

DEVELOPMENT OF A TREATMENT  
SYSTEM FOR ANTIBIOTIC  
WASTEWATER

EMAD SOLIMAN MOHAMMED  
ELMOLLA

DOCTOR OF PHILOSOPHY  
CIVIL ENGINEERING

UNIVERSITI TEKNOLOGI PETRONAS

JULY 2010



STATUS OF THESIS

Title of thesis

DEVELOPMENT OF A TREATMENT SYSTEM FOR ANTIBIOTIC WASTEWATER

I, EMAD SOLIMAN MOHAMMED ELMOLLA  
hereby allow my thesis to be placed at the Information Resource Center (IRC) of Universiti  
Teknologi PETRONAS (UTP) with the following conditions:

The thesis becomes the property of UTP

The IRC of UTP may make copies of the thesis for academic purposes only.

This thesis is classified as

Confidential

Non-confidential

If this thesis is confidential, please state the reason:

\_\_\_\_\_  
\_\_\_\_\_

The contents of the thesis will remain confidential for \_\_\_\_\_ years.

Remarks on disclosure:

\_\_\_\_\_  
\_\_\_\_\_  
\_\_\_\_\_

Endorsed by

\_\_\_\_\_  
Signature of Author

Permanent address:  
Department of Civil Engineering,  
Faculty of Engineering,  
Al-azhar University, Nasr City,  
Cairo, Egypt

Date : \_\_\_\_\_

\_\_\_\_\_  
Signature of Supervisor

Name of Supervisor  
Prof. Malay Chaudhuri

Date : \_\_\_\_\_

UNIVERSITI TEKNOLOGI PETRONAS  
DEVELOPMENT OF A TREATMENT SYSTEM FOR ANTIBIOTIC  
WASTEWATER  
by

EMAD SOLIMAN MOHAMMED ELMOLLA

The undersigned certifies that he has read, and recommends to the Postgraduate Studies Programme for acceptance this thesis for the fulfilment of the requirements for the degree stated.

Signature:

---

Main Supervisor:

Prof. Malay Chaudhuri

Signature:

---

Head of Department:

Assoc. Prof. Dr. Shamsul Rahman Kutty

Date:

---

DEVELOPMENT OF A TREATMENT SYSTEM FOR ANTIBIOTIC  
WASTEWATER

by

EMAD SOLIMAN MOHAMMED ELMOLLA

A Thesis

Submitted to the Postgraduate Studies Programme

as a Requirement for the Degree of

DOCTOR OF PHILOSOPHY

CIVIL ENGINEERING

UNIVERSITI TEKNOLOGI PETRONAS

BANDAR SERI ISKANDAR,

PERAK

JULY 2010

DECLARATION OF THESIS

Title of thesis

DEVELOPMENT OF A TREATMENT SYSTEM FOR ANTIBIOTIC  
WASTEWATER

I, EMAD SOLIMAN MOHAMMED ELMOLLA

hereby declare that the thesis is based on my original work except for quotations and citations which have been duly acknowledged. I also declare that it has not been previously or concurrently submitted for any other degree at UTP or other institutions.

Witnessed by

\_\_\_\_\_  
Signature of Author

\_\_\_\_\_  
Signature of Supervisor

Permanent address:

Department of Civil Engineering,  
Faculty of Engineering, Al-azhar University,  
Nasr City, Cairo, Egypt

Name of Supervisor  
Prof. Malay Chaudhuri

Date : \_\_\_\_\_

Date : \_\_\_\_\_

## ACKNOWLEDGEMENT

The author wishes to thank Allah Al-Mighty, Most Gracious and Most Merciful. The author wishes to express his gratitude to his supervisor, Professor Malay Chaudhuri for his help and supervision in conducting this research.

The author would like to express his sincere appreciation to Associate Professor Dr. Shamsul Rahman Mohamed Kutty and Associate Professor Dr. Mohamed Hasnain Isa and Dr. Amirhossein Malakahmad for their comments and helpful suggestions.

The author also would like to extend his appreciation to the Environmental Engineering Laboratory technicians – Mr Khiarul Anwar and Ms Yousawati as well as Mr Jilani of the Chemical Engineering Department for their help and support in the experimental work. Thanks are also due to the security staff for helping in laboratory access during holidays and to his friends for moral support.

I would like to dedicate this thesis to my parents, wife, son Mohammed and brothers.



## ABSTRACT

Antibiotics are emerging contaminants in the aquatic environment because of their adverse effects on aquatic life and humans. The problem that may be created by the presence of antibiotics at low concentration in the environment is the development of antibiotic resistant bacteria. Antibiotic sources in the environment are antibiotic industry, human excretion and excretion from livestock. No work has been reported on complete treatment of antibiotic wastewater containing amoxicillin, ampicillin and cloxacillin. The overall objective of this work was development of an effective treatment system for antibiotic wastewater from an antibiotic industry producing these antibiotics. The work was conducted in three phases.

In Phase I, four advanced oxidation processes (AOPs) (Fenton, photo-Fenton, UV/TiO<sub>2</sub> and UV/ZnO) were applied for treatment of amoxicillin, ampicillin and cloxacillin antibiotics in aqueous solution. From a technical point of view, Fenton, photo-Fenton and UV/H<sub>2</sub>O<sub>2</sub>/TiO<sub>2</sub> processes were able to degrade the antibiotics and improve biodegradability; however, UV/ZnO process did not improve biodegradability. Based on DOC removal, the photo-Fenton process exhibited the highest rate constant (0.029 min<sup>-1</sup>) followed by the Fenton (0.0144 min<sup>-1</sup>), UV/ZnO (0.00056 min<sup>-1</sup>) and UV/H<sub>2</sub>O<sub>2</sub>/TiO<sub>2</sub> (0.0005 min<sup>-1</sup>). From an economic point of view, the photo-Fenton process appeared to be the most cost-effective compared to the other studied processes. In Phase II, the feasibility of using three combined AOP and sequencing batch reactor (SBR) (Fenton-SBR, photo-Fenton-SBR and UV/H<sub>2</sub>O<sub>2</sub>/TiO<sub>2</sub>-SBR) for complete treatment of an antibiotic wastewater from a local antibiotic industry producing amoxicillin, ampicillin and cloxacillin, was evaluated. Combined systems were operated for several months to study the effect of AOP and SBR operating conditions on the combined system performance. From a technical point of view, both combined Fenton-SBR and photo-Fenton-SBR systems achieved an overall efficiency of 89% for sCOD removal and the final effluent met the discharge standard. However, the combined UV/H<sub>2</sub>O<sub>2</sub>/TiO<sub>2</sub>-SBR system was not a feasible combined system for treatment of the antibiotic wastewater. From an economic point of view, the combined Fenton-SBR system appeared to be more cost-

effective than the combined photo-Fenton-SBR system. The Monod kinetic model was fitted to the results of biodegradation of the Fenton-treated effluent by SBR under the best operating conditions with the kinetic constants  $k_{ob}$   $0.078 \text{ hr}^{-1}$ ,  $Y_{X/S}$   $0.60$  and  $K_d$   $-0.0013 \text{ hr}^{-1}$ . The values of  $k_{ob}$ ,  $Y_{X/S}$  and  $K_d$  for biodegradation of the photo-Fenton-treated effluent under the best operating conditions were similar to those of Fenton-treated effluent. In Phase III, artificial neural network (ANN) was applied for modelling, simulation and prediction of the Fenton process performance. ANN predicted results were very close to the experimental results with correlation coefficient of  $0.997$  and mean square error of  $0.000376$ . The sensitivity analysis showed that all studied variables have strong effect on COD removal and  $\text{H}_2\text{O}_2/\text{Fe}^{2+}$  molar ratio is the most influential parameter. The study showed that neural network modelling could effectively predict and simulate the behaviour of the Fenton process. The study culminated in development of an effective treatment systems for antibiotic wastewater. From technical and economic point of view, combined Fenton-SBR system was the most effective for treatment of the antibiotic wastewater.

## ABSTRAK

Antibiotik yang terdapat dalam perairan telah memberi kesan buruk kepada hidupan akuatik dan manusia. Masalah yang mungkin timbul oleh kehadiran antibiotik pada kepekatan yang rendah dalam persekitaran adalah pertumbuhan bakteria jenis resisten antibiotik. Sumber antibiotik di persekitaran adalah seperti antibiotik dari industri, kumbahan manusia dan kumbahan haiwan ternakan. Tidak ada penyelidikan dilaporkan pada rawatan lengkap yang mengandungi air kumbahan antibiotik jenis amoxicillin, ampicillin dan cloxacillin. Objektif keseluruhan kajian ini adalah pengembangan sistem pemprosesan yang berkesan untuk antibiotik air kumbahan daripada industri antibiotik yang menghasilkan antibiotik ini. Kajian ini telah dilakukan dalam tiga fasa.

Pada Fasa I, empat proses pengoksidaan lanjutan (AOPs) (Fenton, foto-Fenton, UV/TiO<sub>2</sub> dan UV/ZnO) diaplikasikan dalam rawatan antibiotik jenis amoxicillin, ampicillin dan cloxacillin dalam keadaan larutan. Dari segi teknikal, Fenton, foto-Fenton dan proses UV/H<sub>2</sub>O<sub>2</sub>/TiO<sub>2</sub> mampu mendegradasikan antibiotik dan meningkatkan kebolehan degradasi. Namun, kebolehan degradasi dalam proses UV/ZnO tidak meningkat. Dalam penyingkiran DOC, foto-Fenton mempamerkan tahap tertinggi malar (0.029 min<sup>-1</sup>) diikuti oleh Fenton proses (0.0144 min<sup>-1</sup>), UV/ZnO proses (0.00056 min<sup>-1</sup>) dan UV/H<sub>2</sub>O<sub>2</sub>/TiO<sub>2</sub> proses (0.0005 min<sup>-1</sup>). Dari segi ekonomi pula, foto-Fenton mendatangkan kos yang paling efektif berbanding dengan proses-proses yang lain. Pada Fasa II, kajian ini telah menggunakan gabungan ketiga-tiga AOP dan sequencing batch reactor (SBR) (Fenton-SBR, foto-Fenton-SBR dan UV/H<sub>2</sub>O<sub>2</sub>/TiO<sub>2</sub>-SBR) dalam rawatan lengkap untuk antibiotik air kumbahan yang terhasil daripada industri antibiotik tempatan yang menghasilkan amoxicillin, ampicillin dan cloxacillin telah dievaluasi. Sistem gabungan ini telah dijalankan selama beberapa bulan untuk mengkaji kesan SBR dan AOP di bawah sistem gabungan ini. Perbandingan teknikal dan ekonomi dilakukan dalam ketiga-tiga sistem gabungan ini di bawah keadaan yang terbaik sekali. Manakala, dari sudut teknikal, gabungan sistem Fenton-SBR dan foto-Fenton-SBR mencapai kecekapan sebanyak 89% untuk sCOD dan akhirnya mencapai standard pembuangan kumbahan. Namun,

sistem gabungan UV/H<sub>2</sub>O<sub>2</sub>/TiO<sub>2</sub>-SBR bukan sistem gabungan yang terbaik untuk rawatan air kumbahan yang mengandungi antibiotik jenis amoxicillin dan cloxacillin. Dari sudut ekonomi pula, sistem gabungan Fenton-SBR mendatangkan kos yang paling efektif dibandingkan dengan sistem gabungan foto-Fenton- SBR. Monod kinetik model yang dilengkapi dengan keputusan biodegradasi daripada kumbahan yang dirawat oleh Fenton-SBR di bawah keadaan pengendalian terbaik dengan pemalar kinetik  $K_{ob}$  0.078 jam<sup>-1</sup>,  $Y_{X/S}$  0.60 dan  $-0.0013$  k<sub>d</sub> jam<sup>-1</sup>. Nilai-nilai  $K_{ob}$ ,  $Y_{X/S}$  dan  $k_d$  untuk biodegradasi di bawah keadaan pengendalian yang terbaik memberi keputusan yang sama dengan sisa yang dirawat dengan Fenton. Dalam Fasa III, artificial neural network (ANN) telah diterapkan untuk pemodelan, simulasi dan jangkaan daripada rawatan proses Fenton. ANN yang dianggarkan sangat hampir dengan keputusan eksperimen dengan pekali korelasi ( $R^2$ ) of 0.997 dan mean square error (MSE) daripada 0.000376. Analisis sensitiviti menegaskan bahawa semua kajian pembolehubah telah memberi kesan yang impresif terhadap degradasi antibiotik dalam penyingkiran COD. Selain itu, nisbah H<sub>2</sub>O<sub>2</sub>/Fe<sup>2+</sup> adalah paling berpengaruh dengan kepentingan relatif 25.8%. Kajian ini menunjukkan bahawa model rangkaian saraf berkesan dalam memprediksi dan mensimulasikan Fenton proses. Penyelidikan ini memberi pengaruh yang memuncak dalam pembangunan sistem rawatan yang berkesan untuk air kumbahan yang mengandungi antibiotik. Dari sudut teknikal dan ekonomi, penggabungan sistem Fenton-SBR telah memberi kesan yang paling efektif dalam membaikpulih kumbahan air berantibiotik yang mengandungi amoxicillin dan cloxacillin.

## COPYRIGHT

In compliance with the terms of the Copyright Act 1987 and the IP Policy of the university, the copyright of this thesis has been reassigned by the author to the legal entity of the university,

Institute of Technology PETRONAS Sdn Bhd.

Due acknowledgement shall always be made of the use of any material contained in, or derived from, this thesis.

© Emad Soliman Mohammed Elmolla, 2010

Institute of Technology PETRONAS Sdn Bhd

All rights reserved.

## TABLE OF CONTENTS

STATUS OF THESIS.....	i
APPOVAL PAGE.....	ii
TITLE PAGE.....	iii
ACKNOWLEDGEMENT.....	v
ABSTRACT.....	vii
ABSTRAK.....	ix
COPYRIGHT.....	xi
TABLE OF CONTENTS.....	xii
LIST OF TABLES.....	xix
LIST OF FIGURES.....	xxii
ABBREVIATIONS AND NOMENCLATURE.....	xxxii
CHAPTER 1 INTRODUCTION.....	1
1.1 Problem Statement.....	2
1.2 Objectives of the Study.....	3
1.3 Thesis Organisation.....	4
CHAPTER 2 LITERATURE REVIEW.....	6
2.0 Chapter Overview.....	6
2.1 Occurrence and Fate of Pharmaceuticals Including Antibiotics in the Environment.....	6
2.2 Antibiotics.....	8
2.2.1 Classes of Antibiotics.....	8
2.2.1.1 $\beta$ -lactams.....	8
2.2.1.2 Sulfa drugs.....	9
2.2.1.3 Quinolones.....	9
2.2.1.4 Aminoglycosides and Tetracyclines.....	9
2.2.2 Antibiotic Resistance.....	9
2.3 Antibiotic wastewater.....	11
2.4 Advanced Oxidation Processes (AOPs).....	13
2.4.1 Fenton and Photo-Fenton Processes.....	14
2.4.1.1 Fundamentals of Fenton Reactions.....	14
2.4.1.2 Fundamentals of Photo-Fenton Reactions.....	15

2.4.1.3	Factors Affecting Fenton and Photo-Fenton Processes ..	16
2.4.1.4	Application of Fenton and Photo-Fenton Processes in Wastewater Treatment.....	17
2.4.1.5	Benefits and Limitations of Fenton and Photo-Fenton Processes .....	21
2.4.2	Heterogeneous Photocatalysis .....	21
2.4.2.1	Mechanism of the TiO <sub>2</sub> and ZnO Photocatalysed Degradation .....	23
2.4.2.2	Main Factors Affecting Photocatalytic Process.....	24
2.4.2.3	Application of TiO <sub>2</sub> and ZnO Photocatalys for Degradation of Organic Pollutants .....	26
2.5	Antibiotic Wastewater Treatment and Antibiotic Degradation by Advanced Oxidation Processes.....	31
2.6	Biological Wastewater Treatment.....	35
2.6.1	Principle of Aerobic Biological Wastewater Treatment.....	35
2.6.2	Sequencing Batch Reactor (SBR).....	35
2.6.2.1	SBR Operation.....	36
2.6.2.2	Advantages of SBR .....	37
2.7	Combined Advanced Oxidation Process-Biological Treatment.....	38
2.8	Artificial Neural Network (ANN).....	45
2.8.1	Feedforward ANN .....	45
2.8.1.1	Training of Artificial Neural Network.....	46
2.8.2	Application of ANN in Wastewater Treatment .....	47
2.9	Originality and Significance of the Study.....	51
2.10	Summary .....	51
CHAPTER 3	METHODOLOGY .....	52
3.0	Chapter Overview .....	52
3.1	Phase I: Advanced Oxidation Processes Treatment of Antibiotic Aqueous Solution Containing a mixture of Amoxicillin, Ampicillin and Cloxacillin.....	52
3.1.1	Antibiotics and Antibiotic Aqueous Solution .....	53

3.1.2	Chemicals.....	54
3.1.3	Experimental Procedure.....	54
3.1.3.1	Fenton and Photo-Fenton Processes.....	54
3.1.3.2	UV/TiO <sub>2</sub> and UV/ZnO Processes.....	55
3.2	Phase II: Combined Advanced Oxidation Process and Sequencing Batch Reactor for Antibiotic Wastewater Treatment.....	56
3.2.1	Antibiotic Wastewater.....	56
3.2.2	Experimental Set-up.....	57
3.2.3	Experimental Procedure.....	58
3.2.3.1	Stage 1: AOP Pretreatment.....	59
3.2.3.2	Stage 2: Aerobic Sequencing Batch Reactor (SBR).....	59
3.3	Phase III: Artificial Neural Network (ANN) for Modelling and Simulation of Advanced Oxidation Process.....	60
3.4	Analytical Methods.....	61
3.4.1	Antibiotic.....	61
3.4.2	Total Organic Carbon (TOC).....	62
3.4.3	Chemical Oxygen Demand (COD).....	62
3.4.4	Five-day Biochemical Oxygen Demand (BOD <sub>5</sub> ).....	62
3.4.5	Total Suspended Solids (TSS) and Total Volatile Suspended Solids (TVSS).....	62
3.4.6	pH.....	63
3.4.7	Ammonia Nitrogen (NH <sub>3</sub> -N), Nitrate Nitrogen (NO <sub>3</sub> -N) and Total Phosphorus (TP).....	63
3.4.8	Total Kjeldahl Nitrogen (TKN).....	63
3.4.9	Sulphate and Chloride Ions.....	63
3.4.10	Data Analyses.....	63
3.5	Kinetic Study of Antibiotic Oxidation by AOPs.....	64
3.6	Kinetic Study of the biological treatment.....	65
3.7	Summary.....	67
<b>CHAPTER 4 RESULTS AND DISCUSSION</b>		
	<b>PHASE I: ADVANCED OXIDATION PROCESS TREATMENT OF ANTIBIOTIC AQUEOUS SOLUTION.....</b>	<b>68</b>



4.0	Chapter Overview .....	68
4.1	Fenton Process .....	68
4.1.1	Effect of H <sub>2</sub> O <sub>2</sub> /COD Molar Ratio .....	68
4.1.2	Effect of H <sub>2</sub> O <sub>2</sub> /Fe <sup>2+</sup> Molar Ratio.....	72
4.1.3	Effect of pH.....	76
4.1.4	Effect of Initial Antibiotic Concentration and Reaction Time.....	80
4.1.5	Degradation of the Antibiotics in Aqueous Solution, Biodegradability Improvement and Mineralization under Optimum Fenton Operating Conditions.....	84
4.1.6	Kinetic Study .....	86
4.2	Photo-Fenton Process.....	87
4.2.1	Effect of UV Irradiation.....	87
4.2.2	Effect of H <sub>2</sub> O <sub>2</sub> /COD Molar Ratio .....	88
4.2.3	Effect of H <sub>2</sub> O <sub>2</sub> /Fe <sup>2+</sup> Molar Ratio.....	91
4.2.4	Effect of pH.....	95
4.2.5	Effect of Initial Antibiotic Concentration and Irradiation Time..	100
4.2.6	Degradation of the Antibiotics in Aqueous Solution, Biodegradability Improvement and Mineralization under Optimum Photo-Fenton Operating Conditions.....	103
4.2.7	Kinetic Study .....	105
4.3	UV/TiO <sub>2</sub> Process.....	106
4.3.1	Effect of TiO <sub>2</sub> Concentration.....	106
4.3.2	Effect of pH.....	110
4.3.3	Effect of H <sub>2</sub> O <sub>2</sub> Addition.....	115
4.3.4	Effect of H <sub>2</sub> O <sub>2</sub> Addition on Degradation of Antibiotics in Aqueous Solution and Mineralization by UV/TiO <sub>2</sub> process.....	119
4.3.5	Kinetic study .....	122
4.3.5.1	Kinetics of AMX, AMP and CLX Degradation by UV/TiO <sub>2</sub> Process.....	122
4.3.5.2	Kinetics of Antibiotic Mineralization by UV/H <sub>2</sub> O <sub>2</sub> /TiO <sub>2</sub> Process .....	123
4.4	UV/ZnO Process .....	124

4.4.1 Effect of ZnO Concentration .....	124
4.4.2 Effect of pH and Irradiation Time .....	129
4.4.3 Kinetics Study .....	135
4.4.3.1 Kinetics of AMX, AMP and CLX Degradation by UV/ZnO Process.....	135
4.4.3.2 Kinetics of Antibiotic Mineralization by UV/ZnO Process .....	136
4.5 Comparison among the Studied Advanced Oxidation Processes .....	137
4.5.1 Technical Comparison .....	137
4.5.2 Cost Comparison.....	142
4.6 Summary.....	144
<b>CHAPTER 5 RESULTS AND DISCUSSION</b>	
<b>PHASE II: COMBINED ADVANCED OXIDATION PROCESS AND SEQUENCING BATCH REACTOR FOR ANTIBIOTIC WASTEWATER TREATMENT .....</b>	
	<b>147</b>
5.0 Chapter Overview .....	147
5.1 Combined Fenton and Sequencing Batch Reactor Process (Fenton-SBR) .....	147
5.1.1 Pre-treatment of Antibiotic Wastewater Using Fenton Process ..	148
5.1.1.1 Effect of H <sub>2</sub> O <sub>2</sub> /COD Molar Ratio.....	148
5.1.1.2 Effect of H <sub>2</sub> O <sub>2</sub> /Fe <sup>2+</sup> Molar Ratio .....	149
5.1.1.3 Degradation of Antibiotics .....	151
5.1.2 Treatment of Fenton-treated Antibiotic Wastewater by SBR.....	152
5.1.2.1 Effect of Fenton Operating Conditions on SBR and Combined System Performance .....	152
5.1.2.2 Effect of Cycle Period on Performance of SBR.....	158
5.1.2.3 Optimization of Combined Fenton-SBR .....	160
5.2 Combined Photo-Fenton and Sequencing Batch Reactor Process (Photo- Fenton-SBR) .....	168
5.2.1 Pre-treatment of Antibiotic Wastewater Using Photo-Fenton Process .....	169
5.2.1.1 Effect of H <sub>2</sub> O <sub>2</sub> /COD Molar Ratio.....	169

5.2.1.2	Effect of $H_2O_2/Fe^{2+}$ Molar Ratio .....	171
5.2.1.3	Degradation of Antibiotics .....	172
5.2.2	Treatment of Photo-Fenton-Treated Antibiotic Wastewater by SBR.....	173
5.2.2.1	Effect of Photo-Fenton Operating Conditions on SBR and the Combined System Performance.....	173
5.2.2.2	Effect of Cycle Period on the Performance of SBR .	179
5.2.2.3	Optimization of Combined Photo-Fenton-SBR .....	182
5.3	Combined UV/ $H_2O_2$ / $TiO_2$ and Sequencing Batch Reactor Process (UV/ $H_2O_2$ / $TiO_2$ -SBR).....	190
5.3.1	Pre-treatment of Antibiotic Wastewater Using UV/ $H_2O_2$ / $TiO_2$ process.....	190
5.3.1.1	Effect of $TiO_2$ and $H_2O_2$ Dose .....	190
5.3.1.2	Degradation of Antibiotics .....	192
5.3.2	Treatment of UV/ $H_2O_2$ / $TiO_2$ -treated Antibiotic Wastewater by SBR.....	193
5.3.2.1	Effect of UV/ $H_2O_2$ / $TiO_2$ Operating Conditions on SBR Performance .....	193
5.3.2.2	Effect of Cycle Period on the Performance of SBR .	197
5.4	Kinetic Study .....	199
5.5	Proposed Treatment System for Antibiotic Wastewater.....	202
5.5.1	Cost Comparison.....	205
5.6	Summary .....	208

## CHAPTER 6 RESULTS AND DISCUSSION

	PHASE III: ARTIFICIAL NEURAL NETWORK (ANN) FOR MODELLING AND SIMULATION OF ADVANCED OXIDATION PROCESS .....	211
6.0	Chapter Overview .....	211
6.1	Data Sets .....	211
6.2	Selection of Backpropagation Training Algorithm.....	212
6.3	Optimization of Number of Neurons .....	213
6.4	Test and Validation of the Model .....	214

6.5	Sensitivity Analysis .....	215
6.6	Comparison between Predicted and Experimental Results .....	220
6.6.1	Comparison between Measured and Predicted Results at Different H <sub>2</sub> O <sub>2</sub> /COD Molar Ratio .....	220
6.6.2	Comparison between Measured and Predicted Results at Different H <sub>2</sub> O <sub>2</sub> /Fe <sup>2+</sup> Molar Ratio .....	220
6.6.3	Comparison between Measured and Predicted Results at Different pH .....	223
6.7	Summary .....	224
CHAPTER 7 CONCLUSIONS AND RECOMMENDATION .....		225
7.0	Chapter Overview .....	225
7.1	Conclusions .....	225
7.2	Recommendations for Future Work .....	230
PUBLICATIONS AND AWARDS DERIVED FROM THIS STUDY .....		231
REFERENCES .....		234
APPENDIX (A) One-way ANOVA for sCOD and DOC removal at different HRT using Fenton-SBR process .....		258
APPENDIX (B) Two-way ANOVA for sCOD removal at different H <sub>2</sub> O <sub>2</sub> /COD molar ratio and Fenton reaction time using Fenton-SBR process .....		260
APPENDIX (C) One-way ANOVA for sCOD and DOC removal at different HRT using photo-Fenton-SBR process .....		266
APPENDIX (D) Two-way ANOVA for sCOD removal at different H <sub>2</sub> O <sub>2</sub> /COD molar ratio and photo-Fenton irradiation time using photo-Fenton-SBR process .....		268
APPENDIX (E) One-way ANOVA for sCOD and DOC removal at different HRT using TiO <sub>2</sub> photocatalysis-SBR process .....		272
APPENDIX (F) Input data for ANN .....		273
APPENDIX (G) Raw results .....		277

## LIST OF TABLES

Table 2.1	Characteristics of antibiotic wastewater produced from antibiotic synthesis (Zhang et al. 2006) .....	12
Table 2.2	Antibiotic wastewater characteristics produced from antibiotic mixing, compounding and formulating process .....	13
Table 2.3	Classification of AOPs as photochemical and non-photochemical processes .....	14
Table 2.4	Selected review of Fenton and photo-Fenton treatment with related pollutant.....	18
Table 2.5	Selected review of TiO <sub>2</sub> and ZnO photocatalysis with related pollutants .	27
Table 2.6	Antibiotic wastewater treatment and degradation of antibiotic by AOPs..	32
Table 2.7	AOP-biological process for recalcitrant wastewater treatment.....	41
Table 2.8	Applications of ANN in advanced oxidation processes.....	49
Table 3.1	Antibiotic wastewater characteristics.....	57
Table 3.2	The backpropagation training algorithms .....	61
Table 4.1	One-way ANOVA for COD removal at different H <sub>2</sub> O <sub>2</sub> /COD molar ratio, H <sub>2</sub> O <sub>2</sub> /Fe <sup>2+</sup> molar ratio, pH and antibiotic concentration .....	84
Table 4.2	Predominant ferric iron complex species in aqueous solution at different pH ranges .....	100
Table 4.3	One-way ANOVA for AMX, AMP and CLX degradation at different ZnO concentration and pH .....	133
Table 4.4	Operating conditions and results of Fenton and photo-Fenton processes	139
Table 4.5	Operating conditions and results of TiO <sub>2</sub> photocatalysis and UV/ZnO processes .....	140
Table 4.6	Comparison among Fenton, photo-Fenton, UV/H <sub>2</sub> O <sub>2</sub> /TiO <sub>2</sub> and UV/ZnO processes in terms of effluent characteristics under optimum operating conditions .....	141
Table 4.7	Pseudo-first-order rate constant and half-life time for different AOPs under optimum operating condition .....	142
Table 4.8	Price of the chemical reagents .....	143
Table 4.9	Cost estimation for the studied AOPs.....	144
Table 5.1	Fenton operating conditions for SBR.....	152

Table 5.2 Fenton-treated and SBR effluent characteristics and combined system efficiency at different H <sub>2</sub> O <sub>2</sub> /COD molar ratio .....	155
Table 5.3 Fenton-treated and SBR effluent characteristics and combined system efficiency at different H <sub>2</sub> O <sub>2</sub> /Fe <sup>2+</sup> molar ratio .....	157
Table 5.4 One-way ANOVA for SBR efficiency in terms of sCOD and DOC removal at different HRT (combined Fenton-SBR) .....	160
Table 5.5 Operating conditions for combined Fenton-SBR .....	161
Table 5.6 Fenton-treated and SBR effluent characteristics and combined system efficiency at different reaction time and H <sub>2</sub> O <sub>2</sub> /Fe <sup>2+</sup> molar ratio .....	163
Table 5.7 Significance of the difference between two means for sCOD removal in SBR using Tukey HSD method (combined Fenton-SBR).....	166
Table 5.8 Photo-Fenton operating conditions for SBR.....	174
Table 5.9 Photo-Fenton-treated and SBR effluent characteristics and combined system efficiency at different H <sub>2</sub> O <sub>2</sub> /COD molar ratio .....	175
Table 5.10 Photo-Fenton-treated and SBR effluent characteristics and combined system efficiency at different H <sub>2</sub> O <sub>2</sub> /Fe <sup>2+</sup> molar ratios .....	178
Table 5.11 One-way ANOVA for SBR efficiency in terms of sCOD and DOC removal at different HRT (combined photo-Fenton and SBR).....	181
Table 5.12 Operating conditions for combined photo-Fenton-SBR.....	182
Table 5.13 Photo-Fenton-treated and SBR effluent characteristics and combined system efficiency at different irradiation time and H <sub>2</sub> O <sub>2</sub> /Fe <sup>2+</sup> molar ratios .....	184
Table 5.14 Significance of the difference between two means for sCOD removal in SBR using Tukey HSD method (combined photo-Fenton-SBR) .....	187
Table 5.15 UV/H <sub>2</sub> O <sub>2</sub> /TiO <sub>2</sub> operating conditions for SBR .....	194
Table 5.16 UV/H <sub>2</sub> O <sub>2</sub> /TiO <sub>2</sub> -treated and SBR effluent characteristics and combined system efficiency at different H <sub>2</sub> O <sub>2</sub> and TiO <sub>2</sub> dose.....	196
Table 5.17 One-way ANOVA for SBR efficiency in terms of sCOD and DOC removal at different HRT (combined UV/H <sub>2</sub> O <sub>2</sub> /TiO <sub>2</sub> -SBR) .....	199
Table 5.18 Comparison among combined Fenton-SBR, photo-Fenton-SBR and UV/H <sub>2</sub> O <sub>2</sub> /TiO <sub>2</sub> -SBR from technical point of view .....	204
Table 5.19 Price of reagents for estimation of combined AOP-SBR cost.....	206
Table 5.20 Cost estimation for combined Fenton-SBR and photo-Fenton-SBR.....	206

Table 6.1 Backpropagation training algorithms with five neurons in the hidden layer .....	212
Table 6.2 Weight matrix, weights between input and hidden layers (W1) and weights between hidden and output layers (W2).....	217
Table 6.3 Relative importance of input variables .....	217
Table 6.4 Evaluation of combination of input variables .....	219

## LIST OF FIGURES

Figure 2.1 Antibiotic resistance mechanisms (Yim, 2007).....	11
Figure 2.2 Mechanism of semiconductor photocatalysis.....	22
Figure 2.3 Various stages in the SBR cycle.....	37
Figure 2.4 General strategy for wastewater treatment.....	39
Figure 2.5 A feedforward ANN.....	46
Figure 2.6 A supervised learning process (Artificial neural network tutorial, 2008)	47
Figure 3.1 Chemical structure and HPLC chromatograph of (a) amoxicillin, (b) ampicillin sodium and (c) cloxacillin sodium.....	54
Figure 3.2 General schematic of combined AOP-SBR treatment system .....	58
Figure 3.3 SBR setup .....	58
Figure 4.1 Effect of H <sub>2</sub> O <sub>2</sub> /COD molar ratio on antibiotics degradation by Fenton process in terms of COD (a) 1.0, (b) 1.5, (c) 2.0, (d) 2.5, (e) 3.0 and (f) 3.5.....	69
Figure 4.2 Effect of H <sub>2</sub> O <sub>2</sub> /COD molar ratio on antibiotics degradation by Fenton process in terms of COD removal (a) 1.0, (b) 1.5, (c) 2.0, (d) 2.5, (e) 3.0 and (f) 3.5.....	70
Figure 4.3 Effect of H <sub>2</sub> O <sub>2</sub> /COD molar ratio on antibiotics degradation by Fenton process in terms of BOD <sub>5</sub> (a) 1.0, (b) 1.5, (c) 2.0, (d) 2.5, (e) 3.0 and (f) 3.5.....	70
Figure 4.4 Effect of H <sub>2</sub> O <sub>2</sub> /COD molar ratio on antibiotics degradation by Fenton process in terms of BOD <sub>5</sub> /COD ratio (a) 1.0, (b) 1.5, (c) 2.0, (d) 2.5, (e) 3.0 and (f) 3.5.....	71
Figure 4.5 Effect of H <sub>2</sub> O <sub>2</sub> /COD molar ratio on antibiotics degradation by Fenton process in terms of DOC (a) 1.0, (b) 1.5, (c) 2.0, (d) 2.5, (e) 3.0 and (f) 3.5.....	71
Figure 4.6 Effect of H <sub>2</sub> O <sub>2</sub> /COD molar ratio on antibiotics degradation by Fenton process in terms of DOC removal (a) 1.0, (b) 1.5, (c) 2.0, (d) 2.5, (e) 3.0 and (f) 3.5.....	72
Figure 4.7 Effect of H <sub>2</sub> O <sub>2</sub> /Fe <sup>2+</sup> molar ratio on antibiotics degradation by Fenton process in terms of COD (a) 2.0, (b) 5.0, (c) 10.0, (d) 20.0, (e) 50.0, (f) 100 and (g) 150 .....	73



Figure 4.8 Effect of $H_2O_2/Fe^{2+}$ molar ratio on antibiotics degradation by Fenton process in terms of COD removal (a) 2.0, (b) 5.0, (c) 10.0, (d) 20.0, (e) 50.0, (f) 100 and (g) 150 .....	73
Figure 4.9 Effect of $H_2O_2/Fe^{2+}$ molar ratio on antibiotics degradation by Fenton process in terms of $BOD_5$ (a) 2.0, (b) 5.0, (c) 10.0, (d) 20.0, (e) 50.0, (f) 100 and (g) 150 .....	74
Figure 4.10 Effect of $H_2O_2/Fe^{2+}$ molar ratio on antibiotics degradation by Fenton process in terms of $BOD_5/COD$ ratio (a) 2.0, (b) 5.0, (c) 10.0, (d) 20.0, (e) 50.0, (f) 100 and (g) 150 .....	74
Figure 4.11 Effect of $H_2O_2/Fe^{2+}$ molar ratio on antibiotics degradation by Fenton process in terms of DOC (a) 2.0, (b) 5.0, (c) 10.0, (d) 20.0, (e) 50.0, (f) 100 and (g) 150 .....	75
Figure 4.12 Effect of $H_2O_2/Fe^{2+}$ molar ratio on antibiotics degradation by Fenton process in terms of DOC removal (a) 2.0, (b) 5.0, (c) 10.0, (d) 20.0, (e) 50.0, (f) 100 and (g) 150 .....	75
Figure 4.13 Effect of pH on antibiotics degradation by Fenton process in terms of COD (a) 2.0, (b) 2.5, (c) 3.0, (d) 3.5 and (e) 4.0.....	77
Figure 4.14 Effect of pH on antibiotics degradation by Fenton process in terms of COD removal (a) 2.0, (b) 2.5, (c) 3.0, (d) 3.5 and (e) 4.0.....	77
Figure 4.15 Effect of pH on antibiotics degradation by Fenton process in terms of $BOD_5$ (a) 2.0, (b) 2.5, (c) 3.0, (d) 3.5 and (e) 4.0.....	78
Figure 4.16 Effect of pH on antibiotics degradation by Fenton process in terms of $BOD_5/COD$ ratio (a) 2.0, (b) 2.5, (c) 3.0, (d) 3.5 and (e) 4.0.....	78
Figure 4.17 Effect of pH on antibiotics degradation by Fenton process in terms of DOC (a) 2.0, (b) 2.5, (c) 3.0, (d) 3.5 and (e) 4.0.....	79
Figure 4.18 Effect of pH on antibiotics degradation by Fenton process in terms of DOC removal (a) 2.0, (b) 2.5, (c) 3.0, (d) 3.5 and (e) 4.0.....	79
Figure 4.19 Effect of initial antibiotic concentration on antibiotics degradation by Fenton process in terms of COD (a) 100, (b) 250 and (c) 500 mg/L.....	81
Figure 4.20 Effect of initial antibiotic concentration on antibiotics degradation by Fenton process in terms of COD removal (a) 100, (b) 250 and (c) 500 mg/L .....	82

Figure 4.21 Effect of initial antibiotic concentration on antibiotics degradation by Fenton process in terms of BOD <sub>5</sub> (a) 100, (b) 250 and (c) 500 mg/L ....	82
Figure 4.22 Effect of initial antibiotic concentration on antibiotics degradation by Fenton process in terms of BOD <sub>5</sub> /COD ratio (a) 100, (b) 250 and (c) 500 mg/L.....	83
Figure 4.23 Effect of initial antibiotics concentration on antibiotics degradation by Fenton process in terms of DOC (a) 100, (b) 250 and (c) 500 mg/L.....	83
Figure 4.24 Effect of initial antibiotics concentration on antibiotics degradation by Fenton process in terms of DOC removal (a) 100, (b) 250 and (c) 500 mg/L.....	84
Figure 4.25 Degradation of AMX, AMP and CLX under optimum Fenton operating conditions (a) AMX, (b) AMP and (c) CLX.....	85
Figure 4.26 Degradation of antibiotics in terms of COD, BOD <sub>5</sub> and BOD <sub>5</sub> /COD ratio under optimum Fenton operating conditions .....	85
Figure 4.27 Mineralization of organic carbon and nitrogen in terms of DOC removal and nitrate concentration under optimum Fenton operating conditions .	86
Figure 4.28 Kinetics of antibiotic mineralization by the Fenton process .....	87
Figure 4.29 Effect of H <sub>2</sub> O <sub>2</sub> /COD molar ratio on antibiotics degradation by photo-Fenton process in terms of COD (a) 1.0, (b) 1.5, (c) 2.0 and (d) 2.5.....	89
Figure 4.30 Effect of H <sub>2</sub> O <sub>2</sub> /COD molar ratio on antibiotics degradation by photo-Fenton process in terms of COD removal (a) 1.0, (b) 1.5, (c) 2.0 and (d) 2.5.....	89
Figure 4.31 Effect of H <sub>2</sub> O <sub>2</sub> /COD molar ratio on antibiotics degradation by photo-Fenton process in terms of BOD <sub>5</sub> (a) 1.0, (b) 1.5, (c) 2.0 and (d) 2.5 ....	90
Figure 4.32 Effect of H <sub>2</sub> O <sub>2</sub> /COD molar ratio on antibiotics degradation by photo-Fenton process in terms of BOD <sub>5</sub> /COD ratio (a) 1.0, (b) 1.5, (c) 2.0 and (d) 2.5.....	90
Figure 4.33 Effect of H <sub>2</sub> O <sub>2</sub> /COD molar ratio on antibiotics degradation by photo-Fenton process in terms of DOC (a) 1.0, (b) 1.5, (c) 2.0 and (d) 2.5.....	91
Figure 4.34 Effect of H <sub>2</sub> O <sub>2</sub> /COD molar ratio on antibiotics degradation by photo-Fenton process in terms of DOC removal (a) 1.0, (b) 1.5, (c) 2.0 and (d) 2.5.....	91

Figure 4.35 Effect of $\text{H}_2\text{O}_2/\text{Fe}^{2+}$ molar ratio on antibiotics degradation by photo-Fenton process in terms of COD removal (a) 10, (b) 20, (c) 50, (d) 100 and (e) 150.....	92
Figure 4.36 Effect of $\text{H}_2\text{O}_2/\text{Fe}^{2+}$ molar ratio on antibiotics degradation by photo-Fenton process in terms of COD removal (a) 10, (b) 20, (c) 50, (d) 100 and (e) 150.....	93
Figure 4.37 Effect of $\text{H}_2\text{O}_2/\text{Fe}^{2+}$ molar ratio on antibiotics degradation by photo-Fenton process in terms of $\text{BOD}_5$ (a) 10, (b) 20, (c) 50, (d) 100 and (e) 150.....	93
Figure 4.38 Effect of $\text{H}_2\text{O}_2/\text{Fe}^{2+}$ molar ratio on antibiotics degradation by photo-Fenton process in terms of $\text{BOD}_5/\text{COD}$ ratio (a) 10, (b) 20, (c) 50, (d) 100 and (e) 150.....	94
Figure 4.39 Effect of $\text{H}_2\text{O}_2/\text{Fe}^{2+}$ molar ratio on antibiotics degradation by photo-Fenton process in terms of DOC (a) 10, (b) 20, (c) 50, (d) 100 and (e) 150.....	94
Figure 4.40 Effect of $\text{H}_2\text{O}_2/\text{Fe}^{2+}$ molar ratio on antibiotics degradation by photo-Fenton process in terms of DOC removal (a) 10, (b) 20, (c) 50, (d) 100 and (e) 150.....	95
Figure 4.41 Effect of pH on antibiotics degradation by photo-Fenton process in terms of COD for pH (a) 2.0, (b) 2.5, (c) 3.0, (d) 3.5 and (e) 4.0.....	96
Figure 4.42 Effect of pH on antibiotics degradation by photo-Fenton process in terms of COD removal for pH (a) 2.0, (b) 2.5, (c) 3.0, (d) 3.5 and (e) 4.0.....	97
Figure 4.43 Effect of pH on antibiotics degradation by photo-Fenton process in terms of $\text{BOD}_5$ for pH (a) 2.0, (b) 2.5, (c) 3.0, (d) 3.5 and (e) 4.0.....	97
Figure 4.44 Effect of pH on antibiotics degradation by photo-Fenton process in terms of $\text{BOD}_5/\text{COD}$ for pH (a) 2.0, (b) 2.5, (c) 3.0, (d) 3.5 and (e) 4.0.....	98
Figure 4.45 Effect of pH on antibiotics degradation by photo-Fenton process in terms of DOC removal for pH (a) 2.0, (b) 2.5, (c) 3.0, (d) 3.5 and (e) 4.0.....	98
Figure 4.46 Effect of pH on antibiotics degradation by photo-Fenton process in terms of DOC removal for pH (a) 2.0, (b) 2.5, (c) 3.0, (d) 3.5 and (e) 4.0.....	99
Figure 4.47 Effect of initial antibiotic concentration on antibiotics degradation by photo-Fenton process in terms of COD removal (a) 100, (b) 250 and (c) 500 mg/L.....	101

Figure 4.48 Effect of initial antibiotic concentration on antibiotics degradation by photo-Fenton process in terms of COD removal (a) 100, (b) 250 and (c) 500 mg/L.....	101
Figure 4.49 Effect of initial antibiotic concentration on antibiotics degradation by photo-Fenton process in terms of BOD <sub>5</sub> (a) 100, (b) 250, (c) 500 mg/L.....	102
Figure 4.50 Effect of initial antibiotic concentration on antibiotics degradation by photo-Fenton process in terms of BOD <sub>5</sub> /COD ratio (a) 100, (b) 250, (c) 500 mg/L.....	102
Figure 4.51 Effect of initial antibiotic concentration on antibiotics degradation by photo-Fenton process in terms of DOC (a) 100, (b) 250, (c) 500 mg/L.....	103
Figure 4.52 Effect of initial antibiotic concentration on antibiotics degradation by photo-Fenton process in terms of DOC Removal (a) 100, (b) 250, (c) 500 mg/L.....	103
Figure 4.53 Degradation of AMX, AMP and CLX under optimum photo-Fenton operating conditions (a) AMX, (b) AMP and (c) CLX.....	104
Figure 4.54 Degradation of antibiotics under optimum photo-Fenton operating conditions in terms of COD, BOD <sub>5</sub> and BOD <sub>5</sub> /COD ratio.....	104
Figure 4.55 Mineralization of organic carbon and nitrogen in terms of DOC removal and nitrate concentration under optimum photo-Fenton operating conditions.....	105
Figure 4.56 Kinetics of antibiotic mineralization by the photo-Fenton process.....	106
Figure 4.57 Effect of TiO <sub>2</sub> concentration on AMX.....	107
Figure 4.58 Effect of TiO <sub>2</sub> concentration on AMX degradation.....	108
Figure 4.59 Effect of TiO <sub>2</sub> concentration on AMP.....	108
Figure 4.60 Effect of TiO <sub>2</sub> concentration on AMP degradation.....	109
Figure 4.61 Effect of TiO <sub>2</sub> concentration on CLX.....	109
Figure 4.62 Effect of TiO <sub>2</sub> concentration on CLX degradation.....	110
Figure 4.63 Effect of TiO <sub>2</sub> concentration on antibiotics degradation in terms of COD removal.....	110
Figure 4.64 Effect of pH on AMX by UV/TiO <sub>2</sub> process.....	111
Figure 4.65 Effect of pH on AMX degradation by UV/TiO <sub>2</sub> process.....	111

Figure 4.66 Effect of pH on AMP by UV/TiO <sub>2</sub> process .....	112
Figure 4.67 Effect of pH on AMP degradation by UV/TiO <sub>2</sub> process .....	112
Figure 4.68 Effect of pH on CLX by UV/TiO <sub>2</sub> process .....	113
Figure 4.69 Effect of pH on CLX degradation by UV/TiO <sub>2</sub> process.....	113
Figure 4.70 Effect of pH on antibiotics degradation in terms of COD removal by UV/TiO <sub>2</sub> process .....	114
Figure 4.71 Anionic species of amoxicillin at different pH (Chemie, 2005).....	115
Figure 4.72 Effect of H <sub>2</sub> O <sub>2</sub> addition on antibiotics degradation in terms of COD (a) 50, (b) 100, (c) 150, (d) 200 and (e) 300 mg/L .....	117
Figure 4.73 Effect of H <sub>2</sub> O <sub>2</sub> addition on antibiotics degradation in terms of COD removal (a) 50, (b) 100, (c) 150, (d) 200 and (e) 300 mg/L.....	117
Figure 4.74 Effect of H <sub>2</sub> O <sub>2</sub> addition on antibiotics degradation in terms of BOD <sub>5</sub> (a) 50, (b) 100, (c) 150, (d) 200 and (e) 300 mg/L .....	118
Figure 4.75 Effect of H <sub>2</sub> O <sub>2</sub> addition on antibiotics degradation in terms of BOD <sub>5</sub> /COD ratio (a) 50, (b) 100, (c) 150, (d) 200 and (e) 300 mg/L...	118
Figure 4.76 Effect of H <sub>2</sub> O <sub>2</sub> addition on antibiotics degradation in terms of DOC (a) 50, (b) 100, (c) 150, (d) 200 and (e) 300 mg/L .....	119
Figure 4.77 Effect of H <sub>2</sub> O <sub>2</sub> addition on antibiotics degradation in terms of DOC removal (a) 50, (b) 100, (c) 150, (d) 200 and (e) 300 mg/L.....	119
Figure 4.78 Effect of H <sub>2</sub> O <sub>2</sub> addition on AMX, AMP and CLX degradation by the UV/TiO <sub>2</sub> process .....	120
Figure 4.79 Effect of irradiation time on DOC concentration and removal by the UV/H <sub>2</sub> O <sub>2</sub> /TiO <sub>2</sub> process.....	121
Figure 4.80 Effect of irradiation time on NH <sub>3</sub> , NO <sub>3</sub> <sup>-</sup> and SO <sub>4</sub> <sup>2-</sup> formation by the UV/H <sub>2</sub> O <sub>2</sub> /TiO <sub>2</sub> process.....	122
Figure 4.81 Kinetics of AMX, AMP and CLX degradation by UV/TiO <sub>2</sub> process ..	123
Figure 4.82 Kinetic study of antibiotic mineralization by UV/H <sub>2</sub> O <sub>2</sub> /TiO <sub>2</sub> process .	124
Figure 4.83 Effect of ZnO concentration on AMX.....	125
Figure 4.84 Effect of ZnO concentration on AMX degradation.....	125
Figure 4.85 Effect of ZnO concentration on AMP .....	126
Figure 4.86 Effect of ZnO concentration on AMP degradation.....	126
Figure 4.87 Effect of ZnO concentration on CLX degradation .....	126
Figure 4.88 Effect of ZnO concentration on CLX degradation .....	127

Figure 4.89 Effect of ZnO concentration on antibiotics degradation in terms of COD .....	128
Figure 4.90 Effect of ZnO concentration on antibiotics degradation in terms of COD removal.....	128
Figure 4.91 Effect of ZnO concentration on antibiotics degradation in terms of DOC removal and biodegradability improvement .....	129
Figure 4.92 Effect of pH on AMX by UV/ZnO process.....	130
Figure 4.93 Effect of pH on AMX degradation by UV/ZnO process.....	130
Figure 4.94 Effect of pH on AMP by UV/ZnO process .....	131
Figure 4.95 Effect of pH on AMP degradation by UV/ZnO process .....	131
Figure 4.96 Effect of pH on CLX by UV/ZnO process.....	132
Figure 4.97 Effect of pH on CLX degradation by UV/ZnO process.....	132
Figure 4.98 Effect of pH on antibiotics degradation in terms of COD by UV/ZnO process.....	133
Figure 4.99 Effect of pH on antibiotics degradation in terms of COD removal by UV/ZnO process .....	134
Figure 4.100 Effect of pH on on antibiotics degradation in terms of DOC removal and biodegradability improvement .....	134
Figure 4.101 Kinetics of AMX, AMP and CLX degradation by UV/ZnO process.	136
Figure 4.102 Kinetic study of antibiotic mineralization by UV/ZnO process.....	137
Figure 4.103 Kinetics of antibiotic mineralization by different AOPs under optimum operating condition .....	142
Figure 5.1 Effect of H <sub>2</sub> O <sub>2</sub> /COD molar ratio of Fenton process on sCOD and DOC removal, and BOD <sub>5</sub> /COD ratio .....	149
Figure 5.2 Effect of H <sub>2</sub> O <sub>2</sub> /Fe <sup>2+</sup> molar ratio of Fenton process on sCOD and DOC removal, and BOD <sub>5</sub> /COD ratio .....	150
Figure 5.3 Degradation of AMX and CLX in antibiotic wastewater by Fenton process.....	151
Figure 5.4 Performance of SBR in terms of sCOD and DOC as a function of Fenton operating condition (Case F1-F10) .....	153
Figure 5.5 SBR efficiency of Fenton-SBR in terms of sCOD removal at HRT 48, 24 and 12 hr.....	159

Figure 5.6 SBR efficiency of Fenton-SBR in terms of DOC removal at HRT 48, 24 and 12 hr.....	159
Figure 5.7 Performance of SBR in terms of sCOD and DOC as a function of Fenton operating condition (Case F11-F19) .....	161
Figure 5.8 Combined Fenton and SBR efficiency in terms of sCOD removal.....	167
Figure 5.9 Biodegradation of the Fenton-treated effluent in terms of sCOD and DOC in SBR during the cycle period (Case F19) .....	167
Figure 5.10 Nitrification in SBR during the cycle period (Case F19) .....	168
Figure 5.11 Effect of H <sub>2</sub> O <sub>2</sub> /COD molar ratio of photo-Fenton process on sCOD and DOC removal, and BOD <sub>5</sub> /COD ratio .....	170
Figure 5.12 Effect of H <sub>2</sub> O <sub>2</sub> /Fe <sup>2+</sup> molar ratio of photo-Fenton process on sCOD and DOC removal, and BOD <sub>5</sub> /COD ratio .....	172
Figure 5.13 Degradation of AMX and CLX in antibiotic wastewater by photo-Fenton process.....	173
Figure 5.14 Performance of SBR in terms of sCOD and DOC as a function of photo-Fenton operating conditions (Case PF1-PF10) .....	174
Figure 5.15 SBR efficiency of photo-Fenton-SBR in terms of sCOD removal at HRT 48, 24 and 12 hr.....	180
Figure 5.16 SBR efficiency of photo-Fenton-SBR in terms of DOC removal at HRT 48, 24 and 12 hr.....	181
Figure 5.17 Performance of SBR in terms of sCOD and DOC as function of photo-Fenton operating condition (Case PF11-PF19).....	183
Figure 5.18 Combined photo-Fenton and SBR efficiency in terms of sCOD removal .....	188
Figure 5.19 Biodegradation of the photo-Fenton-treated effluent in terms of sCOD and DOC in SBR during the cycle period (Case PF18).....	188
Figure 5.20 Nitrification in SBR during the cycle period (Case PF18).....	189
Figure 5.21 Effect of TiO <sub>2</sub> and H <sub>2</sub> O <sub>2</sub> dose on the sCOD and DOC removal, and BOD <sub>5</sub> /COD ratio .....	192
Figure 5.22 Degradation of AMX and CLX in Antibiotic Wastewater by UV/H <sub>2</sub> O <sub>2</sub> /TiO <sub>2</sub> Process.....	193
Figure 5.23 Performance of SBR in terms of sCOD and DOC as a function of UV/H <sub>2</sub> O <sub>2</sub> /TiO <sub>2</sub> operating conditions (Case T1-T9).....	194

Figure 5.24 SBR efficiency of UV/H <sub>2</sub> O <sub>2</sub> /TiO <sub>2</sub> -SBR in terms of sCOD removal at HRT 48 and 24 hr .....	198
Figure 5.25 SBR efficiency of UV/H <sub>2</sub> O <sub>2</sub> /TiO <sub>2</sub> -SBR in terms of DOC removal at HRT 48 and 24 hr .....	198
Figure 5.26 Kinetics of SBR treatment of Fenton-treated effluent (Case F19) .....	200
Figure 5.27 Kinetics of SBR treatment of photo-Fenton-treated effluent (Case PF18) .....	200
Figure 5.28 Evaluation of Y <sub>X/S</sub> and K <sub>d</sub> for SBR treatment of Fenton-treated effluent (Case F19) .....	202
Figure 5.29 Evaluation of Y <sub>X/S</sub> and K <sub>d</sub> for SBR treatment of photo-Fenton-treated effluent (Case PF18) .....	202
Figure 5.30 Process diagram of the proposed combined system (Fenton-SBR) for the antibiotic wastewater treatment .....	207
Figure 6.1 Relationship between number of neurons and MSE .....	213
Figure 6.2 Artificial neural network optimized structure .....	214
Figure 6.3 Comparison between predicted and measured values of the output .....	215
Figure 6.4 Comparison between predicted and experimental results at different H <sub>2</sub> O <sub>2</sub> /COD molar ratio: (A) 1.0, (B) 1.5, (C) 2.0, (D) 2.5, (E) 3.0 and (F) 3.5 .....	221
Figure 6.5 Comparison between predicted and experimental results at different H <sub>2</sub> O <sub>2</sub> /Fe <sup>2+</sup> molar ratio: (A) 2, (B) 5, (C) 10, (D) 20, (E) 50 and (F) 100 .....	222
Figure 6.6 Comparison between predicted and experimental results at different pH: (A) 2, (B) 3, (C) 3.5 and (D) 4 .....	223



## ABBREVIATIONS AND NOMENCLATURE

Abbreviation		Unit
ANOVA	Analysis of Variance	
AMX	Amoxicillin	
ANN	Artificial Neural Network	
AMP	Ampicillin	
AOPs	Advanced Oxidation Processes	
BOD <sub>5</sub>	5-day Biological Oxygen Demand	mg/L
CLX	Cloxacillin	
COD	Chemical Oxygen Demand	mg/L
DOC	Dissolved Organic Carbon	
DAD	Diode Array Detector	
HPLC	High Performance Chromatograph	Liquid
H <sub>2</sub> O <sub>2</sub>	Hydrogen Peroxide	
HRT	Hydraulic Retention Time	
MSE	Mean Square Error	
MLSS	Mixed Liquor Suspended Solids	mg/L
NH <sub>3</sub> -N	Ammonia-nitrogen	mg/L
NO <sub>3</sub> -N	Nitrate-nitrogen	mg/L
R <sup>2</sup>	Correlation Coefficient	
SBR	Sequencing Batch Reactor	
SS	Suspended Solids	mg/L
TOC	Total Organic Carbon	mg/L
TiO <sub>2</sub>	Titanium Dioxide	mg/L
TSS	Total Suspended Solids	mg/L
DOC	Dissolved Organic Carbon	mg/L

TP	Total Phosphorus	mg/L
UV	Ultraviolet	
MLVSS	Mixed Liquor Volatile Suspended Solids	mg/L
MR	Molar ratio	
MSE	Mean Square Error	
VSS	Volatile Suspended Solids	mg/L
ZnO	Zinc Oxide	

## CHAPTER 1 INTRODUCTION

Generally, antibiotic active ingredients are produced in a bulk form by batch processes and converted to the dosage form for consumer use. Common dosage forms for the consumer market are tablets, capsules and syrup. The necessary production steps typically produce a small wastewater flow because few of the unit operations produce wastewater. The primary use of water is in the actual formulating process, where it is used for cooling and washing of equipment and floor (Jones, 2006).

Usually, the production unit has intermittent and fluctuating wastewater flow with variable wastewater composition depending on the production regime. Because the production regime greatly differs with respect to demand, it is difficult to dedicate the manufacturing lines to a specific product. Thus, the same equipment is used in manufacturing a different range of products. Naturally, this requires thorough cleaning and validation prior to reuse of the equipment. However, the regime of equipment cleaning also varies greatly with the different processes used for each product. Floor and equipment wash water, wet scrubbers and spills are the main sources of wastewater produced from mixing and formulating (Jones, 2006).

It is important to provide solution for treatment of antibiotic wastewater which contains recalcitrant organics and this is a challenging research topic. Advanced oxidation processes (AOPs) appear to be adequate tools for degradation of recalcitrant organics (Liou *et al.*, 2003; Pera-Titus *et al.*, 2004; Tekin *et al.*, 2006) in comparison with the processes such as coagulation-filtration, activated carbon adsorption and reverse osmosis because these processes only transfer the pollutants from one phase to another without destroying them. Biological treatment is limited to wastewaters which contain biodegradable substances and which are not toxic to the biological culture.

## 1.1 Problem Statement

Antibiotics have been observed in surface water (Kolpin *et al.*, 2002; Anderson *et al.*, 2004; Rabiet *et al.*, 2006), ground water (Rabiet *et al.*, 2006), sewage effluents (Carballa *et al.*, 2004; Nikolaou *et al.*, 2007), and even in drinking water (Stackelberg *et al.*, 2004). Antibiotics are emerging contaminants in the aquatic environment because they are introduced in larger amounts and they are bioactive, polar and persistent which may cause adverse effects in aquatic life and humans. Problem that may be created by the presence of antibiotics at low concentration in the environment is the development of antibiotic resistant bacteria. The presence of antibiotics may result in selective pressure that favours organisms that possess genes coding for antibiotic resistance. The incidence of antibiotic resistant bacteria has increased and many people believe the increase is due to the use of antibiotics (Walter and Vennes, 1985). This may pose a serious threat to public health in that more and more infections may no longer be treatable with known antibiotics (Hirsch *et al.*, 1999). In the event that antibiotic resistance is spread from nonpathogenic to pathogenic bacteria, epidemics may result. In fact, bacteria have been observed to transfer their resistance in laboratory settings as well as in the natural environment (Kanay, 1983).

Antibiotic wastewater contains a variety of non-biodegradable organic constituents. Antibiotic compounds can reach the aquatic environment through various sources such as antibiotic industry, and excretion from humans and livestock (Ikehata *et al.*, 2006; Nikolaou *et al.*, 2007; Yang *et al.*, 2008). Antibiotic industries were found to be sources of much higher environmental concentrations than those caused by the humans and livestock usage of drugs (Larsson *et al.*, 2007). In Malaysia, number of pharmaceutical companies is more than 100 and most of these companies produce antibiotics (<http://www.eguide.com.my>). Some of these companies may treat pharmaceutical wastewater containing antibiotics by biological system which could cause development of antibiotic resistance bacteria. Larsson and Fick (2009) highlighted that antibiotic wastewater should not be treated biologically because this increases the risk of antibiotic resistant bacteria development as well as decrease of biological treatment efficiency. In Malaysia, presence of antibiotic resistant bacteria in three sewage treatment plant near Kuala Lumpur has been

detected in 1981 (Yaziz 1981). Recently, a lot of attention has been paid to antibiotic wastewater treatment and degradation of active ingredients before discharge to the environment (Daughton, 2004). Thus, it is important to give a complete treatment for wastewater generated from antibiotic production units to protect the environment from antibiotic resistant bacteria. Research should be conducted into development of a treatment system for antibiotic wastewater.

## **1.2 Objectives of the Study**

The overall objective of the study is to develop an effective treatment system for antibiotic wastewater containing amoxicillin, ampicillin and cloxacillin. In addition, study the degradation of amoxicillin, ampicillin and cloxacillin antibiotics by the treatment system. To fulfill this overall objective, the following specific objectives were taken into consideration:

- 1) To study degradation of amoxicillin, ampicillin and cloxacillin antibiotics in aqueous solution by the Fenton, photo-Fenton, TiO<sub>2</sub> photocatalytic and ZnO photocatalytic process, and the effect of operating conditions of each process on antibiotic mineralization and biodegradability improvement.
- 2) To compare among the AOPs (Fenton, photo-Fenton, UV/TiO<sub>2</sub> and UV/ZnO processes) in terms of technical and economic feasibility.
- 3) To study the feasibility of using combined AOP-sequencing batch reactor (SBR) system for complete treatment of antibiotic wastewater from a local antibiotic industry producing amoxicillin, ampicillin and cloxacillin.
- 4) To apply artificial neural network (ANN) for modelling and simulation of advanced oxidation process in order to estimate the dynamic behaviour of the process.

### 1.3 Thesis Organisation

This thesis has been organised into the following seven chapters:

Chapter 1 introduces antibiotic wastewater and problem statement, and objectives of the study.

Chapter 2 is a literature review on occurrence of antibiotics in the environment, antibiotics, antibiotic wastewater, advanced oxidation processes (Fenton, photo-Fenton, UV/TiO<sub>2</sub> and UV/ZnO) and their application in wastewater treatment, treatment of antibiotic wastewater by advanced oxidation processes, biological wastewater treatment and sequencing batch reactor (SBR) and combined advanced oxidation process-biological treatment. A brief summary of artificial neural network and its application in wastewater treatment is also included.

Chapter 3 describes the study phases, and the materials, experimental procedure and analytical procedure for each phase of the study.

Chapter 4 presents the results of Phase I and discussion. In phase I, four AOPs (Fenton, photo-Fenton, UV/TiO<sub>2</sub> and UV/ZnO) were applied for treatment of amoxicillin, ampicillin and cloxacillin antibiotics in aqueous solution. The chapter is divided into five main sections. Each section presents the results of application of one AOP and discussion, and the fifth section shows a comparison among the AOPs from technical and economic point of view.

Chapter 5 presents the results of Phase II and discussion. In Phase II, the feasibility of using Fenton-SBR, photo-Fenton-SBR and UV/TiO<sub>2</sub>/H<sub>2</sub>O<sub>2</sub>-SBR for the treatment of antibiotic wastewater was evaluated. The chapter is divided into five main sections. The first, second and third section present the results and discussion of the treatment of antibiotic wastewater by combined Fenton-SBR, photo-Fenton-SBR and UV/TiO<sub>2</sub>/H<sub>2</sub>O<sub>2</sub>-SBR, respectively. The fourth and fifth sections present the kinetic study and propose a treatment system for the antibiotic wastewater.

Chapter 6 presents the results of Phase III and discussion. In Phase III, the application of artificial neural network for modelling and simulation of the most promising AOP was implemented.

Chapter 7 gives the conclusions of the work and recommendations for future work.

## CHAPTER 2 LITERATURE REVIEW

### **2.0 Chapter Overview**

This chapter presents a literature review on occurrence of antibiotics in the environment, antibiotics, antibiotic wastewater, advanced oxidation processes (Fenton, photo-Fenton, UV/TiO<sub>2</sub> and UV/ZnO) and their application in wastewater treatment, treatment of antibiotic wastewater by advanced oxidation processes, biological wastewater treatment and sequencing batch reactor (SBR) and combined advanced oxidation process-biological treatment. A brief summary of artificial neural network and its application in wastewater treatment are also included.

### **2.1 Occurrence and Fate of Pharmaceuticals Including Antibiotics in the Environment**

Pharmaceutical compounds including antibiotics and other drugs have been detected in the aquatic environment. These compounds have been observed in surface water (Kolpin *et al.*, 2002; Anderson *et al.*, 2004; Rabiet *et al.*, 2006), ground water (Rabiet *et al.*, 2006), sewage effluents (Carballa *et al.*, 2004; Nikolaou *et al.*, 2007), and even in drinking water (Stackelberg *et al.*, 2004). Antibiotics can reach the aquatic environment through the following routes (Ikehata *et al.*, 2006):

- Pharmaceuticals industry

Pharmaceuticals industry wastewater may be treated separately or combined with municipal wastewater and then treated in sewage treatment plant.



- Human use

The antibiotics excreted in the urine and faeces reach wastewater collection system. In addition, unused surplus/expired antibiotics disposed into toilets go into the sewer (Heberer, 2002; Jones *et al.*, 2005). Hospital wastewater may be treated separately or combined with municipal wastewater and then treated in sewage treatment plant. Some of the antibiotics in wastewater are degraded completely or partially, giving rise to a mixture of parent compounds and a variety of microbial metabolites (Miao *et al.*, 2002; Soulet *et al.*, 2002; Jones *et al.*, 2005). Sewage treatment plant effluent may be discharged to surface water or subjected to groundwater recharge, so that the mixture of compounds enters the aquatic environment. In some cases, biologically treated wastewater may be treated further to produce various reclaimed waters for different purposes including potable reuse. Sorption can also take place during the sewage treatment processes and some of the compounds can be transferred to sewage sludge (Larsen *et al.*, 2004). The sewage sludge may be subjected to anaerobic or aerobic digestion, conditioning and dewatering, and subsequently landfilled, incinerated, or applied to land as a fertilizer. Antibiotic compounds in the sludge can be degraded further during the digestion, although some of them may remain intact. These compounds can seep into groundwater aquifers or be flushed by surface runoff after land application and can cause additional contamination of the aquatic environment. Therefore, the sorption of antibiotics during sewage treatment processes cannot be counted as a removal process unless the sludge is incinerated (Larsen *et al.*, 2004).

- Veterinary use

A large amount of pharmaceutical compounds, especially antibiotics, are used for veterinary therapeutics (Halling-Sørensen *et al.*, 1998). These antibiotics can reach the environment through livestock manure. Land application of livestock manure is often practised and may cause contamination of surface water and groundwater similar to the case of municipal sewage sludge disposal described above.

## 2.2 Antibiotics

Humans and animals serve as hosts to disease-causing organisms, such as bacteria, viruses, fungi and protozoa. In the past and before the development of antibiotics, simple infections often resulted in death. Over time, compounds were observed to possess antimicrobial properties and cure infections. Compounds that have been historically used to fight infections include mercury, silver, and cyanide. Alexander Fleming made the paramount discovery of antibiotics in 1928. He was trying to isolate *Staphylococcus aureus* and one dish had become contaminated. Fleming noticed that bacteria did not grow near the invading substance that he later identified as a common mold of the *Penicillium* genus. After culturing the mold and obtaining a tiny quantity of excreted material, Fleming demonstrated the antimicrobial properties of the product now known as penicillin (Shuler *et al.*, 2002).

### 2.2.1 Classes of Antibiotics

Antibiotics are classified according to their chemical structure and their mode of action to four common classes (Morese, 2003) and are presented herein.

#### 2.2.1.1 $\beta$ -lactams

$\beta$ -lactams are a class of antibiotics that include penicillin, which was discovered by Fleming. They obtain their name from their structure, which contains a  $\beta$ -ring which is a nitrogen structure that gives these compounds their antibiotic properties. The  $\beta$ -lactam antibiotics are classified into penicillin and cephalothin. Penicillins include penicillin G, which is a natural product produced by the fungus *Penicillium chrysogenum*, and amoxicillin, ampicillin and cloxacillin, which are semi-synthetic. Antimicrobial action of  $\beta$ -lactams is to interfere with the synthesis of the bacterial cell wall.  $\beta$ -lactam antibiotics bind to the enzymes that are used in the synthesis of peptidoglycan cell walls. Death of bacteria occurs during cell division as stress is placed on the weakened cell walls.  $\beta$ -lactam antibiotics are some of the most frequently used antibiotics because of their effectiveness and low toxicity.  $\beta$ -lactams contain a carboxyl group that makes them weak acids, resulting in high water solubility which improves diffusion through membranes.

#### *2.2.1.2 Sulfa drugs*

Sulfa drugs such as sulfanilamide and sulfamethoxazole are a class of synthetic antibiotics. Bacteria and humans require folic acid for nucleic acid synthesis and protein synthesis. However, bacteria synthesize their folic acid starting with para-aminobenzoic acid (PABA), while humans must ingest folic acid. Sulfa drugs are PABA analogs, which mean that they compete with PABA. If they are chosen by the cell to be used in folic acid synthesis, they block folic acid synthesis and the bacteria die. Humans are not affected by the PABA analogs because they must ingest their folic acid (Morese, 2003).

#### *2.2.1.3 Quinolones*

Examples of quinolones are ciprofloxacin (i.e., Cipro), norfloxacin, and ofloxacin. Quinolones are DNA gyrase inhibitors, which block the action of bacterial enzymes that relaxes the coils of DNA for replication, transcription, and repair (Morese, 2003).

#### *2.2.1.4 Aminoglycosides and Tetracyclines*

Aminoglycosides are products of actinomycetes, which are soil bacteria, and aminoglycosides may be utilized as natural or synthetic products. Common examples of aminoglycosides are streptomycin, kanamycin, neomycin, and gentamycin. These compounds exert their antimicrobial activity by interfering with the 70s subunit of the bacterial ribosome. Tetracyclines prevent the transfer of activated amino acids to the ribosome subsequently halting protein synthesis. Examples of tetracyclines include chlorotetracycline, also referred to as aureomycin, and oxytetracycline, i.e., terramycin (Morese, 2003).

### **2.2.2 Antibiotic Resistance**

Antibiotic resistance is the ability of microorganisms to withstand the effects of antibiotics designed to fight the infection. The development and proliferation of antibiotic resistance in bacteria is of public health concern because a patient can

develop an antibiotic resistant infection by contacting a resistant organism, or by having a resistant microbe emerge in the body as treatment with antibiotic begins (Lewis, 1995). In 1971, Huber reported non-medical uses of antibiotics were questioned and antimicrobial agents were described as potential environmental contaminants and a threat to public health (Huber, 1971). Since that time, several studies have reported the occurrence of antibiotic resistant organisms in the environment (Pillai *et al.*, 1997; Ash *et al.*, 2002). The antibiotic resistance mechanism includes drug inactivation or modification, alteration of the target site, alteration in the metabolic pathway, and reduced drug accumulation (Katzung 2004). These mechanisms are described in more details in the following paragraphs and shown in Figure 2.1.

- Drug inactivation or modification

Bacteria synthesize enzymes which terminate the antimicrobial activity of the antibiotics. For example  $\beta$ -lactamases synthesized by antibiotic resistant bacteria hydrolyze the  $\beta$ -lactam ring of penicillin thereby inactivating the antibiotic (Katzung, 2004).

- Alteration of target site

Penicillin effects on bacteria by attaching to penicillin binding proteins, which are essential for the bacterial cell wall synthesis. Bacteria develop resistance to penicillin by the overproduction of penicillin binding proteins (Katzung, 2004).

- Alteration of metabolic pathway

Bacteria are able to modify their metabolic pathways in order to evade the effect of antibiotics. For example, sulfonamides inhibit the synthesis of folic acid, and sulfonamide resistant bacteria develop alternate routes for synthesis of folic acid (Katzung, 2004).

- Reduced drug accumulation

Bacteria developing resistance to antibiotics are able to reduce the uptake of the antibiotic by either altering the permeability of the drug or by enhancing active efflux of the drug (Katzung, 2004).

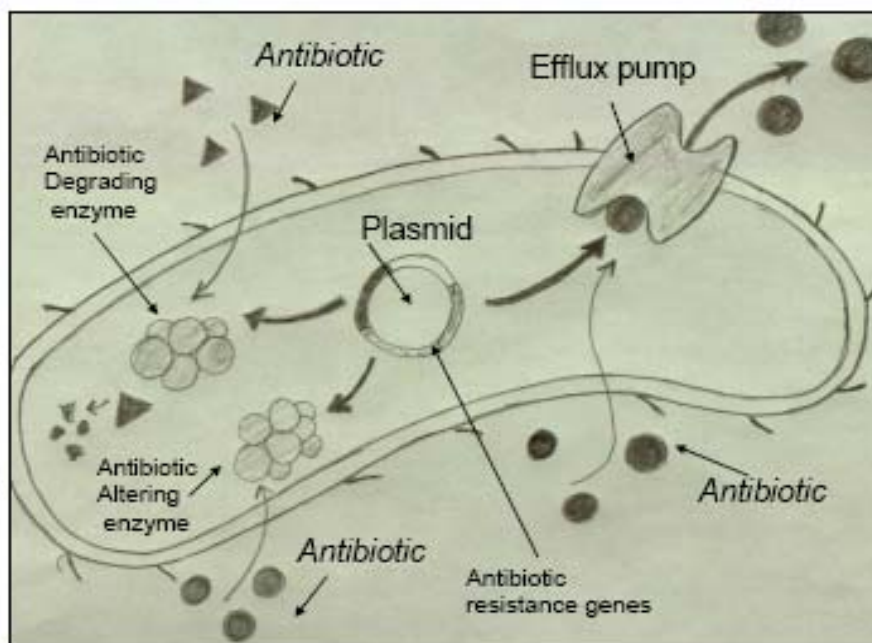


Figure 2.1 Antibiotic resistance mechanisms (Yim, 2007)

Recent studies have shown presence of antibiotic resistant bacteria in various water bodies. Gallert *et al.* (2005) observed antibiotic resistant fecal coliforms and enterococci in influent and effluent of wastewater treatment plants. Antibiotic resistance provides a survival benefit to microorganisms and makes it difficult to eliminate the infections caused by them. Infections caused by antibiotic resistant bacteria are hard to treat. Hence, physicians have to prescribe higher dosage of alternative antibiotics to cure the infections. High doses have side effects and the potential to produce more antibiotic-resistant strains of bacteria.

### 2.3 Antibiotic wastewater

Antibiotic wastewater contains a variety of non-biodegradable organic constituents and it may be high in COD and very low in BOD<sub>5</sub>. The processes involved in

antibiotic production can be classified into four categories which are (a) fermentation, (b) biological and natural extractions, (c) chemical synthesis and (d) mixing, compounding and formulating (US EPA, 2006). Therefore, the composition of antibiotic wastewater can vary widely from one effluent to another depending on the process involved. Unfortunately, there is no reported study about characterization of antibiotic wastewater in Malaysia although the number of pharmaceutical companies is more than 100 and most of these companies produce antibiotics (<http://www.eguide.com.my>). Common practice in Malaysia is to mix antibiotic wastewater with pharmaceutical wastewater to be treated biologically which could cause development of antibiotic resistant bacteria or discharge antibiotic wastewater to evaporation ponds which could contaminate the soil and ground water. Only few studies reported the characteristics of antibiotic wastewater in China (Zhang et al. 2006) and Turkey (Alaton and Dogruel, 2004; Cokgo *et al.*, 2004). Table 2.1 shows an antibiotic wastewater characteristics produced from antibiotic synthesis process. However, Table 2.2 shows an antibiotic wastewater characteristics produced from antibiotic mixing, compounding and formulating process. Comparing between the two tables, it was observed that COD and TOC concentration of antibiotic synthesis wastewater are higher than those values of antibiotic mixing, compounding and formulating wastewater. However BOD<sub>5</sub>/COD ratio of both wastewaters is very low. Hence, biological treatment may be unsuitable for antibiotic wastewater.

Table 2.1 Characteristics of antibiotic wastewater produced from antibiotic synthesis (Zhang et al. 2006)

Parameter	Value
Total COD (mg/L)	80000
TOC (mg/L)	18925
BOD <sub>5</sub> (mg/L)	0
BOD <sub>5</sub> /COD	0
Na <sup>+</sup> (mg/L)	17000
K <sup>+</sup> (mg/L)	9150
Ca <sup>2+</sup> (mg/L)	15.25
Fe <sup>3+</sup> (mg/L)	3.35
Cl <sup>-</sup> (mg/L)	23300

Table 2.2 Antibiotic wastewater characteristics produced from antibiotic mixing, compounding and formulating process

	Value (Alaton and Dogruel, 2004)	Value (Cokgo et al., 2004)
COD (mg/L)	1555	710
sCOD (mg/L)	1250	690
TOC (mg/L)	920	200
BOD <sub>5</sub> (mg/L)	0	0
BOD <sub>5</sub> /COD	0	0
pH	6.95	6.85
Alkalinity (mg CaCO <sub>3</sub> /L)	85	55
TSS (mg/L)	145	-
VSS (mg/L)	105	-
TKN (mg/L)	100	85
TP (mg/L)	8	11
Cl <sup>-</sup> (mg/L)	105	95

#### 2.4 Advanced Oxidation Processes (AOPs)

AOPs are defined by Glaze *et al.* (1987) as near ambient temperature and pressure water treatment processes which involve the generation of highly reactive radicals (especially, hydroxyl radicals (OH<sup>•</sup>)) in sufficient quantity to effect water purification. These treatment processes are considered very promising methods for the remediation of contaminated ground, surface, and wastewaters containing non-biodegradable organic pollutants. Due to the toxic characteristics of non-biodegradable organic pollutants, e.g. antibiotics, a wastewater polluted by these compounds may not suitably be treated by a conventional biological process. In addition, separation technologies such as coagulation-filtration, activated carbon adsorption and reverse osmosis only transfer the pollutants from one phase to another without destroying them. AOPs are promising methods for the remediation of contaminated wastewaters containing non-biodegradable (recalcitrant) organic pollutants.

AOPs can be classified by considering the phase where the process takes place, hence homogenous or heterogeneous processes can be differentiated. AOP classification can also consider the different possible ways of hydroxyl radical production. In this way, photochemical and non-photochemical processes can be distinguished. Table 2.3 shows classification of the most important AOPs into photochemical and non-photochemical processes.

Table 2.3 Classification of AOPs as photochemical and non-photochemical processes

Photochemical processes	Non-photochemical processes
Photo-Fenton (UV/Fe <sup>2+</sup> /H <sub>2</sub> O <sub>2</sub> )	Fenton (Fe <sup>2+</sup> /H <sub>2</sub> O <sub>2</sub> )
UV/O <sub>3</sub>	O <sub>3</sub> /H <sub>2</sub> O <sub>2</sub>
UV/H <sub>2</sub> O <sub>2</sub>	O <sub>3</sub> /Ultrasound
UV/H <sub>2</sub> O <sub>2</sub> /O <sub>3</sub>	Ozonation (O <sub>3</sub> /OH <sup>-</sup> )
Heterogeneous photocatalysis (UV/TiO <sub>2</sub> , UV/ZnO)	H <sub>2</sub> O <sub>2</sub> /Ultrasound

The present work will focus on the Fenton and photo-Fenton (homogeneous reaction phase), and the titanium dioxide (TiO<sub>2</sub>) and the zinc oxide (ZnO) photocatalysis (heterogeneous reaction phase). So, these processes are more extensively described in the following sections.

## 2.4.1 Fenton and Photo-Fenton Processes

Fenton and photo-Fenton are homogenous advanced oxidation process. The Fundamentals of these process as well as the main factors affecting the process are described below.

### 2.4.1.1 Fundamentals of Fenton Reactions

The Fenton reaction was discovered by Fenton (1894) and forty year later, the reaction mechanism was described by Haber and Weiss (1934). In the Fenton reaction, hydroxyl radicals (OH<sup>•</sup>) are generated by interaction of H<sub>2</sub>O<sub>2</sub> with ferrous salts as in Reaction (2.1).





Generated  $\text{Fe}^{3+}$  can be reduced by reaction with exceeding  $\text{H}_2\text{O}_2$  to form again ferrous ion and more radicals. This second process is called Fenton-like and it is slower than Fenton reaction as in Reactions 2.2 and 2.3 (Sychev and Isaak, 1995).



Other important dark reactions involving ferrous ion and hydrogen peroxide in absence of other interfering ions and organic substances are shown in Reactions 2.4-2.6.

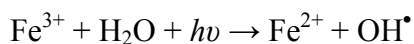


The below listed radical-radical reactions, as well as the auto-decomposition of  $\text{H}_2\text{O}_2$  are also part of the complex process as shown in Reactions 2.7- 2.10.



#### 2.4.1.2 Fundamentals of Photo-Fenton Reactions

Fenton reaction rate is strongly increased by irradiation with UV/visible light (Kiwi *et al.*, 1994; Huston and Pignatello, 1999). During the reaction,  $\text{Fe}^{3+}$  ions accumulate in the system and after  $\text{Fe}^{2+}$  are consumed, the reaction practically stops. Photochemical regeneration (Reaction 2.11) of  $\text{Fe}^{2+}$  ions by photoreduction of  $\text{Fe}^{3+}$  ions was proposed (Huston and Pignatello, 1999). The newly generated ferrous ion reacts with  $\text{H}_2\text{O}_2$  generating a second  $\text{OH}^\bullet$  radical and  $\text{Fe}^{3+}$  and the cycle continues.



Reaction 2.11

Fenton and photo-Fenton processes depend not only on  $\text{H}_2\text{O}_2$  and iron concentration, but also on other factors.

#### 2.4.1.3 Factors Affecting Fenton and Photo-Fenton Processes

The main factors affecting Fenton and photo-Fenton processes are summarized below.

- Initial  $\text{H}_2\text{O}_2$  concentration

Degradation rate of the organics increases with increase of  $\text{H}_2\text{O}_2$  concentration. This could be explained by the effect of the additionally produced  $\text{OH}^\bullet$  radicals (Zhao *et al.*, 2004). However, above a certain  $\text{H}_2\text{O}_2$  concentration, the reaction rate levels off and sometimes is negatively affected by the increase of the  $\text{H}_2\text{O}_2$ . This may be due to scavenging of  $\text{OH}^\bullet$  by  $\text{H}_2\text{O}_2$  as in Reaction 2.6 (Kavitha and Palanivelu, 2005a). Therefore,  $\text{H}_2\text{O}_2$  should be added at an optimal concentration to achieve the best degradation. This optimal  $\text{H}_2\text{O}_2$  concentration depends on the nature and concentration of the pollutants and the iron concentration.

- Initial  $\text{Fe}^{2+}$  concentration

Degradation rate of the organics increases with increase of iron concentration; however, above a certain iron concentration the efficiency decreases. This may be due to the recombination of  $\text{OH}^\bullet$  radicals or increase of turbidity that hinders the absorption of the UV light required for the photo-Fenton process.  $\text{Fe}^{2+}$  reacts with  $\text{OH}^\bullet$  radicals as a scavenger (Reaction 2.5). It is desirable for  $\text{Fe}^{2+}$  or  $\text{Fe}^{3+}$  to be as small as possible, so recombination can be avoided and iron complex production reduced (Kwon *et al.*, 1999).

- pH value

The Fenton and photo-Fenton processes have a maximum activity at about pH 3. The pH value influences the generation of  $\text{OH}^\bullet$  radicals and thus the oxidation efficiency

of the process. At higher pH, generation of  $\text{OH}^\bullet$  radicals decreases and this is due to the decrease of dissolved iron as well as dissociation and auto-decomposition of  $\text{H}_2\text{O}_2$  (Zhao *et al.*, 2004; Tamimi *et al.*, 2008). At low pH, oxidation efficiency is lower due to solvation of hydrogen peroxide in presence of high concentration of  $\text{H}^+$  to form stable oxonium ion ( $\text{H}_3\text{O}_2^+$ ), thus reducing substantially its reactivity with ferrous ions (Kwon *et al.*, 1999).

- Temperature

Fenton and photo-Fenton processes are generally conducted at ambient temperature. However, temperature is a key parameter that has to be taken into account because thermal Fenton process is accelerated with increasing temperature (Arasasinghan *et al.*, 1989). But high temperature (above 40 °C) may decompose hydrogen peroxide to oxygen and water as in Reaction 2.7 (Nesheiwat and Swanson 2000).

#### 2.4.1.4 Application of Fenton and Photo-Fenton Processes in Wastewater Treatment

The degradation of organic pollutants present in wastewater by Fenton and photo-Fenton processes is a fast growing field of applied research. Bench scale studies have been conducted for degradation of many pollutants in wastewater using Fenton and photo-Fenton processes. Degradation of pollutants such as, dyes, pesticides, phenolic compounds and pharmaceutical compounds as well as landfill leachates have been evaluated. Table 2.4 summarizes the treatment conditions and the efficiency of the treatment system.

Large scale photo-Fenton process was applied for treatment of an industrial wastewater contaminated with xylidines (toxic intermediates of pharmaceutical and dyes and pigments industries) in a 500 L pilot plant (Oliveros *et al.*, 1997). Moreover, full scale process was applied for treatment of textile effluents treatment (Vandevivere *et al.*, 1998).

Table 2.4 Selected review of Fenton and photo-Fenton treatment with related pollutant

Pollutant	Light source	H <sub>2</sub> O <sub>2</sub>	Fe <sup>2+</sup> /Fe <sup>3+</sup>	pH	Initial concentration	Removal	Reference
Active Yellow	-	17 mg/L	13.9 mg/L	3	20 -160 mg/L	95- 97%	Solozhenko <i>et al.</i> (1995)
4-chlorophenol	-	45 mM	0.75 mM	2.8	3 mM	90%	Krutzler <i>et al.</i> (1999)
Dichloroacetic acid 2,4-dichlorophenol	Solar	6 mM	0.2-1.5 mM	2.5	1.0 mM	90%	Noguiera <i>et al.</i> (2002)
Nitrobenzene	15 W Hg lamp (low pressure)	21.3 mM	0.54-2.14 mM	2.7-3	0.82 mM	90%	Rodríguez <i>et al.</i> (2002)
Conventional cellulose bleaching effluent	Solar light (0.105 w/cm-2)	103-104 mg/L	50-450 mg/L	3	Colour 649 mg/L	90%	Torrades <i>et al.</i> (2004)
Pharmaceutical wastewater	-	0.3 M – 3 M	0.3 M-3 M	4	COD 362000 mg/L	90%	Martinez <i>et al.</i> (2003)
Reactive Yellow 84 Reactive Red 120	Heroeus UV immerse lamp (15W) solar	5 mM	0.25 mM	3	100 mg/L	98% 99%	Mariana <i>et al.</i> (2003)

Table 2.4 Selected review of Fenton and photo-Fenton treatment with related pollutant (continued)

Pollutant	Light source	H <sub>2</sub> O <sub>2</sub>	Fe <sup>2+</sup> /Fe <sup>3+</sup>	pH	Initial concentration	Removal	Reference
Penicillin wastewater	low pressure mercury arc lamp	20 mM	1 mM	3	COD 1390 mg/L	56%	Alaton and Dogruel (2004)
4-chlorophenol (4-CP)	Solar	10 mM	1.0 mM Ferrioxalate	2.5	1.0 mM	70%	Nogueira <i>et al.</i> (2005)
Diclofenac	Solar	200-400 mg/L	0.03-0.75 mM	2.8	50 mg/L	100%	Estrada <i>et al.</i> (2005)
Reactive orange	Medium pressure mercury lamp	10 mM	0.1 mM	3	0.05 mM	94%	Selvam <i>et al.</i> (2005)
Phenol (C <sub>6</sub> H <sub>5</sub> OH)	Solarbox Reactor 90 cm <sup>3</sup>	21.99 mM	1.07 mM Fe <sup>3+</sup>	3	1.14 mM/L	98%	Rodriguez <i>et al.</i> (2005)
Leachate	-	50 mM	75 mM	2.5	COD 1000 mg/L	61.3%	Zhang <i>et al.</i> (2005)
Alachlor 2-chloro-2,6-diethyl-N methacymethyl acetanilide	Xenon lamp, 990 W, (320-410 nm)	4.0 mM	0.1 mM	5	0.037 mM	85%	Hideyuki <i>et al.</i> (2005)
2-nitrophenol 4-nitrophenol 2, 4-dinitrophenol	Hg lamp, 150 W, 254 nm	17.3 mM	0.45 mM	3	1.43 mM	>92%	Kavitha <i>et al.</i> (2005b)

Table 2.4 Selected review of Fenton and photo-Fenton treatment with related pollutant (continued)

Pollutants	Light source	H <sub>2</sub> O <sub>2</sub>	Fe <sup>2+</sup> /Fe <sup>3+</sup>	pH	Initial concentration	Removal	Reference
Acid Orange 24	Solar (300-650 nm)	5.2 mM 7.8 mM	0.0716 mM 0.1 mM 0.143 mM	5.5	0.446 mM	85%	Chacon <i>et al.</i> (2006)
Pharmaceutical wastewater	-	300 mM	2 mM	3	COD range 900–7000 mg/L	45–65%	Tekin <i>et al.</i> (2006)
Methomyl	High pressure mercury lamp	0.5 mM	1 mM	3	0.123 mM	45% TOC	Tamimi <i>et al.</i> (2008)
Acid Blue 193	150 W black light bulb lamp	35 mM	1.5 mM Fe <sup>3+</sup>	3	COD ≤ 2 00 mg/L	78%	Alaton <i>et al.</i> (2009)

#### 2.4.1.5 Benefits and Limitations of Fenton and Photo-Fenton Processes

Fenton and photo-Fenton are considered the most promising processes for treatment of highly contaminated wastewater (Bossmann *et al.*, 1998). They are considered attractive oxidative processes since they do not require either expensive reagents or sophisticated instrumentation for pollutants degradation (Andreozzi *et al.*, 1999). Hydrogen peroxide is easy to handle, reasonably priced and environmentally benign compared with other bulk oxidants, whereas iron is non toxic and safe (Chen and Pignatello, 1997; Pignatello *et al.*, 2006). At the same time, the Fenton reagent is considered a clean reagent since the dissolved iron can be removed by precipitation at high pH (Huston and Pignatello, 1999; Malato *et al.*, 2003). Moreover, if the employed iron amount is small, it could remain dissolved without affecting the quality of the water. Likewise, residual hydrogen peroxide readily decomposes to O<sub>2</sub> and H<sub>2</sub>O as in Reaction 2.7 (Huston and Pignatello, 1999; Pignatello *et al.*, 2006). From an economic and technical point of view, photoassisted Fenton process (photo-Fenton) may also surpass most of the AOPs because of the possibility of using photons with wavelengths from the near-UV up to visible (~ 550 nm) (Safarzadeh-Amiri *et al.*, 1996; Bauer and Fallman, 1997).

The main drawback of the processes is high operational cost derived from chemical reagent consumption compared to that of biological treatment, instability of the reagent mixture, the necessity of pH adjustment, and the possible iron oxide sludge generation and subsequent disposal (Pignatello *et al.*, 2006). However, their use as a pretreatment step for the enhancement of the biodegradability of recalcitrant wastewater can be justified when the intermediates resulting from the reaction can be readily degraded by microorganisms. Therefore, combination of AOP with inexpensive biological processes appears very promising from an economic point of view.

#### 2.4.2 Heterogeneous Photocatalysis

Heterogeneous photocatalysis is a technology based on the irradiation of a catalyst, usually a semiconductor, which may be photoexcited to form electron-donor sites (reducing sites) and electron-acceptor sites (oxidising sites), providing great scope as

redox reagents. The bands of interest in photocatalysis are the occupied valence band (VB) and the unoccupied conduction band (CB), separated by an energy distance referred to as the band gap ( $E_{bg}$ ). When the semiconductor is illuminated with light of greater energy than that of the band gap, an electron is promoted from the VB to the CB leaving a positive hole in the valence band as illustrated in Figure 2.2 (Cardona, 2001). After separation, the electron ( $e^-$ ) and hole ( $h^+$ ) pair may recombine generating heat or can become involved in electron transfer reactions with other species in solution.

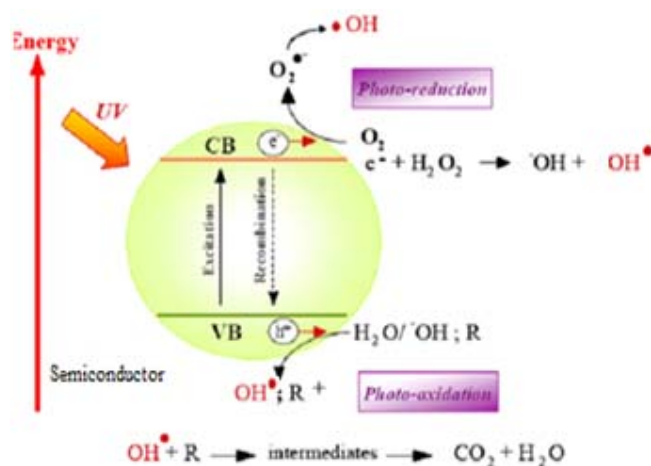


Figure 2.2 Mechanism of semiconductor photocatalysis.

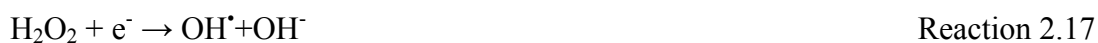
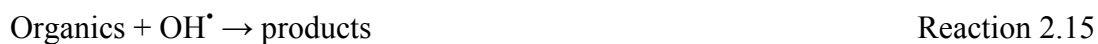
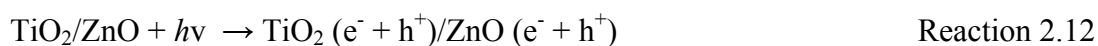
Among the semiconductors, titanium dioxide ( $\text{TiO}_2$ ) has proven to be the most suitable for widespread environmental applications.  $\text{TiO}_2$  is biologically and chemically inert; it is stable to photo and chemical corrosion, and inexpensive. Furthermore,  $\text{TiO}_2$  is of special interest since it can use natural (solar) UV radiation. This is because  $\text{TiO}_2$  has an appropriate energetic separation between its valence and conduction bands, which can be surpassed by the energy of a solar photon. The VB and CB energies of the  $\text{TiO}_2$  are estimated to be +3.1 and  $-0.1$  eV, respectively, which means that its band gap is 3.2 eV and therefore absorbs in the near UV region ( $\lambda < 387$  nm).  $\text{ZnO}$  has been reported to be a suitable alternative to  $\text{TiO}_2$  since its photodegradation mechanism is similar to that of  $\text{TiO}_2$  (Daneshvar *et al.*, 2004).  $\text{ZnO}$  can absorb a larger fraction of the solar spectrum than  $\text{TiO}_2$ , and hence  $\text{ZnO}$



photocatalyst is considered more suitable for photocatalytic degradation in the presence of sunlight (Sakthivel *et al.*, 2003).

#### 2.4.2.1 Mechanism of the TiO<sub>2</sub> and ZnO Photocatalysed Degradation

Reaction mechanisms of photocatalytic processes have been discussed in the literature (Hoffmann *et al.*, 1995; Mills and Le Hunte, 1997; Bhatkhande *et al.*, 2002; Konstantinou and Albanis, 2004; Kabra *et al.*, 2004; Sadik *et al.*, 2007). When a semiconductor such as TiO<sub>2</sub> or ZnO is illuminated by photons having an energy level that exceeds their band gap ( $h\nu > E_{bg} = 3.2$  eV in case of TiO<sub>2</sub> and ZnO) excite electrons ( $e^-$ ) from the valence band to the conduction band and holes ( $h^+$ ) are produced in the valence band (Reaction 2-12). The photogenerated valence band holes react with either water (H<sub>2</sub>O) or hydroxyl ions (OH<sup>-</sup>) adsorbed on the catalyst surface to generate OH<sup>•</sup> radicals which are strong oxidant (Reaction 2-13 and 2-14). The hydroxyl radical reacts readily with surface adsorbed organic molecules, either by electron or hydrogen atom abstraction, forming organic radical cations, or by addition reactions to unsaturated bonds (Sadik *et al.*, 2007) (Reaction 2-15). Since the reaction of the holes on the particle interface is faster than electrons, the particles under illumination contain an excess of electrons. Removal of these excess of electrons is necessary to complete the oxidation reaction, by preventing the recombination of electrons with holes. The most easily available electron acceptor is molecular oxygen and in presence of oxygen the predominant reaction of electrons is that with O<sub>2</sub> to form superoxide ions ( $O_2^{\cdot-}$ ) as in Reaction (2-16). In acidic condition, superoxide ion combines with proton to form a hydroperoxide radical and it reacts with conduction band electron to form hydroperoxide ion. The hydroperoxide ion reacts with proton to form hydrogen peroxide. Cleavage of hydrogen peroxide by the conduction band electrons yields further hydroxyl radicals and hydroxyl ions (Reaction 2-17). The hydroxyl ions can then react with the valence band holes to form additional hydroxyl radicals. Recombination of the photogenerated electrons and holes may occur and indeed it has been suggested that preadsorption of substrate (organic substance) onto the photocatalyst is a prerequisite for highly efficient degradation.



#### 2.4.2.2 Main Factors Affecting Photocatalytic Process

The main factors affecting photocatalysis reactions are described below.

- Catalyst concentration

The reaction rate is affected by the catalyst concentration; however, above a certain concentration value the reaction rate becomes independent of catalyst concentration. This limit depends on the nature of the pollutant and on the geometry and working conditions of the photoreactor corresponding to the maximum catalyst concentration in which all the particles are totally illuminated. Decrease of reaction rate at higher catalyst concentration may be due to decrease of light penetration or increase of light scattering (Kansal *et al.*, 2007). Agglomeration and sedimentation of catalyst under high catalyst concentration may take place and available catalyst surface for photon absorption may decrease (So *et al.*, 2002; San *et al.*, 2007).

- Temperature and pH

Experimental studies on dependence of the reaction rate of degradation of organic compounds on temperature have been conducted. Many researchers established experimental evidence for the dependence of photocatalytic activity on temperature (Tunesi *et al.*, 1987; Fu *et al.*, 1996; Muradov *et al.*, 1996; Evgenidou *et al.*, 2005). Generally, increase in temperature enhances recombination of charge carriers and

desorption process of adsorbed reactant species, resulting in decrease of photocatalytic activity.

The pH of the solution significantly affects the particle size and the surface charge. For TiO<sub>2</sub>, as pH increases overall surface charge of TiO<sub>2</sub> changes from positive ( $pK_{a1} = 2.6$ ) to negative ( $pK_{a2} = 9.0$ ) with zero point charge being at pH 6.4 (Feitz *et al.*, 1999). For ZnO, the zero point charge is  $9.0 \pm 0.3$  and hence the ZnO surface is positively charged at  $pH < 9$  and is negatively charged at  $pH > 9$  (Akyol *et al.*, 2004).

- Nature of the photocatalyst

A very important parameter influencing the performance of photocatalyst in photocatalytic oxidation is the surface morphology (Dinga *et al.*, 2005). Numerous forms of photocatalyst have been synthesized by different methods to arrive at a photocatalyst exhibiting desirable physical properties, activity and stability for photocatalytic application (Gao and Liu, 2005). Smaller particle size is reported to give higher degradation of organic compounds (Maira *et al.*, 2001).

- Light intensity

Photocatalytic reaction rate depends largely on the radiation absorption of the photocatalyst (Curcó *et al.*, 2002). The increase of degradation rate with increase of light intensity during photocatalytic degradation have been reported (Qamar *et al.*, 2006).

- Inorganic ions

Photocatalytic process could be inhibited in the presence of anions. Some anions commonly found in natural or polluted waters (e.g. chloride, bromide, sulphate and phosphate) have an inhibiting effect on the photocatalytic process if they are bound to photocatalyst or close to its surface (Herrmann *et al.*, 1993; Pelizzetti, 1995; Wang *et al.*, 2000). Significant inhibition in the degradation rate of different compounds has been observed in acidic condition, whereas in alkaline condition repulsive forces

between the catalyst and the ions are developed and hence no inhibition effect (Wang *et al.*, 2000).

#### *2.4.2.3 Application of TiO<sub>2</sub> and ZnO Photocatalys for Degradation of Organic Pollutants*

Photocatalytic processes for polluted water treatment have received a lot of attention since these processes exhibited the ability to convert various kinds of toxic and hazardous organic pollutants to non-toxic intermediates or even complete mineralization of the pollutants. Degradation of organic pollutants such as dyes, pesticides, phenolic and pharmaceutical compounds, and other harmful pollutants by TiO<sub>2</sub> photocatalysis and ZnO photocatalysis have been reported. Table 2.5 highlights on experiment and findings on treatment of different pollutants using TiO<sub>2</sub> photocatalysis and ZnO photocatalysis.

Table 2.5 Selected review of TiO<sub>2</sub> and ZnO photocatalysis with related pollutants

Pollutant	Highlight on experiment and findings	Reference
Phenol	TiO <sub>2</sub> does not favour degradation at concentrations higher than 100 ppm.	Pelizzetti and Minero (1993)
4-chlorophenol	Mineralization studied with different samples of TiO <sub>2</sub> . Degussa P-25 proved more effective photocatalyst. Both solar pilot plant and laboratory experiment indicated apparent first order kinetics. Fewer intermediates and faster TOC removal were observed in the solar pilot plant which worked with smaller optimum titania concentration.	Guillard <i>et al.</i> (1999)
Isoproturon	Degradation rate over Degussa TiO <sub>2</sub> was faster than Hombicat 100 and was increased by the addition of electron acceptors.	Vorontsov <i>et al.</i> (2000)
Mixture of 4-chlorophenol, 2,4-dichlorophenol, 2,4,6-trichlorophenol and pentachlorophenol	Sequential photochemical-biological degradation proved useful. There was no removal of chlorophenol with H <sub>2</sub> O <sub>2</sub> or TiO <sub>2</sub> alone.	Mrowetz <i>et al.</i> (2003)
Acid Brown 14	Optimum operation conditions to achieve complete decoloration were pH 10 and ZnO 2.5 g/L	Sakthivel <i>et al.</i> (2003)
Fenamidone	Coated optical fibre photoreactor was used in the study. Slow photocatalytic degradation of fenamidone over TiO <sub>2</sub> was observed. COO <sup>-</sup> and SO <sub>4</sub> <sup>2-</sup> were identified in the reactor.	Haque <i>et al.</i> (2003)

Table 2.5 Selected review of TiO<sub>2</sub> and ZnO photocatalysis with related pollutant (continued)

Pollutant	Highlight on experiment and findings	Reference
Acid Orange 8, Acid Red 1	Sonophotocatalytic degradation was faster than photocatalytic degradation followed by sonolysis.	Qamar <i>et al.</i> (2004)
Sulfadimethoxine	Complete conversion of 15 mg/L sulfadimethoxine in 30 min.	Calza <i>et al.</i> (2004)
Methylene Blue, Methyl Orange, Indigo Carmine and Chicago Sky Blue	TiO <sub>2</sub> photocatalyst was immobilised on glass and used for dye removal. Chicago sky blue was the most resistant to the photodegradation. Methyl orange with t <sub>1/2</sub> 85.6 min was removed faster.	Bertelli and Selli, (2004)
Dichlorvos	Optimum operation conditions to achieve complete destruction were observed to be : pH 7.2, ZnO 0.5 g/L and 120 min irradiation time. Addition of the oxidants such as H <sub>2</sub> O <sub>2</sub> and K <sub>2</sub> S <sub>2</sub> O <sub>8</sub> enhanced the mineralization.	Evgenidou <i>et al.</i> (2005)
Acridine Orange, Ethidium Bromide	Degussa P-25 showed superior photocatalytic activity than PC300. Degradation rate was affected by inorganic additives.	Zainal <i>et al.</i> (2005)
Tetracycline	Complete degradation of 50 mg/L tetracycline in 2 hr; 90% TOC removal in 6 hr.	Addamo <i>et al.</i> (2005)

Table 2.5 Selected review of TiO<sub>2</sub> and ZnO photocatalysis with related pollutant (continued)

Pollutant	Highlight on experiment and findings	Reference
4-fluorophenol	TiO <sub>2</sub> -P25 was found to be more efficient than ZnO under the study conditions. The efficiency of anion and cation oxidation are respectively in the following order IO <sub>4</sub> <sup>-</sup> > BrO <sub>3</sub> <sup>-</sup> > S <sub>2</sub> O <sub>8</sub> <sup>2-</sup> > H <sub>2</sub> O <sub>2</sub> > ClO <sub>3</sub> <sup>-</sup> and Mg <sup>2+</sup> > Fe <sup>3+</sup> > Fe <sup>2+</sup> > Cu <sup>2+</sup> .	Danion <i>et al.</i> (2006)
Lincomycin	Complete conversion of 50 mg/L lincomycin in 2 hr at pH 6; 60% TOC removal in 5 hr.	Paola <i>et al.</i> (2006)
Acid Yellow 23	Optimum operation conditions to achieve complete decoloration were pH 10.9 and ZnO 0.75 g/L.	Behnajady <i>et al.</i> (2006)
Methyl Orange	Photocatalytic activity of ZnO is greater in the presence of solar light as compared to UV light. Optimum operation conditions to achieve maximum decoloration (>95%) were pH 9 and ZnO 1 g/L	Kansal <i>et al.</i> (2007)
Acetone	Vibrofluidized and multiple fixed bed photoreactors were compared. The comparison was based on the quantum efficiency for the photooxidation of acetone using TiO <sub>2</sub> (Hombicat UV 100). Vibrofluidized-bed showed higher activity for photooxidation. Application of ultrasound did not influence the rate of photooxidation of acetone.	Dillert <i>et al.</i> (2007)

Table 2.5 Selected review of TiO<sub>2</sub> and ZnO photocatalysis with related pollutant (continued)

Pollutant	Highlights on experiment and finding	Reference
2-chloroaniline	Slower degradation resulted at low pH in the UV/TiO <sub>2</sub> /H <sub>2</sub> O <sub>2</sub> system.	Chu <i>et al.</i> (2007)
2,4-dichlorophenol	Two kinetic models for photocatalytic degradation of 2,4-dichlorophenol over Degussa P-25 TiO <sub>2</sub> suspension were proposed based on the influence of different variables (pH, radiation and TiO <sub>2</sub> concentration).	Essam <i>et al.</i> (2007)
Rhodamine 6G	Photocatalytic activity of ZnO is greater in the presence of solar light as compared to UV light. Optimum operation conditions to achieve maximum decoloration (>95%) were pH 10 and ZnO 0.5 g/L.	Kansal <i>et al.</i> (2007)
Chrysoidine Y	Degussa P-25 was found to be more effective than ZnO in mineralization of the dye at laboratory scale.	Faisal <i>et al.</i> (2007)
Lignin	Optimum operation conditions to achieve maximum degradation were pH 11 and ZnO 1 g/L	Kansal <i>et al.</i> (2008)
Salicylic acid	Optimum operation conditions for complete mineralization were pH 7 and ZnO 2 g/L	Rao <i>et al.</i> (2009)



## **2.5 Antibiotic Wastewater Treatment and Antibiotic Degradation by Advanced Oxidation Processes**

Several studies on degradation of antibiotics by advanced oxidation processes (AOPs) have been reported. As shown in Table 2.6, applied processes were ozonation, Fenton and photo-Fenton. However, there have been few studies on degradation of antibiotics using heterogeneous advanced oxidation process such as TiO<sub>2</sub> photocatalysis. No previous study on degradation of amoxicillin, ampicillin and cloxacillin in aqueous solution has been reported, except for amoxicillin by Alaton and Dogruel (2004) and Trovó *et al.* (2008). As concentration of antibiotics in antibiotic wastewater may vary from day to day or from batch to batch, some authors considered low antibiotics concentration less than 100 mg/L (Paola *et al.*, 2004; Addamo *et al.*, 2005; Calza *et al.*, 2004; Trovó *et al.*, 2008) while others considered high antibiotics concentration (Alaton and Dogruel, 2004; González *et al.*, 2007).

Table 2.6 Antibiotic wastewater treatment and degradation of antibiotic by AOPs

Antibiotic	Applied process	Influent characteristics	Main findings	Reference
Sulfachlorpyridazine	Ozonation	Sulfachlorpyridazine 50 mg/L	Complete degradation of sulfachlorpyridazine at pH 7.5 in 1.5 min	Adams <i>et al.</i> (2002)
Sulfadimethoxine	Ozonation	Sulfadimethoxine 50 mg/L	Complete degradation of sulfadimethoxine at pH 7.5 in 1.5 min	Adams <i>et al.</i> (2002)
Ceftriaxone	Ozonation	COD 450 mg/L	53%, 74% and 82% COD removal at pH 3, 7, 11	Balcioglu and Ötker (2003)
Enrofloxacin	Ozonation	COD 450 mg/L, TOC 165 mg/L	88% COD removal, 50% TOC removal BOD <sub>5</sub> /COD improved from 0.07 to 0.38	Balcioglu and Ötker (2003)
Ceftriaxone	O <sub>3</sub> /H <sub>2</sub> O <sub>2</sub>	COD 450 mg/L	90% COD removal at pH 7	Balcioglu and Ötker (2003)
	O <sub>3</sub> /H <sub>2</sub> O <sub>2</sub>	COD 830 mg/L	72% COD removal at pH 10.5	Alaton <i>et al.</i> (2004)
Penicillin formulation wash water	Ozonation	Amoxicillin 400 mg/L, COD 1395 mg/L, TOC 920 mg/L	Complete degradation of amoxicillin, 86% COD removal, 40% TOC removal, BOD <sub>5</sub> /COD improved from 0 to 0.08 at pH 11.5	Alaton and Dogruel (2004)
	H <sub>2</sub> O <sub>2</sub> /UV	COD 1395 mg/L, TOC 920 mg/L	22% COD removal, 6% TOC removal, BOD <sub>5</sub> /COD improved from 0 to 0.07 at pH 7, H <sub>2</sub> O <sub>2</sub> 30 mM	Alaton and Dogruel (2004)
	Fenton	COD 1395 mg/L, TOC 920 mg/L	61% COD removal, 33% TOC removal, BOD <sub>5</sub> /COD improved from 0 to 0.1 at pH 3, Fe <sup>2+</sup> 1 mM, H <sub>2</sub> O <sub>2</sub> 20 mM	Alaton and Dogruel (2004)

Table 2.6 Antibiotic wastewater treatment and degradation of antibiotic by AOPs (continued)

Antibiotic	Applied process	Influent characteristics	Main findings	Reference
Penicillin formulation wash water	Fenton-like	COD 1395 mg/L, TOC 920 mg/L	46% COD removal, 18% TOC removal, BOD <sub>5</sub> /COD improved from 0 to 0.08 at pH 3, Fe <sup>3+</sup> 1 mM and H <sub>2</sub> O <sub>2</sub> 20 mM	Alaton and Dogruel (2004)
	Photolysis	COD 1395 mg/L, TOC 920 mg/L	No BOD <sub>5</sub> increase	Alaton and Dogruel (2004)
Sultamicillin	Ozonation	COD 710 mg/L, TOC 200 mg/L	33% COD removal, 24% TOC removal BOD <sub>5</sub> /COD improved from 0.02 to 0.27	Cokgor <i>et al.</i> (2004)
Sulfadimethoxine	UV/TiO <sub>2</sub>	Sulfadiazine 15 mg/L	Complete degradation of sulfadimethoxine in 30 min	Calza <i>et al.</i> (2004)
Tetracycline	UV/TiO <sub>2</sub>	Tetracycline 50 mg/L	Complete degradation of 50 mg/L tetracycline in 2 hr, 90% TOC removal in 6 hr	Paola <i>et al.</i> (2004)
Lincomycin	UV/TiO <sub>2</sub>	Lincomycin 50 mg/L	Complete degradation of lincomycin in 2 h at pH 6, 60% TOC removal in 5 hr	Addamo <i>et al.</i> (2005)
Penicillin G	Ozonation	COD 600 mg/L, TOC 226 mg/L	50% COD removal, TOC removal 50% at pH 12	Alaton and Caglayan (2005)
Penicillin G	Photo-Fenton-like	COD 600 mg/L, TOC 226 mg/L	56% COD removal, 42% TOC removal, BOD <sub>5</sub> /COD improved from 0.25 to 0.45 at pH 3	Alaton and Gurses (2004)

Table 2.6 Antibiotic wastewater treatment and degradation of antibiotic by AOPs (continued)

Antibiotic	Applied process	Influent characteristics	Main findings	Reference
Wastewater from synthesizing of amoxicillin	Extraction (EX), Fenton oxidation (FO)	COD 80000 mg/L, TOC 18925 mg/L	TOC removal 50.6% and 37.8% in the EX and FO at 10 g/l FeSO <sub>4</sub> and 2 g/l H <sub>2</sub> O <sub>2</sub>	Zhang <i>et al.</i> (2006)
Tetracycline	Photo-Fenton	Tetracycline 24 mg/L	Complete degradation of tetracycline in 1 min	Bautitz and Nogueira (2007)
Sulfamethoxazole	Photo-Fenton	Sulfamethoxazole 600 mg/L	Complete degradation of sulfamethoxazole, BOD <sub>5</sub> /COD improved from 0 to 0.3 at pH 2.8, 10 mg/L Fe <sup>2+</sup> and 300 mg/L H <sub>2</sub> O <sub>2</sub>	González <i>et al.</i> (2007)
Amoxicillin	Photo-Fenton	Amoxicillin 43 mg/L	Complete degradation of amoxicillin in both distilled water and STP effluent in 2 min at pH 2.5, 0.20 mM ferric nitrate and 2.0 mM H <sub>2</sub> O <sub>2</sub>	Trovó <i>et al.</i> (2008)

## **2.6 Biological Wastewater Treatment**

Biological treatment is the most common, economically and environmentally attractive method used for wastewater remediation in comparison with other physical and chemical treatment (Chiron *et al.*, 2000). The main categories of biological wastewater treatment are aerobic and anaerobic treatment. The aerobic treatment is performed in the presence of oxygen, whereas the anaerobic treatment is executed in absence of oxygen. Aerobic biological wastewater treatment is most common because it is rapid, easily carried out and effective in degradation of majority of the pollutants (Stephenson and Blackburn, 1998).

### **2.6.1 Principle of Aerobic Biological Wastewater Treatment**

Aerobic biological wastewater treatment is based on the capability of bacteria to assimilate biodegradable organic matter in presence of oxygen. During aerobic degradation, organic compounds are oxidized to carbon dioxide and oxygen is reduced to water (Zitomer and Speece, 1993). The activated sludge process is one of the most widely used biological treatment processes in the world. The process involves a flocculent suspended growth culture in an aerobic reactor and some means of separation of the biomass and other suspended solids from the treated wastewater. There are several conventional activated sludge processes, and some modifications have been used for such a long time that they are accepted worldwide. The list of these processes and process modifications can be found elsewhere (Metcalf and Eddy, 2003).

### **2.6.2 Sequencing Batch Reactor (SBR)**

A sequencing batch reactor is a variant of the activated sludge process and consists of a batch reactor that operates under a series of periods which constitutes a cycle. The cycle generally consists of fill, react, settle, decant and idle periods. The use of these periods allows a single reactor to act as a train of reactors and a clarifier. By manipulating these periods within a single cycle, an SBR can accomplish most of what a continuous flow activated sludge plant can accomplish with several reactors, each operating under a different condition (Orhon *et al.*, 1986).

### *2.6.2.1 SBR Operation*

The SBR uses the fill and draw principal in which unit processes occur sequentially on a cyclical basis. The various stages in the SBR cycle are shown in Figure 2.3 and are the following.

#### Stage 1: Filling

During this stage the SBR tank is filled with the influent wastewater. In order to maintain suitable F/M (food to microorganism) ratio, the wastewater should be admitted into the tank in a rapid and controlled manner.

#### Stage 2: Reaction/Aeration

This stage involves the utilization of substrate by the microorganisms. The length of the aeration period depends on the strength of the wastewater and the degree of nitrification (conversion of ammonia to a less toxic form of nitrate or nitrite) provided for in the treatment.

#### Stage 3: Settling

During this stage, aeration is stopped and the sludge settles leaving clear treated effluent above the sludge blanket. Duration of settling varies from 45 to 60 min depending on the number of cycles per day.

#### Stage 4: Decanting

At this stage of the process, effluent is removed from the tank through the decanter, without disturbing the settled sludge.

#### Stage 5: Idle

The SBR tank remains idle until a batch of wastewater accumulates and excess sludge can be removed in this period.

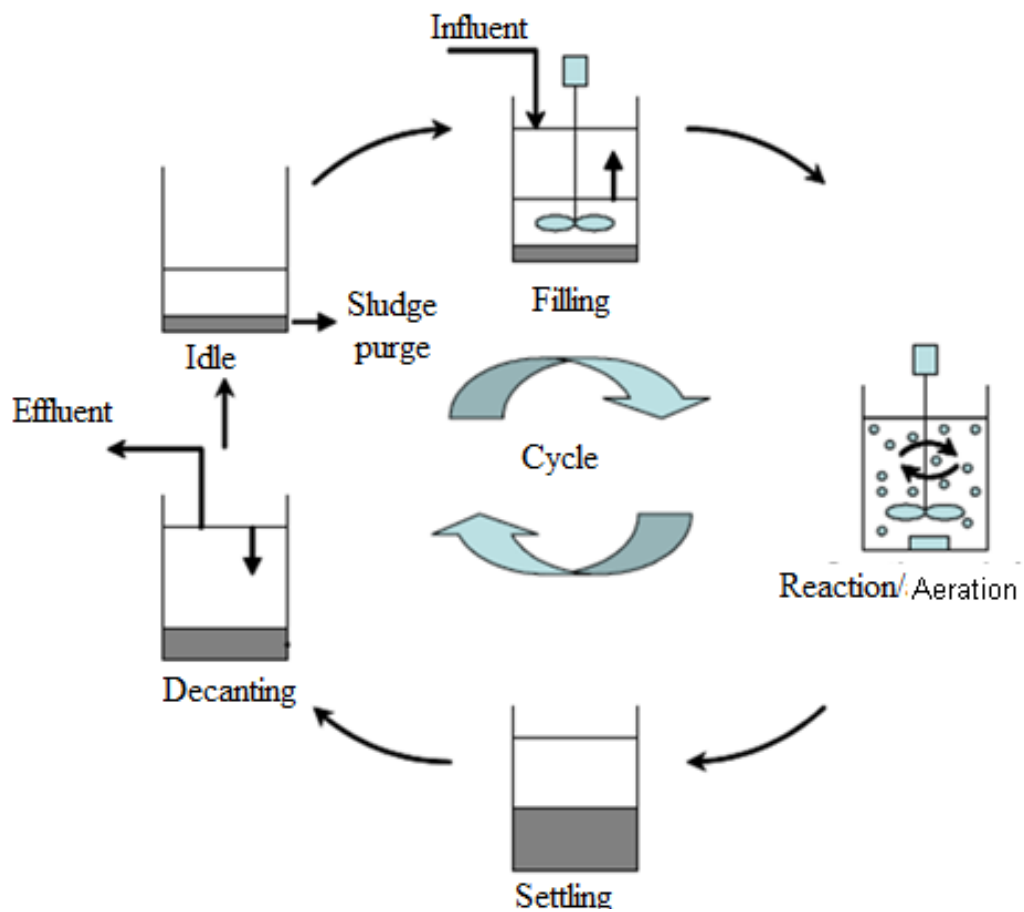


Figure 2.3 Various stages in the SBR cycle

#### 2.6.2.2 Advantages of SBR

The advantages of using an SBR are the following (Edgerton *et al.*, 2000):

- The effluent can be held in the reactor until it is treated and this can minimize the deterioration of the effluent quality which sometimes is associated with influent spikes.
- Biomass will not be washed out from the SBR because of flow surges.
- Simplification of SBR compared to activated sludge systems negates the need for return activated sludge to be pumped from the clarifier.
- Settling occurs when there is no inflow or outflow and therefore, no short-circuiting of the clarifier can occur.

- The nature of an SBR leaves a lot of room for changes to the system.

## **2.7 Combined Advanced Oxidation Process-Biological Treatment**

Several advanced oxidation processes (AOPs) have been carried out to mineralize many recalcitrant organic pollutants. Many examples of recalcitrant wastewater have been proven to lose their toxicity as well as increase their biodegradability upon a chemical treatment before total mineralization has been achieved (Scott and Ollis, 1995). However, cost associated with these processes is the major drawback for application in wastewater treatment.

Combined AOP and biological processes have received a lot of attention in recent years as a promising alternative treatment for recalcitrant wastewater. The main objective of this is to modify the structure of pollutants by transforming them into less toxic and easily biodegradable intermediates by means of an AOP. Then, subsequent mineralization can be achieved in shorter time in the biological treatment (Sarria *et al.*, 2002). Focusing on this strategy, Sarria *et al.* (2002) proposed a general scheme that can be used to plan a combined AOP and biological process for wastewater treatment as depicted in Figure 2.4.



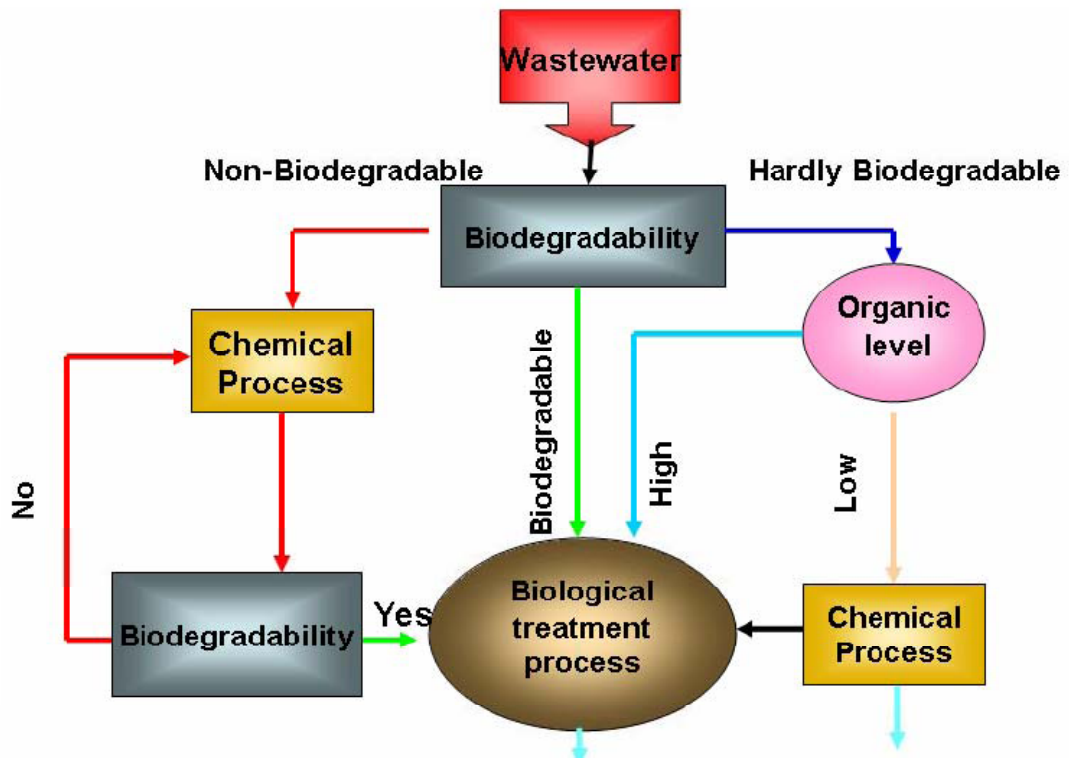


Figure 2.4 General strategy for wastewater treatment

Some practical aspects should be considered for a combined chemical and biological process. Chemical oxidants and the bioculture can not be mixed because the chemical oxidants can cause damaging effects to the microorganisms. Adjustment of pH to approximately 7 is necessary because of generation of acid species in the oxidation process and the required acid pH conditions of some AOPs. Also, the required chemical dosage and how long the reaction should be continued for the effluent to be biodegradable must be known (Scott and Ollis, 1995). Assessment of the biodegradability and toxicity along the chemical process is necessary to determine an optimum pretreatment time that guarantees the success of the combined system. Methods for measuring biodegradability in these systems have been proposed by a number of authors.  $BOD_5$  value and  $BOD_5/COD$  ratio are commonly used (Yu and Hu, 1994; Marco *et al.*, 1997). Other biodegradability measures including by-product identification, oxygen uptake, toxicity measurements also have been used (Scott and Ollis, 1995; Pulgarin *et al.*, 1999).

As shown in Table 2.7, combination of advanced oxidation process (AOPs) and biological process for treatment of many recalcitrant wastewaters have been reported. The studied systems include Fenton, photo-Fenton, TiO<sub>2</sub> photocatalysis and ozone as a pretreatment process, and fixed bed reactor (FBR), sequencing batch reactor (SBR), aerobic immobilised biomass reactor (IBR) and continuous flow activated sludge for biological treatment. The pollutants were, pesticides (Pulgarin *et al.*, 1999; Lapertot *et al.*, 2007; Oller *et al.*, 2007; Ballesteros *et al.*, 2009), herbicides (Sarria *et al.*, 2002; Sarria *et al.*, 2003; Farré *et al.*, 2007), dyes (García-Montaño *et al.*, 2006a and 2006b; Tantak and Chaudhari, 2006; García-Montaño *et al.*, 2008) and pharmaceutical compounds (Raj and Anjaneyulu, 2005). However, only few studies have been reported for the treatment of antibiotic wastewater by combined AOP-biological process and most of them recently reported (Alaton *et al.* 2004; Sirtori *et al.*, 2009, Gonzalez *et al.*, 2009).

Table 2.7 AOP-biological process for recalcitrant wastewater treatment

Pollutant	AOP	Biological process	Reference
p-nitrotolueneortho-sulfonic acid ( <i>p</i> -NTS) wastewater; p-NTS 1000 mg/L, TOC 333 mg/L	Photo Fenton like (Fe <sup>3+</sup> 75 mg/L, H <sub>2</sub> O <sub>2</sub> 0.3 ml/5 min, 95 min irradiation). DOC removal 75 %	Fixed bed reactor (FBR)(1 L volume, Flow 0.5 L/hr). DOC removal of 76% achieved in FBR and 93 % by combined system	Pulgarin <i>et al.</i> (1999)
Herbicide <i>p</i> -NTS	Photo-Fenton (Fe <sup>2+</sup> 1 mM, H <sub>2</sub> O <sub>2</sub> 25 mM 120 min irradiation). DOC removal 65%	Fixed bed reactor (FBR) (1 L volume). DOC removal of 95% achieved by combined system	Sarria <i>et al.</i> (2002)
Herbicide IP	Suspended and supported TiO <sub>2</sub> photocatalytic (120 min irradiation). DOC removal 20%. Disappearance of the target compound	Fixed bed reactor (FBR) (1 L volume). DOC removal of 65% achieved by combined system	Sarria <i>et al.</i> (2002)
Herbicide (5-amino-6-methyl-2-benzimidazolone); AMBI 1 mM, DOC 300 mg/L	Photo-Fenton (Fe <sup>2+</sup> 0.1 mM, H <sub>2</sub> O <sub>2</sub> 10 mM, 120 min irradiation). DOC removal 65%	Continuous aerobic immobilised biomass reactor (35 L volume). DOC removal of 90% achieved by combined system	Sarria <i>et al.</i> (2003)
High-strength semiconductor wastewater	Air stripping and Fenton oxidation (Fenton influent COD 12600 mg/L). COD removal 75%	SBR (HRT 12 hr, VSS, 3100 mg/L). COD removal of 86% achieved by SBR	Lin and Jiang (2003)

Table 2.7 AOP-biological process for recalcitrant wastewater treatment (continued)

Pollutant	AOP	Biological process	Reference
Penicillin formulation effluent (COD 710 mg/L)	Ozonation (ozone dose 1670 mg/L, 40 min reaction, pH 11). COD removal 34%, TOC removal 24%	Bioreactor (wastewater mixture of 0.7 synthetic wastewater and 0.3 ozonated penicillin effluent). COD removal of 80% achieved by bioreactor	Alaton <i>et al.</i> (2004)
Dye (Cibacron Red FN-R); 250 mg/L, DOC 80 mg/L	Photo-Fenton (Fe <sup>2+</sup> 20 mg/L, H <sub>2</sub> O <sub>2</sub> 250 mg/L, 90 min irradiation). DOC removal 49.6%, BOD <sub>5</sub> /COD 0.36	SBR (HRT 1 hr, VSS 560 mg/L). TOC removal of 60% achieved by SBR, 80% by combined system	García-Montaño <i>et al.</i> (2006a)
Dye (Procion Red H-E7B), COD 115 mg/L, DOC 48 mg/L, BOD <sub>5</sub> /COD 0.1	Photo-Fenton (Fe <sup>2+</sup> 10 mg/L, H <sub>2</sub> O <sub>2</sub> 125 mg/L, 60 min irradiation). DOC removal 39%, BOD <sub>5</sub> /COD 0.35	SBR (2 L volume, HRT 1 hr, VSS 1000 mg/L). TOC removal of 60% achieved by SBR, 71% by combined system	García-Montaño <i>et al.</i> (2006b)
Azo dyes (Reactive Black 5 (RB5), Reactive Blue 13 (RB13), and Acid Orange 7 (AO7))	Fenton (Fe <sup>2+</sup> 72 mM, H <sub>2</sub> O <sub>2</sub> 1.05 mM, reaction 60 min). >95% colour removal for all dyes	SBR (HRT 1 hr, MLSS 1000 mg/L). COD removal of 81.9, 85.5, and 77.8% for RB5, RB13, and AO7 achieved by combined system	Tantak and Chaudhari (2006)

Table 2.7 AOP-biological process for recalcitrant wastewater treatment (continued)

Pollutant	AOP	Biological process	Reference
Pesticides (Methomyl, Dimethoate, Oxamyl, Cymoxanil and Pyrimethanil); 50 mg/L for each, DOC 256 mg/L	Photo-Fenton ( $\text{Fe}^{2+}$ 20 mg/L, $\text{H}_2\text{O}_2$ 22 mM, 150 min irradiation). DOC removal 23%	Continuous aerobic immobilised biomass reactor (35L volume), DOC removal of 85% achieved by combined system	Oller <i>et al.</i> (2007)
Pesticides (Alachlor, Atrazine, Chlorfenvinphos, Diuron, Isoproturon); 30 mg/L for each	Photo-Fenton ( $\text{Fe}^{2+}$ 2 mg/L, $\text{H}_2\text{O}_2$ 1000 mg/L, 36 min irradiation). DOC removal 30%	Aerated packed-bed bioreactor (0.24 L total volume, flow rate 0.12 L/day, HRT 2 day). DOC removal of 50% achieved by biological reactor, 80% by combined system	Lapertot <i>et al.</i> (2007)
Herbicides (Diuron, Linuron); TOC 50 mg/L, COD 140 mg/L, $\text{BOD}_5 < 5$ mg/L	Photo-Fenton ( $\text{Fe}^{2+}$ 15.9 mg/L, $\text{H}_2\text{O}_2$ 202 mg/L, 60 min irradiation). $\text{BOD}_5/\text{COD}$ 0.51	SBR (HRT 2 day, VSS 600 mg/L). TOC removal of 80% achieved by SBR	Farré <i>et al.</i> (2007)
Herbicides (Diuron, Linuron in presence of humic acid); TOC 123 mg/L, COD 342 mg/L, $\text{BOD}_5 < 5$ mg/L, humic acid 200 mg/L	Photo-Fenton ( $\text{Fe}^{2+}$ 15.9 mg/L, $\text{H}_2\text{O}_2$ 202 mg/L, 60 min irradiation). $\text{BOD}_5/\text{COD}$ 0.41	SBR (HRT 2 d, VSS 560 mg/L). TOC removal of 42% achieved by SBR	Farré <i>et al.</i> (2007)
Dyes (Cibacron Red FN-R, Procion Red H-E7B)	Photo-Fenton ( $\text{Fe}^{2+}$ 5 mg/L, $\text{H}_2\text{O}_2$ 225 mg/L, 60 min irradiation). DOC removal 39%, for FN-R; ( $\text{Fe}^{2+}$ 2 mg/L, $\text{H}_2\text{O}_2$ 65 mg/L, 90 min irradiation). DOC removal 50% for H-E7B	Batch aerobic immobilised biomass reactor (35L volume). DOC removal of 82% and 86% achieved by combined system for FN-R and H-E7B, respectively	García-Montaño <i>et al.</i> (2008)

Table 2.7 AOP-biological process for recalcitrant wastewater treatment (continued)

Pollutant	AOP	Biological process	Reference
Vulcanization accelerator wastewater (2-mercaptobenzothiazole). COD 7400, TOC 2950, MBT 600 mg/L, BOD <sub>5</sub> /COD 0.45	Fenton (Fe <sup>2+</sup> 50 mM, H <sub>2</sub> O <sub>2</sub> 230 mM). COD removal 56%	Activated sludge (reactor volume 8 L). TOC removal of 29% achieved by biological reactor and 85% by combined system	Ranalli <i>et al.</i> (2008)
Pesticides (Laition, Metasystox, Sevnol and Ultracid). 50 mg/L for each, DOC 180 mg/L	Photo-Fenton (Fe <sup>2+</sup> 5 mg/L, H <sub>2</sub> O <sub>2</sub> 20 mg/L, 140 min irradiation). DOC removal 30 %	SBR (HRT 5 hr, VSS 600 mg/L). DOC removal of 90% achieved by combined system	Martín <i>et al.</i> (2009)
Pharmaceutical wastewater (Alidixic Acid Antibiotic 45 mg/L, DOC 775 mg/L)	Solar photo-Fenton (Fe <sup>2+</sup> 20 mg/L, H <sub>2</sub> O <sub>2</sub> 66 mg/L, 190 min irradiation). DOC removal 33%	Continuous aerobic immobilised biomass reactor (35L volume). DOC removal of 62% achieved by IBR, 92% by combined system	Sirtori <i>et al.</i> (2009)
Antibiotic aqueous solution (Sulfamethoxazole antibiotic 200 mg/L, TOC 94.5, COD 290 mg/L)	Photo-Fenton process (feed A H <sub>2</sub> O <sub>2</sub> 300 mg/L; feed B H <sub>2</sub> O <sub>2</sub> 400 mg/L; and Fe <sup>2+</sup> 10 mg/L). DOC removal 28 %, BOD <sub>5</sub> /COD 0.18 for feed A and DOC removal 52 %, BOD <sub>5</sub> /COD 0.26 for feed B	Sequencing batch biofilm reactor (SBBR) (2.62L, VSS 2000 mg/L, HRT 8 hr). TOC removal of 47 % achieved by SBBR, 75% by combined system for feed A, and TOC removal of 35 % achieved by SBBR, 87 % by combined system for feed B	Gonzalez <i>et al.</i> (2009)

## **2.8 Artificial Neural Network (ANN)**

The ANN modelling technique is considered a kind of artificial intelligence application that simulates the human brain in problem-solving processes. As humans solve a new problem based on the past experience, a neural network takes previously solved examples, looks for patterns in these examples, learns these patterns and develops the ability to correctly classify new patterns. In addition, the neural network has the ability to resemble human characteristics in problem-solving that is difficult to simulate using the logical, analytical techniques of expert system and standard software technologies (Daosud *et al.*, 2005).

A neural network is defined as a system of simple processing elements called neurons, which are connected to a network by a set of weights. The neuron is a processing element that takes a number of inputs, weighs them, sums them up, adds a bias and uses the result as the argument for a single-valued function (transfer function) which results in the neuron's output (Strik *et al.*, 2005). The network is determined by the architecture of the network, the magnitude of the weights and the processing element's mode of operation. At the start of training, the output of each node tends to be small. Consequently, the derivatives of the transfer function and changes in the connection weights are large with respect to the input. As learning progresses and the network reaches a local minimum in error surface, the node outputs approach stable values. Consequently, the derivatives of the transfer function with respect to input, as well as changes in the connection weights, are small (Maier and Dandy, 1998).

The different types of network based on their incremental complexity are: feed-forward network, recurrent network, stochastic network and modular networks (Prakash *et al.*, 2008). The current study will focus on the feedforward network which will be described in details in the next section.

### **2.8.1 Feedforward ANN**

The feedforward ANN is composed of two or more layers of processing elements which are linked by weighted connections (Figure 2.5). The information flow is

unidirectional, no feedback connections are present, data are presented to input layer, passed on to hidden layer and passed on to output layer.

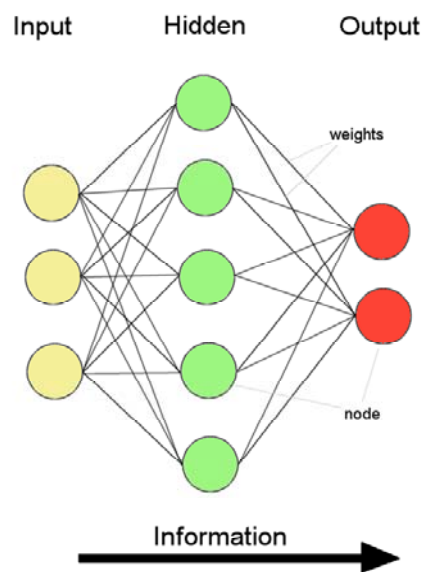


Figure 2.5 A feedforward ANN

### 2.8.1.1 Training of Artificial Neural Network

We can categorise the learning situations as the following (Artificial neural network tutorial, 2008):

- Supervised learning

The network is trained by providing it with input and matching output patterns in supervised learning or associative learning. Backpropagation is a form of supervised training. Using the actual outputs, the backpropagation training algorithm takes a calculated error and adjusts the weights of the various layers backwards from the output layer to the input layer. It means adjusting the weights in neurons with regard to the difference between the outputs predicted by the model and the actual outputs (Figure 2.6).



- Unsupervised learning

An output unit is trained to respond to clusters of pattern within the input in unsupervised learning or self-organisation. In this paradigm, the system is supposed to discover statistically salient features of the input population. Unlike the supervised learning paradigm, there is no *a priori* set of categories into which the patterns are to be classified; rather the system must develop its own representation of the input stimuli.

- Reinforcement learning

This type of learning may be considered as an intermediate form of the above two types of learning. Here the learning machine does some action on the environment and gets a feedback response from the environment. The learning system grades its action as good (rewarding) or bad (punishable) based on the environmental response and accordingly adjusts its parameters. Generally, parameter adjustment is continued until an equilibrium state occurs, following which there will be no more changes in its parameters. The self organizing neural learning may be categorized under this type of learning.

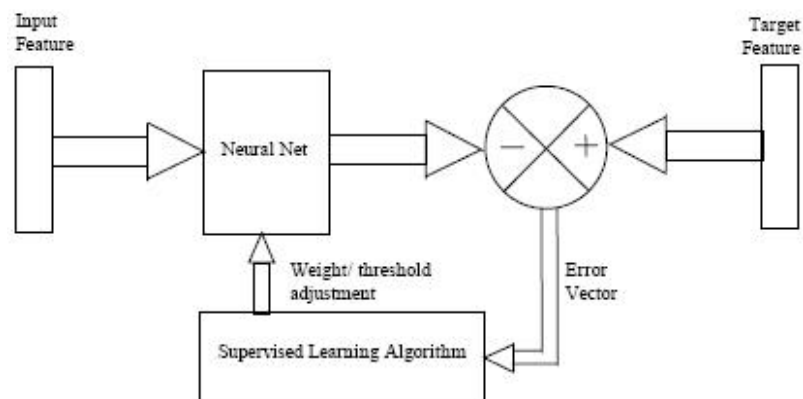


Figure 2.6 A supervised learning process (Artificial neural network tutorial, 2008)

### 2.8.2 Application of ANN in Wastewater Treatment

Artificial neural network (ANN) is now used in many areas of science and engineering and considered as a promising tool because of its simplicity towards

simulation, prediction and modelling (Prakash *et al.*, 2008). The advantages of ANN are that the mathematical description of the phenomena involved in the process is not required, less time is required for model development than the traditional mathematical models and prediction ability with limited number of experiments (Pareek *et al.*, 2002). Disadvantages of artificial neural network include its “black box” nature, the individual relations between the input variables and the output variables are not developed by engineering judgment so that the model tends to be a black box, greater computational burden, proneness to overfitting and the sample size has to be large (Tu, 1996). Application of ANN to solve environmental engineering problems has been reported in many articles. ANN was applied in biological wastewater treatment (Cote *et al.*, 1995; Hack and Kohne, 1996; Zhua *et al.*, 1998; Gontarski *et al.*, 2000; Aubrun *et al.*, 2001; Holubar *et al.*, 2002, Luccarini *et al.*, 2002; Sinha *et al.*, 2002; Zeng *et al.*, 2003; Baruch *et al.*, 2005; Ren *et al.*, 2005; Hong *et al.*, 2007; Machón *et al.*, 2007; Pai *et al.*, 2007; Moral *et al.*, 2008). ANNs were also applied in simulation and prediction of physicochemical wastewater treatment (Daneshvar *et al.*, 2006; Aber *et al.*, 2007; Yetilmezsoy and Demirel, 2008; Prakash *et al.*, 2008). However, few studies on applications of ANN in advanced oxidation processes (AOPs) have been reported as shown in Table 2.8. Most of the studies have been recently reported and published in 2008. The reported studies in the literature also focused on the application of ANNs in UV/H<sub>2</sub>O<sub>2</sub> process.

Table 2.8 Applications of ANN in advanced oxidation processes

ANN application	ANN type	Training method	Sensitivity analysis	Reference
Modeling and optimization of UV/H <sub>2</sub> O <sub>2</sub> for decoloration of C.I. Reactive Red 120	Counter-propagation	Counter propagation	-	Slokar <i>et al.</i> (1999)
Modeling and prediction of TiO <sub>2</sub> photocatalysis efficiency for nitrogen oxides removal	Feed-forward	Quick propagation	-	Toma <i>et al.</i> (2004)
Modeling of the treatment of wastewater containing methyl <i>tert</i> -butyl ether by UV/H <sub>2</sub> O <sub>2</sub>	Feed-forward	Back propagation	-	Salari <i>et al.</i> (2005)
Simulation of photo-Fenton degradation of Reactive Blue 4	Feed-forward	Back propagation (Marquardt non-linear fitting algorithm)	Garson equation	Durán <i>et al.</i> (2006)
Modeling of removal of humic substances by ozonation	Feed-forward	Back propagation	-	Oguz <i>et al.</i> (2008)
Modeling and optimization of UV/H <sub>2</sub> O <sub>2</sub> for decoloration of Acid Orange 52	Feed-forward	Back propagation (Marquardt non-linear fitting algorithm)	-	Guimarães <i>et al.</i> (2008a)
Multivariate experimental design for the photocatalytic degradation of imipramine	Feed-forward	Back propagation, conjugate gradient descent	Statistical software	Calza <i>et al.</i> (2008)

Table 2-8 Applications of ANN in advanced oxidation processes (continued)

ANN application	ANN type	Training method	Sensitivity analysis	Reference
Prediction of azo dye decolorization by UV/H <sub>2</sub> O <sub>2</sub>	Feed-forward	Back propagation, scaled conjugate gradient algorithm	Garson equation	Aleboyeh <i>et al.</i> (2008)
Optimization of the Acid Brown 75 decoloration process by UV/H <sub>2</sub> O <sub>2</sub>	Feed-forward	Back propagation, gradient descent with momentum	-	Guimarães <i>et al.</i> (2008b)
Dosage control of the Fenton process for color removal of textile wastewater applying ORP monitoring	Feed-forward	Back propagation, gradient descent	-	Yu <i>et al.</i> (2009)

## **2.9 Originality and Significance of the Study**

It is evident from the literature review that no study on degradation of the antibiotics amoxicillin, ampicillin and cloxacillin in mixture by AOPs (Fenton, photo-Fenton, UV/TiO<sub>2</sub> and UV/ZnO) has been reported. Treatment of antibiotic wastewater containing these antibiotics by AOPs (Fenton, photo-Fenton, UV/TiO<sub>2</sub> and UV/ZnO) and by combined AOP and sequencing batch reactor (SBR) have also not been reported. Thus, a study on degradation of the antibiotics amoxicillin, ampicillin and cloxacillin in mixture by AOPs (Fenton, photo-Fenton, UV/TiO<sub>2</sub> and UV/ZnO) and treatment of a wastewater containing these antibiotics by combined AOP and sequencing batch reactor (SBR) assume significance.

## **2.10 Summary**

The chapter presented antibiotic wastewater, antibiotic classification and the problem due to presence of antibiotics in the environment and antibiotic resistance. The basic concept of different advanced oxidation processes (AOPs) and previous studies on AOPs as well as antibiotic degradation and treatment of antibiotic wastewater by AOPs were summarized. Operation of sequencing batch reactor (SBR) biological system and advantages of SBR were illustrated. Application of combined AOP and biological system for recalcitrant wastewater treatment was also summarized. The basic concept of artificial neural network (ANN) and its application on wastewater treatment were discussed.

## CHAPTER 3 METHODOLOGY

### **3.0 Chapter Overview**

The study was designed to develop a complete treatment system for antibiotic wastewater and was conducted in three phases. In Phase I, four advanced oxidation processes (Fenton, photo-Fenton, UV/TiO<sub>2</sub> and UV/ZnO) were evaluated for degradation, mineralization and biodegradability improvement of a mixture of amoxicillin, ampicillin and cloxacillin antibiotics in aqueous solution. In Phase II, the feasibility of using three combined systems (Fenton-SBR, photo-Fenton-SBR and UV/H<sub>2</sub>O<sub>2</sub>/TiO<sub>2</sub>-SBR) for treatment of antibiotic wastewater was evaluated. In Phase III, artificial neural network was implemented for prediction and simulation of advanced oxidation process. The following sections describe the materials and the experimental procedure for each phase, and the analytical methods.

### **3.1 Phase I: Advanced Oxidation Processes Treatment of Antibiotic Aqueous Solution Containing a mixture of Amoxicillin, Ampicillin and Cloxacillin**

In Phase I, Fenton, photo-Fenton, UV/TiO<sub>2</sub> and UV/ZnO processes were evaluated for degradation, mineralization and biodegradability improvement of a mixture of amoxicillin, ampicillin and cloxacillin antibiotics in aqueous solution. Materials, antibiotic aqueous solution characteristics and experimental procedure for Phase I are described herein.

### 3.1.1 Antibiotics and Antibiotic Aqueous Solution

Amoxicillin, ampicillin and cloxacillin are semi-synthetic penicillin obtaining their antimicrobial properties from the presence of a  $\beta$ -lactam ring. They are widely used in human and veterinary medicine. Analytical grade of amoxicillin (AMX) and ampicillin (AMP) were purchased from Sigma and cloxacillin (CLX) from Fluka and were used to construct HPLC analytical curves for determination of antibiotic concentration. AMX, AMP and CLX used to prepare antibiotic aqueous solution were obtained from a commercial source (Farmaniage Company). The commercial products were used as received without any further purification. Figure 3.1 shows the chemical structure and HPLC chromatograph of amoxicillin, ampicillin sodium and cloxacillin sodium. Antibiotic aqueous solution was prepared by dissolving specific amounts of AMX, AMP and CLX in distilled water. The aqueous solution characteristics were AMX, AMP and CLX concentration 104, 105 and 103 mg/L, respectively, pH  $\sim$  5, COD 520 mg/L, BOD<sub>5</sub>/COD ratio  $\sim$  0 and DOC 145 mg/L. The selection of antibiotics concentration was based on the values reported in the literature (Paola *et al.*, 2004; Alaton and Dogruel, 2004; Addamo *et al.*, 2005) and preliminary characterization of antibiotic wastewater from a local antibiotic industry producing amoxicillin, ampicillin and cloxacillin which showed that the antibiotic concentration was 110, 80 and 105 mg/L for amoxicillin, ampicillin and cloxacillin, respectively. The antibiotic aqueous solution was prepared weekly and stored at 4°C.

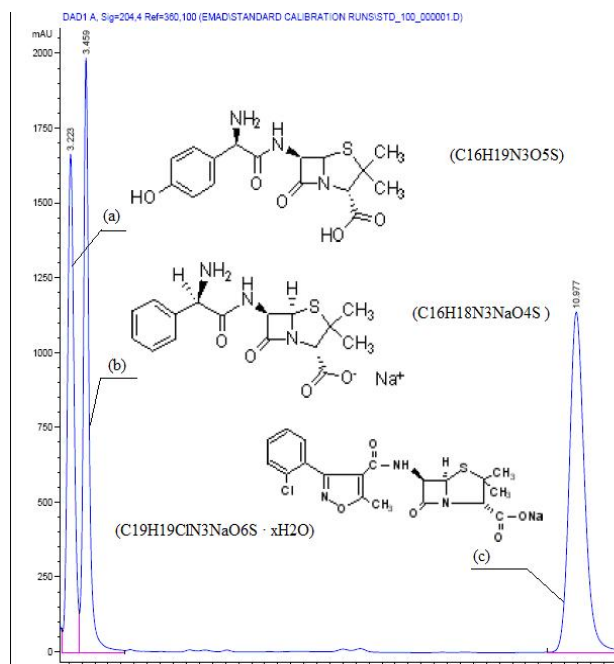


Figure 3.1 Chemical structure and HPLC chromatograph of (a) amoxicillin, (b) ampicillin sodium and (c) cloxacillin sodium.

### 3.1.2 Chemicals

Hydrogen peroxide (H<sub>2</sub>O<sub>2</sub>) (30% w/w), ferrous sulphate heptahydrate (FeSO<sub>4</sub>·7H<sub>2</sub>O), titanium dioxide (TiO<sub>2</sub>) and zinc oxide (ZnO) were purchased from R & M Marketing, Essex, U.K. Sodium hydroxide and sulfuric acid were purchased from HACH Company, USA. Potassium dihydrogen phosphate (KH<sub>2</sub>PO<sub>4</sub>) was purchased from Fluka and acetonitrile HPLC grade from Sigma.

### 3.1.3 Experimental Procedure

The following sections described the experimental procedure of Fenton, photo-Fenton, UV/TiO<sub>2</sub> and UV/ZnO processes.

#### 3.1.3.1 Fenton and Photo-Fenton Processes

Batch experiments were conducted in a 600 mL Pyrex reactor with 500 mL of the antibiotics aqueous solution (AMX, AMP and CLX concentration 104, 105 and 103



mg/L, respectively, COD 520 mg/L, BOD<sub>5</sub>/COD ratio ~ 0 and DOC 145 mg/L) at room temperature (22±2°C). The required amount of iron in the form of FeSO<sub>4</sub>·7H<sub>2</sub>O was added to the aqueous solution and mixed by a magnetic stirrer to ensure complete homogeneity during the reaction. Thereafter, necessary amount of hydrogen peroxide was added to the mixture simultaneously with pH adjustment to the required value using H<sub>2</sub>SO<sub>4</sub>. In case of photo-Fenton process, the mixture was subjected to UV irradiation and the source of UV irradiation was an UV lamp (Spectroline Model EA-160/FE; 230 volts, 0.17 amps, Spectronics Corporation, New York, USA) with nominal power of 6 W, emitting radiation at wave length ≈365 nm and it was placed above the reactor. The time at which hydrogen peroxide was added to the solution was considered the beginning of the experiment. Samples were taken at pre-selected time intervals using a syringe and filtered through a 0.45 µm PTEF syringe filter for soluble chemical oxygen demand (sCOD), 5-day biochemical oxygen demand (BOD<sub>5</sub>) and dissolved organic carbon (DOC) measurement, and through a 0.20 µm PTEF syringe filter for determination of antibiotic concentration by HPLC.

### *3.1.3.2 UV/TiO<sub>2</sub> and UV/ZnO Processes*

A 500 mL aliquot of the antibiotic aqueous solution (AMX, AMP and CLX concentration 104, 105 and 103 mg/L, respectively, COD 520 mg/L, BOD<sub>5</sub>/COD ratio ~ 0 and DOC 145 mg/L) was placed in a 600 mL Pyrex reactor with the required amount of TiO<sub>2</sub> or ZnO and was stirred magnetically at room temperature (22±2°C). The pH of the mixture was adjusted to the required value by 1N H<sub>2</sub>SO<sub>4</sub> or 1N NaOH and the mixture was kept in dark for 30 min for dark adsorption before subjecting to UV irradiation. The source of UV irradiation was a UV lamp (Spectroline Model EA-160/FE; 230 volts, 0.17 amps, Spectronics Corporation, New York, USA) with a nominal power of 6 W, emitting radiation at ≈365 nm and it was placed above the reactor. Samples were taken at pre-selected time intervals using a syringe and filtered through a 0.45 µm PTEF syringe filter for sCOD, BOD<sub>5</sub> and DOC measurement, and through a 0.20 µm PTEF syringe filter for determination of antibiotic concentration by HPLC.

### **3.2 Phase II: Combined Advanced Oxidation Process and Sequencing Batch Reactor for Antibiotic Wastewater Treatment**

In Phase II, the feasibility of using three combined systems (Fenton-SBR, photo-Fenton-SBR and UV/H<sub>2</sub>O<sub>2</sub>/TiO<sub>2</sub>-SBR) for treatment of antibiotic wastewater was evaluated. Antibiotic wastewater characteristics, experimental setup and experimental procedure for Phase II are described herein.

#### **3.2.1 Antibiotic Wastewater**

Antibiotic wastewater used in this study was obtained from a local antibiotic industry producing amoxicillin, ampicillin and cloxacillin. It has three production lines, one for capsules, the second for tablet and the third for syrup. It uses mixing and compounding of antibiotics. The wastewater produced from these processes is approximately 15 m<sup>3</sup>/day. The wastewater was collected from the collection sump, transported to the laboratory and stored at 4°C. Before taking a sample and starting the experiment, the wastewater was mixed well and left for 2 hours to reach room temperature. The wastewater was characterized two times, a preliminary characterization before starting Phase I experiments to find the basis for selecting antibiotic concentration in the aqueous solution and detailed characterization before starting Phase II experiments in which the antibiotic wastewater used. The characteristics of the wastewater before starting Phase I were 110, 80 and 105 mg/L of amoxicillin, ampicillin and cloxacillin, respectively and COD 750 mg/L. The characteristics of the antibiotic wastewater used in Phase II experiments are summarized in Table 3.1.

Table 3.1 Antibiotic wastewater characteristics

Parameter	Value	Parameter	Value
Amoxicillin (mg/L)	138±5	TSS (mg/L)	70±5
Cloxacillin (mg/L)	84±4	TP (mg/L)	7.5
Ampicillin (mg/L)	ND	NO <sub>3</sub> -N (mg/L)	5.1
COD (mg/L)	670±20	NH <sub>3</sub> -N (mg/L)	11.1
Soluble COD (mg/L)	560±20	SO <sub>4</sub> <sup>2-</sup> (mg/L)	0.7
DOC (mg/L)	160±5	Cl <sup>-</sup> (mg/L)	5.92
BOD <sub>5</sub> (mg/L)	65±10	Turbidity (NTU)	45
BOD <sub>5</sub> /COD ratio	0.09	Conductivity (µs/cm)	125
pH	6.8		

### 3.2.2 Experimental Set-up

The antibiotic wastewater was treated by three combined AOP-SBR systems (Fenton-SBR, photo-Fenton-SBR and UV/H<sub>2</sub>O<sub>2</sub>/TiO<sub>2</sub>-SBR). Each combined system was accomplished in two stages, AOP process as stage 1 and aerobic sequencing batch reactor (SBR) as stage 2. In stage 1, batch Fenton, photo Fenton and UV/H<sub>2</sub>O<sub>2</sub>/TiO<sub>2</sub> pretreatment was conducted using a 2200 mL Pyrex reactor with 2000 mL of antibiotic wastewater. In stage 2, three identical SBR were used. SBR total volume was 2 L with operating volume of 1.5 L. The operating volume was divided into 1.0 L decanting volume and 0.5 L sludge volume. The reactor was equipped with an air pump and air diffuser to keep dissolved oxygen above 3 mg/L, and magnetic stirrer for mixing purpose. Feeding and decanting were performed using two peristaltic pumps. The cycle period was divided into five phases: filling (0.25 hr), aeration (variable), settling (1.25 hr), decant (0.25 hr) and idle (0.25 hr). Cycle phases were controlled by an electric control panel. Figure 3.2 shows a general the schematic of combined AOP-SBR treatment system and Figure 3.3 shows the SBR setup.

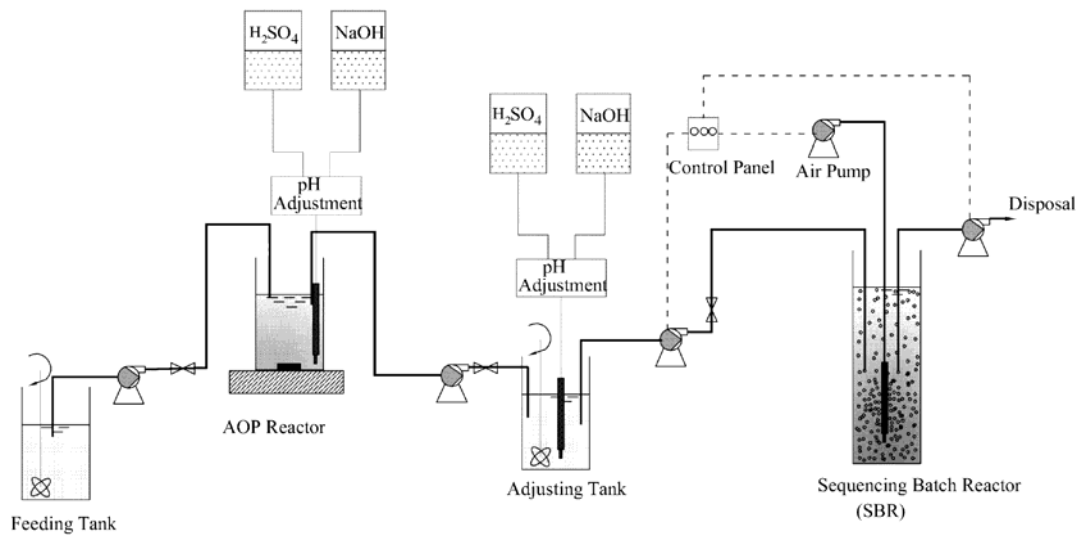


Figure 3.2 General schematic of combined AOP-SBR treatment system



Figure 3.3 SBR setup

### 3.2.3 Experimental Procedure

The antibiotic wastewater treatment by combined advanced oxidation process with sequencing batch reactor was accomplished in two stages. Advanced oxidation process (AOP pretreatment) as stage 1 and aerobic sequencing batch reactor (SBR) as stage 2.

### 3.2.3.1 Stage 1: AOP Pretreatment

Batch Fenton, photo-Fenton and UV/H<sub>2</sub>O<sub>2</sub>/TiO<sub>2</sub> pretreatment were conducted using a 2200 mL Pyrex reactor with 2000 mL of the antibiotic wastewater. The antibiotic wastewater characteristics were shown in table 3.1. The required amount of iron (FeSO<sub>4</sub>·7H<sub>2</sub>O) for Fenton and photo-Fenton or TiO<sub>2</sub> for UV/H<sub>2</sub>O<sub>2</sub>/TiO<sub>2</sub> was added to the wastewater and mixed by a magnetic stirrer to ensure complete homogeneity during reaction. Thereafter, necessary amount of hydrogen peroxide was added to the mixture simultaneously with pH adjustment to the required value using H<sub>2</sub>SO<sub>4</sub> or NaOH. The processes were conducted at room temperature (22±2°C). The mixture was subjected to UV irradiation in case of photo-Fenton and UV/TiO<sub>2</sub> processes. The source of UV light was an UV lamp (Spectroline Model EA-160/FE; 230 volts, 0.17 amps, Spectronics Corporation, New York, USA) with nominal power of 6 W, emitting radiations at wave length ≈365 nm. The time at which hydrogen peroxide was added to the solution was considered the beginning of the experiment. The reaction was allowed to continue for the required time and thereafter, pH was elevated to more than 10 for iron precipitation and decomposing residual H<sub>2</sub>O<sub>2</sub> (Talinli and Anderson, 1999). Precipitated iron or TiO<sub>2</sub> was separated and samples were taken and filtered through a 0.45µm membrane syringe filter for sCOD, BOD<sub>5</sub> and DOC measurement, and filtered through a 0.20 µm membrane syringe filter for antibiotic measurement using HPLC.

### 3.2.3.2 Stage 2: Aerobic Sequencing Batch Reactor (SBR)

Fenton-treated, photo-Fenton-treated and UV/H<sub>2</sub>O<sub>2</sub>/TiO<sub>2</sub>-treated antibiotic wastewater was used to feed three SBR reactors after pH adjustment to 6.8 and 7.2. The SBR was inoculated with 200 mL of aerobic sludge. The source of the sludge was the aeration tank of the sewage treatment plant (STP), Universiti Teknologi PETRONAS. Concentration of biomass in the reactors after inoculation was 2200-2400 mg/L. In order to acclimate the biomass, HRT was chosen to be 2 days and pretreated antibiotic wastewater was mixed with wastewater obtained from the STP, with mixing ratio 25%:75%, 50%:50%, 75%:25% and 100, and the acclimation period was extended to 10 days. The SBR cycle was repeated 6-9 times to allow cell

acclimation and/or to obtain repetitive results. Daily analyses of sCOD and DOC for both influent and effluent were carried out. Concentration of mixed liquor suspended solids (MLSS), mixed liquor volatile suspended solids (MLVSS), ammonia (NH<sub>3</sub>-N), total Kjeldahl nitrogen (TKN), nitrate (NO<sub>3</sub>-N) and BOD<sub>5</sub> were monitored throughout the operation.

### **3.3 Phase III: Artificial Neural Network (ANN) for Modelling and Simulation of Advanced Oxidation Process**

A three-layered backpropagation neural network with tangent sigmoid transfer function (tansig) at hidden layer and a linear transfer function (purelin) at output layer was used. Neural Network Toolbox V4.0 of MATLAB mathematical software was used for AOP simulation. Data set was divided into input matrix [p] and target matrix [t]. The input variables were reaction time (t), H<sub>2</sub>O<sub>2</sub>/COD molar ratio, H<sub>2</sub>O<sub>2</sub>/Fe<sup>2+</sup> molar ratio, pH and COD. The corresponding COD removal percent was used as a target. Principal component analysis (PCA) was performed as an effective procedure for removing data noise. The data sets were divided into training (one half), validation (one fourth) and test (one fourth) subsets, each of which contained 60, 30 and 30 samples, respectively. Ten backpropagation training algorithms (Table 3.2) were used for network training.

Table 3.2 The backpropagation training algorithms

SN	Backpropagation (BP) algorithms	Function
1	Levenberg–Marquardt backpropagation	trainlm
2	Scaled conjugate gradient backpropagation	trainsecg
3	BFGS quasi-Newton backpropagation	trainbfg
4	One step secant backpropagation	trainoss
5	Batch gradient descent	traingd
6	Vairable learning rate backpropagation	traingdx
7	Batch gradient descent with momentum	traingdm
8	Fletcher–Reeves conjugate gradient backpropagation	traincgf
9	Polak–Ribi’ere conjugate gradient backpropagation	traincgp
10	Powell–Beale conjugate gradient backpropagation	traincgb

### 3.4 Analytical Methods

Analytical methods for the measured parameters such as amoxicillin, ampicillin, cloxacillin, TOC, COD, BOD<sub>5</sub>, TSS, TVSS, pH, NH<sub>3</sub>-N, NO<sub>3</sub>-N, TKN, TP, sulphate and chloride ions were detailed. In addition, the methods of data analyses were described.

#### 3.4.1 Antibiotic

Antibiotic concentration was determined by a high performance liquid chromatograph (HPLC) (Agilent 1100 Series) equipped with a micro-vacuum degasser (Agilent 1100 Series), quaternary pump, diode array and multiple wavelength detector (DAD) (Agilent 1100 Series) at wavelength 204 nm. The data were recorded by a chemstation software. The column was ZORBAX SB-C18 (4.6 mm x 150 mm, 5 µm) and its temperature was 60°C. The mobile phase was 55% 0.025 M KH<sub>2</sub>PO<sub>4</sub> buffer solution in ultra pure water and 45% acetonitrile at a flow rate of 0.50 mL/min.

### **3.4.2 Total Organic Carbon (TOC)**

A TOC analyzer (Model 1010; O & I Analytical) was used for determining total carbon (TC) and total inorganic carbon, and the difference between total carbon (TC) and total inorganic carbon is equal to total organic carbon (TOC). When the samples are filtered through a 0.45  $\mu\text{m}$  membrane filter, total organic carbon is equal to dissolved organic carbon (DOC).

### **3.4.3 Chemical Oxygen Demand (COD)**

COD was measured according to Hach method (Method 8000) using Hach reagent (Hach, 2002). Colorimetric determination of COD was carried out at 620 nm using a Hach spectrophotometer DR 2000 (Hach, 2002). When the sample contained  $\text{H}_2\text{O}_2$ , to reduce interference in COD determination pH was increased to above 10 to decompose  $\text{H}_2\text{O}_2$  to oxygen and water (Talinli and Anderson, 1999).

### **3.4.4 Five-day Biochemical Oxygen Demand (BOD<sub>5</sub>)**

BOD<sub>5</sub> was determined according to the Standard Methods (APHA, 1992). Dissolved oxygen (DO) was measured by an YSI 5000 dissolved oxygen meter. Bacterial seed for the BOD<sub>5</sub> test was obtained from the STP, Universiti Teknologi PETRONAS campus.

### **3.4.5 Total Suspended Solids (TSS) and Total Volatile Suspended Solids (TVSS)**

TSS was determined according to the Standard Methods Section 2540 D. Total Suspended Solids Dried at 103-105°C Method (APHA, 1992). In TVSS measurement, the residue from the TSS measurement was ignited to constant weight at 550°C in the furnace (Nabertherm L15/12/P320) according to the Standard Methods Section 2540 E Fixed and Volatile Solids Ignited at 550°C Method (APHA, 1992). Mixed liquor suspended solids (MLSS) was measured by the TSS method and Mixed Liquor Volatile Suspended Solids (MLVSS) was measured by the TVSS method with proper dilution.



### **3.4.6 pH**

A pH meter (HACH Sension 4) with a pH electrode (HACH platinum series pH electrode model 51910, HACH company, USA) was used for pH measurement. The pH meter was calibrated with pH 4.0, 7.0 and 10.0 buffers.

### **3.4.7 Ammonia Nitrogen (NH<sub>3</sub>-N), Nitrate Nitrogen (NO<sub>3</sub>-N) and Total Phosphorus (TP)**

NH<sub>3</sub>-N was measured by the Nessler Method (Method 8038), NO<sub>3</sub>-N by the Cadmium Reduction Method (High Range) using Hach powder pillow and TP by PhosVer 3 Method using Hach powder pillow (Hach, 2002).

### **3.4.8 Total Kjeldahl Nitrogen (TKN)**

TKN was measured according to the Standard Methods Section 4500-Norg B Macro-Kjeldahl Method (APHA, 1992). Digestion was conducted using a Buchi K-424 digestion unit and Buchi B-414 scrubber unit. Distillation and titration were conducted using using a Buchi Auto Kjeldal unit, K-370.

### **3.4.9 Sulphate and Chloride Ions**

Sulphate and chloride were determined by ion chromatograph (Metrohm). The eluent phase consisted of 3.2 mM Na<sub>2</sub>CO<sub>3</sub> and 1.0 mM NaHCO<sub>3</sub>. The analytical column was METROSEP A SUPP 5-150 (4.0 mm x 150 mm, 5 µm). The flow rate was 0.7 mL and the temperature was 20°C.

### **3.4.10 Data Analyses**

Statistical analyses (ANOVA) was conducted using SPSS software and Microsoft excel. One-way and two-way ANOVA were applied to the results to determine the significant difference between the data that were obtained for each variable of the experiments.

### 3.5 Kinetic Study of Antibiotic Oxidation by AOPs

The kinetics of antibiotic oxidation by advanced oxidation processes (AOPs) can be represented as a second-order rate equation as follows:

$$\frac{dC_{anti}}{dt} = -k_{anti} C_{anti} C_{OH\bullet} \quad \text{Equation 3.1}$$

where,  $C_{anti}$  is the concentration of the antibiotics,  $C_{OH\bullet}$  is the concentration of hydroxyl radicals and  $k_{anti}$  is the second-order rate constant for the reaction. In case of constant  $OH\bullet$  radical concentration and in excess compared to antibiotic concentration, Equation 3.1 can be reduced to a pseudo-first-order rate equation (Kavitha and Palanivelu, 2005b).

$$\frac{dC_{anti}}{dt} = -k_{anti} C_{anti} \quad \text{Equation 3.2}$$

where,  $k_{anti}$  is the pseudo-first-order rate constant. When  $t = 0$ ,  $C_{anti}$  is equal to  $C_{anti_0}$ , and the solution of Equation 3.2 becomes:

$$\ln \frac{[C_{anti}]}{[C_{anti_0}]} = -k_{anti} t \quad \text{Equation 3.3}$$

When antibiotics degradation takes place immediately and leading to the formation of intermediates, it would be appropriate to assess the rate constant with respect to DOC rather than to a particular antibiotic. Thus, Equation 3.3 is represented as:

$$\ln \frac{[DOC]}{[DOC_0]} = -k_0 t \quad \text{Equation 3.4}$$

where,  $k_0$  represents the overall pseudo-first-order rate constant for antibiotic mineralization.

Pseudo-first-order rate constant ( $k_0$ ) can be obtained through a linear least-square fit of the DOC data. The corresponding half-life time ( $t_{1/2}$ ) was calculated according to the following equation:

$$t_{1/2} = \frac{0.693}{k_0} \quad \text{Equation 3.5}$$

### 3.6 Kinetic Study of the biological treatment

Kinetic evaluation is important for design and operation of biological wastewater treatment processes. Several models relating growth rate and the substrate utilization rate with the substrate concentration are available (Bailey and Ollis, 1986). Among these models, Monod model (Monod, 1949) is widely used because it gives good fit to the experimental results. The model is expressed as:

$$\mu = \mu_m \frac{S}{K_s + S} \quad \text{Equation 3.6}$$

where,  $\mu$  = specific growth rate,  $\text{hr}^{-1}$ ;  $\mu_m$  = maximum specific growth rate,  $\text{hr}^{-1}$ ;  $S$  = substrate concentration,  $\text{mg/L}$ ; and  $K_s$  = half velocity constant,  $\text{mg/L}$ .

In batch and continuous biological processes, the growth rate can be defined by the following relationship:

$$r_g = \mu X \quad \text{Equation 3.7}$$

where,  $r_g$  = rate of bacterial growth,  $\text{mg/L/hr}$ , and  $X$  = microorganism concentration,  $\text{mg/L}$ .

In batch process,  $r_g = \frac{dX}{dt}$  and hence the following relationship is also valid:

$$\frac{dX}{dt} = \mu X \quad \text{Equation 3.8}$$

If the value of  $\mu$  is substituted in Equation 3.6, the resulting equation for the growth rate is:

$$\frac{dX}{dt} = \mu_m \frac{XS}{K_s + S} \quad \text{Equation 3.9}$$

The relationship between the growth rate and substrate utilization rate is:

$$\frac{dX}{dt} = -Y \frac{dS}{dt} \quad \text{Equation 3.10}$$

where,  $Y$  = maximum yield coefficient (ratio of the mass of cell formed to the mass of substrate consumed) and  $\frac{dS}{dt}$  = substrate utilization rate,  $\text{mg/L/ hr}^{-1}$

From Equation 3.9 and 3.10,  $\frac{dS}{dt}$  can be expressed as:

$$\frac{dS}{dt} = -\mu_m \frac{XS}{Y(K_s+S)} \quad \text{Equation 3.11}$$

The term  $\frac{\mu_m}{Y}$  can be replaced by a constant  $K$ , where  $K$  is the maximum specific substrate utilization rate (mg sCOD mg MLSS<sup>-1</sup> hr<sup>-1</sup>) or (hr<sup>-1</sup>):

$$K = \frac{\mu_m}{Y} \quad \text{Equation 3.12}$$

If the value of  $K$  is substituted in Equation 3.11, the resulting equation for substrate utilization rate is

$$\frac{dS}{dt} = -\frac{KXS}{(K_s+S)} \quad \text{Equation 3.13}$$

At limited concentration of the substrate, it would be consumed first and the growth would cease. Beltran-Heredia *et al.* (2000) reported that at low substrate concentration ( $K_s \gg S$ ), Monod model can be defined using the following first order kinetic expression:

$$\frac{dS}{dt} = -k_{ob}S \quad \text{Equation 3.14}$$

where,  $k_{ob}$  is biological first order kinetic constant (hr<sup>-1</sup>)

For  $S_0 > 0$ , the differential equation is solved by the method of separation of variables:

$$\ln \frac{S}{S_0} = k_{ob}t \quad \text{Equation 3.15}$$

According to Equation 3.15, plot of  $\ln \frac{S}{S_0}$  versus time should give a straight line whose slope will be the biological first order kinetic constant ( $k_{ob}$ ).

### **3.7 Summary**

The chapter described the materials, experimental procedure and analytical methods used in each phase of the study. The antibiotics and the antibiotic aqueous solution characteristics were presented. The sources of the materials were mentioned. Experimental procedure for each process (Fenton, photo-Fenton, UV/TiO<sub>2</sub> and UV/ZnO) were described. The characteristics of the antibiotic wastewater in Phase II were presented and the experimental setup was illustrated. Details of experimental procedure and the start up of the SBR were outlined. The analytical methods and data analyses were described. The details of application of artificial neural network for modelling of AOP were presented.

CHAPTER 4  
RESULTS AND DISCUSSION  
PHASE I: ADVANCED OXIDATION PROCESS TREATMENT OF ANTIBIOTIC  
AQUEOUS SOLUTION

#### **4.0 Chapter Overview**

This chapter presents the experimental results and discussion of Phase I study. Four advanced oxidation processes (AOPs) were studied for treatment of antibiotic aqueous solution containing a mixture of amoxicillin, ampicillin and cloxacillin. The chapter is divided into five main sections, Fenton process, photo-Fenton process, UV/TiO<sub>2</sub> process and UV/ZnO process and a comparison (technical and cost) of the processes. This chapter has been the basis of the following peer-reviewed journal publications:

#### **4.1 Fenton Process**

Effect of the operating conditions of the Fenton process such as H<sub>2</sub>O<sub>2</sub>/COD molar ratio, H<sub>2</sub>O<sub>2</sub>/Fe<sup>2+</sup> molar ratio, pH, initial antibiotic concentration and reaction time on antibiotic degradation, mineralization and biodegradability improvement were studied.

##### **4.1.1 Effect of H<sub>2</sub>O<sub>2</sub>/COD Molar Ratio**

To determine the optimum H<sub>2</sub>O<sub>2</sub>/COD molar ratio, initial H<sub>2</sub>O<sub>2</sub> concentration was varied in the range 15-54 mM at constant initial COD 520 mg/L (16.25 mM). The corresponding H<sub>2</sub>O<sub>2</sub>/COD molar ratios were 1, 1.5, 2, 2.5, 3 and 3.5. Initial AMX, AMP and CLX concentrations were 104, 105 and 103 mg/L, respectively. The other operating conditions were fixed at pH 3 and H<sub>2</sub>O<sub>2</sub>/Fe<sup>2+</sup> molar ratio 50. Figures 4.1 and 4.2 show the effect of H<sub>2</sub>O<sub>2</sub>/COD molar ratio on AMX, AMX and CLX

degradation in terms of COD and COD removal. COD after 60 min reaction time was 387, 288, 236, 207, 197 and 198 mg/L (Figure 4.1); however, COD removal after 60 min reaction time was 25.6, 44.6, 54.6, 60.2, 62.1 and 60.9% (Figure 4.2) at  $H_2O_2/COD$  molar ratio 1, 1.5, 2, 2.5, 3 and 3.5, respectively.  $BOD_5$  after 60 min reaction time was 20, 20, 50, 58, 62 and 57 mg/L (Figure 4.3); however,  $BOD_5/COD$  ratio after 60 min reaction time was 0.05, 0.07, 0.21, 0.28, 0.31 and 0.29 (Figure 4.4) at  $H_2O_2/COD$  molar ratio 1, 1.5, 2, 2.5, 3 and 3.5, respectively. DOC after 60 min reaction time was 129, 120, 104, 103, 98 and 96 mg/L (Figure 4.5); however, DOC removal after 60 min reaction time was 13.3, 19.8, 30.1, 34.4 and 35.6% (Figure 4.6) at  $H_2O_2/COD$  molar ratio 1, 1.5, 2, 2.5, 3 and 3.5, respectively. The results show that increasing COD removal,  $BOD_5/COD$  ratio and DOC removal at  $H_2O_2/COD$  molar ratio 1-3 and further increase in  $H_2O_2/COD$  did not improve degradation. This may be due to scavenging of  $OH^\bullet$  by  $H_2O_2$  as in Reaction 2.6 (Kavitha and Palanivelu 2005a). Based on the results, maximum COD removal, biodegradability ( $BOD_5/COD$  ratio) improvement and DOC removal for the antibiotic aqueous solution containing AMX, AMP and CLX was achieved at  $H_2O_2/COD$  molar ratio 3.

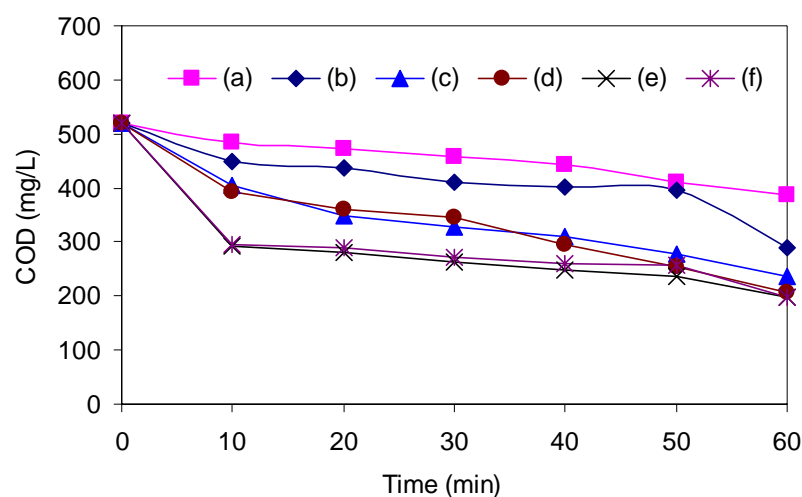


Figure 4.1 Effect of  $H_2O_2/COD$  molar ratio on antibiotics degradation by Fenton process in terms of COD (a) 1.0, (b) 1.5, (c) 2.0, (d) 2.5, (e) 3.0 and (f) 3.5

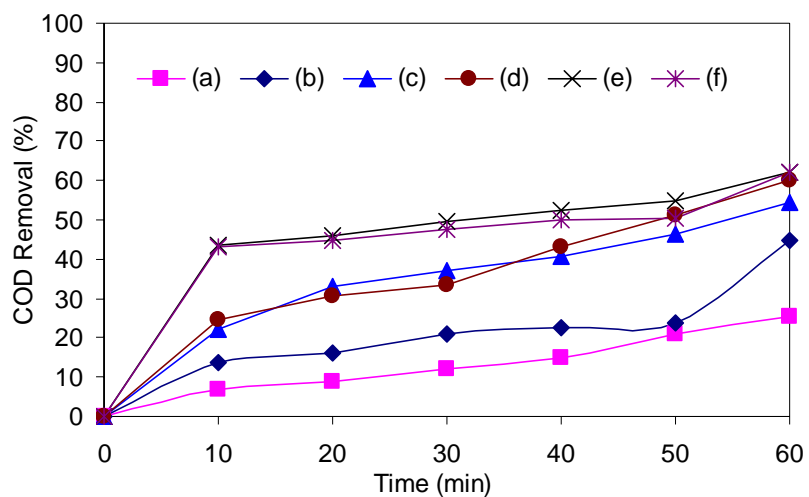


Figure 4.2 Effect of H<sub>2</sub>O<sub>2</sub>/COD molar ratio on antibiotics degradation by Fenton process in terms of COD removal (a) 1.0, (b) 1.5, (c) 2.0, (d) 2.5, (e) 3.0 and (f) 3.5

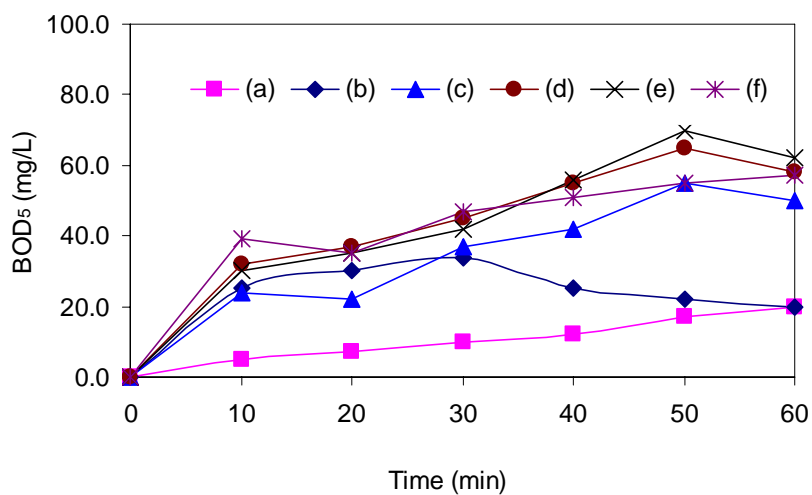


Figure 4.3 Effect of H<sub>2</sub>O<sub>2</sub>/COD molar ratio on antibiotics degradation by Fenton process in terms of BOD<sub>5</sub> (a) 1.0, (b) 1.5, (c) 2.0, (d) 2.5, (e) 3.0 and (f) 3.5



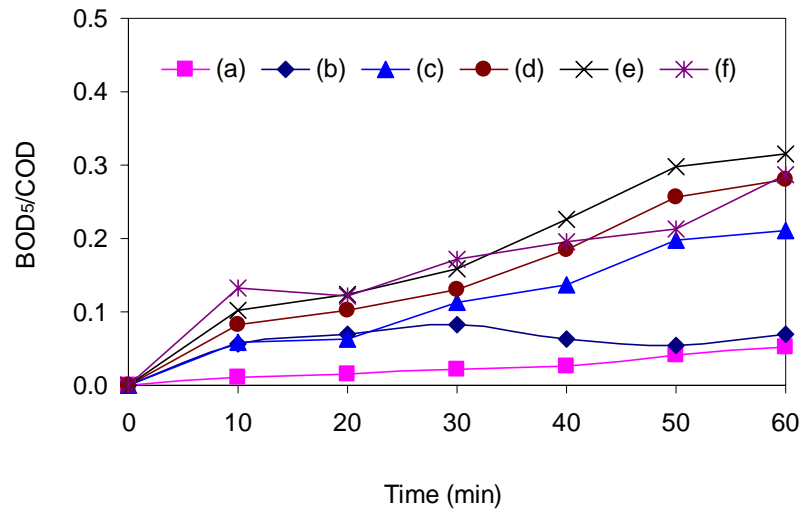


Figure 4.4 Effect of H<sub>2</sub>O<sub>2</sub>/COD molar ratio on antibiotics degradation by Fenton process in terms of BOD<sub>5</sub>/COD ratio (a) 1.0, (b) 1.5, (c) 2.0, (d) 2.5, (e) 3.0 and (f) 3.5

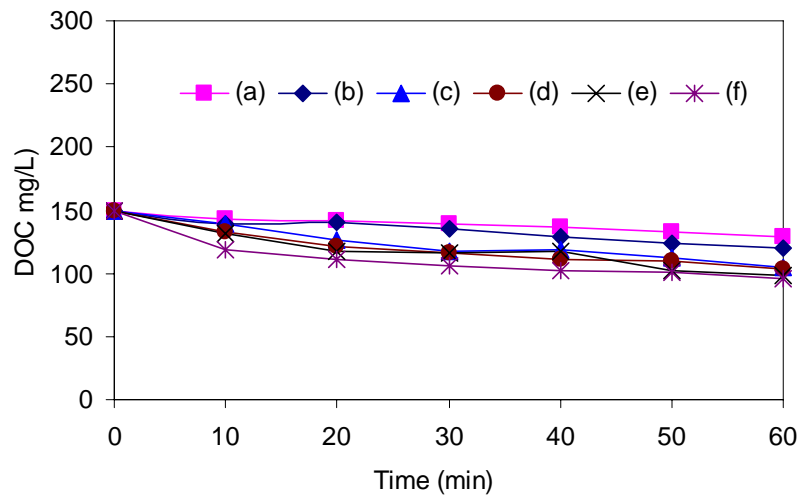


Figure 4.5 Effect of H<sub>2</sub>O<sub>2</sub>/COD molar ratio on antibiotics degradation by Fenton process in terms of DOC (a) 1.0, (b) 1.5, (c) 2.0, (d) 2.5, (e) 3.0 and (f) 3.5

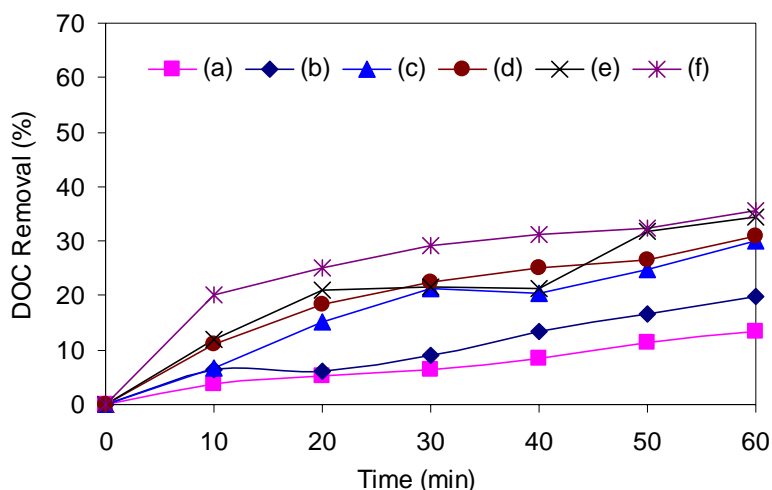


Figure 4.6 Effect of  $\text{H}_2\text{O}_2/\text{COD}$  molar ratio on antibiotics degradation by Fenton process in terms of DOC removal (a) 1.0, (b) 1.5, (c) 2.0, (d) 2.5, (e) 3.0 and (f) 3.5

#### 4.1.2 Effect of $\text{H}_2\text{O}_2/\text{Fe}^{2+}$ Molar Ratio

In Fenton process, iron and hydrogen peroxide are two major chemicals determining the operation cost as well as efficiency. To determine the optimal  $\text{H}_2\text{O}_2/\text{Fe}^{2+}$  molar ratio, experiments were conducted at pH 3 with constant initial COD of 520 mg/L (16.25 mM) and  $\text{H}_2\text{O}_2$  concentration of 46.87 mM ( $\text{H}_2\text{O}_2/\text{COD}$  molar ratio 3).  $\text{Fe}^{2+}$  concentration was varied in the range 0.32-24.3 mM and the corresponding  $\text{H}_2\text{O}_2/\text{Fe}^{2+}$  molar ratio was in the range 2-150. Initial AMX, AMP and CLX concentration were 104, 105 and 103 mg/L, respectively. Figures 4.7 and 4.8 show the effect of  $\text{H}_2\text{O}_2/\text{Fe}^{2+}$  molar ratio on AMX, AMX and CLX degradation in terms of COD and COD removal. COD after 60 min reaction time was 142, 127, 105, 140, 197, 253 and 300 mg/L (Figure 4.7); however, COD removal after 60 min reaction time was 72.7, 75.6, 79.8, 73.1, 62.1 and 42.3% (Figure 4.8) at  $\text{H}_2\text{O}_2/\text{Fe}^{2+}$  molar ratio 2, 5, 10, 20, 50, 100 and 150, respectively.  $\text{BOD}_5$  after 60 min reaction time was 28, 30, 48, 52, 62, 38 and 23 mg/L (Figure 4.9); however,  $\text{BOD}_5/\text{COD}$  ratio after 60 min reaction time was 0.20, 0.29, 0.38, 0.37, 0.31, 0.15 and 0.08 (Figure 4.10) at  $\text{H}_2\text{O}_2/\text{Fe}^{2+}$  molar ratio 2, 5, 10, 20, 50, 100 and 150, respectively. DOC after 60 min reaction time was 88, 74, 75, 92, 98, 121 and 127 mg/L (Figure 4.11); however, DOC removal after 60 min reaction time was 41, 50.5, 50, 38.2, 34.4, 18.5 and 14.9% (Figure 4.12) at  $\text{H}_2\text{O}_2/\text{Fe}^{2+}$  molar ratio 2, 5, 10, 20, 50, 100 and 150,

respectively. The results show that COD removal, BOD<sub>5</sub>/COD ratio and DOC removal increased with the decrease of H<sub>2</sub>O<sub>2</sub>/Fe<sup>2+</sup> molar ratio up to 10. Further decrease in H<sub>2</sub>O<sub>2</sub>/Fe<sup>2+</sup> molar ratio below 10 did not improve degradation of the antibiotics. This may be due to direct reaction of OH<sup>•</sup> radical with metal ions at high concentration of Fe<sup>2+</sup> (Joseph *et al.*, 2000) as in Reaction 2.5. Maximum COD removal, biodegradability improvement and DOC removal for the antibiotic aqueous solution containing AMX, AMP, and CLX was achieved at H<sub>2</sub>O<sub>2</sub>/Fe<sup>2+</sup> molar ratio 10.

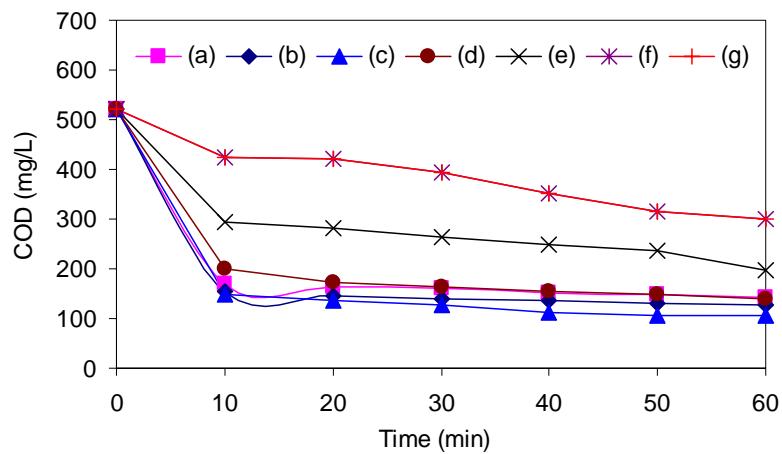


Figure 4.7 Effect of H<sub>2</sub>O<sub>2</sub>/Fe<sup>2+</sup> molar ratio on antibiotics degradation by Fenton process in terms of COD (a) 2.0, (b) 5.0, (c) 10.0, (d) 20.0, (e) 50.0, (f) 100 and (g)

150

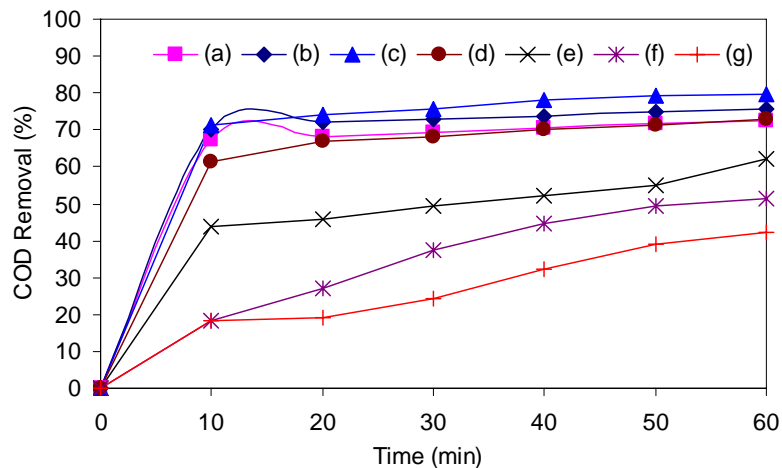


Figure 4.8 Effect of H<sub>2</sub>O<sub>2</sub>/Fe<sup>2+</sup> molar ratio on antibiotics degradation by Fenton process in terms of COD removal (a) 2.0, (b) 5.0, (c) 10.0, (d) 20.0, (e) 50.0, (f) 100 and (g) 150

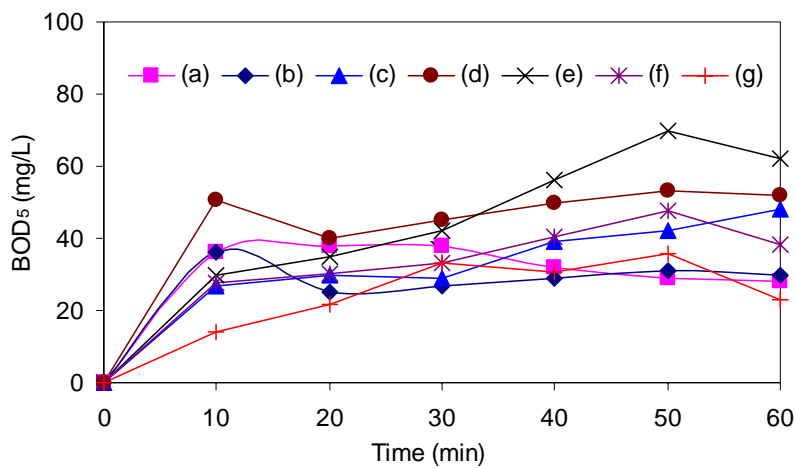


Figure 4.9 Effect of  $H_2O_2/Fe^{2+}$  molar ratio on antibiotics degradation by Fenton process in terms of BOD<sub>5</sub> (a) 2.0, (b) 5.0, (c) 10.0, (d) 20.0, (e) 50.0, (f) 100 and (g) 150

150

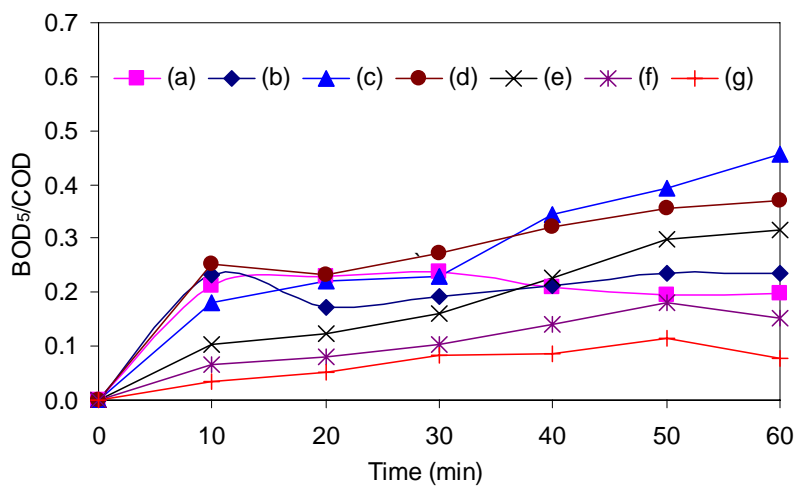


Figure 4.10 Effect of  $H_2O_2/Fe^{2+}$  molar ratio on antibiotics degradation by Fenton process in terms of BOD<sub>5</sub>/COD ratio (a) 2.0, (b) 5.0, (c) 10.0, (d) 20.0, (e) 50.0, (f) 100 and (g) 150

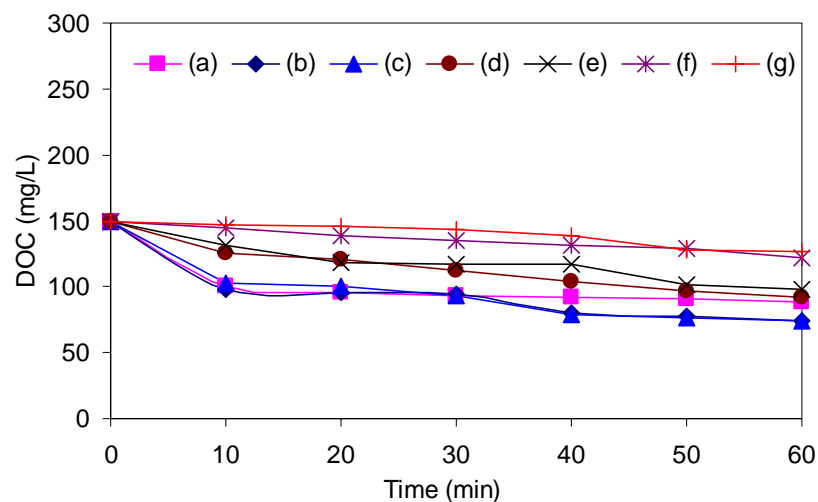


Figure 4.11 Effect of  $H_2O_2/Fe^{2+}$  molar ratio on antibiotics degradation by Fenton process in terms of DOC (a) 2.0, (b) 5.0, (c) 10.0, (d) 20.0, (e) 50.0, (f) 100 and (g) 150

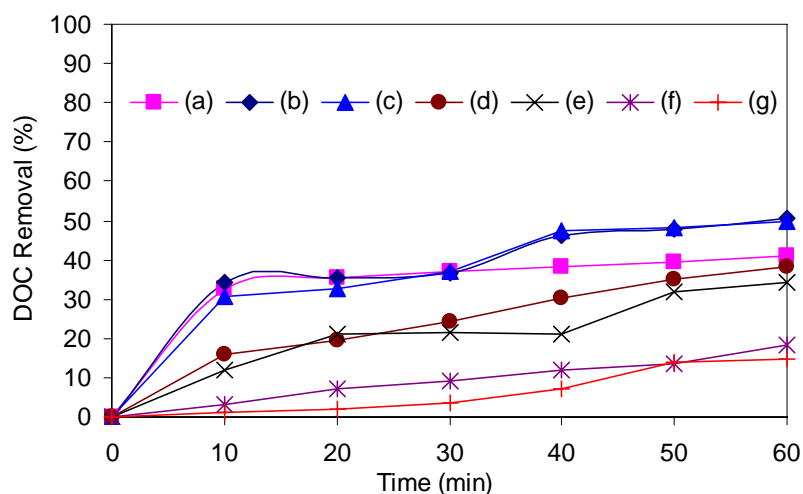


Figure 4.12 Effect of  $H_2O_2/Fe^{2+}$  molar ratio on antibiotics degradation by Fenton process in terms of DOC removal (a) 2.0, (b) 5.0, (c) 10.0, (d) 20.0, (e) 50.0, (f) 100 and (g) 150

The results agree well with the reported results for various pollutants – the optimum  $H_2O_2/Fe^{2+}$  molar ratio was 10 and 40 for chlorophenol and chlorinated aliphatics degradation (Tang and Huang, 1997; Pera-Titus *et al.*, 2004), 6.5 for cresols destruction (Kavitha and Palanivelu, 2005a), 5-40 for degradation of aromatic amines (Casero *et al.*, 1997) and 1.9–3.7 for degradation of trihalomethanes (Tang and Tassos, 1997). In the present study, COD and DOC removal and

BOD<sub>5</sub>/COD ratio improvement at low H<sub>2</sub>O<sub>2</sub>/Fe<sup>2+</sup> molar ratio is higher than that for high H<sub>2</sub>O<sub>2</sub>/Fe<sup>2+</sup> molar ratio. This may be explained taking into consideration the intermediates formed during reaction. Lower H<sub>2</sub>O<sub>2</sub>/Fe<sup>2+</sup> molar ratio causes a high removal of the target compound and formation of early intermediates (Pera-Titus *et al.*, 2004; González *et al.*, 2007).

### 4.1.3 Effect of pH

The pH value influences the generation of hydroxyl radicals in the Fenton process and hence the oxidation efficiency. To determine the optimum pH, experiments were conducted by varying the pH in the range 2-4. Initial AMX, AMP and CLX concentrations were 104, 105 and 103 mg/L, respectively (COD 520 mg/L; 16.25 mM). The other operating conditions were H<sub>2</sub>O<sub>2</sub>/COD molar ratio 3, H<sub>2</sub>O<sub>2</sub>/Fe<sup>2+</sup> molar ratio 10. Figures 4.13 and 4.14 show the effect of pH on AMX, AMP and CLX degradation in terms of COD and COD removal. COD after 60 min reaction time was 265, 220, 96, 120 and 127 mg/L (Figure 4.13); however, COD removal after 60 min reaction time was 49, 57.7, 81.5, 76.9 and 75.6% (Figure 4.14) at pH 2, 2.5, 3, 3.5 and 4, respectively. BOD<sub>5</sub> after 60 min reaction time was 35, 42, 32, 30 and 25 mg/L (Figure 4.15); however, BOD<sub>5</sub>/COD ratio after 60 min reaction time was 0.13, 0.19, 0.33, 0.35, 0.25 and 0.20 (Figure 4.16) at pH 2, 2.5, 3, 3.5 and 4, respectively. DOC after 60 min reaction time was 99, 84, 68, 75 and 77 mg/L (Figure 4.17); however, DOC removal after 60 min reaction time was 33.9, 43.5, 54.3, 50 and 48.4% (Figure 4.18) at pH 2, 2.5, 3, 3.5 and 4, respectively. Maximum COD removal, biodegradability improvement and DOC removal for the antibiotic aqueous solution containing AMX, AMP, and CLX was achieved at pH 3.

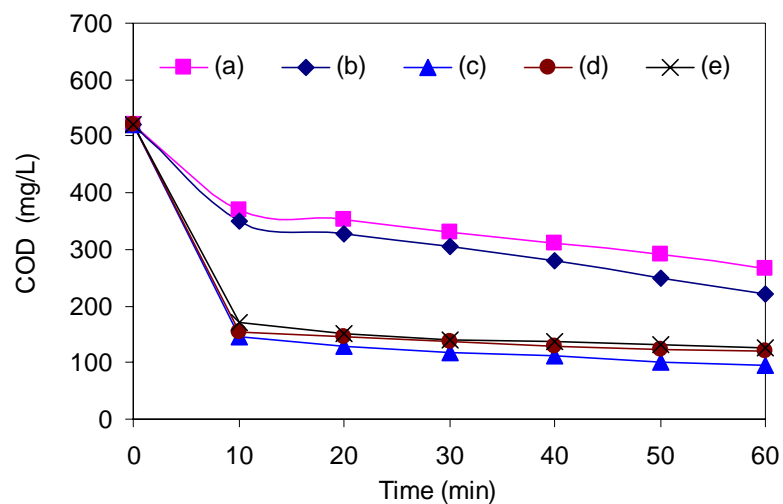


Figure 4.13 Effect of pH on antibiotics degradation by Fenton process in terms of COD (a) 2.0, (b) 2.5, (c) 3.0, (d) 3.5 and (e) 4.0

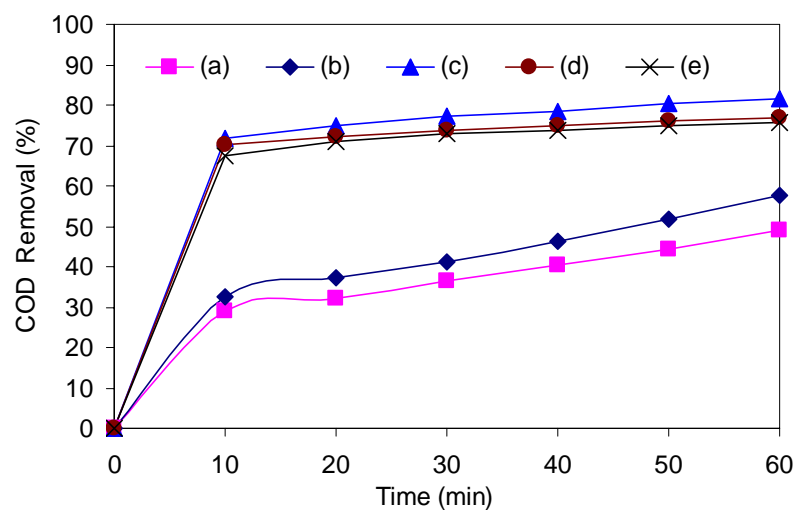


Figure 4.14 Effect of pH on antibiotics degradation by Fenton process in terms of COD removal (a) 2.0, (b) 2.5, (c) 3.0, (d) 3.5 and (e) 4.0

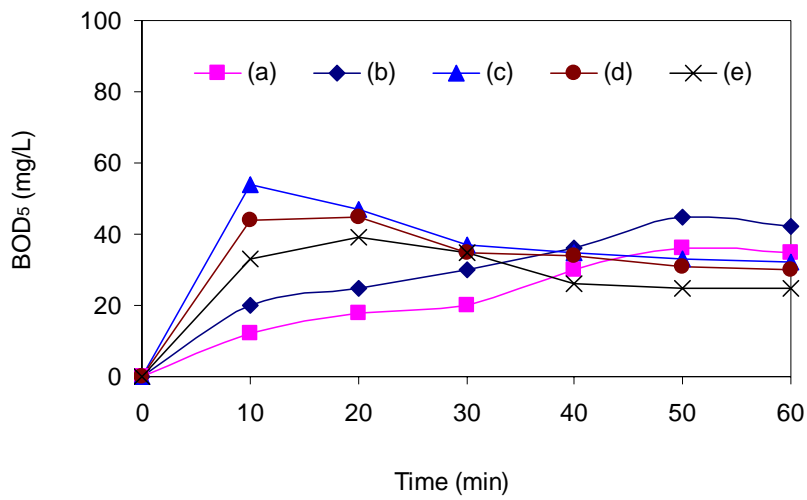


Figure 4.15 Effect of pH on antibiotics degradation by Fenton process in terms of BOD<sub>5</sub> (a) 2.0, (b) 2.5, (c) 3.0, (d) 3.5 and (e) 4.0

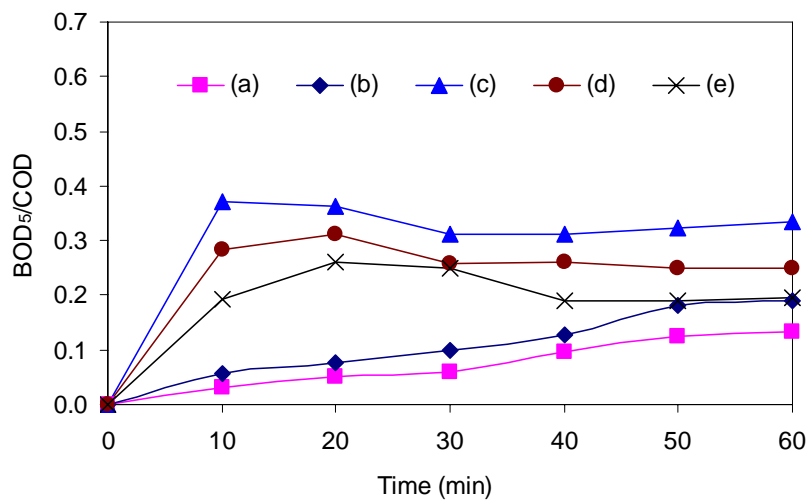


Figure 4.16 Effect of pH on antibiotics degradation by Fenton process in terms of BOD<sub>5</sub>/COD ratio (a) 2.0, (b) 2.5, (c) 3.0, (d) 3.5 and (e) 4.0



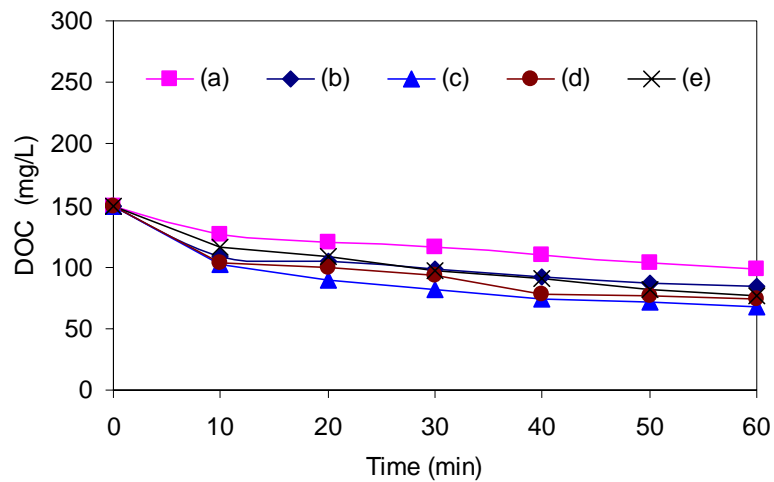


Figure 4.17 Effect of pH on antibiotics degradation by Fenton process in terms of DOC (a) 2.0, (b) 2.5, (c) 3.0, (d) 3.5 and (e) 4.0

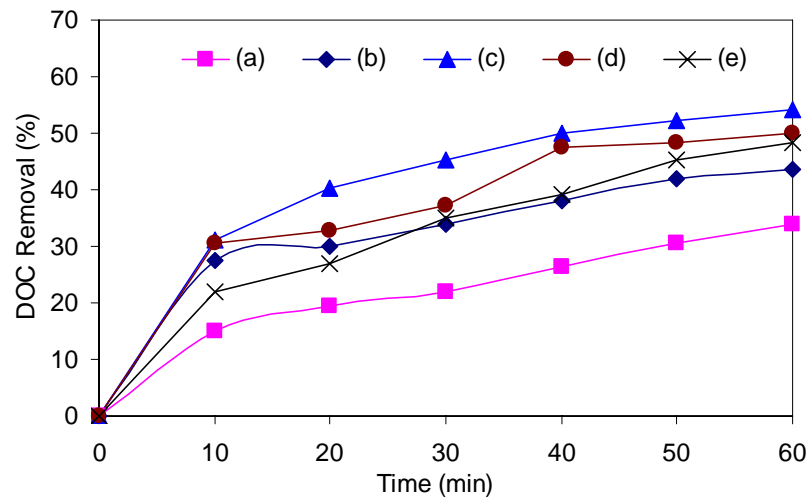


Figure 4.18 Effect of pH on antibiotics degradation by Fenton process in terms of DOC removal (a) 2.0, (b) 2.5, (c) 3.0, (d) 3.5 and (e) 4.0

The results show that pH significantly influences COD removal, biodegradability ( $BOD_5/COD$  ratio) improvement and DOC removal. Decrease in COD and DOC removal and biodegradability improvement at pH higher than 3 may be due to the decrease in dissolved iron (Zhao *et al.*, 2004; Kavitha and Palanivelu, 2005a; Tamimi *et al.*, 2008). At lower pH, organic degradation is lower and this may be due to the solvation of hydrogen peroxide in presence of high concentration of  $H^+$  to form

stable oxonium ion ( $\text{H}_3\text{O}_2^+$ ), thus reducing substantially its reactivity with ferrous ions (Kwon *et al.*, 1999). Therefore, the amount of hydroxyl radicals would decrease at low pH, decreasing degradation of antibiotic intermediates.

The calculated average oxidation state (AOS) using Equation 4.1 given by Bowers *et al.* (1989) reflects the degree of change in antibiotic structure after oxidation.

$$AOS = \frac{4(DOC-COD)}{DOC} \quad \text{Equation 4.1}$$

where, COD is expressed in moles  $\text{O}_2$  per litre and DOC in moles C per litre.

AOS of the treated antibiotic solution at pH 2 and 3 was 0.76 and 2.3, respectively. The high AOS value of the treated antibiotic solution at pH 3 indicates that the byproducts formed during the oxidation of antibiotic are highly biodegradable and less toxic (Kavitha and Palanivelu, 2005a). These results agree well with the reported results of oxidation of organic substances in wastewater such as creosol (Kavitha and Palanivelu, 2005a), methomyl (Tamimi *et al.*, 2008), dimethyl phthalate (Zhao *et al.*, 2004), p-chlorophenol (Kwon *et al.*, 1999) and p-nitroaniline (Sun *et al.*, 2008).

#### 4.1.4 Effect of Initial Antibiotic Concentration and Reaction Time

The efficiency of the Fenton process depends on the formation of hydroxyl radicals and less scavenging of hydroxyl radicals occurs as initial organic substrate concentration increases (Tekin *et al.*, 2006). To observe the effect of initial antibiotic concentration, experiments were conducted by varying the initial concentration of AMX, AMP and CLX as 100, 250 and 500 mg/L for each antibiotic in the aqueous solution. The corresponding COD were 520, 1229 and 2440 mg/L. The operating conditions were  $\text{H}_2\text{O}_2/\text{COD}$  molar ratio 3,  $\text{H}_2\text{O}_2/\text{Fe}^{2+}$  molar ratio 10 and pH 3.

Figures 4.13 and 4.14 show the effect of pH on AMX, AMX and CLX degradation in terms of COD and COD removal. COD after 60 min reaction time was 96, 290 and 595 mg/L (Figure 4.19); however, COD removal after 60 min reaction time was 81.4, 76.4 and 75.6% at initial antibiotic concentration 100, 250

and 500 mg/L, respectively for each antibiotic in the aqueous solution (Figure 4.20). BOD<sub>5</sub> after 60 min reaction time was 32, 80 and 170 mg/L (Figure 4.21). Figure 4.22 shows that the maximum BOD<sub>5</sub>/COD ratio was achieved at different reaction times – it was 0.37, 0.36 and 0.36 at reaction time 10, 20 and 40 min for initial antibiotics concentration 100, 250 and 500 mg/L, respectively. This may be due to the fact that concentration of recalcitrant byproducts is different at the same time for different antibiotic concentration. DOC after 60 min reaction time 68, 250 and 467 mg/L (Figure 4.23); however, DOC removal after 60 min reaction time was 54.3, 43.1 and 47.1% at initial antibiotic concentration 100, 250 and 500 mg/L, respectively for each antibiotic (Figure 4.24). The results show a marginal decrease in COD and DOC removal with increase in antibiotic concentration, indicating that the selected COD/H<sub>2</sub>O<sub>2</sub>/Fe<sup>2+</sup> molar ratio (1:3:0.30) is optimum for treatment of antibiotic wastewater with a wide range of antibiotic concentration.

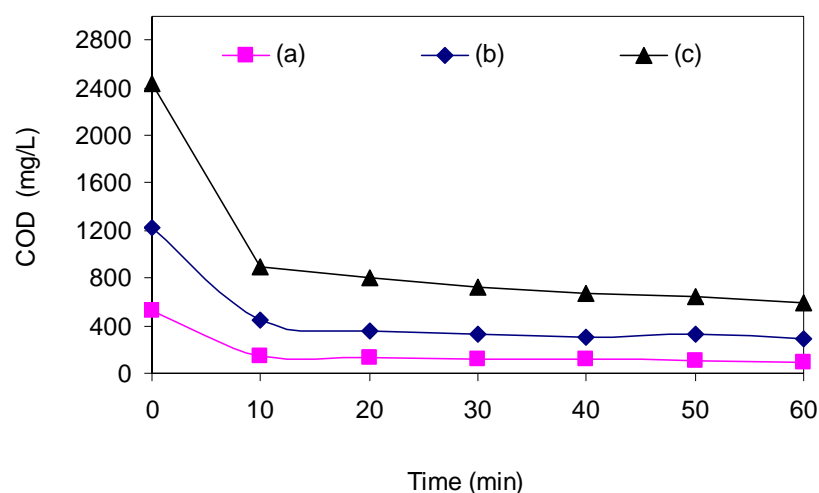


Figure 4.19 Effect of initial antibiotic concentration on antibiotics degradation by Fenton process in terms of COD (a) 100, (b) 250 and (c) 500 mg/L

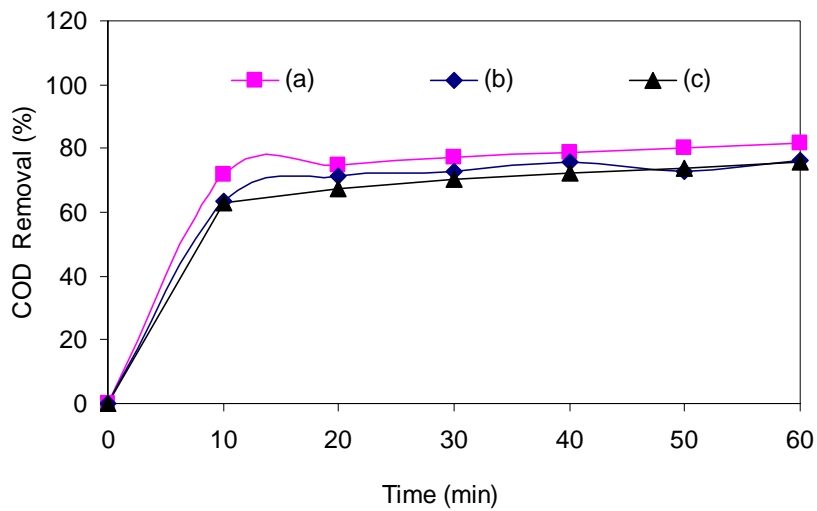


Figure 4.20 Effect of initial antibiotic concentration on antibiotics degradation by Fenton process in terms of COD removal (a) 100, (b) 250 and (c) 500 mg/L

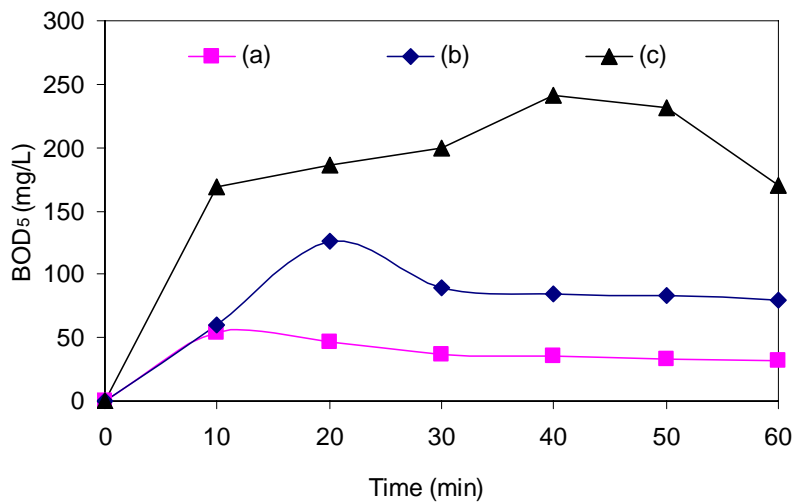


Figure 4.21 Effect of initial antibiotic concentration on antibiotics degradation by Fenton process in terms of BOD<sub>5</sub> (a) 100, (b) 250 and (c) 500 mg/L

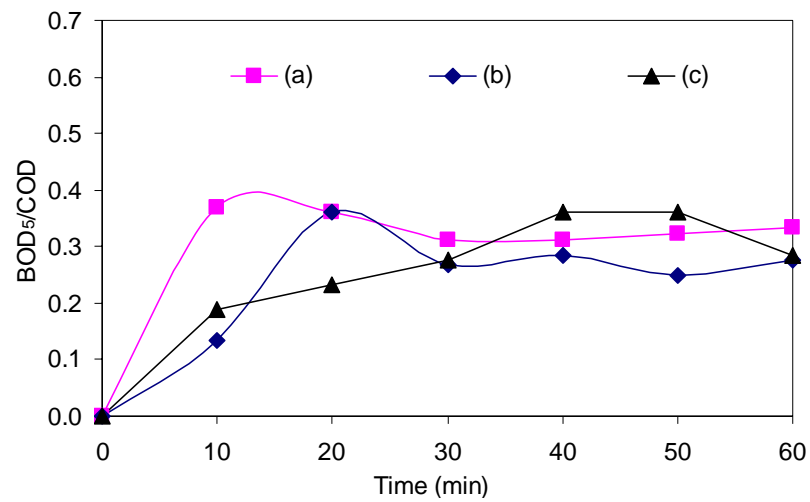


Figure 4.22 Effect of initial antibiotic concentration on antibiotics degradation by Fenton process in terms of BOD<sub>5</sub>/COD ratio (a) 100, (b) 250 and (c) 500 mg/L

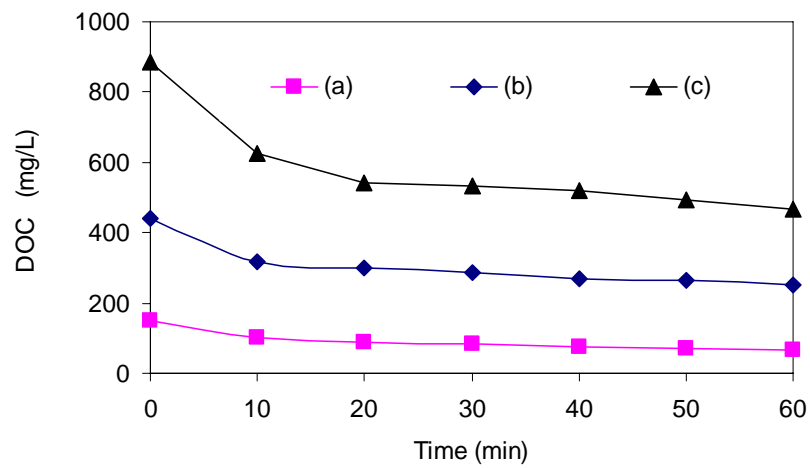


Figure 4.23 Effect of initial antibiotics concentration on antibiotics degradation by Fenton process in terms of DOC (a) 100, (b) 250 and (c) 500 mg/L

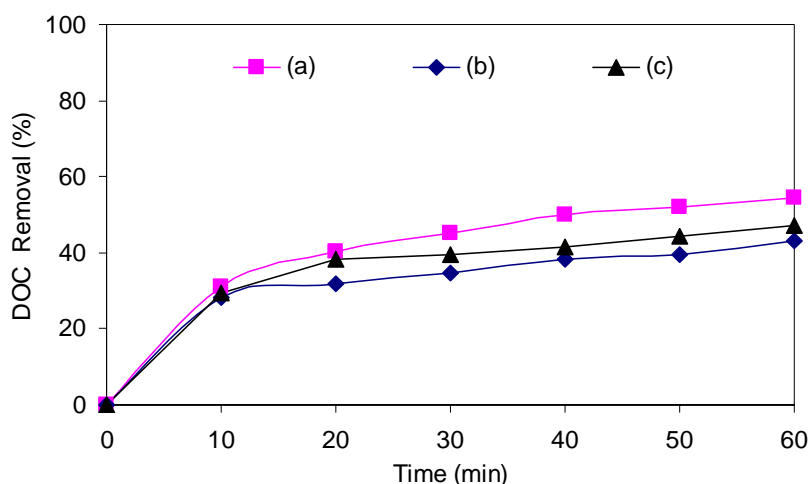


Figure 4.24 Effect of initial antibiotics concentration on antibiotics degradation by Fenton process in terms of DOC removal (a) 100, (b) 250 and (c) 500 mg/L

A statistical analysis (one-way ANOVA) performed on the results at a 5% level of significance indicated that COD removal was significantly affected by  $\text{H}_2\text{O}_2/\text{COD}$  molar ratio,  $\text{H}_2\text{O}_2/\text{Fe}^{2+}$  molar ratio and pH (Table 4.1). However there was no significant effect of antibiotic concentration on the COD removal.

Table 4.1 One-way ANOVA for COD removal at different  $\text{H}_2\text{O}_2/\text{COD}$  molar ratio,  $\text{H}_2\text{O}_2/\text{Fe}^{2+}$  molar ratio, pH and antibiotic concentration

parameter	No. of groups	F	P-value	F crit
$\text{H}_2\text{O}_2/\text{COD}$	6	3.662	0.009	2.477
$\text{H}_2\text{O}_2/\text{Fe}^{2+}$	7	3.162	0.012	2.324
pH	5	2.862	0.040	2.690
Antibiotic concentration	3	0.088	0.917	3.555

#### 4.1.5 Degradation of the Antibiotics in Aqueous Solution, Biodegradability Improvement and Mineralization under Optimum Fenton Operating Conditions

Figure 4.25 shows the degradation of the antibiotics (AMX 104 mg/L, AMP 105 mg/L and CLX 103 mg/L) in aqueous solution (COD 520 mg/L; 16.25 mM) under optimum operating conditions ( $\text{COD}/\text{H}_2\text{O}_2/\text{Fe}^{2+}$  molar ratio 1:3:0.3 and pH 3). Complete degradation of all antibiotics was achieved in 2.0 min. These results agree

well with that reported by Trovo' et al (2008) for degradation of amoxicillin and bezafibrate in aqueous solution by the photo-Fenton process.

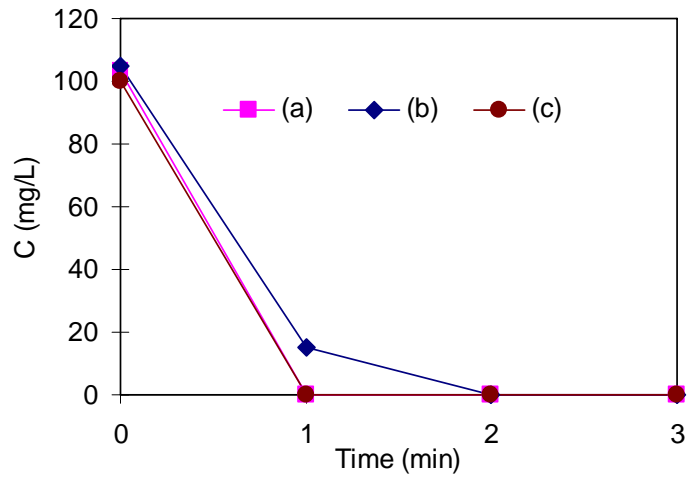


Figure 4.25 Degradation of AMX, AMP and CLX under optimum Fenton operating conditions (a) AMX, (b) AMP and (c) CLX

Figure 4.26 shows degradation of the antibiotics AMX, AMP and CLX in aqueous solution in terms of COD, BOD<sub>5</sub> and biodegradability (BOD<sub>5</sub>/COD ratio) improvement. COD decreased from 520 mg/L (initial value) to 146 mg/L in 10 min, whereas BOD<sub>5</sub> increased from zero to 54 mg/L. The corresponding BOD<sub>5</sub>/COD ratio was 0.37 which may be considered adequate for biological treatment as a wastewater is biodegradable if BOD<sub>5</sub>/COD ratio is 0.4 (Al-Momani *et al.*, 2002).

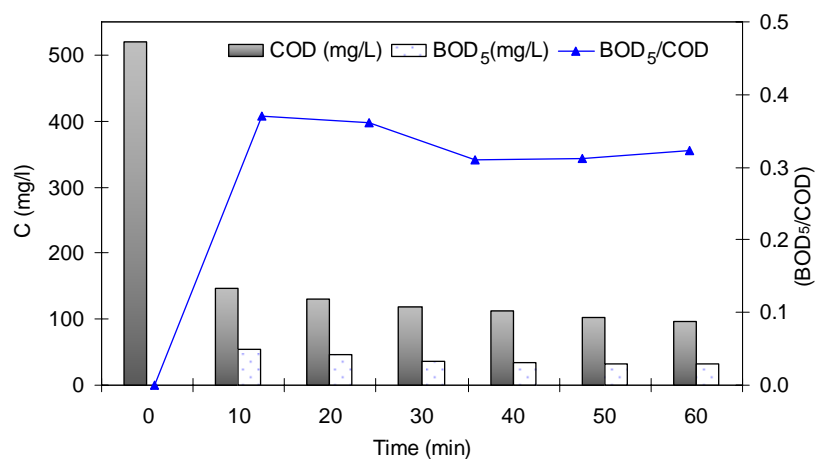


Figure 4.26 Degradation of antibiotics in terms of COD, BOD<sub>5</sub> and BOD<sub>5</sub>/COD ratio under optimum Fenton operating conditions

To assess the degree of mineralization, DOC removal and increase in nitrate concentration were measured. Mineralization of organic carbon and nitrogen compounds are verified by the results presented in Figure 4.27. DOC removal was 31.2, 40.3, 45.2, 50, 52.2 and 54.3% at reaction time 10, 20, 30, 40, 50 and 60 min, respectively and concentration of nitrate ( $\text{NO}_3^-$ ) increased from 0.3 to 10 mg/L in 60 min.

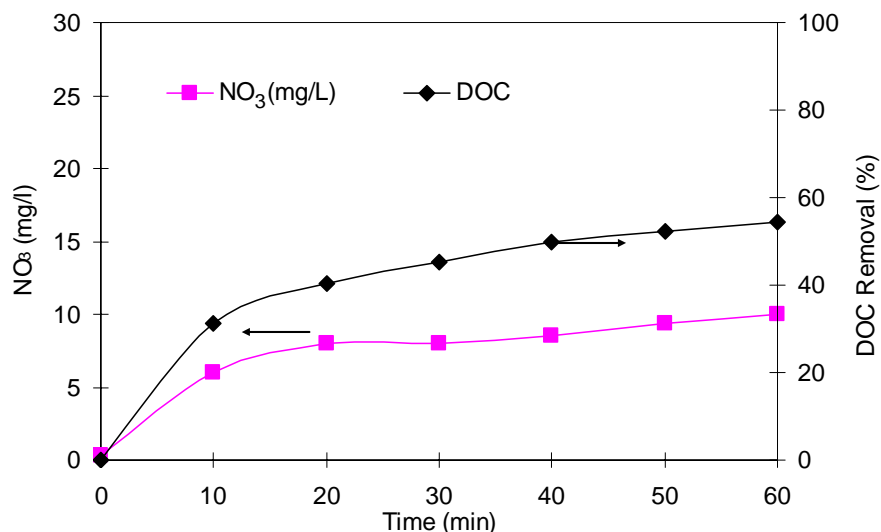


Figure 4.27 Mineralization of organic carbon and nitrogen in terms of DOC removal and nitrate concentration under optimum Fenton operating conditions

#### 4.1.6 Kinetic Study

Figure 4.28 shows the plots of  $-\ln \frac{[DOC]}{[DOC_0]}$  versus reaction time for antibiotic mineralization by the Fenton process under optimum operating conditions (COD/ $\text{H}_2\text{O}_2$ / $\text{Fe}^{2+}$  molar ratio 1:3:0.3 and pH 3). The linearity of the plot suggests that the Fenton reaction approximately followed the pseudo-first order kinetics with rate constant of  $0.01 \text{ min}^{-1}$  and  $t_{1/2}$  69.3 min.



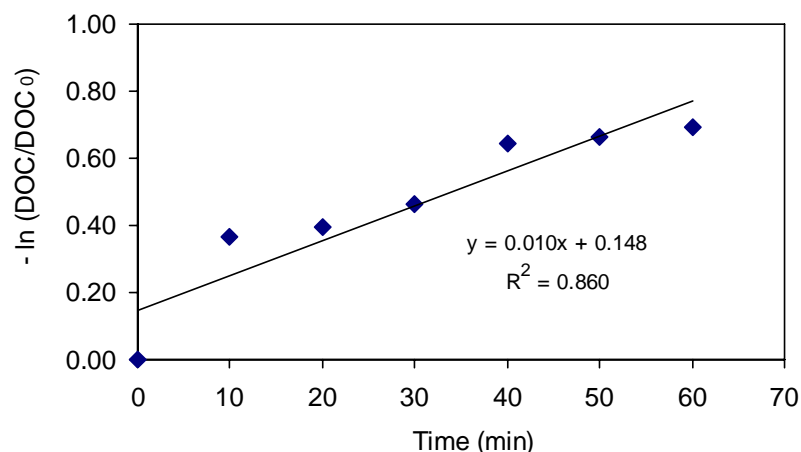


Figure 4.28 Kinetics of antibiotic mineralization by the Fenton process

## 4.2 Photo-Fenton Process

Effect of the operating conditions of the photo-Fenton process such as  $\text{H}_2\text{O}_2/\text{COD}$  molar ratio,  $\text{H}_2\text{O}_2/\text{Fe}^{2+}$  molar ratio, pH, initial antibiotic concentration and irradiation time on antibiotic degradation, mineralization and biodegradability improvement were studied.

### 4.2.1 Effect of UV Irradiation

Photolysis occurs when chemical substances absorb light. The photolysis of the antibiotics due to UV irradiation *per se* was studied. The experimental conditions were initial AMX, AMP and CLX concentration 104, 105, 103 mg/L, respectively and pH 5. By 5-hr UV irradiation, degradation was 2.9, 3.8 and 4.9% for AMX, AMP and CLX, respectively. Amoxicillin and cloxacillin show maximum absorbance at 245 and 250 nm, respectively and they can absorb light below 300 nm. So, no significant degradation was expected due to UV 365 nm irradiation *per se* and presumably the degradation was due to antibiotic hydrolysis. The hydrolysis reaction would proceed through the attack of the nucleophile  $\text{H}_2\text{O}$  to the  $\beta$ -lactam ring followed by ring opening (Andreozzi *et al.*, 2005). Further, it is known that  $\text{H}_2\text{O}_2$  has a maximum absorbance at 210–230 nm and  $\text{H}_2\text{O}_2$  proteolysis takes place to a small extent at wavelength 365 nm (Pignatello, 1992) and iron photo-redox also takes

place under wave length  $\approx 365$  nm (Al Momani, 2006). Consequently, degradation of the studied antibiotics when subjected to photo-Fenton reaction at wavelength 365 nm will be mainly due to the hydroxyl radical produced from the photo-Fenton reaction as in Reaction 2.1 and 2.11.

#### 4.2.2 Effect of $H_2O_2$ /COD Molar Ratio

To determine the optimum  $H_2O_2$ /COD molar ratio, initial AMX, AMP and CLX concentration were 104, 105 and 103 mg/L, respectively in the aqueous solution (COD 520 mg/L; 16.25 mM) and  $H_2O_2$  concentration was varied in the range 15-40 mM, corresponding  $H_2O_2$ /COD molar ratios were 1, 1.5, 2 and 2.5. The other operating conditions were pH 3.5 and  $H_2O_2/Fe^{2+}$  molar ratio 50. Figures 4.29 and 4.30 show the effect of  $H_2O_2$ /COD molar ratio on AMX, AMX and CLX degradation in terms of COD and COD removal. COD after 50 min reaction time was 175, 145, 205 and 280 mg/L (Figure 4.29); however, COD removal after 50 min reaction time was 66.3, 72.1, 60.6 and 46.2% at  $H_2O_2$ /COD molar ratio 1, 1.5, 2 and 2.5, respectively (Figure 4.30).  $BOD_5$  after 50 min reaction time was 32, 34, 33 and 31 mg/L (Figure 4.31); however,  $BOD_5$ /COD ratio after 50 min reaction time was 0.05, 0.07, 0.21, 0.28, 0.31 and 0.29 (Figure 4.32) at  $H_2O_2$ /COD molar ratio 1, 1.5, 2 and 2.5, respectively. DOC after 50 min reaction time was 88, 81, 89 and 88 mg/L (Figure 4.33); however, DOC removal after 50 min reaction time was 13.3, 19.8, 30.1, 34.4 and 35.6% (Figure 4.34) at  $H_2O_2$ /COD molar ratio 1, 1.5, 2 and 2.5, respectively. Maximum COD removal, biodegradability ( $BOD_5$ /COD ratio) improvement and DOC removal was achieved at  $H_2O_2$ /COD molar ratio 1.5. The results show increase in COD removal,  $BOD_5$ /COD ratio and DOC removal at  $H_2O_2$ /COD molar ratio 1-1.5 and further increase in  $H_2O_2$ /COD molar ratio did not improve the degradation. This may be due to scavenging of  $OH^\bullet$  by  $H_2O_2$  as in Reaction 2.6 (Kavitha and Palanivelu, 2005a).

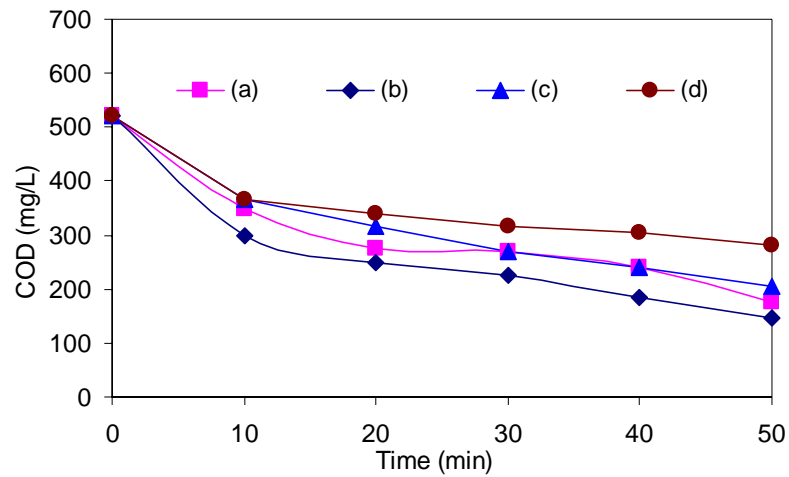


Figure 4.29 Effect of  $H_2O_2$ /COD molar ratio on antibiotics degradation by photo-Fenton process in terms of COD (a) 1.0, (b) 1.5, (c) 2.0 and (d) 2.5

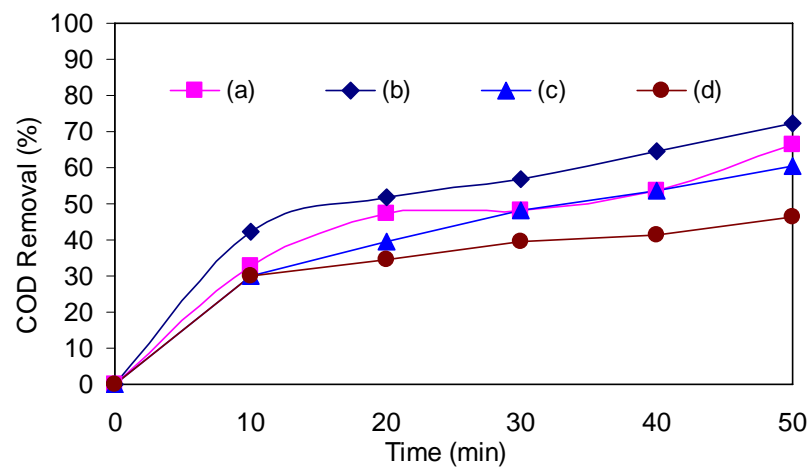


Figure 4.30 Effect of  $H_2O_2$ /COD molar ratio on antibiotics degradation by photo-Fenton process in terms of COD removal (a) 1.0, (b) 1.5, (c) 2.0 and (d) 2.5

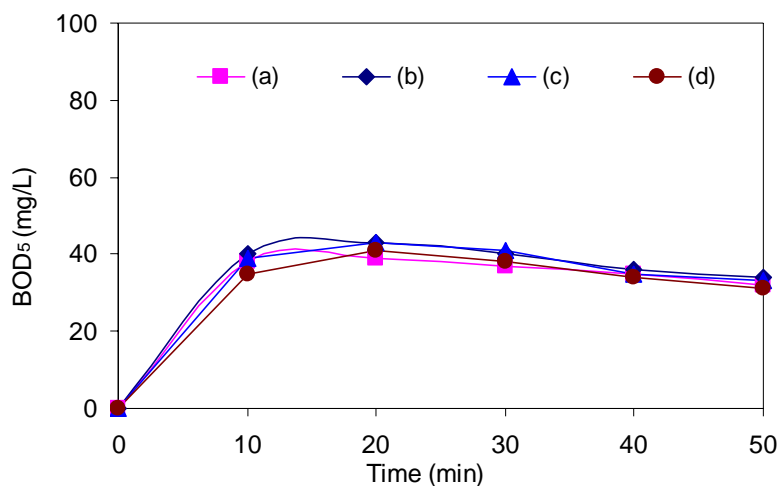


Figure 4.31 Effect of  $H_2O_2/COD$  molar ratio on antibiotics degradation by photo-Fenton process in terms of  $BOD_5$  (a) 1.0, (b) 1.5, (c) 2.0 and (d) 2.5

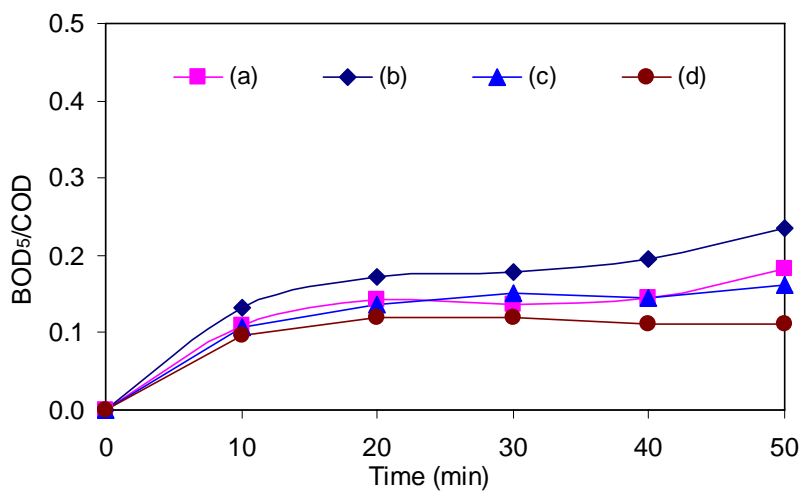


Figure 4.32 Effect of  $H_2O_2/COD$  molar ratio on antibiotics degradation by photo-Fenton process in terms of  $BOD_5/COD$  ratio (a) 1.0, (b) 1.5, (c) 2.0 and (d) 2.5

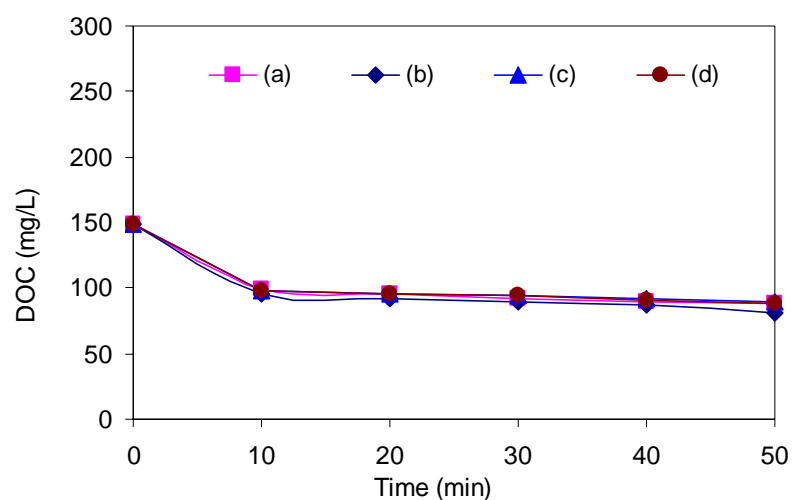


Figure 4.33 Effect of H<sub>2</sub>O<sub>2</sub>/COD molar ratio on antibiotics degradation by photo-Fenton process in terms of DOC (a) 1.0, (b) 1.5, (c) 2.0 and (d) 2.5

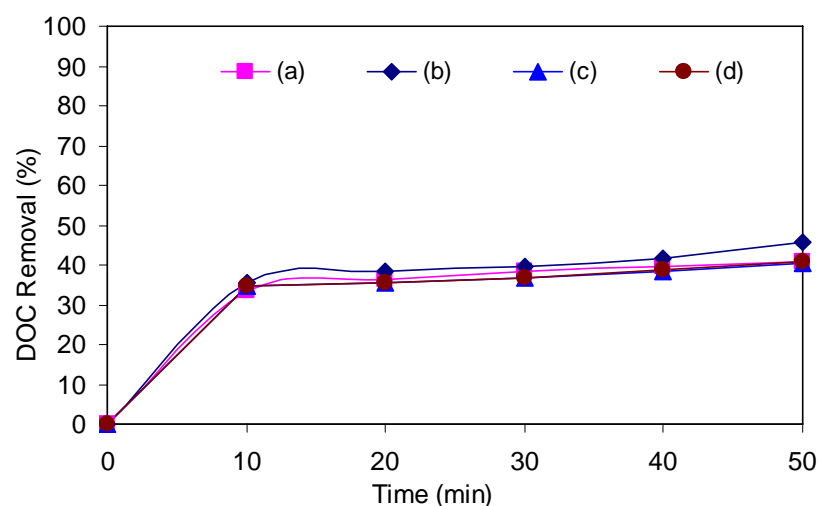


Figure 4.34 Effect of H<sub>2</sub>O<sub>2</sub>/COD molar ratio on antibiotics degradation by photo-Fenton process in terms of DOC removal (a) 1.0, (b) 1.5, (c) 2.0 and (d) 2.5

#### 4.2.3 Effect of H<sub>2</sub>O<sub>2</sub>/Fe<sup>2+</sup> Molar Ratio

To determine the optimum H<sub>2</sub>O<sub>2</sub>/Fe<sup>2+</sup> molar ratio, experiments were conducted at pH 3.5 with constant H<sub>2</sub>O<sub>2</sub> concentration of 24.3 mM and varying Fe<sup>2+</sup> concentration in the range 0.16-2.4 mM. The corresponding H<sub>2</sub>O<sub>2</sub>/Fe<sup>2+</sup> molar ratio was in the range 10-150. Initial AMX, AMP and CLX concentration were 104, 105 and 103 mg/L, respectively in the aqueous solution (COD 520 mg/L; 16.25 mM), giving a

$\text{H}_2\text{O}_2/\text{COD}$  molar ratio 1.5. Figures 4.7 and 4.8 show the effect of  $\text{H}_2\text{O}_2/\text{Fe}^{2+}$  molar ratio on AMX, AMX and CLX degradation in terms of COD and COD removal. COD after 50 min reaction time was 125, 130, 145, 240 and 270 mg/L (Figure 4.35); however, COD removal after 50 min reaction time was 76.0, 76.0, 72.1, 53.8 and 48.1% (Figure 4.36) at  $\text{H}_2\text{O}_2/\text{Fe}^{2+}$  molar ratio 10, 20, 50, 100 and 150, respectively.  $\text{BOD}_5$  after 50 min reaction time was 43, 44, 34, 33 and 33 mg/L (Figure 4.37); however,  $\text{BOD}_5/\text{COD}$  ratio after 50 min reaction time was 0.34, 0.34, 0.23, 0.14 and 0.12 (Figure 4.38) at  $\text{H}_2\text{O}_2/\text{Fe}^{2+}$  molar ratio 10, 20, 50, 100 and 150, respectively. DOC after 50 min reaction time was 80, 80, 81, 96 and 99 mg/L (Figure 4.39); however, DOC removal after 50 min reaction time was 46.6, 46.3, 45.6, 35.6 and 33.6% (Figure 4.40) at  $\text{H}_2\text{O}_2/\text{Fe}^{2+}$  molar ratio 10, 20, 50, 100 and 150, respectively.

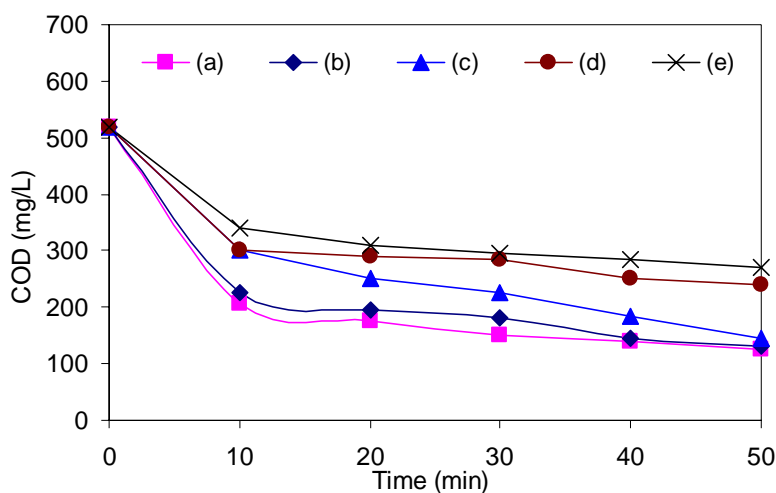


Figure 4.35 Effect of  $\text{H}_2\text{O}_2/\text{Fe}^{2+}$  molar ratio on antibiotics degradation by photo-Fenton process in terms of COD removal (a) 10, (b) 20, (c) 50, (d) 100 and (e) 150

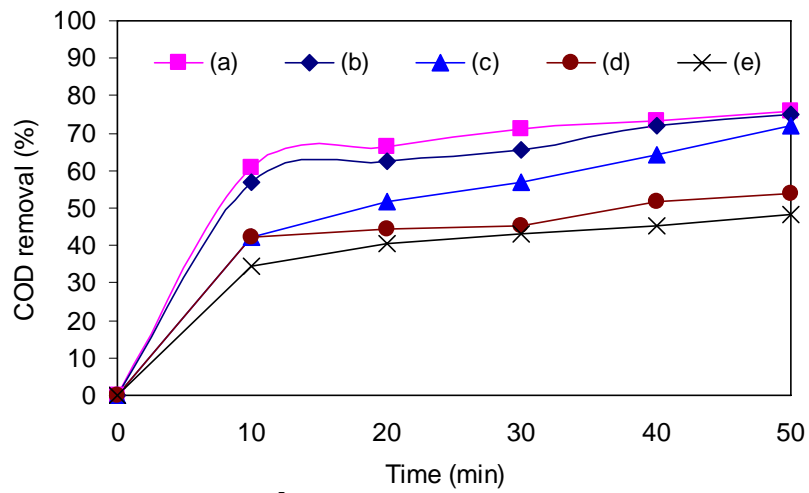


Figure 4.36 Effect of  $\text{H}_2\text{O}_2/\text{Fe}^{2+}$  molar ratio on antibiotics degradation by photo-Fenton process in terms of COD removal (a) 10, (b) 20, (c) 50, (d) 100 and (e) 150

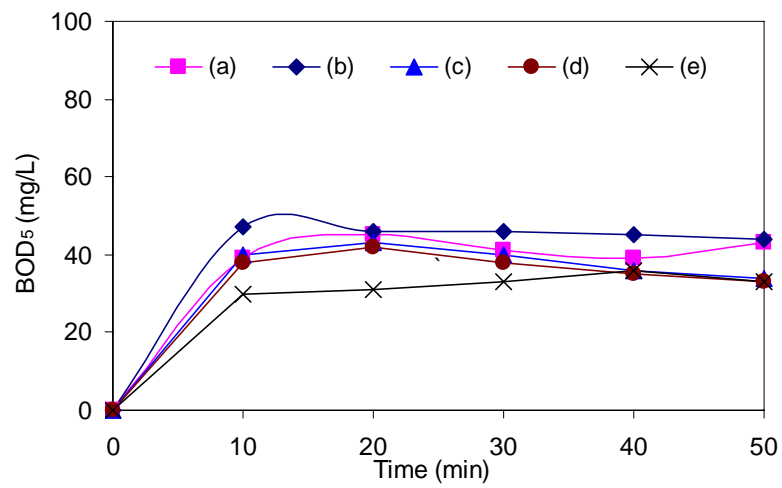


Figure 4.37 Effect of  $\text{H}_2\text{O}_2/\text{Fe}^{2+}$  molar ratio on antibiotics degradation by photo-Fenton process in terms of BOD<sub>5</sub> (a) 10, (b) 20, (c) 50, (d) 100 and (e) 150

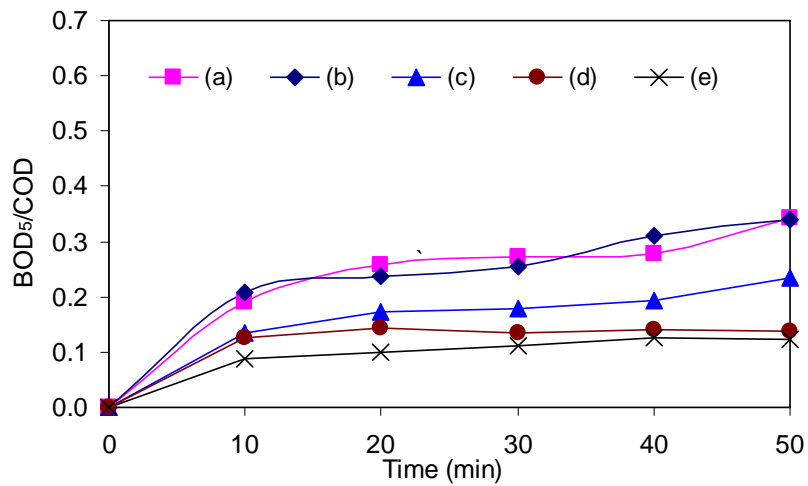


Figure 4.38 Effect of H<sub>2</sub>O<sub>2</sub>/Fe<sup>2+</sup> molar ratio on antibiotics degradation by photo-Fenton process in terms of BOD<sub>5</sub>/COD ratio (a) 10, (b) 20, (c) 50, (d) 100 and (e)

150

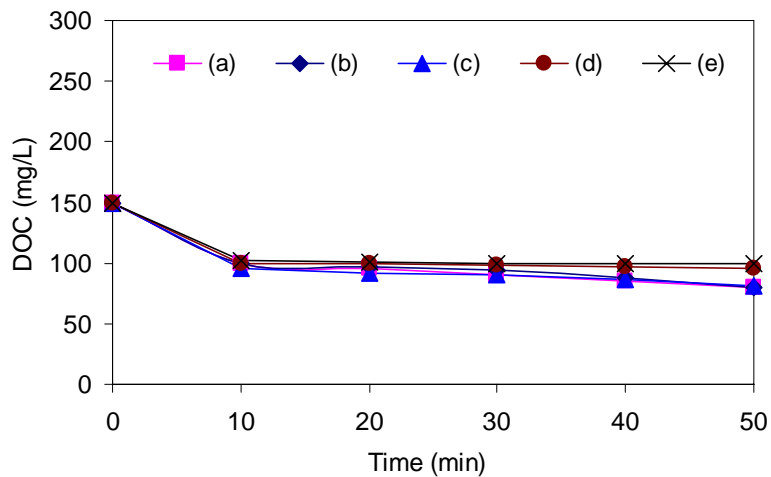


Figure 4.39 Effect of H<sub>2</sub>O<sub>2</sub>/ Fe<sup>2+</sup> molar ratio on antibiotics degradation by photo-Fenton process in terms of DOC (a) 10, (b) 20, (c) 50, (d) 100 and (e) 150



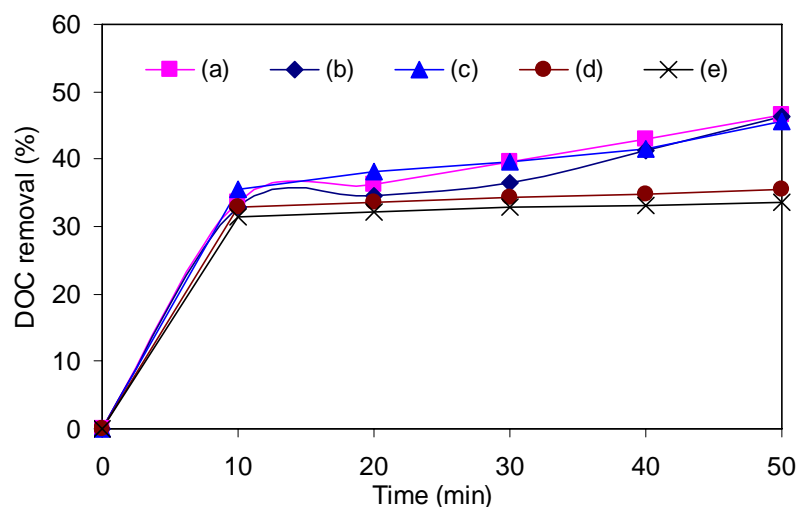


Figure 4.40 Effect of  $\text{H}_2\text{O}_2/\text{Fe}^{2+}$  molar ratio on antibiotics degradation by photo-Fenton process in terms of DOC removal (a) 10, (b) 20, (c) 50, (d) 100 and (e) 150

The results show increase in COD removal,  $\text{BOD}_5/\text{COD}$  ratio and DOC removal with decrease in  $\text{H}_2\text{O}_2/\text{Fe}^{2+}$  molar ratio up to 20. Further decrease in  $\text{H}_2\text{O}_2/\text{Fe}^{2+}$  molar ratio did not improve the degradation. This may be due to direct reaction of  $\text{OH}^\bullet$  radical with metal ions at high concentration of  $\text{Fe}^{2+}$  as in Reaction 2.5 (Joseph *et al.*, 2000).

Due to the similarity of the results for  $\text{H}_2\text{O}_2/\text{Fe}^{2+}$  molar ratio 20 and 10, a statistical analysis (one-way ANOVA) was performed on the COD removal results at a 5% level of significance in order to determine the optimum  $\text{H}_2\text{O}_2/\text{Fe}^{2+}$  molar ratio. The statistical analysis indicated that P-value between two variables ( $\text{H}_2\text{O}_2/\text{Fe}^{2+}$  molar ratio 20 and 10) was 0.878 ( $> 0.05$ ) and therefore the null hypothesis that performance of the photo-Fenton process was different at  $\text{H}_2\text{O}_2/\text{Fe}^{2+}$  molar ratio 20 and 10 was rejected. Thus, the optimum  $\text{H}_2\text{O}_2/\text{Fe}^{2+}$  molar ratio for treatment of the antibiotic aqueous solution is 20.

#### 4.2.4 Effect of pH

The pH value influences the generation of hydroxyl radicals in the photo-Fenton process and hence the oxidation efficiency. To determine the optimum pH, experiments were conducted by varying the pH in the range 2-4. Initial AMX, AMP and CLX concentration were 104, 105 and 103 mg/L, respectively in the aqueous

solution (COD 520 mg/L; 16.25 mM). The other operating conditions were  $\text{H}_2\text{O}_2/\text{COD}$  molar ratio 1.5 and  $\text{H}_2\text{O}_2/\text{Fe}^{2+}$  molar ratio 20.

Figures 4.41 and 4.42 show the effect of pH on AMX, AMX and CLX degradation in terms of COD and COD removal. COD after 50 min reaction time was 300, 150, 100, 130 and 140 mg/L (Figure 4.41); however, COD removal after 50 min reaction time was 42.3, 73.1, 80.8, 76.0 and 74.1% (Figure 4.42) at pH 2, 2.5, 3, 3.5 and 4, respectively.  $\text{BOD}_5$  after 50 min reaction time was 40, 42, 39, 44 and 38 mg/L (Figure 4.43); however,  $\text{BOD}_5/\text{COD}$  ratio after 50 min reaction time was 0.13, 0.3, 0.4, 0.34 and 0.29 (Figure 4.44) at pH 2, 2.5, 3, 3.5 and 4, respectively. DOC after 50 min reaction time was 100, 89, 62, 80 and 81mg/L (Figure 4.45); however, DOC removal after 50 min reaction time was 32.9, 40.3, 58.4, 46.3 and 45.6% (Figure 4.46) at pH 2, 2.5, 3, 3.5 and 4, respectively. Based on the results, the optimum pH for treatment of the antibiotic aqueous solution is 3.

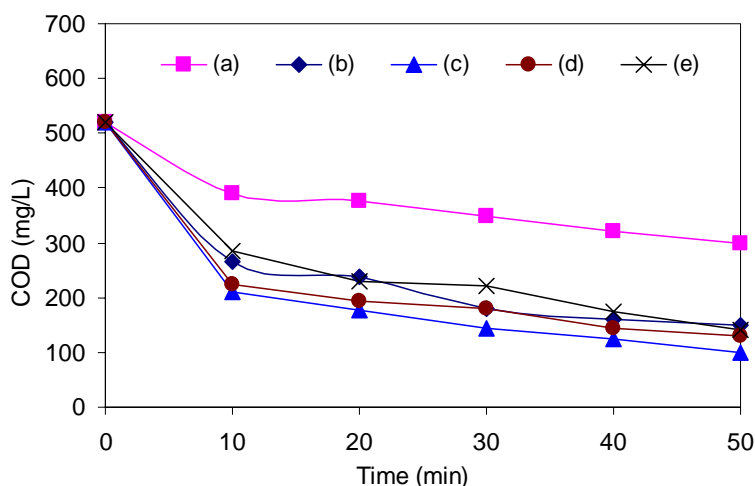


Figure 4.41 Effect of pH on antibiotics degradation by photo-Fenton process in terms of COD for pH (a) 2.0, (b) 2.5, (c) 3.0, (d) 3.5 and (e) 4.0

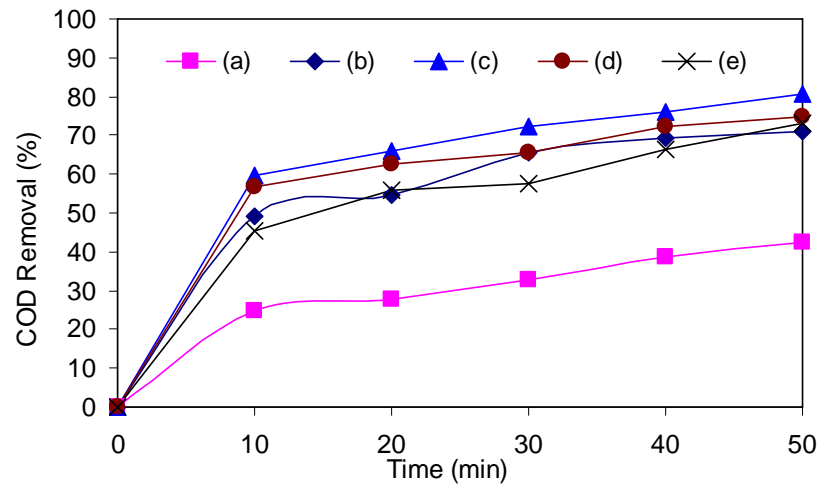


Figure 4.42 Effect of pH on antibiotics degradation by photo-Fenton process in terms of COD removal for pH (a) 2.0, (b) 2.5, (c) 3.0, (d) 3.5 and (e) 4.0

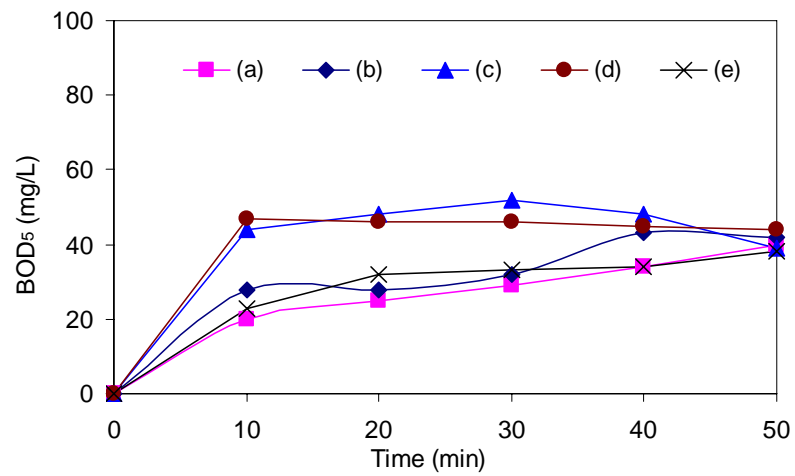


Figure 4.43 Effect of pH on antibiotics degradation by photo-Fenton process in terms of BOD<sub>5</sub> for pH (a) 2.0, (b) 2.5, (c) 3.0, (d) 3.5 and (e) 4.0

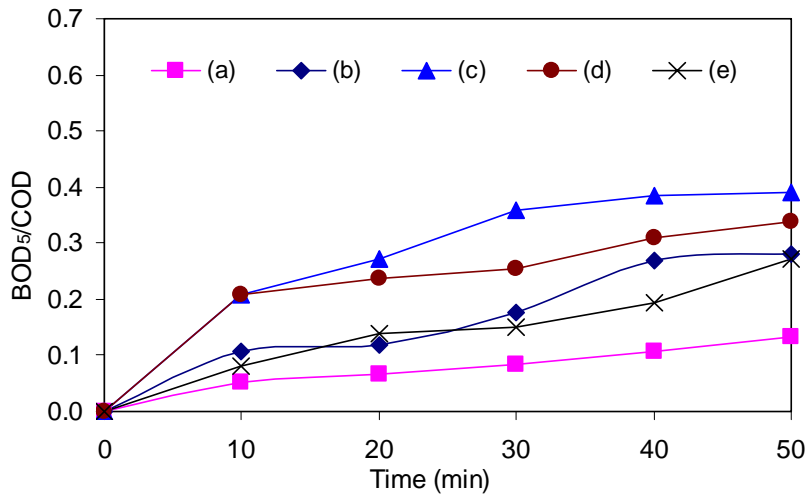


Figure 4.44 Effect of pH on antibiotics degradation by photo-Fenton process in terms of BOD<sub>5</sub>/COD for pH (a) 2.0, (b) 2.5, (c) 3.0, (d) 3.5 and (e) 4.0

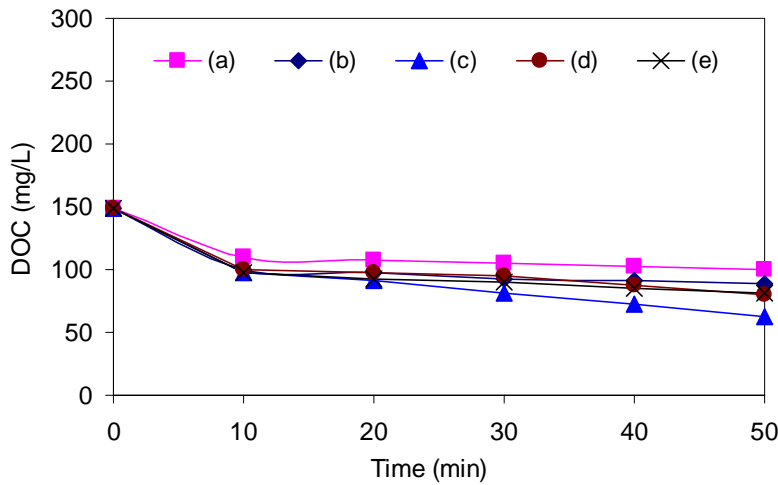


Figure 4.45 Effect of pH on antibiotics degradation by photo-Fenton process in terms of DOC removal for pH (a) 2.0, (b) 2.5, (c) 3.0, (d) 3.5 and (e) 4.0

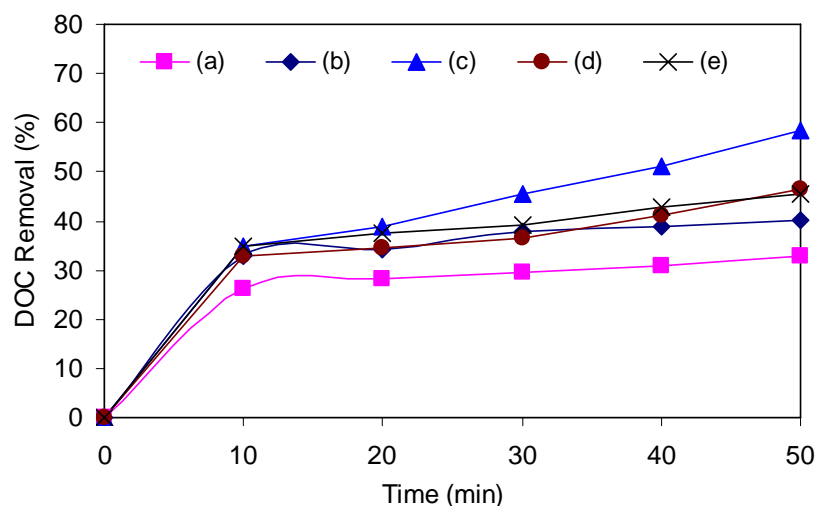


Figure 4.46 Effect of pH on antibiotics degradation by photo-Fenton process in terms of DOC removal for pH (a) 2.0, (b) 2.5, (c) 3.0, (d) 3.5 and (e) 4.0

The results show that pH significantly influences COD removal, biodegradability ( $BOD_5/COD$  ratio) improvement and DOC removal. Maximum degradation was achieved at pH 3 and it decreased at lower and higher pH. This can be explained by taking into consideration the effect of pH on the formation of ferric iron complex species in aqueous solution (Table 4.2). At pH 2-3, the main ferric iron complex species is  $[Fe(OH)(H_2O)_5]^{2+}$  which has the largest light absorption coefficient and quantum yield for  $OH^\bullet$  production, along with  $Fe^{2+}$  regeneration in the range 280–370 nm (Benkelberg and Warneck, 1995). At lower pH,  $[Fe(H_2O)_6]^{3+}$  is more predominant and so the effectiveness of light absorption, regeneration of  $Fe^{2+}$  and organic degradation is lower. In addition, hydrogen peroxide gets solvated in the presence of high concentration of  $H^+$  to form stable oxonium ion ( $H_3O_2^+$ ), thus reducing substantially its reactivity with ferrous ions (Kwon *et al.*, 1999). At higher pH  $[Fe(OH)_2(H_2O)_4]^+$  dominates, but the solution becomes unstable with  $Fe(OH)_3$  precipitation (Benkelberg and Warneck, 1999).

Table 4.2 Predominant ferric iron complex species in aqueous solution at different pH ranges

Ferric iron species	pH range
$[\text{Fe}(\text{H}_2\text{O})_6]^{3+}$	1–2
$[\text{Fe}(\text{OH})(\text{H}_2\text{O})_5]^{2+}$	2–3
$[\text{Fe}(\text{OH})_2(\text{H}_2\text{O})_4]^+$	3–4

Also, the calculated average oxidation state (AOS) using Equation 4.1 given by Bowers *et al.* (1989) reflects the degree of change in antibiotic structure after oxidation. AOS of the treated antibiotic aqueous solution at pH 2 and 3 are -0.50 and 1.58, respectively. The high AOS value of the treated antibiotic aqueous solution at pH 3 indicates that the byproducts formed during oxidation of the antibiotics are highly biodegradable and less toxic (Kavitha and Palanivelu, 2005a). These results agree well with that of oxidation of organic substances in wastewater such as p-chlorophenol (Bowers *et al.*, 1989), methomyl (Tamimi *et al.*, 2008), dimethyl phthalate (Zhao *et al.*, 2004), creosol (Kavitha and Palanivelu, 2005a) and p-nitroaniline (Sun *et al.*, 2008).

#### 4.2.5 Effect of Initial Antibiotic Concentration and Irradiation Time

To determine the effect of initial antibiotic concentration, experiments were conducted by varying the initial concentration of AMX, AMP and CLX as 100, 250 and 500 mg/L for each antibiotic in the aqueous solution. The corresponding COD were 520, 1229 and 2440 mg/L, respectively. The operating conditions were  $\text{H}_2\text{O}_2/\text{COD}$  molar ratio 1.5,  $\text{H}_2\text{O}_2/\text{Fe}^{2+}$  molar ratio 20 and pH 3.

Figures 4.47 and 4.48 show the effect of pH on AMX, AMX and CLX degradation in terms of COD and COD removal. COD after 50 min reaction time was 100, 302 and 680mg/L (Figure 4.47); however, COD removal after 50 min reaction time was 80.8, 74.9 and 72.3% at initial antibiotic concentration 100, 250 and 500 mg/L, respectively for each antibiotic in the aqueous solution (Figure 4.48).  $\text{BOD}_5$  after 50 min reaction time was 39, 109 and 236 mg/L (Figure 4.49); however,  $\text{BOD}_5/\text{COD}$  ratio after 50 min reaction time was 0.4, 0.36 and 0.34 at initial antibiotics concentration 100, 250 and 500 mg/L, respectively for each antibiotic in

the aqueous solution (Figure 4.50). DOC after 50 min reaction time 62, 169 and 434 mg/L (Figure 4.51); however, DOC removal after 50 min reaction time was 58.4, 47.4 and 33.2% at initial antibiotic concentration 100, 250 and 500 mg/L, respectively for each antibiotic (Figure 4.52). Marginal decrease in COD degradation and BOD<sub>5</sub>/COD ratio with increasing antibiotic concentration indicate that the selected operating conditions (H<sub>2</sub>O<sub>2</sub>/COD molar ratio 1.5, H<sub>2</sub>O<sub>2</sub>/Fe<sup>2+</sup> molar ratio 20 and pH 3) are optimum for treatment of antibiotic wastewater with a wide range of antibiotic concentration.

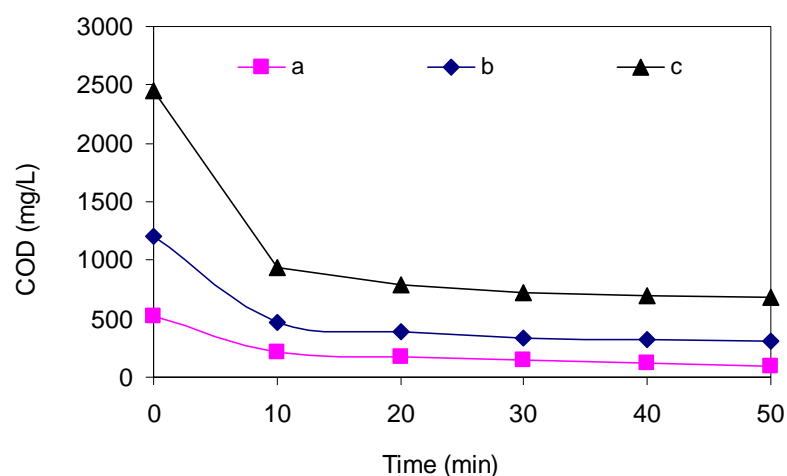


Figure 4.47 Effect of initial antibiotic concentration on antibiotics degradation by photo-Fenton process in terms of COD removal (a) 100, (b) 250 and (c) 500 mg/L

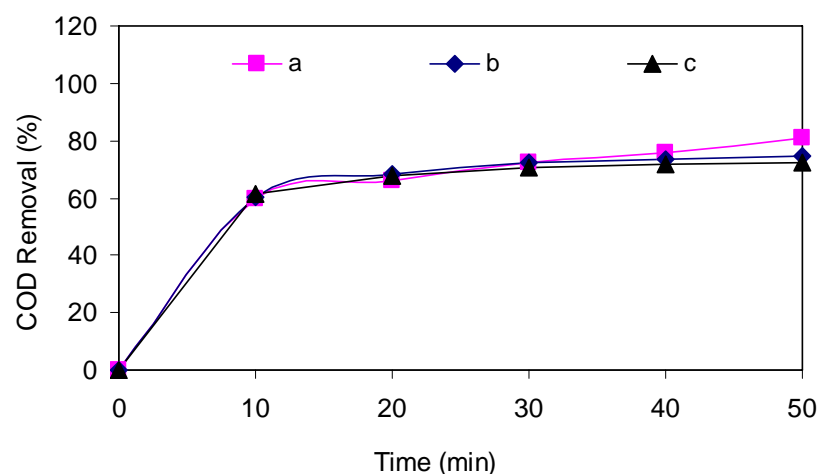


Figure 4.48 Effect of initial antibiotic concentration on antibiotics degradation by photo-Fenton process in terms of COD removal (a) 100, (b) 250 and (c) 500 mg/L

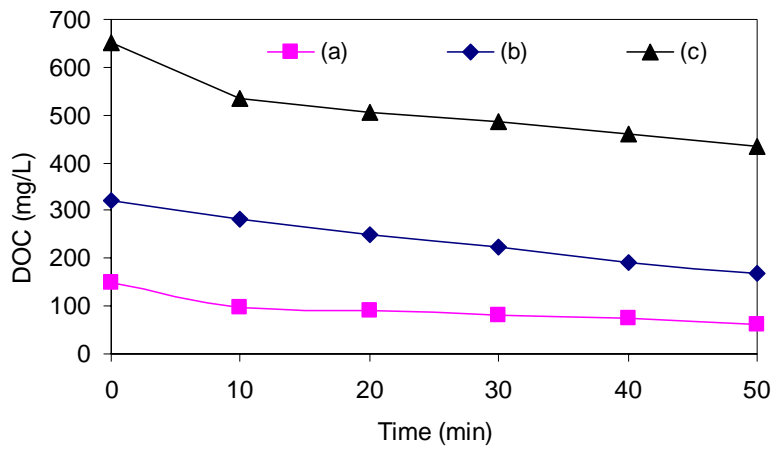


Figure 4.49 Effect of initial antibiotic concentration on antibiotics degradation by photo-Fenton process in terms of BOD<sub>5</sub> (a) 100, (b) 250, (c) 500 mg/L

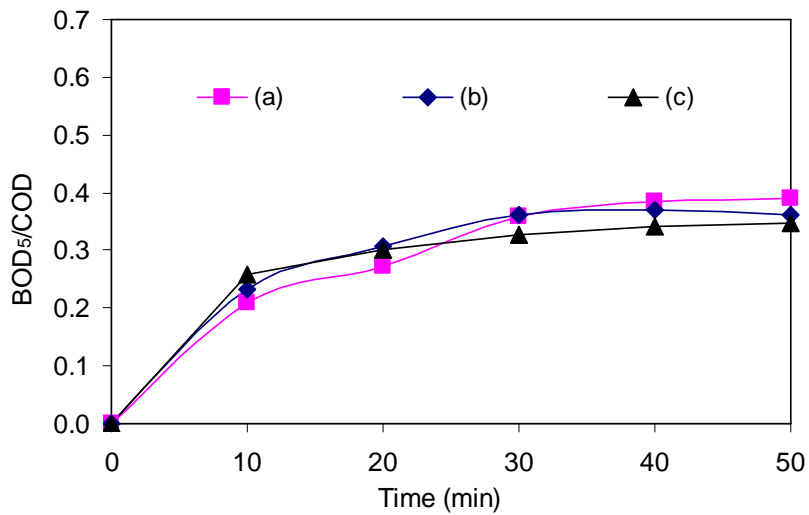


Figure 4.50 Effect of initial antibiotic concentration on antibiotics degradation by photo-Fenton process in terms of BOD<sub>5</sub>/COD ratio (a) 100, (b) 250, (c) 500 mg/L



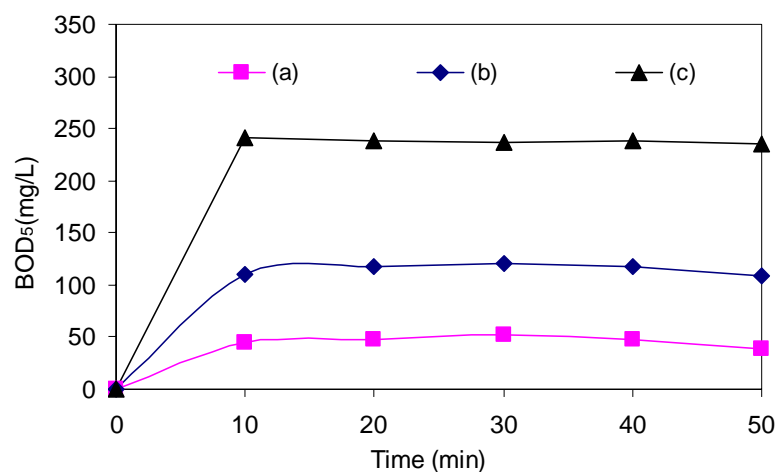


Figure 4.51 Effect of initial antibiotic concentration on antibiotics degradation by photo-Fenton process in terms of DOC (a) 100, (b) 250, (c) 500 mg/L

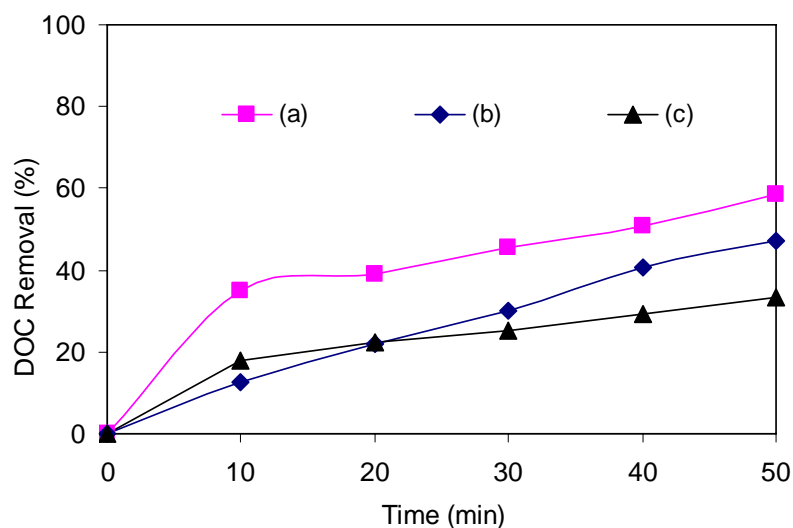


Figure 4.52 Effect of initial antibiotic concentration on antibiotics degradation by photo-Fenton process in terms of DOC Removal (a) 100, (b) 250, (c) 500 mg/L

#### 4.2.6 Degradation of the Antibiotics in Aqueous Solution, Biodegradability Improvement and Mineralization under Optimum Photo-Fenton Operating Conditions

Figure 4.53 shows degradation of the antibiotics (AMX 104 mg/L, AMP 105 mg/L and CLX 103 mg/L) in aqueous solution (COD 520 mg/L; 16.25 mM) under optimum operating conditions ( $H_2O_2/COD$  molar ratio 1.5,  $H_2O_2/Fe^{2+}$  molar ratio 20 and pH 3). Complete degradation of all three antibiotics was achieved in 2 min.

These results agree well with that reported by Trovó *et al.* (2008) for degradation of amoxicillin and bezafibrate in aqueous solution by the photo-Fenton process.

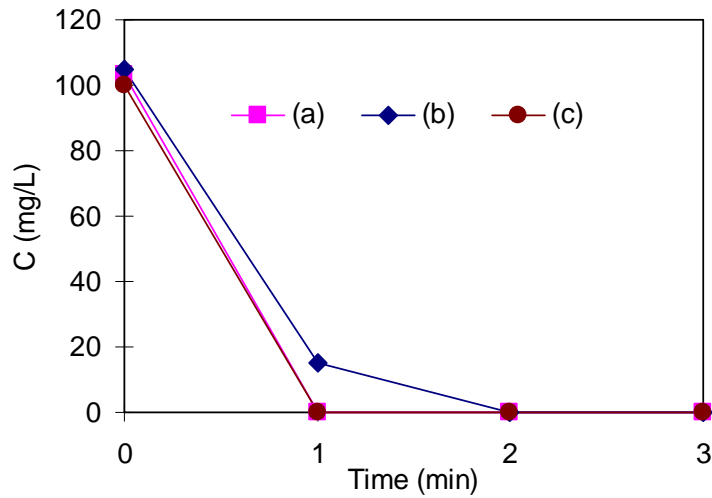


Figure 4.53 Degradation of AMX, AMP and CLX under optimum photo-Fenton operating conditions (a) AMX, (b) AMP and (c) CLX

Figure 4.54 shows degradation of AMX, AMP and CLX in aqueous solution in terms of COD, BOD<sub>5</sub> and BOD<sub>5</sub>/COD ratio. COD decreased from 520 mg/L (initial value) to 100 mg/L and BOD<sub>5</sub> increased from zero to 40 mg/L in 50 min irradiation time and the corresponding BOD<sub>5</sub>/COD ratio was 0.4 which is considered adequate for biological treatment (Al-Momani *et al.*, 2002).

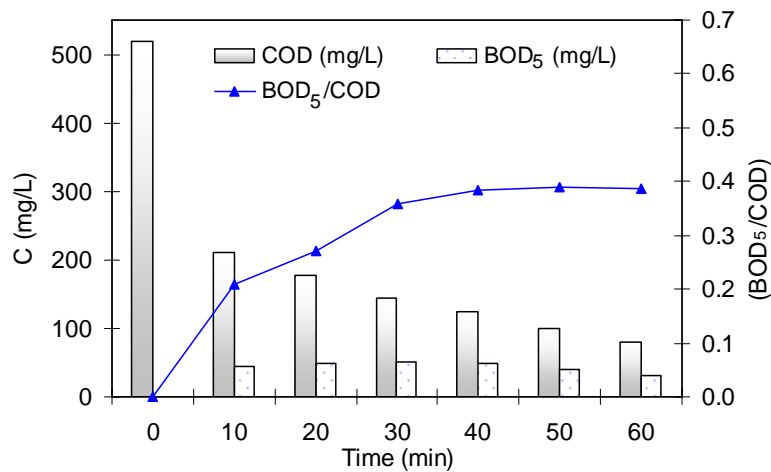


Figure 4.54 Degradation of antibiotics under optimum photo-Fenton operating conditions in terms of COD, BOD<sub>5</sub> and BOD<sub>5</sub>/COD ratio.

To assess the degree of mineralization, DOC removal and increase in nitrate concentration were measured. Mineralization of organic carbon and nitrogen compounds are verified by the results presented in Figure 4.55. DOC removal was 34.2, 38.3, 42.3, 50.3 and 58.4% in 10, 20, 30, 40 and 50 min, respectively. Nitrate increased from 0.3 to 14.2 mg/L in 50 min.

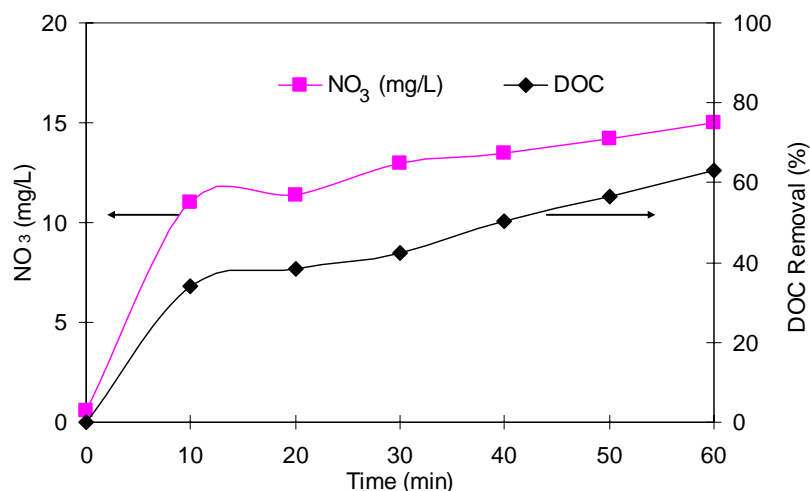


Figure 4.55 Mineralization of organic carbon and nitrogen in terms of DOC removal and nitrate concentration under optimum photo-Fenton operating conditions

#### 4.2.7 Kinetic Study

Figure 4.56 shows the plots of  $-\ln \frac{[DOC]}{[DOC_0]}$  versus irradiation time for antibiotic mineralization by the photo-fenton process under optimum operating conditions (COD/H<sub>2</sub>O<sub>2</sub>/Fe<sup>2+</sup> molar ratio 1:1.5:0.075 and pH 3). The linearity of the plot suggests that the photo-Fenton reaction approximately followed the pseudo-first order kinetics with rate constant of 0.014 min<sup>-1</sup> and  $t_{1/2}$  49.5 min.

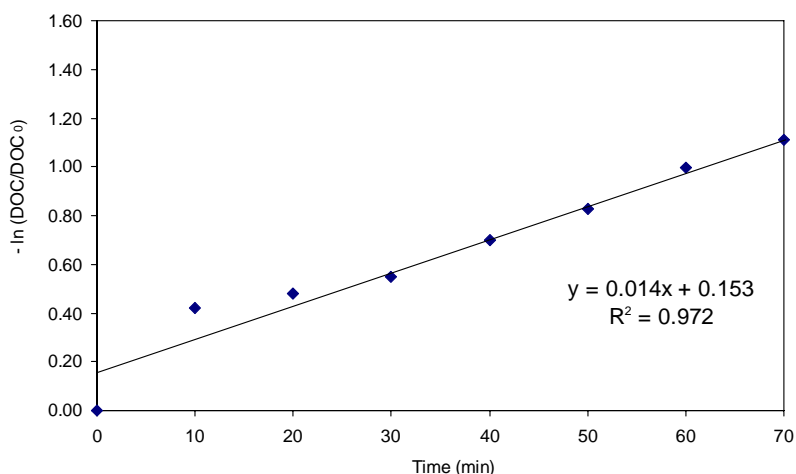


Figure 4.56 Kinetics of antibiotic mineralization by the photo-Fenton process

### 4.3 UV/TiO<sub>2</sub> Process

Effect of the operating conditions of the UV/TiO<sub>2</sub> process such as TiO<sub>2</sub> concentration, pH and irradiation time and addition of H<sub>2</sub>O<sub>2</sub> on antibiotic degradation, biodegradability improvement and mineralization were studied.

#### 4.3.1 Effect of TiO<sub>2</sub> Concentration

To observe the effect of TiO<sub>2</sub> concentration on AMX, AMP and CLX degradation, initial TiO<sub>2</sub> concentration was varied in the range 0.5-2.0 g/L. The experimental conditions were AMX, AMP and CLX concentration 104, 105 and 103 mg/L, respectively (COD 520 mg/L) and pH 5. AMX after 300 min irradiation time was 40, 47, 42 and 30 mg/L (Figure 4.57); however, AMX degradation was 42.3, 54.8, 55.8 and 58.7% (Figure 4.58) at TiO<sub>2</sub> concentration 0.5, 1.0, 1.5 and 2.0 g/L, respectively. AMP after 300 min irradiation time was 23, 50, 27 and 9 mg/L (Figure 4.59); however, AMP degradation was 33.3, 52.4, 54.3 and 52.4% (Figure 4.60) at TiO<sub>2</sub> concentration 0.5, 1.0, 1.5 and 2.0 g/L, respectively. CLX after 300 min irradiation time was 5, 43, 19 and 0 mg/L (Figure 4.61); however, CLX degradation was 46.6, 58.3, 59.2 and 60.2% (Figure 4.62) at TiO<sub>2</sub> concentration 0.5, 1.0, 1.5 and 2.0 g/L, respectively. Degradation of antibiotics increased with increasing TiO<sub>2</sub> concentration in the range 0.5-1.0 g/L. Further increase of TiO<sub>2</sub> concentration above 1 g/L did not

produce significant improvement in antibiotic degradation. This may be due to decreasing light penetration, increasing light scattering (Kansal *et al.*, 2008), agglomeration and sedimentation of TiO<sub>2</sub> under high catalyst concentration (So *et al.*, 2002; San *et al.*, 2007). These results agree well with previous studies on degradation of bisphenol (Kaneco *et al.*, 2004), chloramphenicol (Chatzitakis *et al.*, 2008), hymatoxylin (Sioi *et al.*, 2006) and paracetamol (Yang *et al.*, 2008).

Based on the results, the optimum TiO<sub>2</sub> concentration for degradation of amoxicillin, ampicillin and cloxacillin antibiotics in aqueous solution is 1.0 g/L and it was used to study the effect of other operating conditions. It is worth noting that dissolved oxygen decreased under the experimental condition from initial value 8.4 to 6.8 mg/L in 300 min. This may be due to the reaction of oxygen with conduction band electrons to form superoxide ions ( $\cdot\text{O}_2^-$ ) as in Reaction (2.16). The role of dissolved oxygen in photocatalytic degradation is dual. It accepts a photogenerated electron from the conduction band and thus promotes the charge separation (minimizing the electron-hole pair recombination).

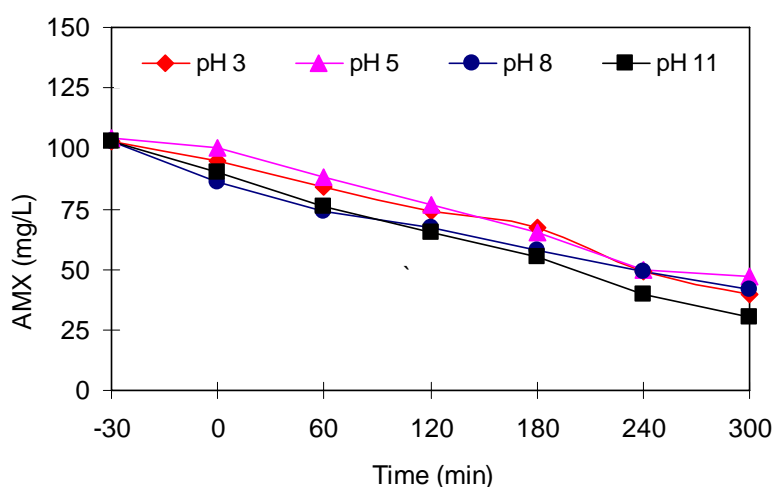


Figure 4.57 Effect of TiO<sub>2</sub> concentration on AMX

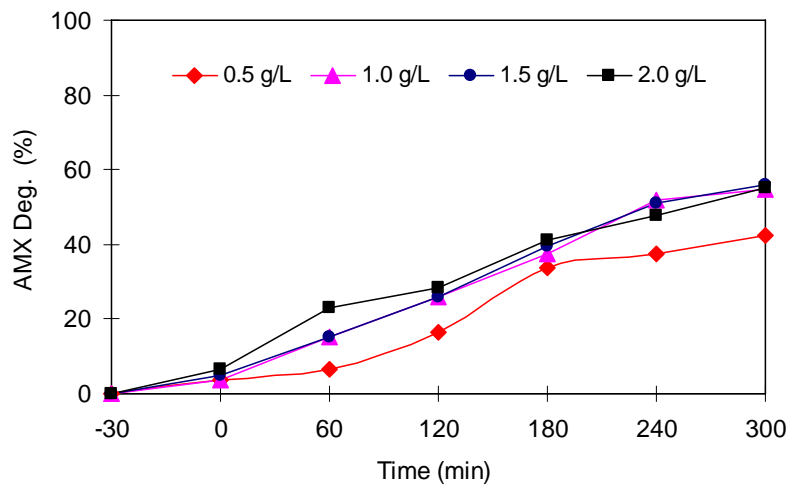


Figure 4.58 Effect of TiO<sub>2</sub> concentration on AMX degradation

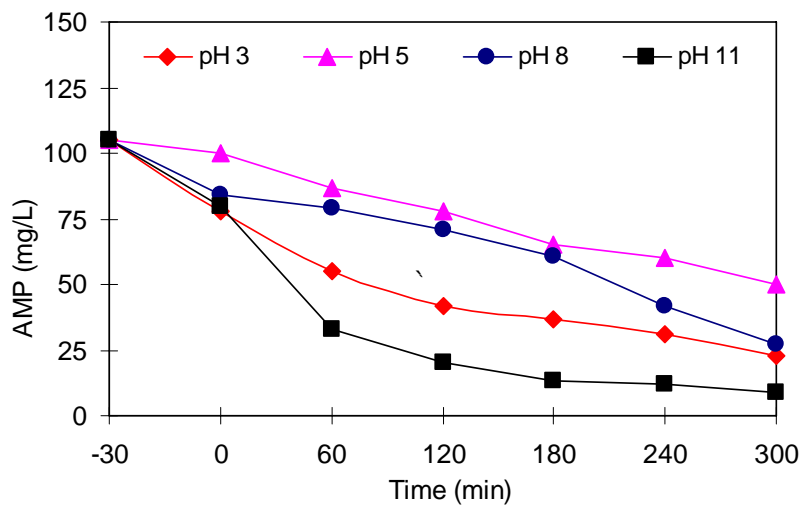


Figure 4.59 Effect of TiO<sub>2</sub> concentration on AMP

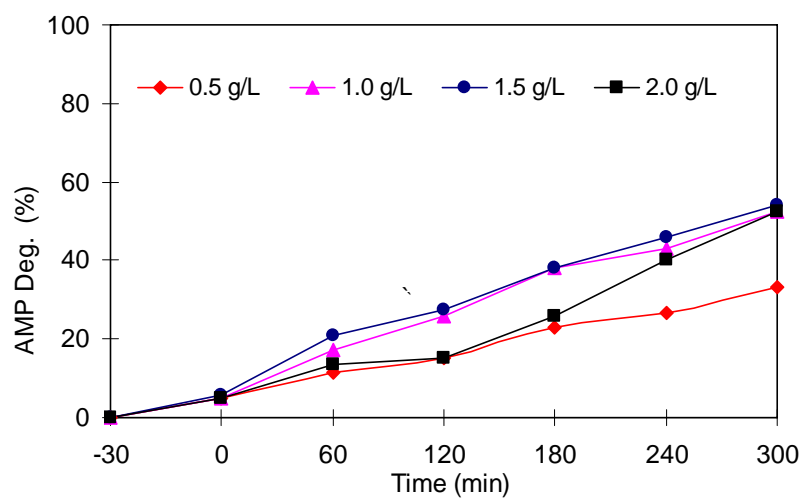


Figure 4.60 Effect of TiO<sub>2</sub> concentration on AMP degradation

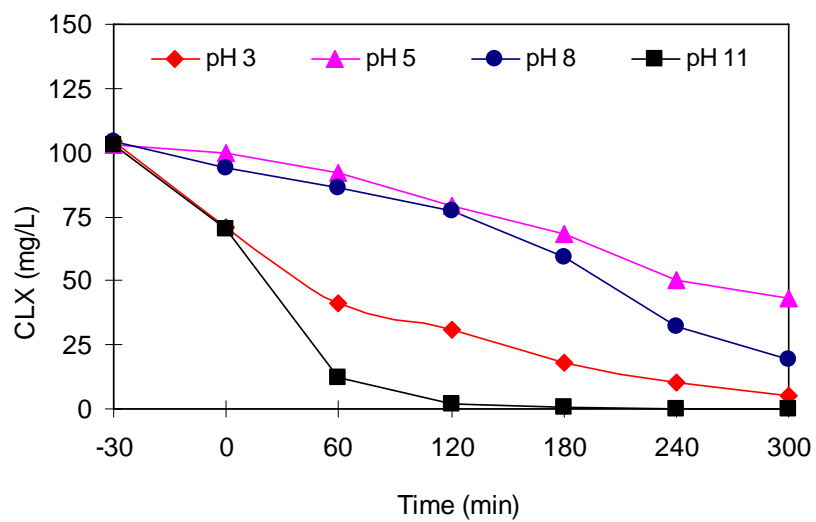


Figure 4.61 Effect of TiO<sub>2</sub> concentration on CLX

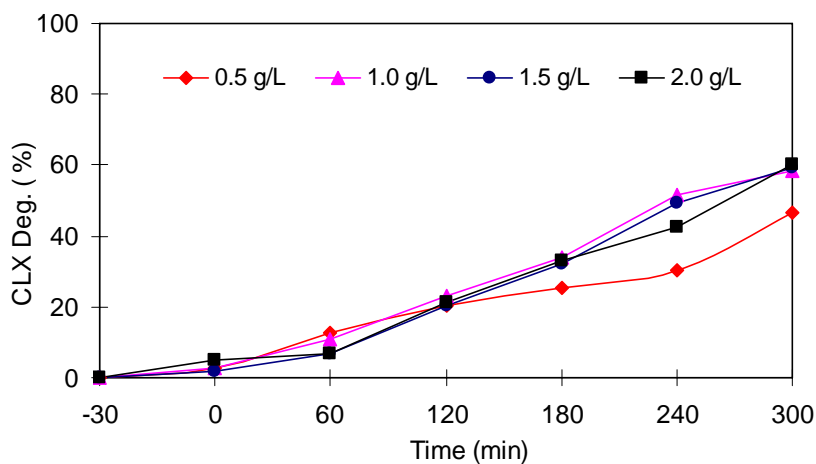


Figure 4.62 Effect of TiO<sub>2</sub> concentration on CLX degradation

Figure 4.36 shows the effect of TiO<sub>2</sub> concentration on antibiotics degradation in terms of COD removal. COD removal after 300 min irradiation time was 6.2, 9.2, 10.0 and 9.6%, respectively. No significant improvement in biodegradability (BOD<sub>5</sub>/COD ratio) occurred and maximum DOC removal was 2%.

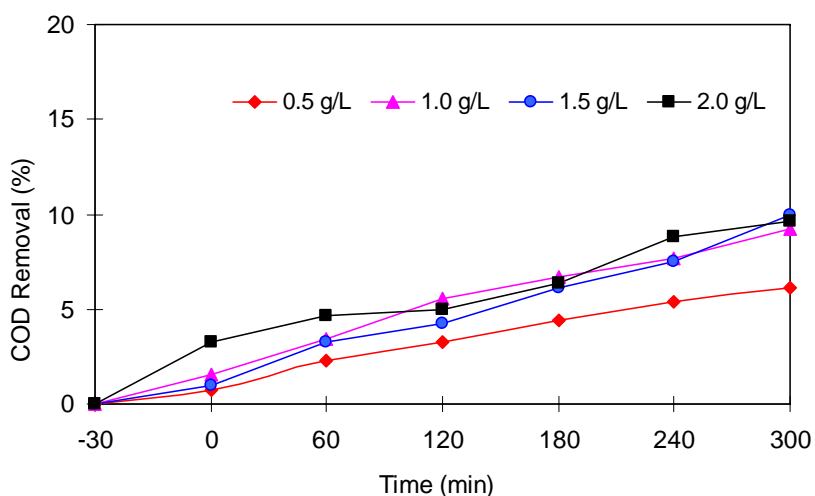


Figure 4.63 Effect of TiO<sub>2</sub> concentration on antibiotics degradation in terms of COD removal

### 4.3.2 Effect of pH

To study the effect of initial pH on degradation of AMX, AMP and CLX, experiments were conducted by varying the pH in the range 3-11. The experimental



conditions were AMX, AMP and CLX concentration 104, 105 and 103 mg/L, respectively (COD 520 mg/L) and  $\text{TiO}_2$  1.0 g/L. AMX after 300 min irradiation time was 40, 47, 42 and 30 mg/L (Figure 4.64); however, AMX degradation was 61.2, 54.8, 59.2 and 70.9% (Figure 4.65) at pH 3, 5, 8 and 11, respectively. AMP after 300 min irradiation time was 23, 50, 27 and 9 mg/L (Figure 4.66); however, AMP degradation was 78.1, 52.4, 74.3 and 91.4% (Figure 4.67) at at pH 3, 5, 8 and 11, respectively. CLX after 300 min irradiation time was 5, 43, 19 and 0 mg/L (Figure 4.68); however, CLX degradation was 95.2, 58.3, 81.7 and 100% (Figure 4.69) at at pH 3, 5, 8 and 11, respectively.

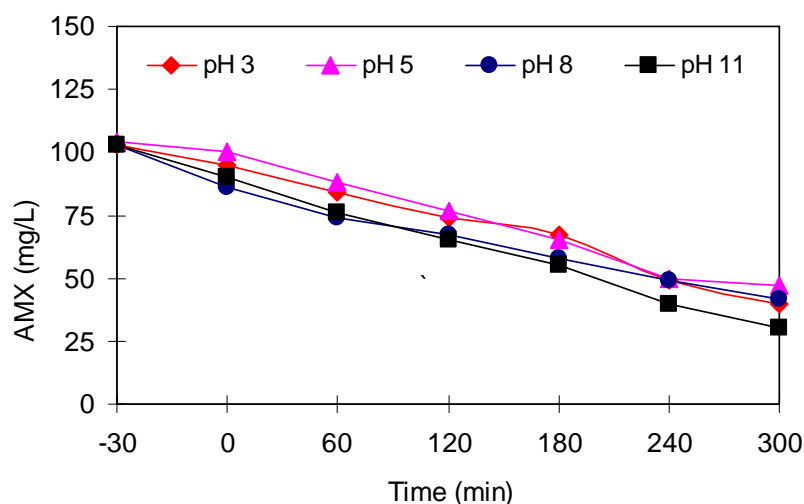


Figure 4.64 Effect of pH on AMX by UV/ $\text{TiO}_2$  process

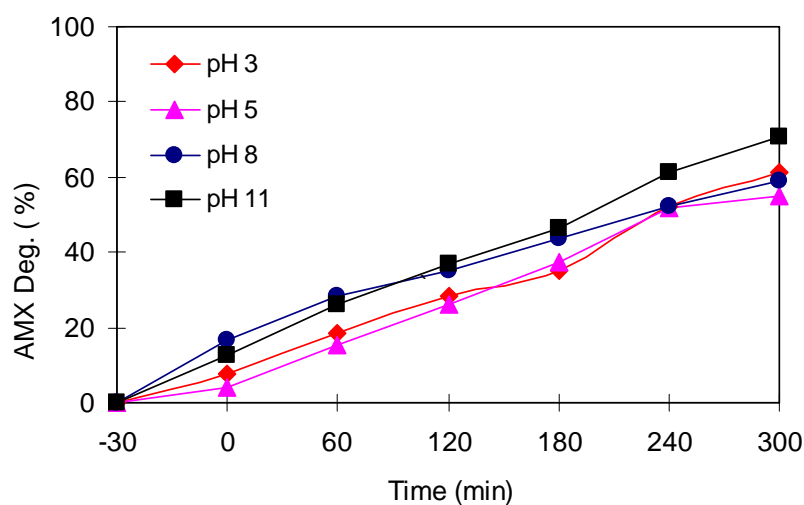


Figure 4.65 Effect of pH on AMX degradation by UV/ $\text{TiO}_2$  process

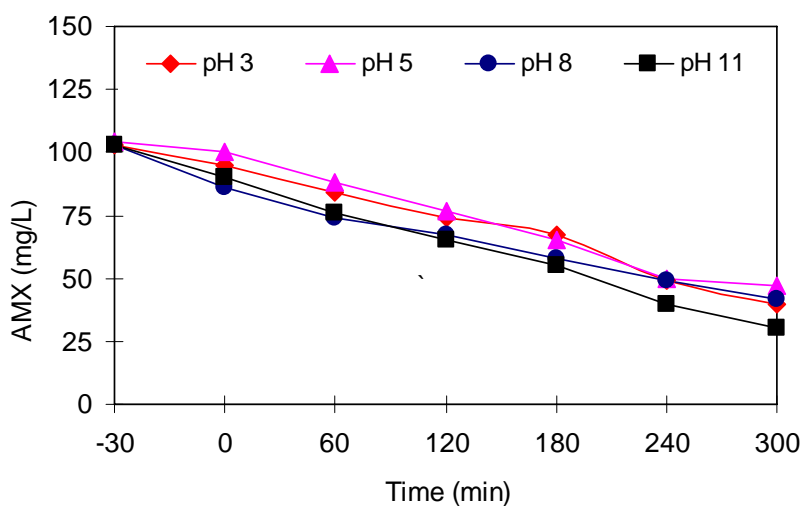


Figure 4.66 Effect of pH on AMP by UV/TiO<sub>2</sub> process

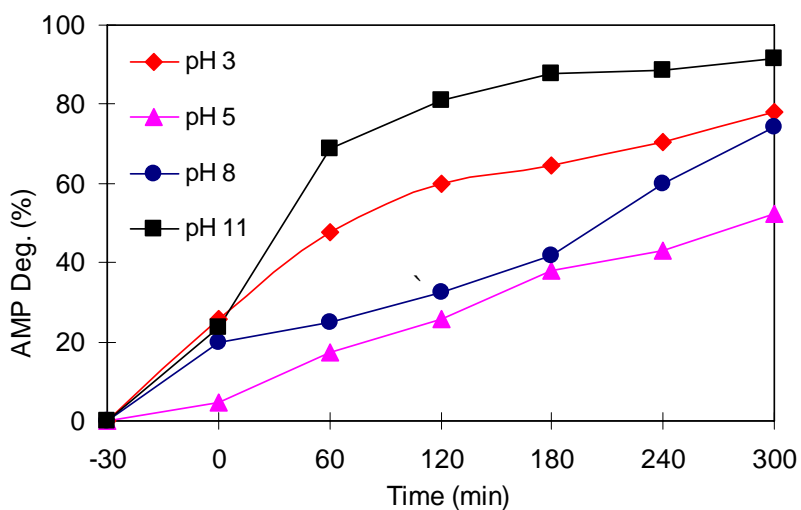


Figure 4.67 Effect of pH on AMP degradation by UV/TiO<sub>2</sub> process

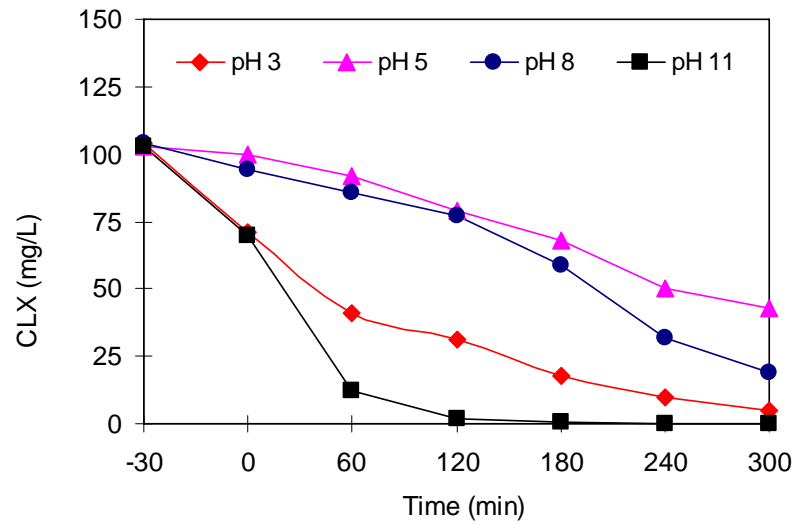


Figure 4.68 Effect of pH on CLX by UV/TiO<sub>2</sub> process

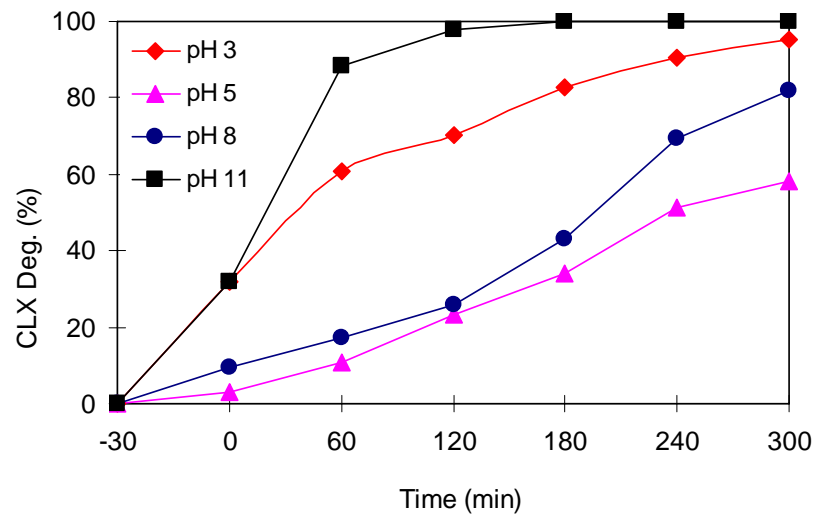


Figure 4.69 Effect of pH on CLX degradation by UV/TiO<sub>2</sub> process

Effect of pH on antibiotics degradation in terms of COD removal was also studied. As shown in Figure 4.70, COD removal after 300 min irradiation was 11.7, 9.2, 10.2 and 11.2% at pH 3, 5, 8 and 11, respectively. No significant improvement in BOD<sub>5</sub>/COD ratio occurred and the maximum DOC removal was 3 %.

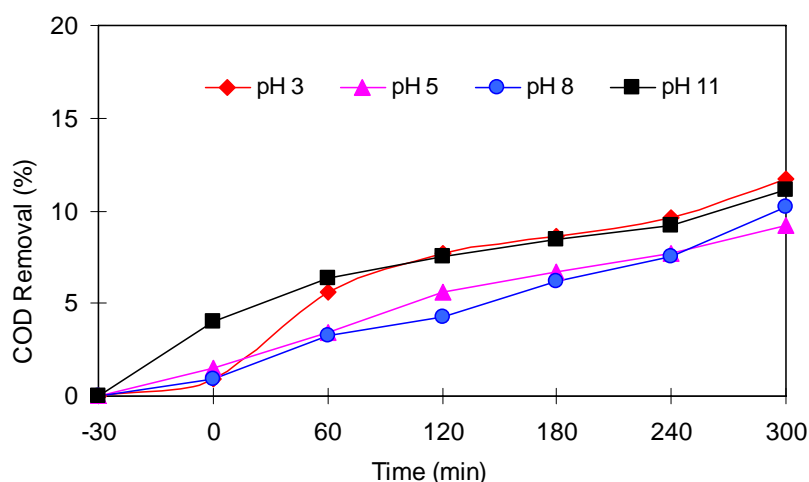


Figure 4.70 Effect of pH on antibiotics degradation in terms of COD removal by UV/TiO<sub>2</sub> process

The effect of pH on antibiotic degradation can be explained by taking into consideration the properties of both catalyst and antibiotic at different pH. For TiO<sub>2</sub>, as pH increases overall surface charge of TiO<sub>2</sub> changes from positive (pK<sub>a1</sub> = 2.6) to negative (pK<sub>a2</sub> = 9.0) with point of zero charge being pH 6.4 (Feitz *et al.*, 1999). Chemie (2005) reported that ionic amoxicillin species change from positive charge at acidic pH to negative charge at alkaline pH as shown in Figure 4.71. At acidic pH, both TiO<sub>2</sub> and amoxicillin are positively charged and hence, the adsorption on the surface of TiO<sub>2</sub> is limited. The high degradation of antibiotics at acidic pH compared to that at neutral pH may be due to the hydrolysis of antibiotics as reported by Hou and Pool (1971). At alkaline pH, both amoxicillin and TiO<sub>2</sub> are negatively charged and so repulsive forces between the catalyst and the antibiotics are developed. High degradation of antibiotics in alkaline condition may be due to two facts. First is the enhancement of hydroxyl radical formation at high pH due to the availability of hydroxyl ions on TiO<sub>2</sub> surface that can easily be oxidized to form hydroxyl radical as in Reaction (2.15) (Yang *et al.*, 2008; Zheng *et al.*, 1997; Galindo *et al.*, 2000). Second is the hydrolysis of the antibiotics due to instability of the  $\beta$ -lactam ring at high pH (Deshpande *et al.*, 2004).

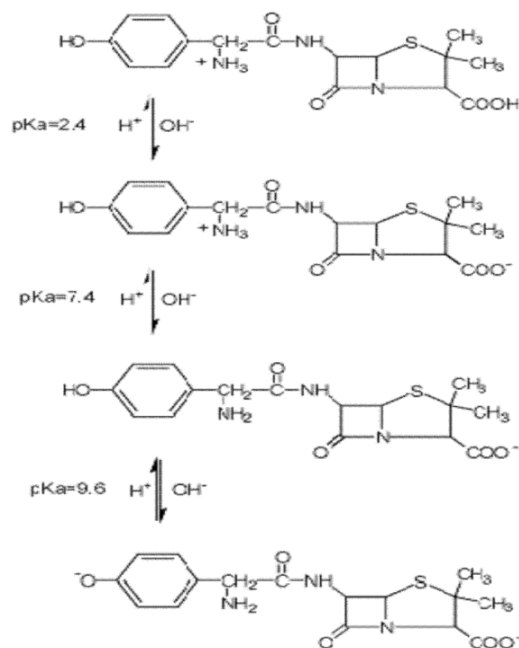


Figure 4.71 Anionic species of amoxicillin at different pH (Chemie, 2005).

### 4.3.3 Effect of H<sub>2</sub>O<sub>2</sub> Addition

Addition of a powerful oxidizing agent such as H<sub>2</sub>O<sub>2</sub> to the TiO<sub>2</sub> suspension is a well-known procedure and in many cases leads to an increase in the rate of photocatalytic oxidation (Malato *et al.*, 2000; Poulios *et al.*, 2003). In order to keep the efficiency of the added H<sub>2</sub>O<sub>2</sub>, it is necessary to choose the optimum concentration of H<sub>2</sub>O<sub>2</sub> according to the type and concentration of the pollutants. H<sub>2</sub>O<sub>2</sub> is considered to have two functions in the photocatalytic oxidation. It accepts a photogenerated electron from the conduction band of the semiconductor to form OH<sup>•</sup> radical (Reaction 2.17). In addition, it forms OH<sup>•</sup> radicals according to Reaction (4.1) (Kositzki *et al.*, 2004).



In order to investigate the effect of H<sub>2</sub>O<sub>2</sub> addition on degradation of antibiotics by the UV/TiO<sub>2</sub> process, experiments were conducted by varying the initial H<sub>2</sub>O<sub>2</sub> concentration in the range 50-300 mg/L. The experimental conditions were AMX, AMP and CLX concentration 104, 105 and 103 mg/L respectively (COD 520 mg/L), TiO<sub>2</sub> 1.0 g/L and ambient pH ~ 5. Ambient pH ~ 5 was chosen because H<sub>2</sub>O<sub>2</sub>

decomposes in alkaline pH (Talinli and Anderson, 1992). COD after 300 min irradiation time was 495, 383, 400, 435 and 456 mg/L (Figure 4.72); however, COD removal after 300 min irradiation time was 14.8, 26.3, 23.1, 16.3 and 12.3% (Figure 4.73) at H<sub>2</sub>O<sub>2</sub> concentration 50, 100, 150, 200 and 300 mg/L, respectively. BOD<sub>5</sub> after 300 min irradiation time was 10, 38, 36, 30 and 28 mg/L (Figure 4.74); however, BOD<sub>5</sub>/COD ratio after 300 min irradiation time was 0.05, 0.10, 0.09, 0.07 and 0.06 at H<sub>2</sub>O<sub>2</sub> concentration 50, 100, 150, 200 and 300 mg/L, respectively (Figure 4.75). DOC after 300 min irradiation time was 139, 125, 131, 135 and 137 mg/L (Figure 4.76); however, DOC removal after 300 min irradiation time was 6.4, 13.9, 9.6, 6.9 and 5.3% at H<sub>2</sub>O<sub>2</sub> concentration 50, 100, 150, 200 and 300 mg/L, respectively (Figure 4.77). Maximum COD and DOC removal were achieved at H<sub>2</sub>O<sub>2</sub> concentration 100 mg/L. Degradation increased as the concentration of H<sub>2</sub>O<sub>2</sub> increased and it reached the highest value at H<sub>2</sub>O<sub>2</sub> concentration 100 mg/L. Further increase in H<sub>2</sub>O<sub>2</sub> concentration caused decrease in COD and DOC removal, and BOD<sub>5</sub>/COD ratio. Similar observation has been reported for degradation of chloramphenicol (Chatzitakis *et al.*, 2008). This may be due to the fact that excess H<sub>2</sub>O<sub>2</sub> reacts with OH<sup>•</sup> and contributes to the OH<sup>•</sup> and hole (h<sup>+</sup>) scavenging as in Reactions 2.6 and Reaction 4.2 to form HO<sub>2</sub><sup>•</sup> (Zhao *et al.*, 2004; Behnajady *et al.*, 2006). Based on the results, the optimum H<sub>2</sub>O<sub>2</sub> concentration for antibiotics degradation is 100 mg/L.



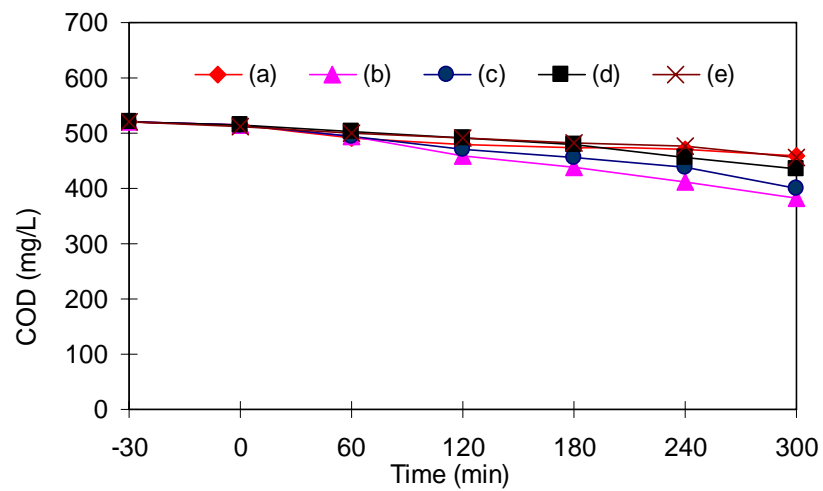


Figure 4.72 Effect of H<sub>2</sub>O<sub>2</sub> addition on antibiotics degradation in terms of COD (a) 50, (b) 100, (c) 150, (d) 200 and (e) 300 mg/L

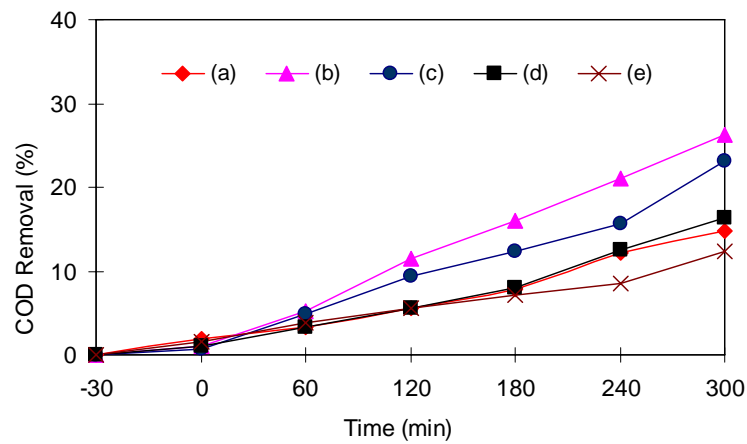


Figure 4.73 Effect of H<sub>2</sub>O<sub>2</sub> addition on antibiotics degradation in terms of COD removal (a) 50, (b) 100, (c) 150, (d) 200 and (e) 300 mg/L

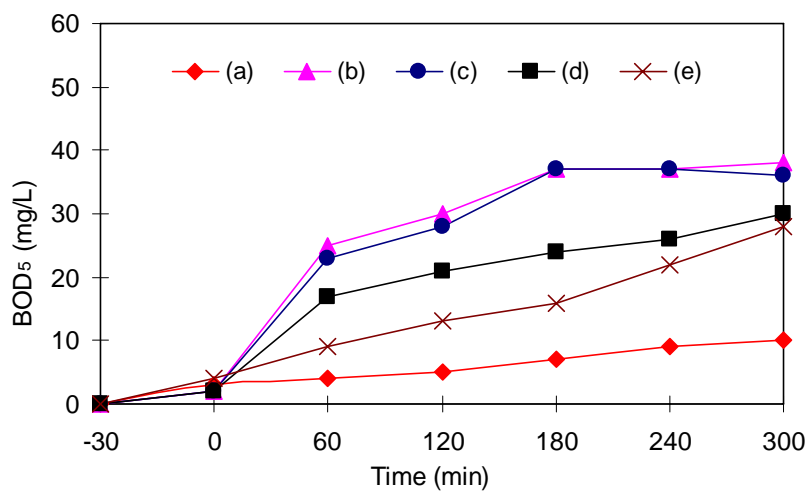


Figure 4.74 Effect of H<sub>2</sub>O<sub>2</sub> addition on antibiotics degradation in terms of BOD<sub>5</sub> (a) 50, (b) 100, (c) 150, (d) 200 and (e) 300 mg/L

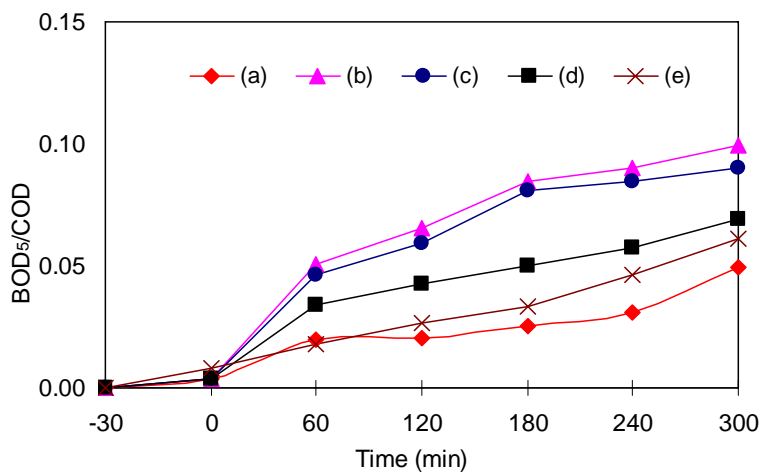


Figure 4.75 Effect of H<sub>2</sub>O<sub>2</sub> addition on antibiotics degradation in terms of BOD<sub>5</sub>/COD ratio (a) 50, (b) 100, (c) 150, (d) 200 and (e) 300 mg/L



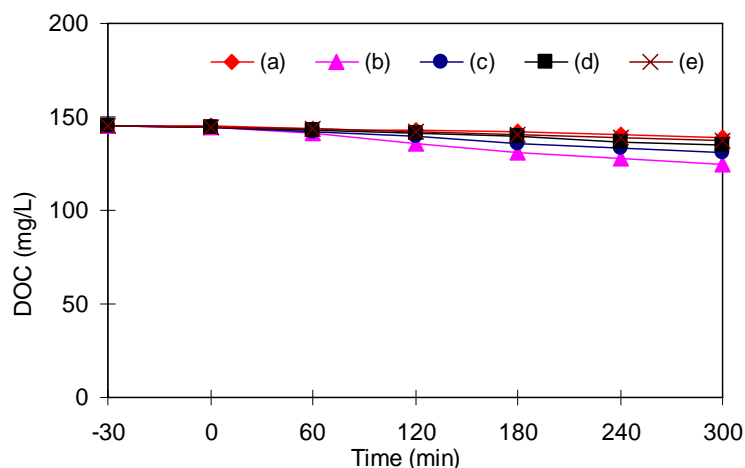


Figure 4.76 Effect of H<sub>2</sub>O<sub>2</sub> addition on antibiotics degradation in terms of DOC (a) 50, (b) 100, (c) 150, (d) 200 and (e) 300 mg/L

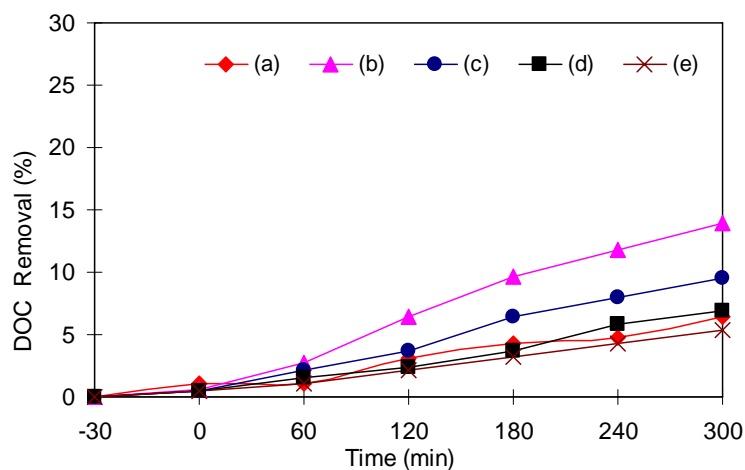


Figure 4.77 Effect of H<sub>2</sub>O<sub>2</sub> addition on antibiotics degradation in terms of DOC removal (a) 50, (b) 100, (c) 150, (d) 200 and (e) 300 mg/L

#### 4.3.4 Effect of H<sub>2</sub>O<sub>2</sub> Addition on Degradation of Antibiotics in Aqueous Solution and Mineralization by UV/TiO<sub>2</sub> process

To study the effect of H<sub>2</sub>O<sub>2</sub> addition on the degradation of AMX, AMP and CLX by the UV/TiO<sub>2</sub> process, an experiment was conducted under the optimum operating conditions (TiO<sub>2</sub> 1.0 g/L, H<sub>2</sub>O<sub>2</sub> 100 mg/L and pH 5). Initial AMX, AMP and CLX concentration was 104, 105 and 103 mg/L, respectively (COD 520 mg/L). Figure 4.78 shows the effect of H<sub>2</sub>O<sub>2</sub> addition on AMX, AMP and CLX degradation.

Complete degradation of amoxicillin and cloxacillin was achieved in 20 min, whereas complete degradation of ampicillin was achieved in 30 min.

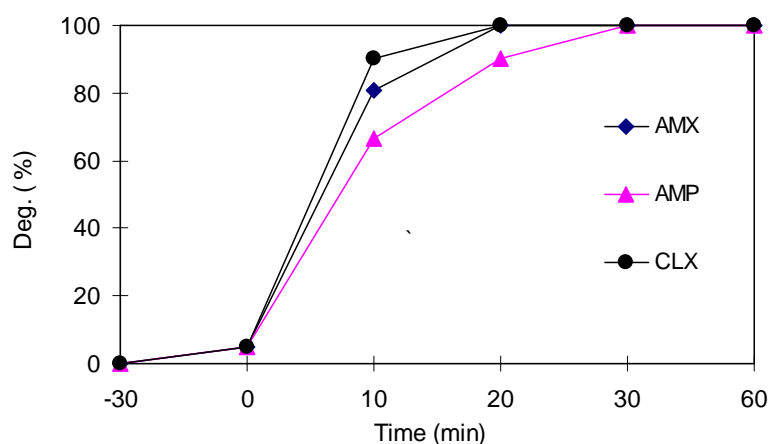


Figure 4.78 Effect of H<sub>2</sub>O<sub>2</sub> addition on AMX, AMP and CLX degradation by the UV/TiO<sub>2</sub> process

TiO<sub>2</sub> photocatalysis would result in the mineralization of organic carbon, and release of nitrogen and sulphur from the antibiotic molecule. To assess the degree of mineralization, dissolved organic carbon (DOC), nitrate (NO<sub>3</sub><sup>-</sup>), ammonia (NH<sub>3</sub>) and sulphate (SO<sub>4</sub><sup>2-</sup>) in the solution were measured. The experimental conditions were TiO<sub>2</sub> concentration 1.0 g/L, H<sub>2</sub>O<sub>2</sub> concentration 100 mg/L, pH 5, initial AMX, AMP and CLX concentration 104, 105 and 103 mg/L, respectively (COD 520 mg/L). Mineralization of organic carbon, and formation of nitrogen and sulphur compounds are verified by the results presented in Figures 4.79 and 4.80. Figure 4.79 shows increase of DOC removal with irradiation time (DOC removal 24.3 and 41% at 10 and 24 hr, respectively). Figure 4.80 shows the formation of NO<sub>3</sub><sup>-</sup>, NH<sub>3</sub> and SO<sub>4</sub><sup>2-</sup> as a result of AMX, AMP and CLX degradation.

According to the structure of the antibiotics (Figure 3.1), each antibiotic has three nitrogen atoms and one sulphur atom. Photocatalytic transformation of the nitrogen moieties to N<sub>2</sub>, NH<sub>4</sub><sup>+</sup>, NO<sub>2</sub><sup>-</sup> or NO<sub>3</sub><sup>-</sup> depends on the initial oxidation state of nitrogen and on the structure of the organic molecule (Calza *et al.*, 2005). Low *et al.* (1991) reported that ammonium to nitrate concentration ratio in aliphatic amines is higher than that in compounds containing ring nitrogen. For amoxicillin and ampicillin, each molecule contains three nitrogen atoms, two of them in aliphatic

bond and the other in aromatic bond, and for cloxacillin, only one atom in aliphatic bond. This indicates that mineralization of organic nitrogen in case of cloxacillin is more complex than that of amoxicillin and ampicillin. The results show that the initial  $\text{NH}_3$  concentration was 6.1 mg/L and slightly increased to 7.6 mg/L and  $\text{NO}_3^-$  gradually increased from zero (initial value) to 1.2 mg/L in 24 hr. This agrees with previous studies on degradation of lincomycin and sulfamethoxazole antibiotics by photocatalytic processes. Paola *et al.* (2006) reported that at pH 5.6,  $\text{TiO}_2$  0.4 g/L and UV ( $< 300$  nm) irradiation for 6 hr, ammonium ions were quickly formed and accumulated throughout the irradiation period. Abellán *et al.* (2007) reported that at pH 5,  $\text{TiO}_2$  0.5 g/L, sulfamethoxazole 100 mg/L and UV ( $>290$  nm) irradiation for 6 hr, mineralization of organic nitrogen in sulfamethoxazole molecule to  $\text{NH}_3$  or to  $\text{NO}_2^-$  and/or  $\text{NO}_3^-$  occurred, and at the end of the experiment 5 mg/L of  $\text{NH}_4^+$  was released. As shown in Figure 4.46, sulphate ions were not detected in the first 6 hr, but were detected in small value in the time between 6-10 hr and in high concentration of 39 mg/L after 24 hr. This indicates that release of sulphur needs long irradiation time. The results indicate that degradation of AMX, AMP and CLX antibiotics presumably involves cleavage of  $\beta$ -lactam ring, followed by subsequent reactions to form carbon dioxide, water, nitrate, ammonia and sulphate.

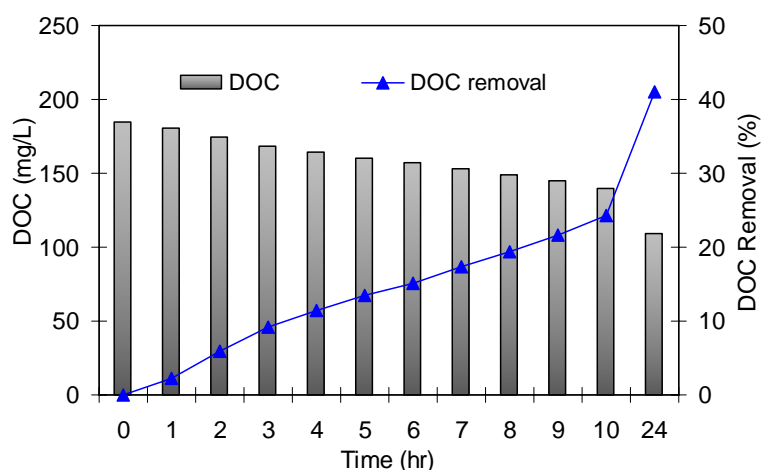


Figure 4.79 Effect of irradiation time on DOC concentration and removal by the UV/ $\text{H}_2\text{O}_2$ / $\text{TiO}_2$  process

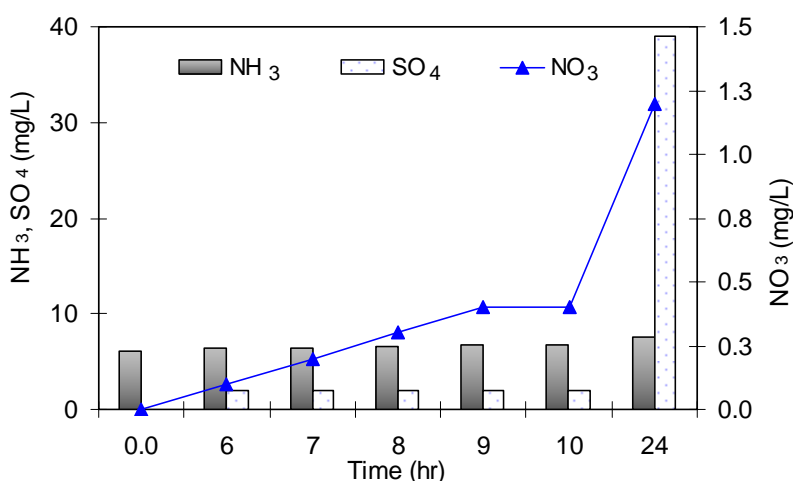


Figure 4.80 Effect of irradiation time on NH<sub>3</sub>, NO<sub>3</sub><sup>-</sup> and SO<sub>4</sub><sup>2-</sup> formation by the UV/H<sub>2</sub>O<sub>2</sub>/TiO<sub>2</sub> process

#### 4.3.5 Kinetic study

Kinetics of AMX, AMP and CLX Degradation by UV/TiO<sub>2</sub> Process as well as Kinetics of Antibiotic Mineralization by UV/H<sub>2</sub>O<sub>2</sub>/TiO<sub>2</sub> Process are presented herein.

##### 4.3.5.1 Kinetics of AMX, AMP and CLX Degradation by UV/TiO<sub>2</sub> Process

To study the kinetics of amoxicillin, ampicillin and cloxacillin degradation by UV/TiO<sub>2</sub> process, experiments were conducted at TiO<sub>2</sub> concentration 1.0 g/L, irradiation time 300 min and pH 11. The concentration of AMX, AMP and CLX after 30 min dark adsorption was taken as initial AMX, AMP and CLX concentration for kinetic analysis. Figure 4.81 shows the plots of  $-\ln \frac{[Antibiotic]}{[Antibiotic_0]}$  versus irradiation time for amoxicillin, ampicillin and cloxacillin. The linearity of the plots suggests that the photocatalytic degradation approximately followed a pseudo-first order kinetics. Degradation of cloxacillin exhibited the highest rate constant (0.029 min<sup>-1</sup>), followed by amoxicillin (0.007 min<sup>-1</sup>) and ampicillin (0.004 min<sup>-1</sup>).

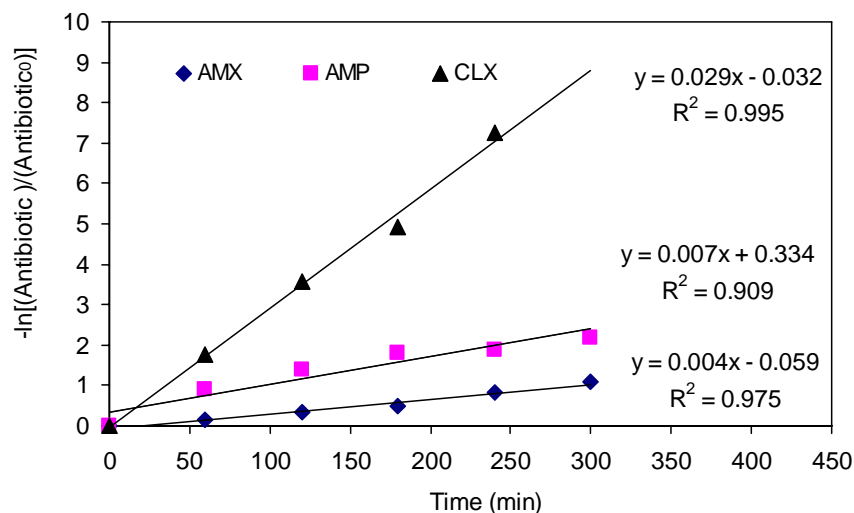


Figure 4.81 Kinetics of AMX, AMP and CLX degradation by UV/TiO<sub>2</sub> process

#### 4.3.5.2 Kinetics of Antibiotic Mineralization by UV/H<sub>2</sub>O<sub>2</sub>/TiO<sub>2</sub> Process

It was shown before in Section 4.3.4 that addition of H<sub>2</sub>O<sub>2</sub> resulted in complete degradation of AMX, AMP in 20 min, and complete degradation of AMP in 30 min (Figure 4.78). Hence, it would be appropriate to assess the rate constant with respect to DOC rather than to a particular antibiotic and Equation 3.4 can be used in the kinetic study. Pseudo-first-order rate constant ( $k_0$ ) can be obtained through a linear least-square fit of the DOC data. Half-life time ( $t_{1/2}$ ) was calculated according to Equation 3.5.

Figure 4.82 shows the plots of  $-\ln \frac{[DOC]}{[DOC_0]}$  versus irradiation time for antibiotic mineralization by the UV/H<sub>2</sub>O<sub>2</sub>/TiO<sub>2</sub> process under optimum operating conditions (TiO<sub>2</sub> 1 g/l, H<sub>2</sub>O<sub>2</sub> 100 mg/L and ambient pH 5). The linearity of the plot suggests that the UV/H<sub>2</sub>O<sub>2</sub>/TiO<sub>2</sub> process approximately followed the pseudo-first order kinetics with rate constant of 0.00050 min<sup>-1</sup> and  $t_{1/2}$  1386 min.

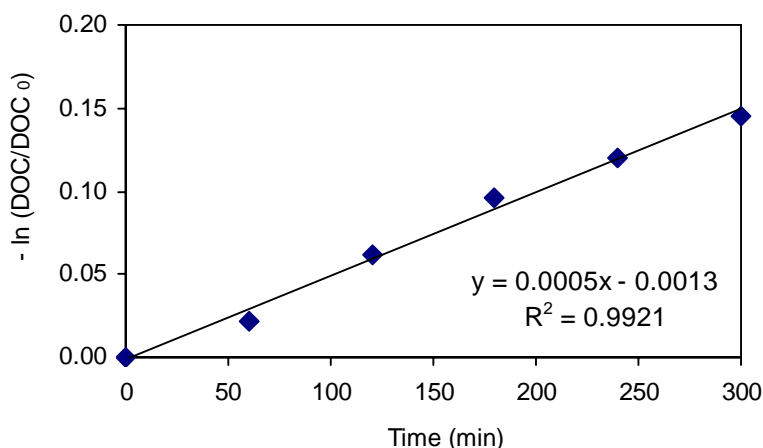


Figure 4.82 Kinetic study of antibiotic mineralization by UV/H<sub>2</sub>O<sub>2</sub>/TiO<sub>2</sub> process

#### 4.4 UV/ZnO Process

Effect of the operating conditions of the UV/ZnO process such as ZnO concentration, pH and irradiation time on antibiotic degradation, biodegradability improvement and mineralization were studied.

##### 4.4.1 Effect of ZnO Concentration

To observe the effect of ZnO concentration on antibiotic degradation, initial ZnO concentration was varied in the range 0.2-2.0 g/L. The experimental conditions were AMX, AMP and CLX concentration 104, 105 and 103 mg/L, respectively (COD 520 mg/L), pH 8 and irradiation time 300 min. AMX after 300 min irradiation time was 58, 50, 29, 30, 31 and 33 mg/L (Figure 4.83); however, AMX degradation was 44.2, 51.2, 72.1, 71.2, 70.2 and 68.6% (Figure 4.84) at ZnO concentration 0.20, 0.35, 0.50, 1.0, 1.5 and 2.0 g/L, respectively. AMP after 300 min irradiation time was 42, 33, 28, 31, 33 and 34 mg/L (Figure 4.85); however, AMP degradation was 60.0, 68.6, 73.3, 70.5, 68.6 and 67.6% (Figure 4.86) at ZnO concentration 0.20, 0.35, 0.50, 1.0, 1.5 and 2.0 g/L, respectively. CLX after 300 min irradiation time was 4, 0, 0, 0, 0, 0 mg/L (Figure 4.87); however, CLX degradation was 96.1, 100, 100, 100, 100 and 100% (Figure 4.88) at ZnO concentration 0.20, 0.35, 0.50, 1.0, 1.5 and 2.0 g/L, respectively. It is seen that degradation of antibiotics increased with ZnO concentration presumably due to increase of OH<sup>•</sup> radical production. However,

increasing ZnO concentration above 0.5 g/L did not produce any significant improvement in antibiotic degradation. This may be due to decreasing UV light penetration as a result of increasing turbidity and thus decreasing the photoactivated volume of the suspension (Daneshvar *et al.*, 2004).

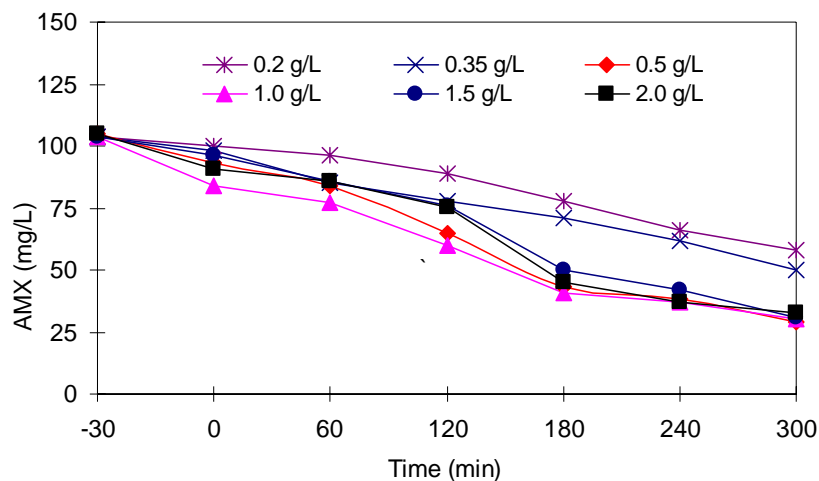


Figure 4.83 Effect of ZnO concentration on AMX

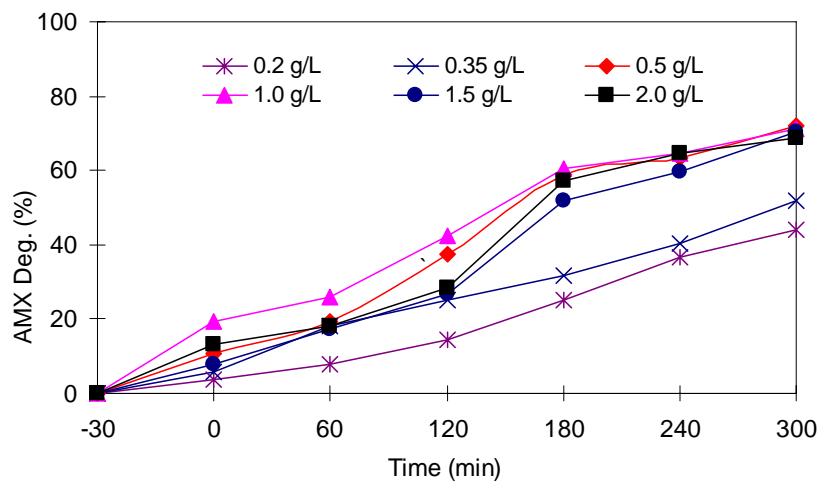


Figure 4.84 Effect of ZnO concentration on AMX degradation

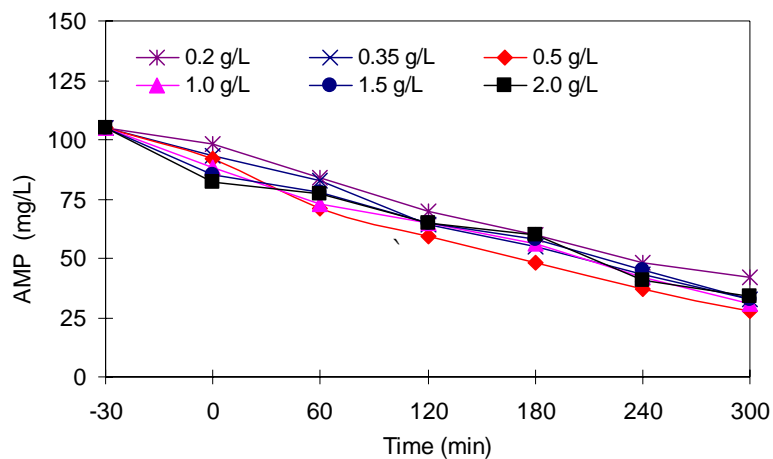


Figure 4.85 Effect of ZnO concentration on AMP

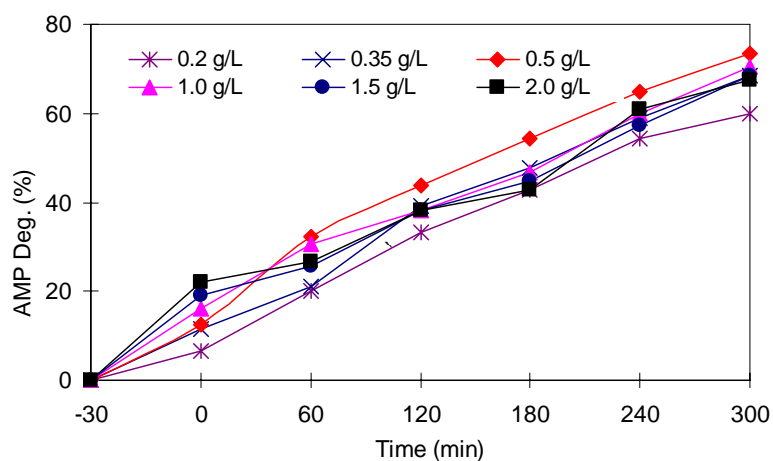


Figure 4.86 Effect of ZnO concentration on AMP degradation

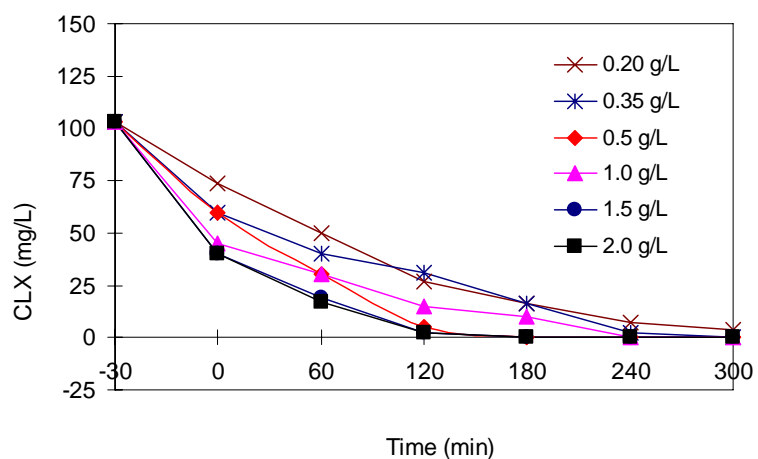


Figure 4.87 Effect of ZnO concentration on CLX degradation



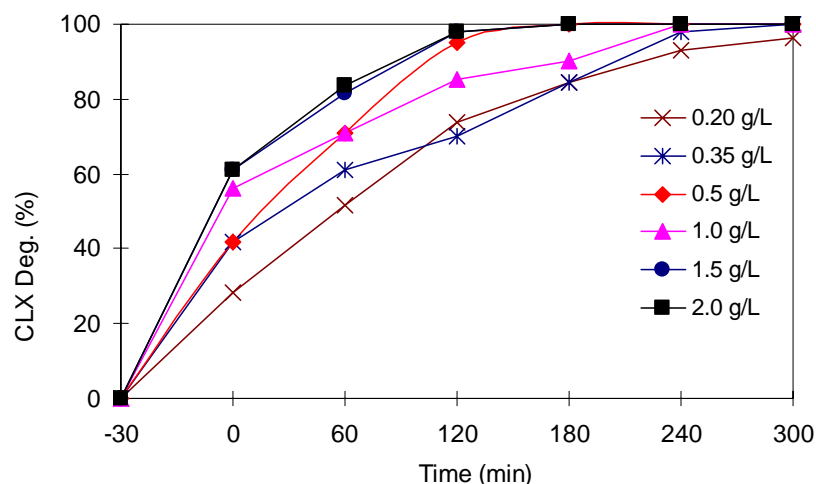


Figure 4.88 Effect of ZnO concentration on CLX degradation

Figures 4.89 and 4.90 show the effect of ZnO concentration on antibiotics degradation in terms of COD and COD removal. COD after 300 min irradiation time was 416, 400, 330, 356, 380 and 384 mg/L (Figure 4.89); however, COD removal after 300 min irradiation time was 18, 22, 33, 30, 25 and 25 % at ZnO concentration 0.20, 0.35, 0.50, 1.0, 1.5 and 2.0 g/L, respectively (Figure 4.90). Figure 4.91 shows the effect of ZnO concentration on antibiotics degradation in terms of DOC removal and biodegradability ( $BOD_5/COD$  ratio) improvement. The results show that DOC removal after 300 min irradiation time were 5.2, 12.6, 15.6, 14.1, 11.9 and 11.1% at ZnO concentration 0.20, 0.35, 0.50, 1.0, 1.5 and 2.0 g/L, respectively. No significant improvement in biodegradability was observed and the maximum  $BOD_5/COD$  ratio was 0.034. Low biodegradability may be due to the toxicity of antibiotics degradation products and dissolved zinc. Based on the results, the optimum ZnO concentration for degradation of amoxicillin, ampicillin and cloxacillin in aqueous solution is 0.5 g/L.

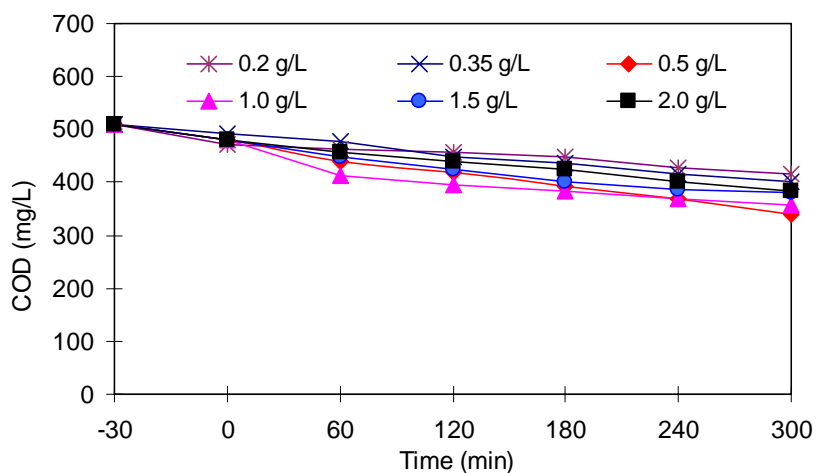


Figure 4.89 Effect of ZnO concentration on antibiotics degradation in terms of COD

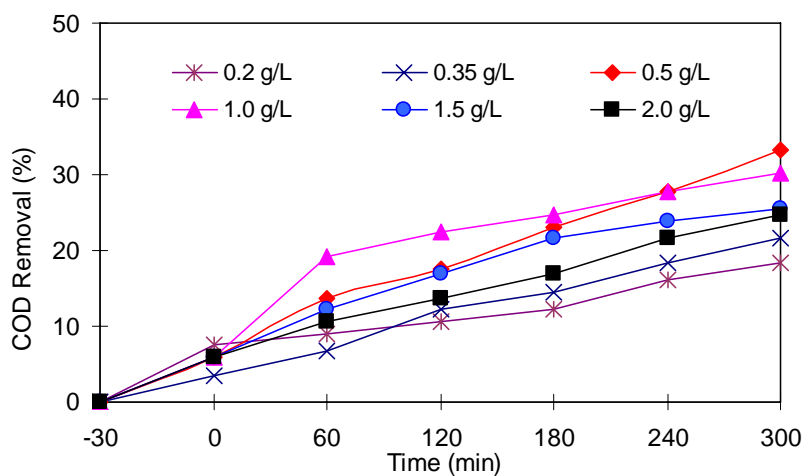


Figure 4.90 Effect of ZnO concentration on antibiotics degradation in terms of COD removal

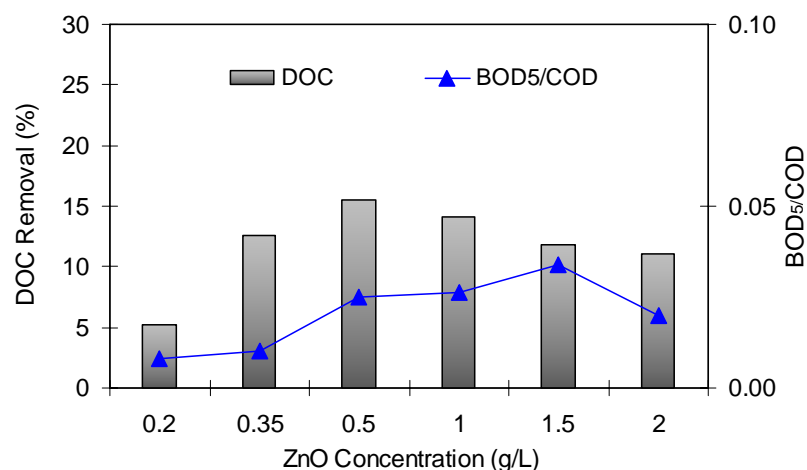


Figure 4.91 Effect of ZnO concentration on antibiotics degradation in terms of DOC removal and biodegradability improvement

#### 4.4.2 Effect of pH and Irradiation Time

The pH value is considered an important factor since it influences the surface charge properties of the semiconductor. To study the effect of initial pH on the degradation of AMX, AMP and CLX, experiments were conducted by varying the pH in the range 5-11. The experimental conditions were AMX, AMP and CLX concentration 104, 105 and 103 mg/L, respectively (COD 520 mg/L) and ZnO concentration 0.5 g/L. AMX after 300 min irradiation time was 42, 29 and 0 mg/L (Figure 4.92); however, AMX degradation was 59.2, 72.1 and 100% (Figure 4.93) at pH 5, 8 and 11, respectively. AMP after 300 min irradiation time was 60, 30 and 0 mg/L (Figure 4.94); however, AMP degradation was 42.9, 71.4 and 100% (Figure 4.95) at pH 3, 5, 8 and 11, respectively. CLX after 300 min irradiation time was 0, 0 and 0 mg/L (Figure 4.96); however, CLX degradation was 100, 100 and 100% (Figure 4.97) at pH 3, 5, 8 and 11, respectively. Based on the results, the optimum pH and irradiation time for degradation of amoxicillin, ampicillin and cloxacillin in aqueous solution are 11 and 180 min, respectively.

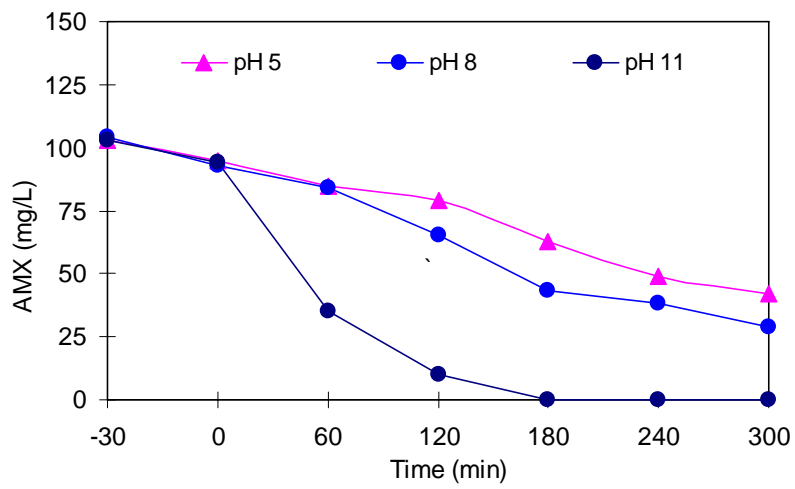


Figure 4.92 Effect of pH on AMX by UV/ZnO process

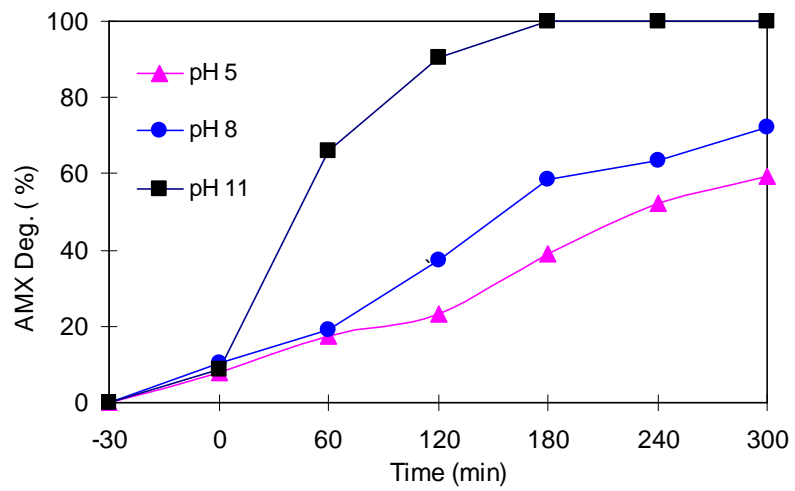


Figure 4.93 Effect of pH on AMX degradation by UV/ZnO process

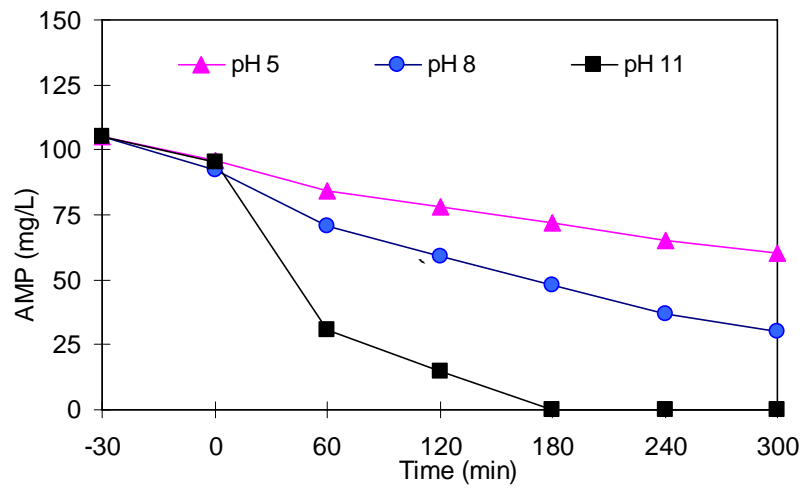


Figure 4.94 Effect of pH on AMP by UV/ZnO process

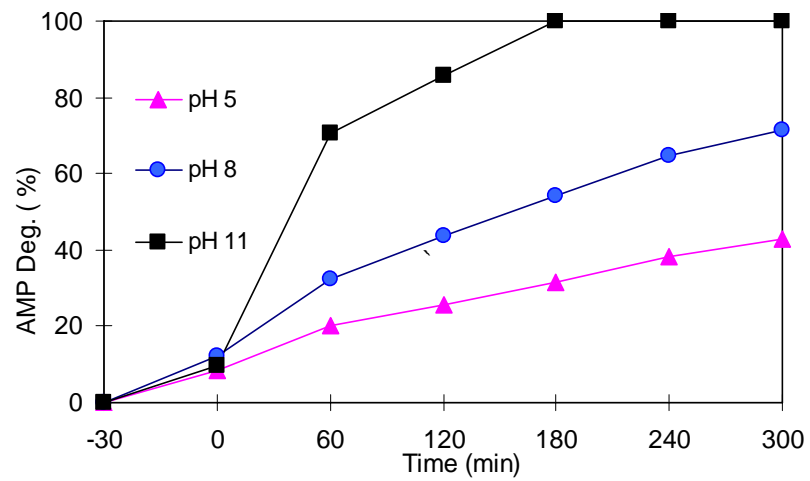


Figure 4.95 Effect of pH on AMP degradation by UV/ZnO process

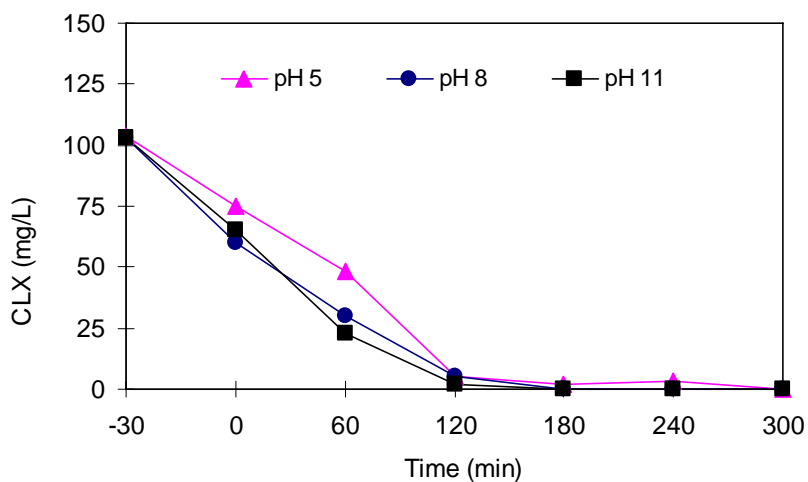


Figure 4.96 Effect of pH on CLX by UV/ZnO process

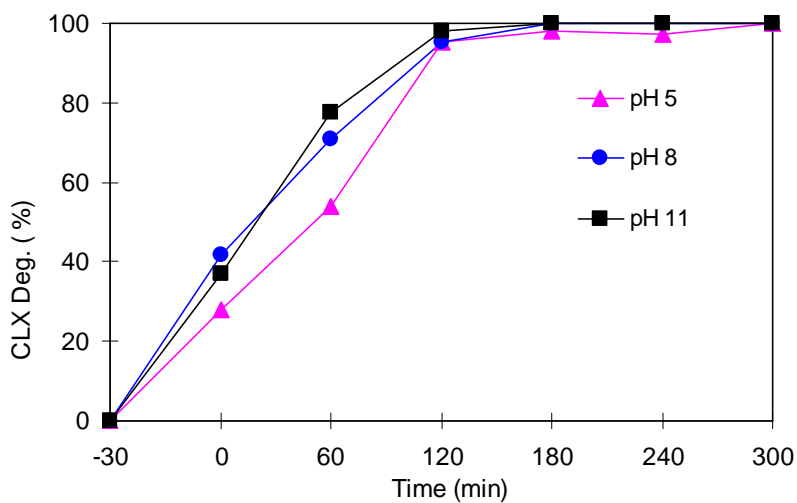


Figure 4.97 Effect of pH on CLX degradation by UV/ZnO process

A statistical analysis (one-way ANOVA) performed on the results at a 5% level of significance indicated that AMX, AMP and CLX degradation were significantly affected by ZnO concentration and pH (Table 4.3).

Table 4.3 One-way ANOVA for AMX, AMP and CLX degradation at different ZnO concentration and pH

Parameter	Antibiotic	No. of groups	F	P-value	F crit
ZnO	AMX	6	34.3	2.96E <sup>-13</sup>	2.4
	AMP	6	211.9	5.30E <sup>-26</sup>	2.4
	CLX	6	99.8	1.57E <sup>-20</sup>	2.4
pH	AMX	3	4.9	0.0067	2.8
	AMP	3	3.6	0.0225	2.8
	CLX	3	158.6	4.72E <sup>-12</sup>	2.8

Figures 4.98 and 4.99 show the effect of pH on antibiotics degradation in terms of COD and COD removal. COD after 300 min irradiation time was 384, 376 and 366 mg/L (Figure 4.98); however, COD removal after 300 min irradiation time was 24.7, 26.3 and 28.2% at pH 5, 8 and 11, respectively (Figure 4.99). Figure 4.100 shows the effect of pH on antibiotics degradation in terms of DOC removal and biodegradability (BOD<sub>5</sub>/COD ratio) improvement. DOC removal after 300 min irradiation time was 11.1, 15.6 and 16.3% at pH 5, 8 and 11, respectively. No significant improvement in biodegradability was observed and the maximum BOD<sub>5</sub>/COD ratio at pH 11 was 0.036.

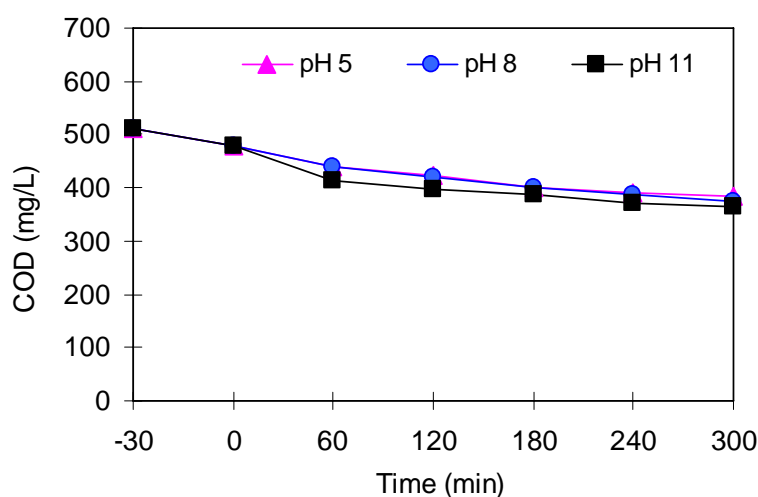


Figure 4.98 Effect of pH on antibiotics degradation in terms of COD by UV/ZnO process

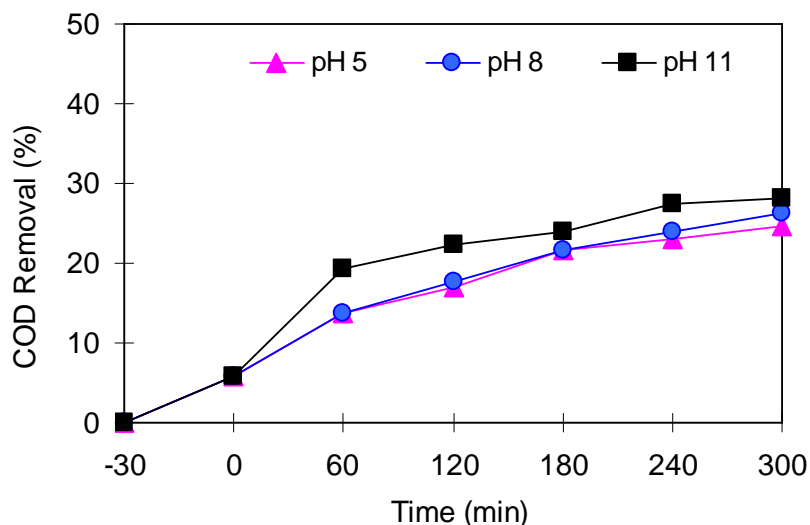


Figure 4.99 Effect of pH on antibiotics degradation in terms of COD removal by UV/ZnO process

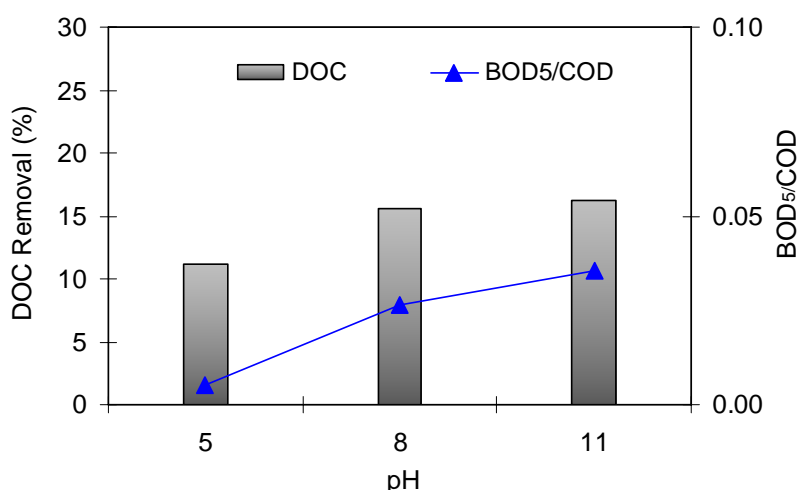


Figure 4.100 Effect of pH on antibiotics degradation in terms of DOC removal and biodegradability improvement

The effect of pH on antibiotic degradation can be explained by taking into consideration the properties of both the catalyst and antibiotic at different pH. For ZnO, the zero point charge is  $9.0 \pm 0.3$  (Akyol *et al.*, 2004) and hence the ZnO surface is positively charged at  $\text{pH} < 9$  and is negatively charged at  $\text{pH} > 9$ . It is reported that ionic amoxicillin species changes from positive charge at acidic pH to negative charge at alkaline pH as shown in Figure 4.71 (Chemie, 2005). At acidic pH, both



ZnO and amoxicillin are positively charged and hence, adsorption on the surface of ZnO is limited. At near neutral pH, amoxicillin has negative charge, whereas ZnO still has same positive charge favouring adsorption. At pH > 9, both amoxicillin and the ZnO are negatively charged and so repulsive forces between the catalyst and the antibiotics are developed. The results show that the adsorption of the antibiotics after 30 min dark adsorption was slightly higher at pH 8 compared to pH 11 and 5, and the adsorption percent varied for each antibiotic depending on their property (Figures 4.54, 4.55 and 4.56). High degradation of antibiotics in alkaline condition may be due to two facts. First is the presence of large quantities of OH<sup>-</sup> ions on ZnO surface favoring formation of OH<sup>•</sup> radicals (Kansal *et al.*, 2007). Second is the hydrolysis of the antibiotics due to instability of the β-lactam ring at high pH as reported by Hou and Pool (1971).

#### 4.4.3 Kinetics Study

Kinetics of AMX, AMP and CLX Degradation as well as Kinetics of Antibiotic Mineralization by UV/ZnO Process are presented herein.

##### 4.4.3.1 Kinetics of AMX, AMP and CLX Degradation by UV/ZnO Process

To study the kinetics of amoxicillin, ampicillin and cloxacillin degradation by UV/ZnO process, experiments were conducted under optimum operating conditions (ZnO concentration 0.5 g/L, irradiation time 180 min and pH 11). The concentration of AMX, AMP and CLX concentration after 30 min dark adsorption was taken as initial AMX, AMP and CLX concentration for kinetic analysis. Figure 4.101 shows the plots of  $-\ln \frac{[Antibiotic]}{[Antibiotic_0]}$  versus irradiation time for amoxicillin, ampicillin and cloxacillin. The linearity of the plots suggest that the photocatalytic reaction approximately followed a pseudo-first order kinetics. Degradation of cloxacillin exhibited the highest rate constant (0.029 min<sup>-1</sup>), followed by amoxicillin (0.018 min<sup>-1</sup>) and ampicillin (0.015 min<sup>-1</sup>).

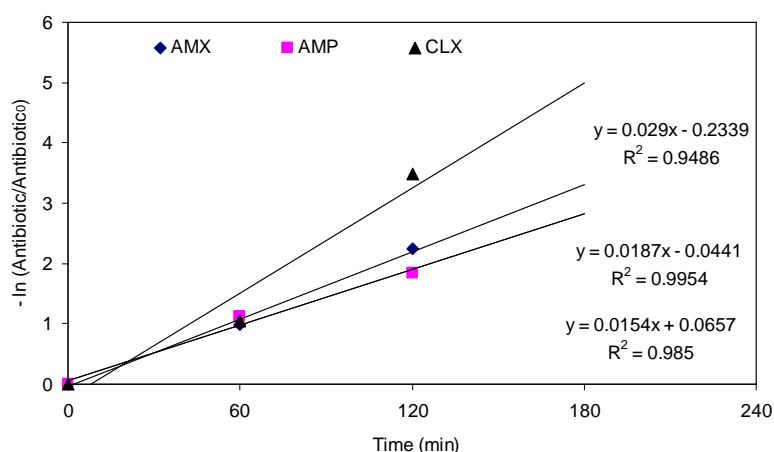


Figure 4.101 Kinetics of AMX, AMP and CLX degradation by UV/ZnO process

#### 4.4.3.2 Kinetics of Antibiotic Mineralization by UV/ZnO Process

For a comparison with the previous processes (Fenton, photo-Fenton and UV/H<sub>2</sub>O<sub>2</sub>/TiO<sub>2</sub>), it would be appropriate to assess the rate constant with respect to DOC rather than to a particular antibiotic and Equation 3.4 can be used in the kinetic study. Pseudo-first-order rate constant ( $k_0$ ) can be obtained through a linear least-square fit of the DOC data. Half-life time ( $t_{1/2}$ ) was calculated according to Equation 3.5. Figure 4.102 shows the plot of  $-\ln \frac{[DOC]}{[DOC_0]}$  versus irradiation time for antibiotic mineralization by the UV/ZnO process under optimum operating conditions (ZnO 0.5 g/L and pH 11). The linearity of the plots suggests that the UV/ZnO process approximately followed the pseudo-first order kinetic with rate constant of 0.00056 min<sup>-1</sup> and  $t_{1/2}$  1238 min.

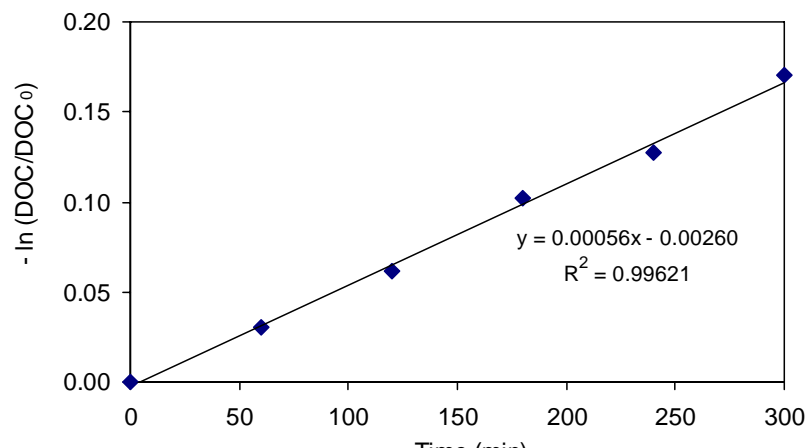


Figure 4.102 Kinetic study of antibiotic mineralization by UV/ZnO process

## 4.5 Comparison among the Studied Advanced Oxidation Processes

In order to identify the most promising advanced oxidation process for degradation of the antibiotic, mineralization and biodegradability improvement, a technical as well as cost comparison among the studied advanced oxidation processes (AOPs) were made.

### 4.5.1 Technical Comparison

A comparison among the studied AOPs was made in terms of antibiotics degradation, mineralization, biodegradability (BOD<sub>5</sub>/COD ratio) improvement, kinetic constants and half-life time ( $t_{1/2}$ ) under their optimum operating conditions. Tables 4.4 and 4.5 summarize the effect of operating conditions such as oxidant and catalyst concentration, and pH on the treatment of antibiotic aqueous solution by Fenton, photo-Fenton, TiO<sub>2</sub> photocatalysis (UV/TiO<sub>2</sub> and UV/H<sub>2</sub>O<sub>2</sub>/TiO<sub>2</sub>) and UV/ZnO processes. Homogeneous advanced oxidation processes (Fenton and photo-Fenton) appeared to be more effective for antibiotics degradation and mineralization, and biodegradability improvement compared to heterogeneous advanced oxidation processes (TiO<sub>2</sub> photocatalysis and UV/ZnO process). The optimum operating conditions for degradation, mineralization and biodegradability improvement of amoxicillin, ampicillin, and cloxacillin antibiotics in aqueous solution were observed to be: Fenton process – H<sub>2</sub>O<sub>2</sub>/COD molar ratio 3, H<sub>2</sub>O<sub>2</sub>/Fe<sup>2+</sup> molar ratio 10

(COD/H<sub>2</sub>O<sub>2</sub>/Fe<sup>2+</sup> molar ratio 1:3:0.30) and pH 3; photo-Fenton process – H<sub>2</sub>O<sub>2</sub>/COD molar ratio 1.5, H<sub>2</sub>O<sub>2</sub>/Fe<sup>2+</sup> molar ratio 20 (COD/H<sub>2</sub>O<sub>2</sub>/Fe<sup>2+</sup> molar ratio 1:1.5:0.075) and pH 3; TiO<sub>2</sub> photocatalysis – TiO<sub>2</sub> concentration 1 g/L, ambient pH ~ 5 and H<sub>2</sub>O<sub>2</sub> concentration 100 g/L; and ZnO photocatalysis – ZnO concentration 0.5 g/L and pH 11.

Table 4.4 Operating conditions and results of Fenton and photo-Fenton processes

Process	pH	H <sub>2</sub> O <sub>2</sub> /COD	H <sub>2</sub> O <sub>2</sub> /Fe <sup>2+</sup>	Time (min)	COD removal (%)	BOD <sub>5</sub> /COD	DOC removal (%)
F01	3	1	50	50	21	0.04	11
F02	3	1.5	50	50	24	0.06	17
F03	3	2	50	50	47	0.20	25
F04	3	2.5	50	50	51	0.26	27
F05	3	3	50	50	55	0.30	32
F06	3	3.5	50	50	50	0.21	32
F07	3	3	2	50	72	0.20	39
F08	3	3	5	50	75	0.24	48
F09	3	3	10	50	79	0.35	52
F10	3	3	20	50	71	0.36	35
F11	3	3	50	50	55	0.30	32
F12	3	3	100	50	49	0.18	13
F13	3	3	150	50	39	0.11	14
F14	2	3	10	50	44	0.12	31
F15	2.5	3	10	50	52	0.18	42
F16	3	3	10	50	80	0.35	53
F17	3.5	3	10	50	76	0.25	48
F18	4	3	10	50	75	0.19	45
PF01	3.5	1	50	50	66	0.18	41
PF02	3.5	1.5	50	50	72	0.23	46
PF03	3.5	2	50	50	61	0.16	40
PF04	3.5	2.5	50	50	46	0.11	41
PF05	3.5	1.5	10	50	76	0.34	47
PF06	3.5	1.5	20	50	75	0.34	46
PF07	3.5	1.5	50	50	72	0.23	46
PF08	3.5	1.5	100	50	54	0.14	36
PF09	3.5	1.5	150	50	48	0.12	34
PF10	2	1.5	20	50	42	0.13	33
PF11	2.5	1.5	20	50	71	0.28	40
PF12	3	1.5	20	50	81	0.39	58
PF13	3.5	1.5	20	50	75	0.34	46
PF14	4	1.5	20	50	73	0.27	46

Irradiation or reaction time for the experiments was 50 min  
 Complete degradation of the antibiotics in 2 min

Table 4.5 Operating conditions and results of TiO<sub>2</sub> photocatalysis and UV/ZnO processes

Process	pH	TiO <sub>2</sub>	H <sub>2</sub> O <sub>2</sub>	ZnO	Antibiotic degradation (%)			BOD <sub>5</sub> /COD	COD removal	DOC removal
		(g/L)	(mg/L)	(g/L)	AMX	AMP	CLX		(%)	(%)
T01	5	0.5	-	-	42	33	47	<0.05	6	3.4
T02	5	1.0	-	-	55	52	58	<0.05	9	6.3
T03	5	1.5	-	-	56	54	59	<0.05	10	6.0
T04	5	2.0	-	-	55	52	60	<0.05	10	5.3
T05	3	1.0	-	-	61	78	95	<0.05	12	4.0
T06	5	1.0	-	-	55	52	58	<0.05	9	6.3
T07	8	1.0	-	-	59	74	82	<0.05	10	4.5
T08	11	1.0	-	-	71	91	100	<0.05	11	5.0
T09	5	1.0	50	-	100	100	100	0.05	15	6.4
T10	5	1.0	100	-	100	100	100	0.10	26	14.0
T11	5	1.0	150	-	100	100	100	0.09	23	9.6
T12	5	1.0	200	-	100	100	100	0.07	16	6.9
T13	5	1.0	300	-	100	100	100	0.06	12	5.3
Z01	8	-	-	0.2	100	44	60	<0.05	18	5.2
Z02	8	-	-	0.4	100	52	69	<0.05	22	12.6
Z03	8	-	-	0.5	100	72	73	<0.05	33	15.6
Z04	8	-	-	1.0	100	71	70	<0.05	30	14.1
Z05	8	-	-	1.5	100	70	69	<0.05	25	11.9
Z06	8	-	-	2.0	100	69	68	<0.05	25	11.1
Z07	5	-	-	0.5	100	59	43	<0.05	25	11.1
Z08	8	-	-	0.5	100	72	71	<0.05	26	15.6
Z09	11	-	-	0.5	100	100	100	<0.05	28	16.3

Irradiation time for the experiments was 300 min

Table 4.6 shows a comparison among Fenton, photo-Fenton, UV/H<sub>2</sub>O<sub>2</sub> /TiO<sub>2</sub> and UV/ZnO processes in terms of effluent characteristics under their optimum operating conditions. All studied AOPs were able to degrade and mineralize the antibiotics and improve the biodegradability, except UV/ZnO which did not improve the biodegradability. Hence, Fenton, photo-Fenton and UV/TiO<sub>2</sub>/H<sub>2</sub>O<sub>2</sub> processes are

considered promising AOPs for treatment of the antibiotic aqueous solution containing AMX, AMP and CLX.

Table 4.6 Comparison among Fenton, photo-Fenton, UV/H<sub>2</sub>O<sub>2</sub>/TiO<sub>2</sub> and UV/ZnO processes in terms of effluent characteristics under optimum operating conditions

	Parameter	Fenton	Photo-Fenton	UV/H <sub>2</sub> O <sub>2</sub> /TiO <sub>2</sub>	UV/ZnO
Operating conditions	H <sub>2</sub> O <sub>2</sub> /COD	3.0	1.5	-	-
	H <sub>2</sub> O <sub>2</sub> /Fe <sup>2+</sup>	10	20	-	-
	COD/H <sub>2</sub> O <sub>2</sub> /Fe <sup>2+</sup>	1:3:0.3	1:1.5:0.075	-	-
	TiO <sub>2</sub> (g/L)/H <sub>2</sub> O <sub>2</sub> (mg/L)	-	-	1/100	-
	ZnO (g/L)	-	-	-	0.5
	pH	3	3	5	11
Effluent Characteristics	Complete Antibiotics degradation time (min)	2	2	30	180
	COD removal (%) <sup>*</sup>	80	81	26	28
	DOC removal (%) <sup>*</sup>	53	58	14	16
	BOD <sub>5</sub> /COD <sup>*</sup>	0.35	0.39	0.1	<0.05

\*At 50 min for Fenton and photo-Fenton; at 300 min for UV/H<sub>2</sub>O<sub>2</sub>/TiO<sub>2</sub> and UV/ZnO process

The kinetics of antibiotics mineralization by Fenton, photo-Fenton processes, and UV/H<sub>2</sub>O<sub>2</sub>/TiO<sub>2</sub> and UV/ZnO processes can be represented as a first-order rate by Equation 3.4. The half-life time ( $t_{1/2}$ ) was calculated according to Equation 3.5. Value of the pseudo-first order rate constant ( $k_0$ ) was obtained by fitting the experimental data to a straight line (Figure 4.103) and the results are summarized in Table 4.7. The values of half-life time ( $t_{1/2}$ ) are also presented in Table 4.7. Photo-Fenton showed the highest  $k_0$  and it is 1.4, 28 and 25 times higher than that of Fenton, UV/H<sub>2</sub>O<sub>2</sub>/TiO<sub>2</sub> and UV/ZnO processes, respectively.

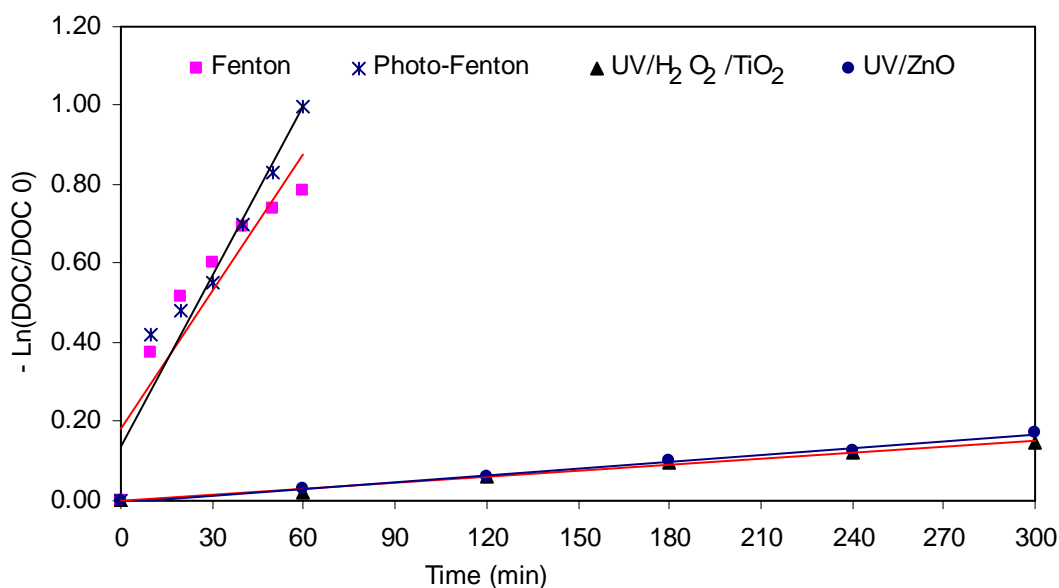


Figure 4.103 Kinetics of antibiotic mineralization by different AOPs under optimum operating condition

Table 4.7 Pseudo-first-order rate constant and half-life time for different AOPs under optimum operating condition

Process	$k_0(\text{min}^{-1})$	$t_{1/2}$	$R^2$
Fenton	0.01	69.3	0.86
Photo-Fenton	0.014	49.5	0.97
UV/H <sub>2</sub> O <sub>2</sub> /TiO <sub>2</sub>	0.00050	1386	0.99
UV/ZnO	0.00056	1238	0.99

#### 4.5.2 Cost Comparison

Estimation of the treatment cost is an important aspect. The overall cost of the treatment process is represented by the sum of the capital, operating and maintenance cost. For a full-scale system, these costs strongly depend on the nature and concentration of the pollutants, flow rate of the influent and configuration of the reactor (Andreozzi *et al.*, 1999). In the literature, some efforts have been made for estimation of electrical consumption for UV lamps (Bolton *et al.*, 1996; Andreozzi *et al.*, 1999). One of these procedures to estimate the electrical energy is based on the electrical energy ( $EE$ ) in kilowatt hours (kWh) required to bring about the



degradation of a unit mass (one kilogram, kg) of a contaminant in polluted water and can be calculated by Equation 4.2.

$$EE = \frac{p \times t \times 1000}{V \times M \times 60 \times (c_i - c_f)} \quad \text{Equation 4.2}$$

where,  $EE$  is the energy requirement per kilogram of organic pollutant as DOC,  $p$  is the lamp power (kW),  $V$  is the polluted water volume (litres),  $t$  is the half-life time (min) for achieving 50% mineralization of DOC,  $M$  is the molecular weight of the pollutant (g/mol),  $c_i$ ,  $c_f$  are the initial and final concentrations of the pollutant (mol/L) and the factor of 1000 converts g to kg (Cañizares *et al.*, 2009). Price of electricity is highly dependent on the particular country and the electricity price was taken \$0.10/kwh as an average value (Cañizares *et al.*, 2009). The average price of the chemical reagents is shown in Table 4.8. An estimation of the operating cost per kg of DOC was calculated for mineralization of 50% of the initial DOC and shown in Table 4.9. Photo-Fenton process appeared to be the most cost-effective. However, the cost may be decreased considerably for photocatalytic processes when solar light is used (Curcó *et al.*, 1996; Giménez *et al.*, 1997; Giménez *et al.*, 1999).

Table 4.8 Price of the chemical reagents

Reagent	Unit	Price (\$)
H <sub>2</sub> O <sub>2</sub> (35%) (Cañizares <i>et al.</i> , 2009)	kg	0.35
FeSO <sub>4</sub> ·7H <sub>2</sub> O (Cañizares <i>et al.</i> , 2009)	kg	0.5
TiO <sub>2</sub> (Cañizares <i>et al.</i> , 2009)	kg	3
ZnO (Chen and McHale, 2009)	kg	2.2

Table 4.9 Cost estimation for the studied AOPs

	Reagent	Fenton	Photo-Fenton	UV/H <sub>2</sub> O <sub>2</sub> /TiO <sub>2</sub>	UV/ZnO
Chemical requirement (kg/ kg DOC)	H <sub>2</sub> O <sub>2</sub>	25.49	12.74	1.54	-
	FeSO <sub>4</sub> ·7H <sub>2</sub> O	20.85	5.2	-	-
	TiO <sub>2</sub>	-	-	15.38	-
	ZnO	-	-	-	7.69
Cost estimation (\$/kg DOC)	H <sub>2</sub> O <sub>2</sub>	9	4	1	-
	FeSO <sub>4</sub> ·7H <sub>2</sub> O	10	3	-	-
	TiO <sub>2</sub>	-	-	46	-
	ZnO	-	-	-	17
	UV	-	8	213	190
Total cost (\$/kg DOC)		19	15	260	207

#### 4.6 Summary

The feasibility of using four advanced oxidation processes (AOPs) (Fenton, photo-Fenton, UV/TiO<sub>2</sub> and UV/ZnO) for treatment of amoxicillin, ampicillin and cloxacillin antibiotics in aqueous solution was evaluated. In the first process (Fenton process), the effect of operating conditions on biodegradability (BOD<sub>5</sub>/COD ratio) improvement and mineralization of amoxicillin, ampicillin and cloxacillin antibiotics in aqueous solution was studied. In addition, degradation of amoxicillin, ampicillin and cloxacillin under optimum operating conditions was also evaluated. The optimum operating conditions for treatment of an aqueous solution containing 104, 105 and 103 mg/L amoxicillin, ampicillin and cloxacillin, respectively were observed to be H<sub>2</sub>O<sub>2</sub>/COD molar ratio 3 and H<sub>2</sub>O<sub>2</sub>/Fe<sup>2+</sup> molar ratio 10 (COD/H<sub>2</sub>O<sub>2</sub>/Fe<sup>2+</sup> molar ratio 1:3:0.3) and pH 3. Under optimum operating conditions, complete degradation of amoxicillin, ampicillin and cloxacillin occurred in 2 min. In addition, biodegradability improved from ~ 0 to 0.4, and COD removal was 81.4% in 60 min. DOC removal was 54.3% and nitrate increased from 0.3 to 10 mg/L, indicating mineralization of organic carbon and nitrogen.

In the second process (photo-Fenton process), the effect of operating conditions on biodegradability improvement and mineralization of amoxicillin, ampicillin and cloxacillin antibiotics in aqueous solution was examined. In addition, degradation of amoxicillin, ampicillin and cloxacillin under optimum operating conditions was also studied. The optimum operating conditions for treatment of the antibiotic aqueous solution was observed to be  $\text{H}_2\text{O}_2/\text{COD}$  molar ratio 1.5 and  $\text{H}_2\text{O}_2/\text{Fe}^{2+}$  molar ratio 20 ( $\text{COD}/\text{H}_2\text{O}_2/\text{Fe}^{2+}$  molar ratio 1:1.5:0.075) and pH 3. Under optimum operating conditions, complete degradation of amoxicillin, ampicillin and cloxacillin occurred in 2 min. Biodegradability improved from  $\sim 0$  to 0.4, and COD and DOC removal were 80.8 and 58.4%, respectively in 50 min. Photo-Fenton treatment resulted in mineralization of organic carbon and nitrogen. DOC removal increased to 58.4% and nitrate increased from 0.3 to 14.2 mg/L in 50 min.

In the third process (UV/ $\text{TiO}_2$  process), the effect of operating conditions ( $\text{TiO}_2$  concentration, pH and irradiation time) on degradation of amoxicillin, ampicillin and cloxacillin in aqueous solution was examined. In addition, enhancement of photocatalysis by addition of  $\text{H}_2\text{O}_2$  (UV/ $\text{H}_2\text{O}_2/\text{TiO}_2$ ) was also evaluated. The pH had a great effect on antibiotic degradation. Antibiotics degradation by UV/ $\text{TiO}_2$  approximately followed a pseudo-first order kinetics and the rate constants ( $k_0$ ) were 0.007, 0.003 and 0.029  $\text{min}^{-1}$  for amoxicillin, ampicillin and cloxacillin, respectively. Under optimum operating conditions ( $\text{TiO}_2$  1 g/L, ambient pH  $\sim 5$  and  $\text{H}_2\text{O}_2$  100 g/L), complete degradation of amoxicillin, ampicillin and cloxacillin occurred in 30 min. Dissolved organic carbon (DOC) removal, and nitrate ( $\text{NO}_3^-$ ), ammonia ( $\text{NH}_3$ ) and sulphate ( $\text{SO}_4^{2-}$ ) formation during degradation indicated mineralization of organic carbon, nitrogen and sulphur.

In the fourth process (UV/ $\text{ZnO}$  process), the effect of operating conditions ( $\text{ZnO}$  concentration, pH and irradiation time) on degradation of amoxicillin, ampicillin and cloxacillin in aqueous solution was evaluated. The pH had a great effect on amoxicillin, ampicillin and cloxacillin degradation. The optimum operating conditions for complete degradation of the antibiotics were  $\text{ZnO}$  0.5 g/L, irradiation time 180 min and pH 11. Under optimum operating conditions, complete degradation of amoxicillin, ampicillin and cloxacillin occurred and COD and DOC

removal were 23.9 and 5.97%, respectively. Antibiotic degradation by UV/ZnO process under the optimum conditions approximately followed a pseudo-first order kinetics with rate constant ( $k_0$ ) 0.018, 0.015 and 0.029  $\text{min}^{-1}$  for amoxicillin, ampicillin and cloxacillin, respectively.

In comparison among the AOPs, all studied processes were able to degrade the antibiotics and improve biodegradability, except for UV/ZnO process which did not improve biodegradability. Photo-Fenton process exhibited the highest rate constant (0.029  $\text{min}^{-1}$ ) followed by Fenton (0.0144  $\text{min}^{-1}$ ), UV/ZnO (0.00056  $\text{min}^{-1}$ ) and UV/H<sub>2</sub>O<sub>2</sub>/TiO<sub>2</sub> (0.0005  $\text{min}^{-1}$ ). Photo-Fenton process appeared to be the most cost-effective compared to the other processes.

CHAPTER 5  
RESULTS AND DISCUSSION  
PHASE II: COMBINED ADVANCED OXIDATION PROCESS AND  
SEQUENCING BATCH REACTOR FOR ANTIBIOTIC WASTEWATER  
TREATMENT

## **5.0 Chapter Overview**

This chapter presents the experimental results and discussion of Phase II study. Three combined advanced oxidation process (AOP) and sequencing batch reactor (SBR) were evaluated for treatment of a real antibiotic wastewater produced from a local antibiotic industry. The chapter is divided into five main sections. Section 5.1 presents the results and discussion of the combined Fenton-SBR. It includes the effect of Fenton-SBR operating conditions on the SBR and combined system performance. Results and discussion of the performance of SBR and the combined photo-Fenton-SBR are presented in Section 5.2. Section 5.3 details the performance of the UV/H<sub>2</sub>O<sub>2</sub>/TiO<sub>2</sub>-SBR process including the effect of the operating conditions on the SBR and combined system performance. Section 5.4 presents the kinetic study and in Section 5.5 a treatment system for antibiotic wastewater is proposed.

### **5.1 Combined Fenton and Sequencing Batch Reactor Process (Fenton-SBR)**

Any variation in performance of the pre-treatment and/or post-treatment process is reflected on the performance of the combined process. The combined Fenton and sequencing batch reactor process (Fenton-SBR) may be affected by the Fenton operating conditions such as the oxidant and catalyst dose, and reaction time as well as the SBR operating conditions such as the hydraulic retention time (HRT). The key to efficient integration of advanced oxidation process and biological treatment for recalcitrant wastewater is knowing the required chemical dosages and the reaction or

irradiation time of the AOP process for the effluent to be biodegradable and the hydraulic retention time required for biological treatment. Experiments were designed to answer these questions. In the experimental design,  $\text{H}_2\text{O}_2/\text{COD}$  molar ratio,  $\text{H}_2\text{O}_2/\text{Fe}^{2+}$  molar ratio and reaction time were varied in order to study the performance of the Fenton process. The SBR was fed with the Fenton-treated effluent under different operating conditions to study the performance of the SBR under these conditions. In addition, the SBR cycle period was also varied.

### 5.1.1 Pre-treatment of Antibiotic Wastewater Using Fenton Process

In this section, the effect of operating conditions ( $\text{H}_2\text{O}_2/\text{COD}$  molar ratio and  $\text{H}_2\text{O}_2/\text{Fe}^{2+}$  molar ratio) on biodegradability ( $\text{BOD}_5/\text{COD}$  ratio) improvement and mineralization of the antibiotic wastewater was studied.

#### 5.1.1.1 Effect of $\text{H}_2\text{O}_2/\text{COD}$ Molar Ratio

The effect of  $\text{H}_2\text{O}_2/\text{COD}$  molar ratio (the ratio was calculated based on sCOD but denoted as  $\text{H}_2\text{O}_2/\text{COD}$  molar ratio) on sCOD and DOC removal, and biodegradability ( $\text{BOD}_5/\text{COD}$  ratio) improvement are shown in Figure 5.1. The operating conditions were pH 3, initial sCOD 575 mg/L (17.97 mM), DOC 165 mg/L, reaction time 30 min and  $\text{H}_2\text{O}_2/\text{Fe}^{2+}$  molar ratio 50. To study the effect of  $\text{H}_2\text{O}_2/\text{COD}$  molar ratio on biodegradability improvement and mineralization, initial  $\text{H}_2\text{O}_2$  concentration was varied in the range 17.97–53.9 mM. The corresponding  $\text{H}_2\text{O}_2/\text{COD}$  and  $\text{COD}/\text{H}_2\text{O}_2/\text{Fe}^{2+}$  molar ratio were 1, 1.5, 2, 2.5 and 3, and 1.0/1.0/0.02, 1.0/1.5/0.03, 1.0/2.0/0.04, 1.0/2.5/0.05 and 1.0/3.0/0.06, respectively. It was expected that as the  $\text{H}_2\text{O}_2/\text{COD}$  molar ratio increased, more hydroxyl radicals would be available to attack the substrate and therefore degradation would increase. As can be seen in Figure 5.1, the COD removal was  $43\pm 2$ ,  $47\pm 1$ ,  $49\pm 1$ ,  $52\pm 1$  and  $54\pm 1\%$  at  $\text{H}_2\text{O}_2/\text{COD}$  molar ratio 1, 1.5, 2.0, 2.5 and 3.0, respectively. The  $\text{BOD}_5/\text{COD}$  ratio was  $0.32\pm 0.01$ ,  $0.37\pm 0.01$ , and  $0.39\pm 0.01$ ,  $0.46\pm 0.03$  and  $0.43\pm 0.01$  at  $\text{H}_2\text{O}_2/\text{COD}$  molar ratios 1, 1.5, 2.0, 2.5 and 3.0, respectively. It may be noted that a wastewater is considered biodegradable if the  $\text{BOD}_5/\text{COD}$  ratio is 0.40 (Al-Momani *et al.*, 2002). The DOC removal was  $16\pm 4$ ,  $27\pm 6$ ,  $29\pm 1$ ,  $39\pm 1$  and

42±1% at H<sub>2</sub>O<sub>2</sub>/COD molar ratio 1, 1.5, 2.0, 2.5 and 3.0, respectively. The results show that COD and DOC removal, and biodegradability (BOD<sub>5</sub>/COD ratio) improved with increasing H<sub>2</sub>O<sub>2</sub>/COD molar ratio. Addition of H<sub>2</sub>O<sub>2</sub> in excess of H<sub>2</sub>O<sub>2</sub>/COD molar ratio 2.5-3 did not improve removal and biodegradability. This may be due to scavenging of OH<sup>•</sup> by H<sub>2</sub>O<sub>2</sub> as in Reaction 2.6 (Kavitha and Palanivelu, 2005a).

Based on the results, it may be considered that optimal H<sub>2</sub>O<sub>2</sub>/COD molar ratio is 2.5-3 for biodegradability improvement and mineralization and it agrees well with the Phase I results (Section 4.1.1). A H<sub>2</sub>O<sub>2</sub>/COD molar ratio 2.5 was used in all subsequent experiments.

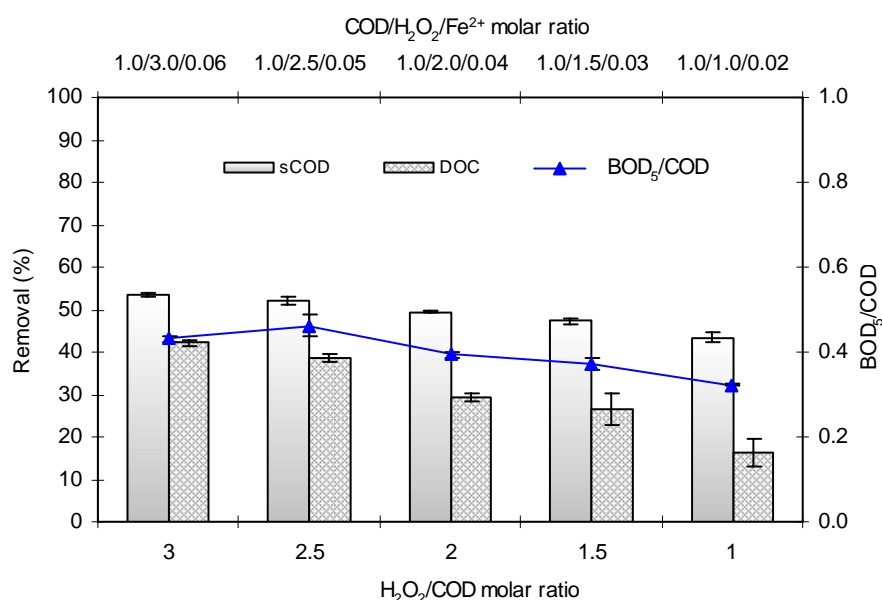


Figure 5.1 Effect of H<sub>2</sub>O<sub>2</sub>/COD molar ratio of Fenton process on sCOD and DOC removal, and BOD<sub>5</sub>/COD ratio

#### 5.1.1.2 Effect of H<sub>2</sub>O<sub>2</sub>/Fe<sup>2+</sup> Molar Ratio

In Fenton process, iron and hydrogen peroxide are two major chemicals determining the operation cost as well as efficiency. The effect of H<sub>2</sub>O<sub>2</sub>/Fe<sup>2+</sup> molar ratio on sCOD and DOC removal, and biodegradability (BOD<sub>5</sub>/COD ratio) improvement are shown in Figure 5.2. The operating conditions were pH 3, initial sCOD 575 mg/L (17.97 mM), DOC 165 mg/L, reaction time 30 min and H<sub>2</sub>O<sub>2</sub>/COD molar ratio 2.5. To

study the effect of  $\text{H}_2\text{O}_2/\text{Fe}^{2+}$  molar ratio on biodegradability improvement and mineralization, experiments were conducted at constant  $\text{H}_2\text{O}_2$  concentration (44.9 mM) and varying  $\text{Fe}^{2+}$  concentration in the range 4.5-0.3 mM. The corresponding  $\text{H}_2\text{O}_2/\text{Fe}^{2+}$  and  $\text{COD}/\text{H}_2\text{O}_2/\text{Fe}^{2+}$  molar ratio were 10, 20, 50, 100 and 150, and 1.0/2.5/0.25, 1.0/2.5/0.125, 1.0/2.5/0.05, 1.0/2.5/0.025 and 1.0/2.5/0.017, respectively. The sCOD removal was  $63\pm 1$ ,  $62\pm 1$ ,  $49\pm 1$ ,  $38\pm 1$  and  $29\pm 1\%$  at  $\text{H}_2\text{O}_2/\text{Fe}^{2+}$  molar ratio 10, 20, 50, 100 and 150, respectively. The  $\text{BOD}_5/\text{COD}$  ratio was  $0.49\pm 0.01$ ,  $0.49\pm 0.02$ ,  $0.37\pm 0.01$ ,  $0.27\pm 0.01$  and  $0.17\pm 0.03$  at  $\text{H}_2\text{O}_2/\text{Fe}^{2+}$  molar ratio 10, 20, 50, 100 and 150, respectively. The DOC removal was  $38\pm 3$ ,  $37\pm 3$ ,  $32\pm 2$ ,  $17\pm 2$  and  $11\pm 1\%$  at  $\text{H}_2\text{O}_2/\text{Fe}^{2+}$  molar ratio 10, 20, 50, 100 and 150, respectively.

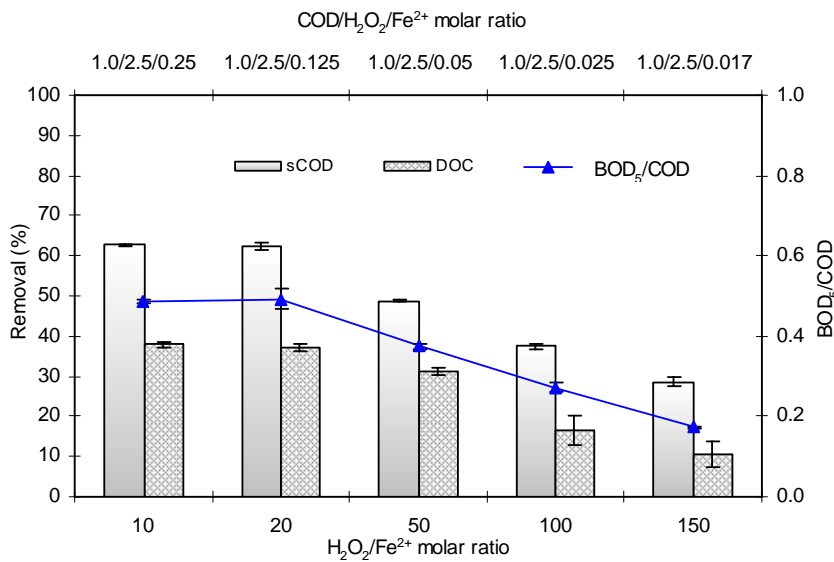


Figure 5.2 Effect of  $\text{H}_2\text{O}_2/\text{Fe}^{2+}$  molar ratio of Fenton process on sCOD and DOC removal, and  $\text{BOD}_5/\text{COD}$  ratio

The results show that sCOD and DOC removal and  $\text{BOD}_5/\text{COD}$  ratio increased with decrease of  $\text{H}_2\text{O}_2/\text{Fe}^{2+}$  molar ratio up to 20-10. Decrease of  $\text{H}_2\text{O}_2/\text{Fe}^{2+}$  molar ratio below 20 did not significantly improve sCOD and DOC removal, and  $\text{BOD}_5/\text{COD}$  ratio. This may be due to direct reaction of  $\text{OH}^\bullet$  radical with metal ions at high concentration of  $\text{Fe}^{2+}$  as in Reaction 2.5 (Joseph *et al.*, 2000).



Based on the results, it may be considered that optimal  $\text{H}_2\text{O}_2/\text{Fe}^{2+}$  molar ratio is 10-20 for biodegradability improvement, sCOD removal and mineralization of the antibiotic wastewater.

### 5.1.1.3 Degradation of Antibiotics

To confirm degradation of the antibiotics and study the matrix effect, an experiment was conducted under the following operating conditions:  $\text{H}_2\text{O}_2/\text{COD}$  molar ratio 2.5,  $\text{H}_2\text{O}_2/\text{Fe}^{+2}$  molar ratio 20 and pH 3. As shown in Figure 5.3, complete degradation of amoxicillin (AMX) and cloxacillin (CLX) occurred in one min. This agrees well with Phase I results (Section 4.1.5) for degradation of antibiotics in aqueous solution and thus, the effect of water matrix can be neglected. It also agrees well with the results reported by Trovó *et al.* (2008) on degradation of amoxicillin, bezafibrate and paracetamol by the Fenton process. They observed 90 and 89% amoxicillin degradation in one min in distilled water and in sewage treatment plant effluent, respectively.

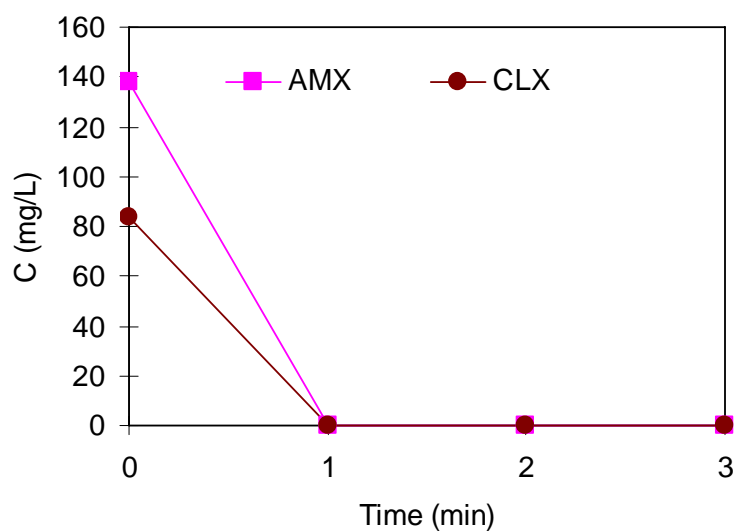


Figure 5.3 Degradation of AMX and CLX in antibiotic wastewater by Fenton process

## 5.1.2 Treatment of Fenton-treated Antibiotic Wastewater by SBR

The SBR was operated for 239 days with Fenton-treated effluent. The Fenton-treated effluent characteristics depended on the Fenton operating conditions. The study covered the effect of the Fenton and SBR operating conditions on the SBR and combined system performance. These conditions are oxidant and catalyst concentration, and Fenton reaction time and SBR hydraulic retention time (HRT).

### 5.1.2.1 Effect of Fenton Operating Conditions on SBR and Combined System Performance

To study the effect of Fenton operating conditions and Fenton-treated effluent characteristics on SBR and combined system performance, ten Fenton-treated effluents (Case F1-F10, Table 5.1) under different COD/H<sub>2</sub>O<sub>2</sub>/Fe<sup>2+</sup> molar ratios were used to feed the SBR. The SBR was operated for 71 days at cycle period 24 hr. The cycle was repeated 6-9 times to allow cell acclimation and/or to obtain repetitive results for each feed. Some of the cases (F1-F5) examined the effect of decreasing H<sub>2</sub>O<sub>2</sub> concentration (decreasing H<sub>2</sub>O<sub>2</sub>/COD molar ratio) and the rest (F6-F10) examined the effect of decreasing Fe<sup>2+</sup> concentration (increasing H<sub>2</sub>O<sub>2</sub>/Fe<sup>2+</sup> molar ratio). Performance of SBR in terms of sCOD and DOC as a function of Fenton operating conditions is shown in Figure 5.4.

Table 5.1 Fenton operating conditions for SBR

Case	H <sub>2</sub> O <sub>2</sub> /COD (MR)	H <sub>2</sub> O <sub>2</sub> /Fe <sup>2+</sup> (MR)	COD/H <sub>2</sub> O <sub>2</sub> /Fe <sup>2+</sup> (MR)
F1	3	50	1.0/3.0/0.06
F2	2.5	50	1.0/2.5/0.05
F3	2	50	1.0/2.0/0.04
F4	1.5	50	1.0/1.5/0.03
F5	1	50	1.0/1.0/0.02
F6	2.5	10	1.0/2.5/0.25
F7	2.5	20	1.0/2.5/0.125
F8	2.5	50	1.0/2.5/0.05
F9	2.5	100	1.0/2.5/0.025
F10	2.5	150	1.0/2.5/0.017

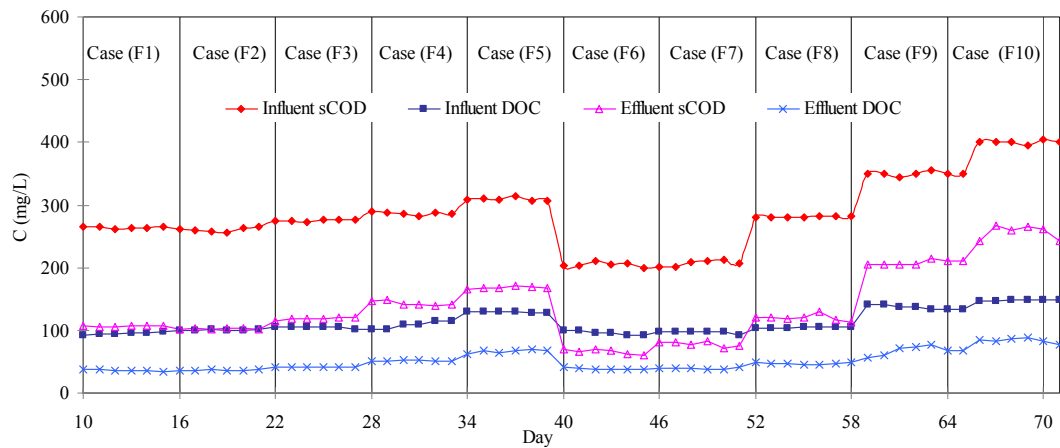


Figure 5.4 Performance of SBR in terms of sCOD and DOC as a function of Fenton operating condition (Case F1-F10)

Table 5.2 shows the Fenton operating conditions, Fenton-treated and SBR effluent characteristics and the combined system efficiency. The effect of decreasing  $\text{H}_2\text{O}_2/\text{COD}$  molar ratio from 3 to 2.5, 2, 1.5 and 1 (decrease of  $\text{H}_2\text{O}_2$  concentration) on SBR performance was examined (Case F1-F5). The other operating conditions of the Fenton process were fixed at  $\text{H}_2\text{O}_2/\text{Fe}^{2+}$  molar ratio 50, reaction time 30 min and pH 3. The SBR cycle period was 24 hr and it was divided into 0.25 hr filling, 22.0 hr aeration, 1.25 hr settling, 0.25 hr decanting and 0.25 hr idle period. The  $\text{H}_2\text{O}_2/\text{COD}$  molar ratio 3 ( $\text{H}_2\text{O}_2$  1832 mg/L) was considered as the starting point. The characteristics of the Fenton-treated effluent (Case F1) were sCOD  $264 \pm 2$  mg/L, DOC  $95 \pm 2$  mg/L and  $\text{BOD}_5/\text{COD}$  ratio  $0.43 \pm 0.01$ . SBR efficiency was  $60 \pm 1$  and  $62 \pm 2\%$  for sCOD and DOC removal, respectively. When  $\text{H}_2\text{O}_2$  concentration was reduced to 1527 mg/L (Case F2), the characteristics of the Fenton-treated effluent were sCOD  $261 \pm 4$  mg/L, DOC  $100 \pm 2$  mg/L and  $\text{BOD}_5/\text{COD}$  ratio  $0.46 \pm 0.03$ , and SBR efficiency was  $61 \pm 1$  and  $64 \pm 1\%$  for sCOD and DOC removal, respectively.

It is seen in Table 5.2 that increasing  $\text{H}_2\text{O}_2/\text{COD}$  molar ratio to more than 2.5 did not improve the SBR efficiency. This is presumably due to the fact that biodegradability ( $\text{BOD}_5/\text{COD}$  ratio) of the Fenton-treated effluents was more than 0.40 in both cases, which is considered biodegradable (Al-Momani *et al.*, 2002). Decreasing SBR efficiency with decreasing  $\text{H}_2\text{O}_2/\text{COD}$  molar ratios below 2.5 may be ascribed to decrease of biodegradability below 0.4 and this indicates inhibition of the aerobic oxidation by the antibiotic intermediates.

MLSS varied from 2350 mg/L at BOD<sub>5</sub>/COD ratio 0.43±0.01 (Case F1) to 2250 mg/L at BOD<sub>5</sub>/COD ratio 0.32±0.01 (Case F5). The reduction in MLSS concentration is considered small and it may be due to biomass growth on the SBR wall as well as inhibition of aerobic oxidation by antibiotic intermediates. The F/M ratio varied in the range 0.074-0.087 day<sup>-1</sup> and this is mainly due to variation in sCOD concentration of the Fenton-treated effluent.

Table 5.2 Fenton-treated and SBR effluent characteristics and combined system efficiency at different H<sub>2</sub>O<sub>2</sub>/COD molar ratio

Case	Fenton-treated effluent							SBR effluent					Combined efficiency		
	H <sub>2</sub> O <sub>2</sub> /COD (MR)	sCOD		DOC		BOD <sub>5</sub>	BOD <sub>5</sub> /COD	sCOD		DOC		MLSS	F/M	sCOD	DOC
		mg/L	R%	mg/L	R%	mg/L		mg/L	R%	mg/L	R%	mg/L	day <sup>-1</sup>	%	%
F1	3	264±2	54±1	95±2	42±1	114±1	0.43±0.01	107±1	60±1	36±1	62±2	2350	0.074	82	77
F2	2.5	261±4	52±1	100±2	39±1	120±6	0.46±0.03	103±1	61±1	36±1	64±1	2320	0.074	81	73
F3	2	275±2	49±1	105±2	29±1	109±3	0.39±0.01	119±2	57±1	41±1	60±1	2280	0.080	78	64
F4	1.5	286±3	47±1	109±6	27±4	107±3	0.37±0.01	143±4	50±1	54±1	50±3	2290	0.083	74	63
F5	1	309±3	43±1	129±1	16±4	100±2	0.32±0.01	168±2	46±1	67±2	48±2	2250	0.087	69	57

The next step was to study the effect of increasing  $\text{H}_2\text{O}_2/\text{Fe}^{2+}$  molar ratio (decrease of  $\text{Fe}^{2+}$  concentration) from 10 to 20, 50, 100 and 150 on SBR performance (Case F6-F10, Table 5.3). The  $\text{H}_2\text{O}_2/\text{Fe}^{2+}$  molar ratio 10 ( $\text{Fe}^{2+}$  250 mg/L) was considered as the starting point. Other operating conditions of the Fenton process were fixed at  $\text{H}_2\text{O}_2/\text{COD}$  molar ratio 2.5, reaction time 30 min and pH 3. The SBR cycle period was 24 hr and it was divided into 0.25 hr filling, 22.0 hr aeration, 1.25 hr settling and 0.25 hr decanting and 0.25 hr idle period. The characteristics of the Fenton-treated effluent (Case F6) were sCOD  $205\pm 4$  mg/L, DOC  $95\pm 3$  mg/L and  $\text{BOD}_5/\text{COD}$  ratio  $0.49\pm 0.01$ . SBR efficiency was  $68\pm 2$  and  $59\pm 1\%$  for sCOD and DOC removal, respectively. When ferrous iron concentration was reduced to 125 mg/L (Case F7), the characteristics of the Fenton-treated effluent were sCOD  $207\pm 4$  mg/L, DOC  $97\pm 3$  mg/L and  $\text{BOD}_5/\text{COD}$  ratio  $0.49\pm 0.02$ , and SBR efficiency was  $62\pm 2$  and  $59\pm 2\%$  for sCOD and DOC removal, respectively. The Fenton-treated effluent characteristics were similar in Case F6 and F7 and hence the expected SBR efficiency. Both Fenton-treated effluents were biodegradable since the  $\text{BOD}_5/\text{COD}$  ratio threshold for a wastewater to be considered biodegradable is 0.4 (Al-Momani *et al.*, 2002). The results show that ferrous iron concentration ( $\text{H}_2\text{O}_2/\text{Fe}^{2+}$  molar ratio) is an important parameter of the combined Fenton-SBR system. Decreasing SBR efficiency with decrease of  $\text{Fe}^{2+}$  concentration (increase of  $\text{H}_2\text{O}_2/\text{Fe}^{2+}$  molar ratios) is presumably due to decrease of biodegradability below 0.4 and this indicates inhibition of aerobic oxidation by the antibiotic intermediates. It is noteworthy that SBR efficiency in terms of sCOD and DOC is very sensitive to  $\text{BOD}_5/\text{COD}$  ratio below 0.40. SBR efficiency in terms of sCOD removal decreased from  $68\pm 2\%$  at  $\text{BOD}_5/\text{COD}$  ratio  $0.48\pm 0.01$  to  $36\pm 3\%$  at  $\text{BOD}_5/\text{COD}$  ratio  $0.17\pm 0.03$ .

A marked decline in MLSS concentration was observed at higher influent sCOD and low  $\text{BOD}_5/\text{COD}$  ratio (Case F10). This reduction in MLSS concentration may be ascribed to wall growth (Farré *et al.*, 2007) and inhibition of aerobic oxidation by antibiotic intermediates. The F/M ratio varied in the range 0.058-0.122  $\text{day}^{-1}$  and this is mainly due to variation in sCOD concentration of the Fenton-treated effluent as well as change in biomass concentration.

Table 5.3 Fenton-treated and SBR effluent characteristics and combined system efficiency at different H<sub>2</sub>O<sub>2</sub>/Fe<sup>2+</sup> molar ratio

Case	Fenton-treated effluent							SBR effluent					Combined efficiency		
	H <sub>2</sub> O <sub>2</sub> /Fe <sup>2+</sup> (MR)	sCOD		DOC		BOD <sub>5</sub>	BOD <sub>5</sub> /COD	sCOD		DOC		MLSS	F/M	sCOD	DOC
		mg/L	R%	mg/L	R%	mg/L		mg/L	R%	mg/L	R%	mg/L	day <sup>-1</sup>	%	%
F6	10	205±4	63±1	95±3	38±3	99±3	0.49±0.1	66±4	68±2	39±1	59±1	2340	0.058	88	79
F7	20	207±4	62±1	97±3	37±3	102±3	0.49±0.02	78±4	62±2	39±1	59±2	2300	0.059	86	74
F8	50	281±1	49±1	105±1	32±2	105±2	0.37±0.01	119±5	58±2	47±1	55±1	2320	0.080	79	74
F9	100	350±4	38±1	137±4	17±3	95±4	0.27±0.01	208±4	40±1	68±8	51±6	2250	0.103	63	59
F10	150	400±4	29±1	148±1	11±1	69±10	0.17±0.03	257±11	36±3	84±4	43±3	2160	0.122	54	49

The combined efficiency achieved by the Fenton-SBR process was similar to those observed in the reported studies. Farré *et al.* (2007) reported 80% DOC removal for treatment of diuron and linuron pesticides by combined photo-Fenton-SBR system at  $\text{H}_2\text{O}_2/\text{Fe}^{2+}$  molar ratio  $\sim 12.7$ , HRT 2 days and VSS  $0.60\pm 0.03$  g /L. Garcia-Montaña *et al.* (2006a) reported 80% DOC removal for treatment of a synthetic textile effluent containing a hetero-bioreactive dye (Cibacron Red FN-R, 250 mg /L) by combined photo-Fenton-SBR system at  $\text{H}_2\text{O}_2/\text{Fe}^{2+}$  molar ratio 12.5, HRT 1 day, irradiation time 90 min and VSS  $0.56\pm 0.03$  g/L. Gonzalez *et al.* (2009) reported 75.7% TOC removal for treatment of a synthetic wastewater containing 200 mg/L sulfamethoxazole by photo-Fenton-sequencing batch biofilm reactor (SBBR). The treatment conditions were 300 mg/L  $\text{H}_2\text{O}_2$  and 10 mg/L  $\text{Fe}^{2+}$  for photo-Fenton process and HRT 8 hr for SBBR.

It should be noted that the Malaysian Standards (B) set for discharge of treated industrial wastewater into receiving water bodies (lakes, rivers) is 100 mg/L in terms of total COD (Malaysian Environmental Quality, 1979). Assuming that COD contribution by suspended solids is  $\sim 30$  mg/L, minimum sCOD in the final effluent should be around 70 mg/L. It is obvious from Tables 5.2 and 5.3 (Case F1-F10) that discharge standard is met by the Fenton-SBR treated antibiotic wastewater (Case F6).

#### 5.1.2.2 Effect of Cycle Period on Performance of SBR

In order to examine the effect of cycle period on SBR performance, HRT was varied in the range 12-48 hr. The SBR was operated for 203 days at HRT 48, 24 and 12 hr and was fed by ten Fenton-treated effluents (Cases F1-F10, Table 5.1). Figures 5.5 and 5.6 show the SBR efficiency in terms of sCOD and DOC removal, respectively at HRT 48, 24 and 12 hr. No remarkable improvement in SBR efficiency in terms of sCOD and DOC removal is seen due to HRT increasing from 12 to 48 hr. This indicates that most of the substrate degradation takes place during the first 12 hr and a smaller portion is degraded in rest of the retention time. In order to this, a statistical analysis (one-way ANOVA) was made on the results at a 5% level of significance. The statistical analysis results are presented in more details in Appendix (A). As



shown in Table 5.4, the statistical analysis indicated that increase of HRT from 24 to 48 hr did not significantly improve sCOD removal (P-value 0.227 > 0.05) or DOC removal (P-value 0.135 > 0.05). HRT decreasing from 24 hr to 12 hr did not also significantly reduce sCOD removal (P-value 0.055 > 0.05) or DOC removal (P-value 0.106 > 0.05).

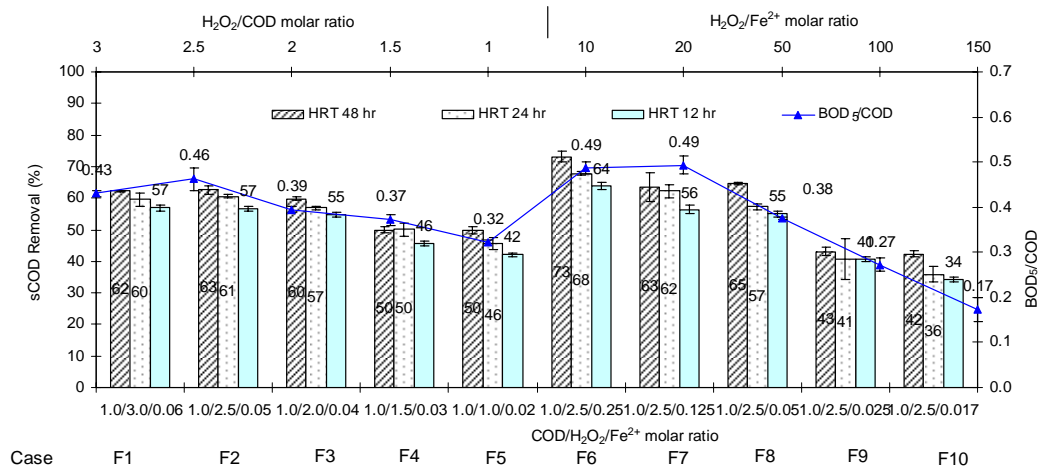


Figure 5.5 SBR efficiency of Fenton-SBR in terms of sCOD removal at HRT 48, 24 and 12 hr

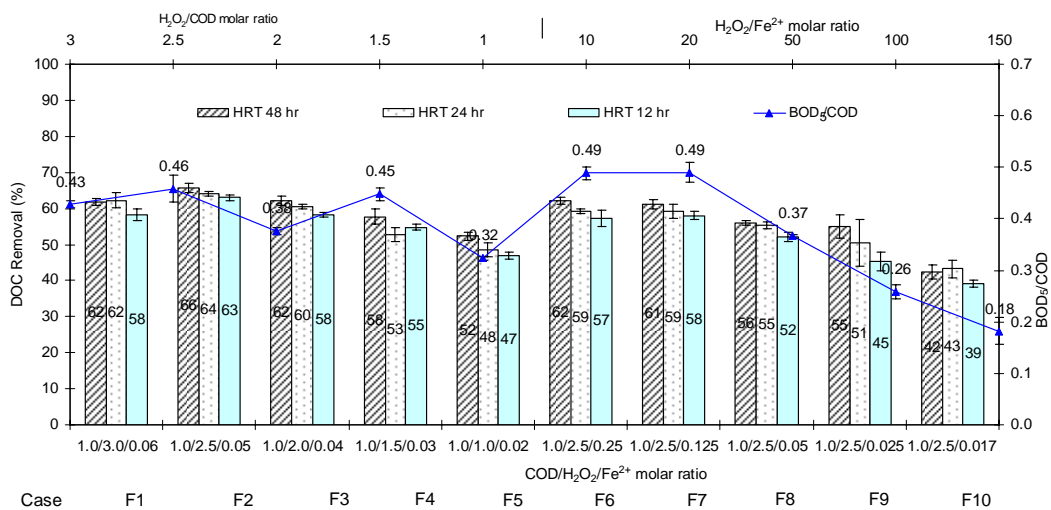


Figure 5.6 SBR efficiency of Fenton-SBR in terms of DOC removal at HRT 48, 24 and 12 hr

Table 5.4 One-way ANOVA for SBR efficiency in terms of sCOD and DOC removal at different HRT (combined Fenton-SBR)

One-way ANOVA	Parameter	No. of groups	F	P-value	F crit
24 hr vs. 48 hr	sCOD	2	1.5	0.227	3.9
12 hr vs. 24 hr	sCOD	2	4.2	0.055	3.9
12 hr vs. 24 hr vs. 48 hr	sCOD	3	5.4	0.006	3.1
24 hr vs. 48 hr	DOC	2	2.3	0.135	3.9
12 hr vs. 24 hr	DOC	2	2.7	0.106	3.9
12 hr vs. 24 hr vs. 48 hr	DOC	3	5.0	0.008	3.1

From the results it can be concluded that SBR efficiency mainly depends on the nature of the by-products generated in the Fenton treatment and no remarkable improvement in SBR efficiency due to HRT increase. It was decided to operate the SBR at 12 hr HRT for subsequent experiments. The results agree well with the reported studies by García-Montaño *et al.* (2006a, 2006b). They reported no remarkable decrease in DOC removal due to increasing HRT from 1 to 2 and 4 days for degradation of a commercial hetero-bioreactive dye and Procion Red H-E7B reactive dye by combined photo-Fenton-SBR system.

### 5.1.2.3 Optimization of Combined Fenton-SBR

In section 5.1.2.1 and 5.1.2.2 it was observed that  $H_2O_2/COD$  molar ratio and  $H_2O_2/Fe^{2+}$  molar ratio significantly affected the SBR performance, whereas HRT increase did not significantly improve the SBR performance. It was found that  $H_2O_2/COD$  molar ratio 2.5 and HRT 12 hr were suitable for the combined Fenton-SBR process in this study. For  $H_2O_2/Fe^{2+}$  molar ratio, it was found that Case F6 ( $H_2O_2/Fe^{2+}$  molar ratio 10) met the discharge standard in terms of sCOD (Table 5.3). So, the next step would be to study the effect of increasing the Fenton reaction time to more than 30 min as well as increasing  $H_2O_2/Fe^{2+}$  molar ratio (decreasing  $Fe^{2+}$  dose) on the combined system performance. The experimental design consisted of nine Fenton-treated effluents (Case F11-F19, Table 5.5).

Table 5.5 Operating conditions for combined Fenton-SBR

Case	Reaction time (min)	H <sub>2</sub> O <sub>2</sub> /COD (MR)	H <sub>2</sub> O <sub>2</sub> /Fe <sup>2+</sup> (MR)	COD/H <sub>2</sub> O <sub>2</sub> /Fe <sup>2+</sup> (MR)	HRT (hr)
F11	60	2.5	50	1.0/2.5/0.05	12
F12	90	2.5	50	1.0/2.5/0.05	12
F13	120	2.5	50	1.0/2.5/0.05	12
F14	60	2.5	100	1.0/2.5/0.025	12
F15	90	2.5	100	1.0/2.5/0.025	12
F16	120	2.5	100	1.0/2.5/0.025	12
F17	60	2.5	150	1.0/2.5/0.017	12
F18	90	2.5	150	1.0/2.5/0.017	12
F19	120	2.5	150	1.0/2.5/0.017	12

The SBR was operated from day 204-239 (36 days) at HRT 12 hr and the cycle was repeated 8 times to obtain repetitive results for each feed. Figure 5.7 shows the performance of the SBR in terms of sCOD and DOC as a function of Fenton operating conditions.

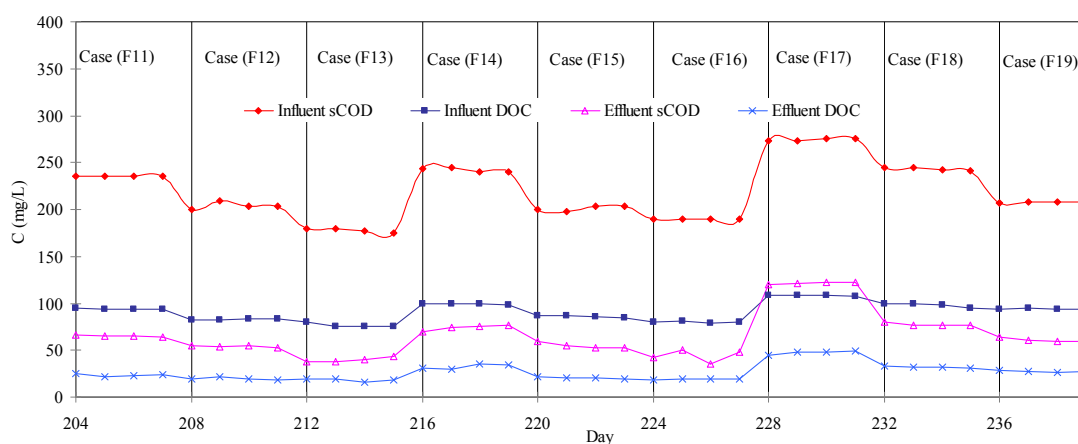


Figure 5.7 Performance of SBR in terms of sCOD and DOC as a function of Fenton operating condition (Case F11-F19)

Table 5.6 shows a summary of Fenton-treated and SBR effluent characteristics and combined system efficiency at different Fenton reaction time and H<sub>2</sub>O<sub>2</sub>/Fe<sup>2+</sup> molar ratio. The other operating conditions of the Fenton process were fixed at H<sub>2</sub>O<sub>2</sub>/COD 2.5 molar ratio and pH 3. The SBR cycle period was 12 hr and it was

divided into 0.25 hr filling, 10 hr aeration, 1.25 hr settling, 0.25 decanting and 0.25 hr idle period.  $\text{H}_2\text{O}_2/\text{Fe}^{2+}$  molar ratio 50 ( $\text{Fe}^{2+}$  250 mg/L) was considered as the starting point since it did not meet the discharge standard as described in Table 5.3. The reaction time was increased from 30 to 60 min (Case F11). The characteristics of the Fenton-treated effluent (Case F11) were sCOD  $236\pm 1$  mg/L, DOC  $94\pm 1$  mg/L and  $\text{BOD}_5/\text{COD}$  ratio  $0.42\pm 0.01$ . SBR efficiency was  $72\pm 1$  and  $75\pm 1\%$  for sCOD and DOC removal, respectively. Considering the similarity between Case F8 (Table 5.3) and F11 (Table 5.6) in Fenton operating conditions except reaction time which was increased from 30 min to 60 min, the SBR efficiency improved in Case F11. Increased Fenton reaction time produced less recalcitrant intermediates ( $\text{BOD}_5/\text{COD}$  ratio  $0.37\pm 0.01$  in Case F8 and  $0.42\pm 0.01$  in Case F11) and hence SBR efficiency improved ( $58\pm 2\%$  Case F8 and  $72\pm 1\%$  Case F11). With regard to the final effluent, the final sCOD was  $65\pm 1$  mg/L which met the discharge standard. When the Fenton reaction time was increased to 90 min (Case F12) and 120 min (Case F13), SBR efficiency improved further ( $74\pm 1\%$  and  $78\pm 2\%$ ).

Table 5.6 Fenton-treated and SBR effluent characteristics and combined system efficiency at different reaction time and  $H_2O_2/Fe^{2+}$  molar ratio

Case	Fenton-treated effluent								SBR effluent					Combined efficiency		
	Reaction time	$H_2O_2/Fe^{2+}$	sCOD		DOC		BOD <sub>5</sub>	BOD <sub>5</sub> /COD	sCOD		DOC		MLSS	F/M	sCOD	DOC
	min	(MR)	mg/L	R%	mg/L	R%	mg/L		mg/L	R%	mg/L	R%	mg/L	day <sup>-1</sup>	%	%
F11	60	50	236±1	57±1	94±1	43±1	98±2	0.42±0.01	65±1	72±1	24±1	75±1	2170	0.074	88	85
F12	90	50	210±8	63±1	83±1	45±1	96±2	0.46±0.02	54±1	74±1	20±2	76±1	2150	0.065	91	85
F13	120	50	178±3	69±1	76±3	54±2	101±1	0.57±0.01	40±3	78±2	18±1	76±2	2100	0.056	93	94
F14	60	100	242±3	58±1	99±1	39±1	91±2	0.38±0.01	74±3	69±1	33±3	67±3	2050	0.078	88	80
F15	90	100	201±3	65±1	86±1	52±1	95±1	0.47±0.01	55±3	73±2	21±1	76±1	2020	0.066	90	87
F16	120	100	190±1	69±1	80±1	54±1	91±2	0.48±0.01	44±6	77±3	19±1	76±1	2100	0.060	93	94
F17	60	150	274±1	51±1	109±1	35±1	94±1	0.34±0.01	121±2	56±1	48±3	56±2	2000	0.091	85	83
F18	90	150	243±2	58±1	98±2	41±2	96±1	0.39±0.01	78±2	68±2	32±1	67±1	1950	0.082	86	81
F19	120	150	207±1	64±1	94±1	44±1	87±1	0.42±0.01	61±1	71±1	28±1	71±1	1940	0.071	89	84

The final SBR effluent in Case F11, F12 and F13 amply met the discharge standard of less than 100 mg/L COD and 70 mg/L sCOD. Based on these results, it was decided to increase  $\text{H}_2\text{O}_2/\text{Fe}^{2+}$  molar ratio to 100 (decrease  $\text{Fe}^{2+}$  to 125 mg/L). The reaction time was 60 min (Case F14), 90 min (Case F15) and 120 min (Case F16). The characteristics of the Fenton-treated effluent (Case F14) were sCOD  $242\pm 3$  mg/L, DOC  $99\pm 1$  mg/L and  $\text{BOD}_5/\text{COD}$  ratio  $0.38\pm 0.01$ . The SBR efficiency was  $69\pm 1$  and  $67\pm 3\%$  for sCOD and DOC removal, respectively. Considering the similarity in the Fenton operating conditions between Case F9 (Table 5.3) and F14 (Table 5.6), the SBR efficiency in terms of sCOD removal increased from  $40\pm 1\%$  in Case F9 (30 min reaction time) to  $69\pm 1\%$  in Case F14 (60 min reaction time). This may be due to the decrease of the recalcitrant intermediates as reaction time increased. With regard to the final effluent, the sCOD concentration was  $74\pm 3$  mg/L which did not meet discharge standard.

In order improve the final effluent characteristics and instead of increasing chemical dosage, Fenton reaction time was increased from 60 min to 90 min (Case F15) at same  $\text{H}_2\text{O}_2/\text{Fe}^{2+}$  molar ratio 100. The characteristics of the Fenton-treated effluent were sCOD  $201\pm 3$  mg/L, DOC  $86\pm 1$  mg/L and  $\text{BOD}_5/\text{COD}$  ratio  $0.47\pm 0.01$ . The SBR efficiency was  $73\pm 2$  and  $76\pm 1\%$  for sCOD and DOC removal, respectively. The sCOD removal by SBR in Case F12 and F15 are similar ( $74\pm 1\%$  and  $73\pm 2\%$ ) which means that reducing  $\text{Fe}^{2+}$  dose from 250 to 125 mg/L at same Fenton reaction time (90 min) did not affect the SBR efficiency. This can be explained by taking into consideration that the biodegradability in both cases is more than 0.40. With regard to the final effluent, the sCOD was  $55\pm 3$  mg/L which met the discharge standard. When Fenton reaction time was increased further to 120 min (Case F16), SBR efficiency improved to  $77\pm 3\%$  and final sCOD was  $44\pm 6$  mg/L.

From the previous results, the final SBR effluent of the combined Fenton-SBR process at  $\text{H}_2\text{O}_2/\text{Fe}^{2+}$  molar ratio 100 and Fenton reaction time 90 and 120 min (Case F15 and F16) amply met the discharge standard. In order to assess the effect of further increasing  $\text{H}_2\text{O}_2/\text{Fe}^{2+}$  molar ratio (reducing  $\text{Fe}^{2+}$  dose) on SBR performance,  $\text{H}_2\text{O}_2/\text{Fe}^{2+}$  molar ratio 150 was used with Fenton reaction time 60, 90 and 120 min (Case F17, F18 and F19). For Case F19 (Fenton reaction time 120 min), the SBR

efficiency was  $71\pm 1\%$  for both sCOD and DOC removal, and the final SBR effluent sCOD was  $61\pm 1$  mg/L.

Since the target was to minimize the use of chemicals ( $\text{Fe}^{2+}$  dose) in the treatment, it was important to know if increasing Fenton reaction time and reducing  $\text{Fe}^{2+}$  dose significantly affected the SBR performance. In order to do that, a two-way analysis of variance (ANOVA) was conducted using SPSS statistical software. Table 5.7 shows the significance of the difference between the two means for sCOD removal in SBR at  $\text{H}_2\text{O}_2/\text{Fe}^{2+}$  molar ratio 50, 100 and 150 and Fenton reaction time 30, 60, 90 and 120 min using Tukey HSD method. The statistical analysis results are presented in more details in Appendix (B). When the value of significance is less than 0.05, it indicates that COD removal in SBR is significantly different and is not significantly different if the value of significance is more than 0.05 (the highlighted values in Table 6.7). There is no difference between the SBR efficiency at  $\text{H}_2\text{O}_2/\text{Fe}^{2+}$  molar ratio 100 and 90 min reaction time (100 MR - 90 min), and SBR efficiency at  $\text{H}_2\text{O}_2/\text{Fe}^{2+}$  molar ratio 150 and 120 reaction time (150 MR - 120 min). If the final SBR effluent in both cases can meet the discharge standard, it may be more economic to choose  $\text{H}_2\text{O}_2/\text{Fe}^{2+}$  molar ratio 150 and 120 min Fenton reaction time as optimum condition (Case F19, Table 5.6).

Table 5.7 Significance of the difference between two means for sCOD removal in SBR using Tukey HSD method (combined Fenton-SBR)

H <sub>2</sub> O <sub>2</sub> /Fe <sup>2+</sup> (MR) and Reaction time (min)	50 MR - 30 min (F8)	50 MR - 60 min (F11)	50 MR - 90 min (F12)	50 MR - 120 min (F13)	100 MR - 30 min (F19)	100 MR - 60 min (F14)	100 MR - 90 min (F15)	100 MR - 120 min (F16)	150 MR - 30 min (F10)	150 MR - 60 min (F17)	150 MR - 90 min (F18)	150 MR - 120 min (F19)
50 MR - 30 min (F8)												
50 MR - 60 min (F11)	0.0											
50 MR - 90 min (F12)	0.0	1.0										
50 MR - 120 min (F13)	0.0	0.0	0.0									
100 MR - 30 min (F9)	0.0	0.0	0.0	0.0								
100 MR - 60 min (F14)	0.0	0.1	0.0	0.0	0.0							
100 MR - 90 min (F15)	0.0	1.0	1.0	0.0	0.0	0.1						
100 MR - 120 min (F16)	0.0	0.0	0.0	1.0	0.0	0.0	0.0					
150 MR - 30 min (F10)	0.0	0.0	0.0	0.0	0.0	0.0	0.0	0.0				
150 MR - 60 min (F17)	1.0	0.0	0.0	0.0	0.0	0.0	0.0	0.0	0.0			
150 MR - 90 min (F18)	0.0	0.0	0.0	0.0	0.0	1.0	0.0	0.0	0.0	0.0		
150 MR - 120 min (F19)	0.0	0.8	0.2	0.0	0.0	1.0	0.6	0.0	0.0	0.0	0.3	

The combined system efficiency also confirmed the finding. As shown in Figure 5.8, the combined system efficiency in terms of sCOD at H<sub>2</sub>O<sub>2</sub>/Fe<sup>2+</sup> molar ratio 50, 100 and 150 with 120 min reaction time was 93, 93 and 89%, respectively. With regard to the final effluent, the final sCOD decreased to 61±1 mg/L (Case F19, Table 5.6) which meets the discharge standard of less than 100 mg/L as COD. Based on the results, the best H<sub>2</sub>O<sub>2</sub>/Fe<sup>2+</sup> molar ratio is 150 and the best reaction time is 120 min.



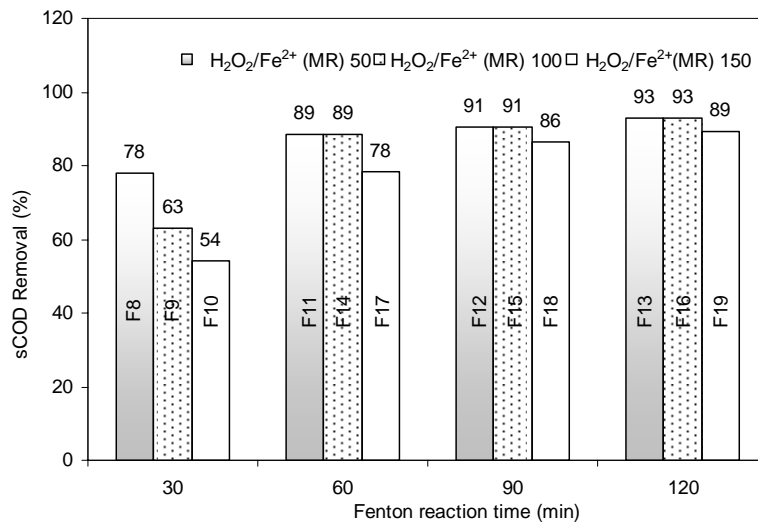


Figure 5.8 Combined Fenton and SBR efficiency in terms of sCOD removal

To study biodegradation of the Fenton-treated effluent and nitrification in SBR, sCOD, DOC, NH<sub>3</sub>, TKN and NO<sub>3</sub><sup>-</sup> were measured during the cycle period (12 hr) for Case F19 and shown in Figures 5.9 and 5.10. The data show that bulk of sCOD and DOC degradation occurred initially (Figure 5.9). Oxidation of NH<sub>3</sub> was complete in 6 hr, residual TKN was 3 mg/L in 12 hr (90% TKN removal) and NO<sub>3</sub><sup>-</sup> concentration was 34 mg/L in 12 hr, indicating adequate nitrification (Figure 5.10).

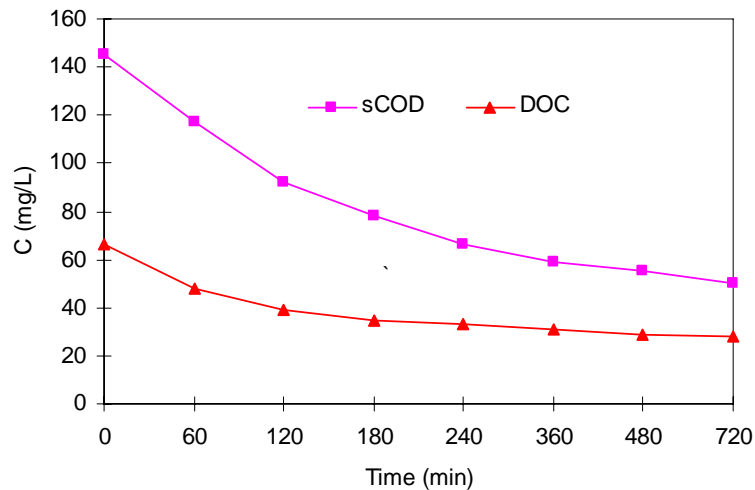


Figure 5.9 Biodegradation of the Fenton-treated effluent in terms of sCOD and DOC in SBR during the cycle period (Case F19)

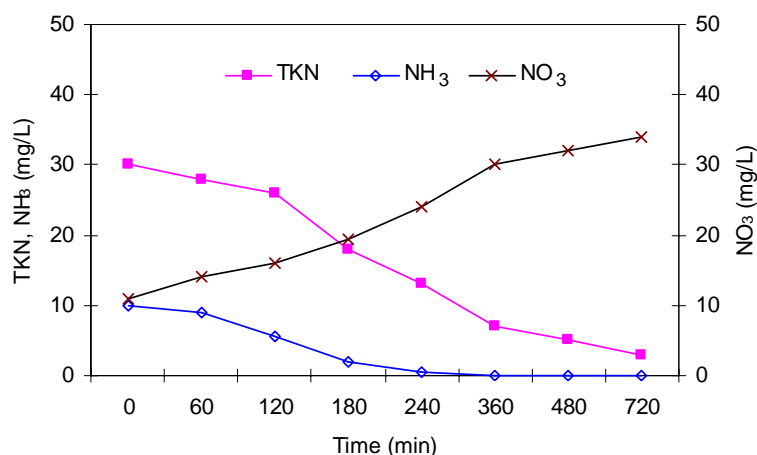


Figure 5.10 Nitrification in SBR during the cycle period (Case F19)

In summary, the SBR was operated for 239 days and fed with Fenton-treated effluent under different Fenton and SBR operating conditions. The  $\text{H}_2\text{O}_2/\text{COD}$  molar ratio 2.5 was found to be the best ratio among five studied ratios (Case F1-F5, Table 5.2). The hydraulic retention time (HRT) of 12 hr was found suitable for the SBR and increasing HRT to 24 and 48 hr did not significantly improve the SBR efficiency in terms of sCOD and DOC removal. The  $\text{H}_2\text{O}_2/\text{Fe}^{2+}$  molar ratio and reaction time of the Fenton process were found to be the most influential parameters. Statistical analysis (two-way ANOVA) was made on the results to optimize the  $\text{H}_2\text{O}_2/\text{Fe}^{2+}$  molar ratio and reaction time and it was found possible to reduce the  $\text{Fe}^{2+}$  dose and increase the Fenton reaction time. Based on the results, the best operating conditions for treatment of the antibiotic wastewater by the combined Fenton-SBR were  $\text{H}_2\text{O}_2/\text{COD}$  molar ratio 2.5,  $\text{H}_2\text{O}_2/\text{Fe}^{2+}$  molar ratio 150, reaction time 120 min and HRT 12 hr. Under the best operating conditions, the Fenton-SBR achieved a combined efficiency of 89% for sCOD removal. Final sCOD of the effluent was 61 mg/L and almost complete nitrification occurred in the SBR.

## 5.2 Combined Photo-Fenton and Sequencing Batch Reactor Process (Photo-Fenton-SBR)

The second treatment train was a combined photo-Fenton and SBR process. The combined photo-Fenton-SBR process may be affected by the photo-Fenton operating

conditions such as the oxidant and catalyst dose, and UV irradiation time as well as the SBR operating conditions such as the hydraulic retention time (HRT). The key to efficient integration of the photo-Fenton process and SBR for recalcitrant wastewater treatment is knowing the required chemical dosages and UV irradiation time for the effluent to be biodegradable and the required hydraulic retention time of the SBR. Experiments were designed to answer these questions. In the experimental design,  $\text{H}_2\text{O}_2/\text{COD}$  molar ratio,  $\text{H}_2\text{O}_2/\text{Fe}^{2+}$  molar ratio and irradiation time were varied in order to study the performance of the photo-Fenton process. The SBR was fed with the photo-Fenton-treated effluent under different operating conditions to study the performance of the SBR under these conditions. In addition, the SBR cycle period was also varied. The operating conditions chosen for combined photo-Fenton-SBR were similar to the combined Fenton-SBR operating conditions, to compare the process performance and evaluate the effect of UV irradiation.

### **5.2.1 Pre-treatment of Antibiotic Wastewater Using Photo-Fenton Process**

In this section, the effect of operating conditions ( $\text{H}_2\text{O}_2/\text{COD}$  molar ratio and  $\text{H}_2\text{O}_2/\text{Fe}^{2+}$  molar ratio) on biodegradability ( $\text{BOD}_5/\text{COD}$  ratio) improvement and mineralization of the antibiotic wastewater was studied.

#### *5.2.1.1 Effect of $\text{H}_2\text{O}_2/\text{COD}$ Molar Ratio*

The effect of  $\text{H}_2\text{O}_2/\text{COD}$  molar ratio on sCOD and DOC removal, and biodegradability ( $\text{BOD}_5/\text{COD}$  ratio) improvement are shown in Figure 5.11. The operating conditions were pH 3, initial sCOD 575 mg/L (17.97 mM), DOC 165 mg/L, irradiation time 30 min and  $\text{H}_2\text{O}_2/\text{Fe}^{2+}$  molar ratio 50. To study the effect of  $\text{H}_2\text{O}_2/\text{COD}$  molar ratio on biodegradability improvement and mineralization of the antibiotic wastewater, initial  $\text{H}_2\text{O}_2$  concentration was varied in the range 17.97–53.9 mM. The corresponding  $\text{H}_2\text{O}_2/\text{COD}$  and  $\text{COD}/\text{H}_2\text{O}_2/\text{Fe}^{2+}$  molar ratio were 1, 1.5, 2, 2.5 and 3, and 1.0/1.0/0.02, 1.0/1.5/0.03, 1.0/2.0/0.04, 1.0/2.5/0.05 and 1.0/3.0/0.06, respectively. It was expected that as the  $\text{H}_2\text{O}_2/\text{COD}$  molar ratio increased, more hydroxyl radicals would be available to attack the substrate and therefore degradation would increase. As can be seen in Figure 5.11, the COD removal was

45±1, 51±1, 57±1, 59±1 and 58±1% at H<sub>2</sub>O<sub>2</sub>/COD molar ratio 1, 1.5, 2.0, 2.5 and 3.0, respectively. The BOD<sub>5</sub>/COD ratio was 0.34±0.01, 0.41±0.02, 0.43±0.01, 0.44±0.01 and 0.42±0.01 at H<sub>2</sub>O<sub>2</sub>/COD molar ratios 1, 1.5, 2.0, 2.5 and 3.0, respectively. It may be noted that a wastewater is considered biodegradable if the BOD<sub>5</sub>/COD ratio is 0.40 (Al-Momani *et al.*, 2002). The DOC removal was 32±3, 34±1, 36±1, 49±1 and 48±1% at H<sub>2</sub>O<sub>2</sub>/COD molar ratio 1, 1.5, 2.0, 2.5 and 3.0, respectively. The results show that COD and DOC removal, and biodegradability (BOD<sub>5</sub>/COD ratio) improved with increasing H<sub>2</sub>O<sub>2</sub>/COD molar ratio. Addition of H<sub>2</sub>O<sub>2</sub> in excess of H<sub>2</sub>O<sub>2</sub>/COD molar ratio 2.5 did not improve removal and biodegradability. This may be due to scavenging of OH<sup>•</sup> by H<sub>2</sub>O<sub>2</sub> as in Reaction 2.6 (Kavitha and Palanivelu 2005a).

Based on the results, it may be considered that optimal H<sub>2</sub>O<sub>2</sub>/COD molar ratio is 2.5 for biodegradability improvement and mineralization. Comparing with the results of Phase I (Section 4.2.2), the optimum H<sub>2</sub>O<sub>2</sub>/COD molar ratio in this case (2.5) is higher than that reported in Phase I (1.5). This is may be ascribed to decreasing light penetration and presence of inorganic ions in the real wastewater. A H<sub>2</sub>O<sub>2</sub>/COD molar ratio 2.5 was used in all subsequent experiments.

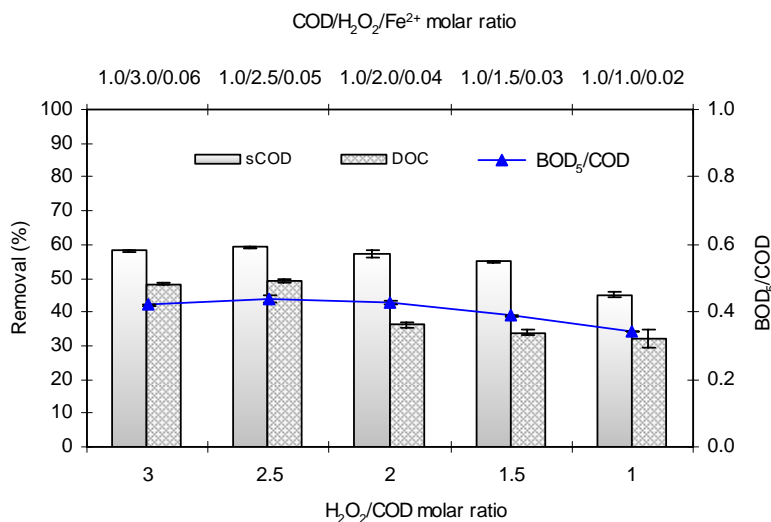


Figure 5.11 Effect of H<sub>2</sub>O<sub>2</sub>/COD molar ratio of photo-Fenton process on sCOD and DOC removal, and BOD<sub>5</sub>/COD ratio

### 5.2.1.2 Effect of $H_2O_2/Fe^{2+}$ Molar Ratio

In photo-Fenton process, iron and hydrogen peroxide are two major chemicals determining the operation cost as well as efficiency. The effect of  $H_2O_2/Fe^{2+}$  molar ratio on sCOD and DOC removal, and biodegradability ( $BOD_5/COD$  ratio) improvement are shown in Figure 5.12. The operating conditions were pH 3, initial sCOD 575 mg/L (17.97 mM), DOC 165 mg/L, irradiation time 30 min and  $H_2O_2/COD$  molar ratio 2.5. To study the effect of  $H_2O_2/Fe^{2+}$  molar ratio on biodegradability improvement and mineralization of the antibiotic wastewater, experiments were conducted at constant  $H_2O_2$  dose (44.9 mM) and varying  $Fe^{2+}$  dose in the range 0.3-4.5 mM. The corresponding  $H_2O_2/Fe^{2+}$  and  $COD/H_2O_2/Fe^{2+}$  molar ratio were 10, 20, 50, 100 and 150, and 1.0/2.5/0.25, 1.0/2.5/0.125, 1.0/2.5/0.05, 1.0/2.5/0.025 and 1.0/2.5/0.017, respectively. The COD removal was  $67\pm 1$ ,  $67\pm 1$ ,  $59\pm 1$ ,  $46\pm 1$  and  $30\pm 1\%$  at  $H_2O_2/Fe^{2+}$  molar ratio 10, 20, 50, 100 and 150, respectively. The  $BOD_5/COD$  ratio was  $0.48\pm 0.04$ ,  $0.50\pm 0.01$ ,  $0.44\pm 0.01$ ,  $0.32\pm 0.02$  and  $0.19\pm 0.02$  at  $H_2O_2/Fe^{2+}$  molar ratio 10, 20, 50, 100 and 150, respectively.

The DOC removal was  $48\pm 1$ ,  $51\pm 2$ ,  $45\pm 1$ ,  $36\pm 1$  and  $24\pm 2\%$  at  $H_2O_2/Fe^{2+}$  molar ratio 10, 20, 50, 100 and 150, respectively. The results show that COD and DOC removal and  $BOD_5/COD$  ratio increased with decrease of  $H_2O_2/Fe^{2+}$  molar ratio up to 20. Decrease of  $H_2O_2/Fe^{2+}$  molar ratio below 20 did not improve COD and DOC removal and  $BOD_5/COD$  ratio. This may be due to direct reaction of  $OH^\bullet$  radicals with metal ions at high concentration of  $Fe^{2+}$  as in Reaction 2.5 (Joseph *et al.* 2000):

Based on the results, it may be considered that optimal  $H_2O_2/Fe^{2+}$  molar ratio is 20 for biodegradability improvement, sCOD removal and mineralization of antibiotic wastewater and this agrees well with the Phase I results (Section 4.2.2).

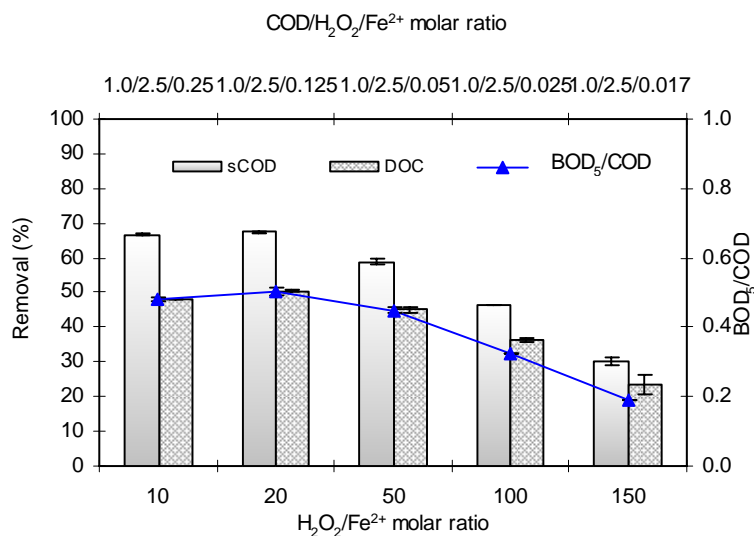


Figure 5.12 Effect of  $\text{H}_2\text{O}_2/\text{Fe}^{2+}$  molar ratio of photo-Fenton process on sCOD and DOC removal, and  $\text{BOD}_5/\text{COD}$  ratio

### 5.2.1.3 Degradation of Antibiotics

To confirm degradation of the antibiotics and study the matrix effect, an experiment was conducted under the following operating conditions:  $\text{H}_2\text{O}_2/\text{COD}$  molar ratio 2.5,  $\text{H}_2\text{O}_2/\text{Fe}^{+2}$  molar ratio 20 and pH 3. As shown in Figure 5.13, complete degradation of amoxicillin and cloxacillin occurred in one min. This agrees well with the Phase I results (Section 4.2.6) for degradation of antibiotics in aqueous solution and thus, the effect of water matrix can be neglected. It also agrees well with the results reported by Trovó *et al.* (2008) on degradation of amoxicillin, bezafibrate and paracetamol by the Fenton process. They observed 90 and 89% amoxicillin degradation in one min in distilled water and in sewage treatment plant effluent, respectively.

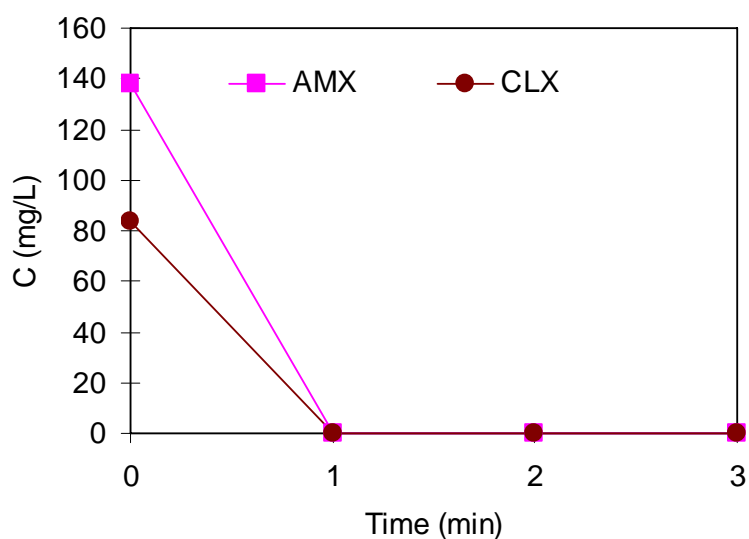


Figure 5.13 Degradation of AMX and CLX in antibiotic wastewater by photo-Fenton process

## 5.2.2 Treatment of Photo-Fenton-Treated Antibiotic Wastewater by SBR

The second SBR was operated for 239 days with photo-Fenton-treated effluent. The photo-Fenton-treated effluent characteristics depended mainly on the photo-Fenton process operating conditions. The study covered the effect of the photo-Fenton and SBR operating conditions on the SBR and combined system performance. These conditions are oxidant and catalyst dose, and photo-Fenton irradiation time and SBR hydraulic retention time (HRT).

### 5.2.2.1 Effect of Photo-Fenton Operating Conditions on SBR and the Combined System Performance

To study the effect of photo-Fenton operating conditions and photo-Fenton-treated effluent characteristics on SBR and combined system performance, ten photo-Fenton-treated effluents (Case PF1-PF10, Table 5.8) under different COD/H<sub>2</sub>O<sub>2</sub>/Fe<sup>2+</sup> molar ratios were used to feed the SBR. The SBR was operated for 71 days at cycle period 24 hr. The cycle was repeated 6-9 times to allow cell acclimation and/or to obtain repetitive results for each feed. Some of the cases (PF1-PF5) examined the effect of decreasing H<sub>2</sub>O<sub>2</sub> dose (decreasing H<sub>2</sub>O<sub>2</sub>/COD molar ratio) and the rest (PF6-PF10) examined the effect of decreasing Fe<sup>2+</sup> dose (increasing H<sub>2</sub>O<sub>2</sub>/Fe<sup>2+</sup> molar

ratio). The performance of SBR in terms of sCOD and DOC as a function of the photo-Fenton operating conditions is shown in Figure 5.14.

Table 5.8 Photo-Fenton operating conditions for SBR

Case	H <sub>2</sub> O <sub>2</sub> /COD (MR)	H <sub>2</sub> O <sub>2</sub> /Fe <sup>2+</sup> (MR)	COD/H <sub>2</sub> O <sub>2</sub> /Fe <sup>2+</sup> (MR)
PF1	3	50	1.0/3.0/0.06
PF2	2.5	50	1.0/2.5/0.05
PF3	2	50	1.0/2.0/0.04
PF4	1.5	50	1.0/1.5/0.03
PF5	1	50	1.0/1.0/0.02
PF6	2.5	10	1.0/2.5/0.25
PF7	2.5	20	1.0/2.5/0.125
PF8	2.5	50	1.0/2.5/0.05
PF9	2.5	100	1.0/2.5/0.025
PF10	2.5	150	1.0/2.5/0.017

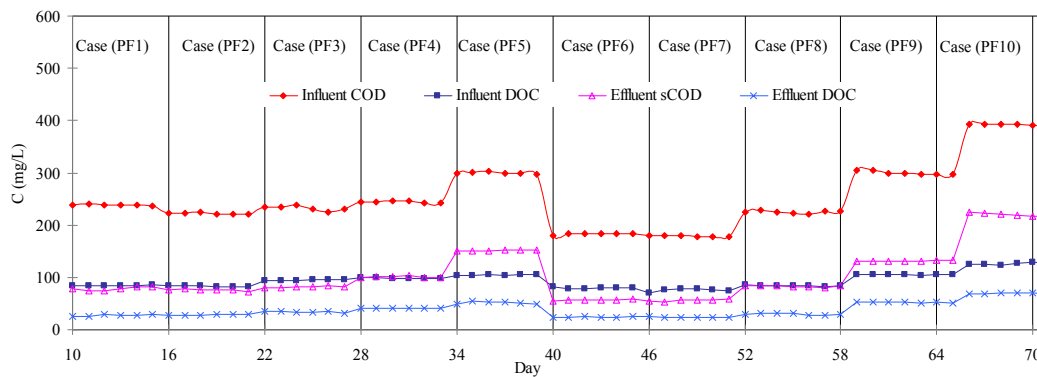


Figure 5.14 Performance of SBR in terms of sCOD and DOC as a function of photo-Fenton operating conditions (Case PF1-PF10)

Table 5.9 shows the photo-Fenton operating conditions, photo-Fenton-treated and SBR effluent characteristics, and the combined system efficiency. The effect of decreasing H<sub>2</sub>O<sub>2</sub>/COD molar ratio from 3 to 2.5, 2, 1.5 and 1 (decrease of H<sub>2</sub>O<sub>2</sub> dose) on SBR performance was examined (Case PF1-PF5). The other operating conditions of the photo-Fenton process were fixed at H<sub>2</sub>O<sub>2</sub>/Fe<sup>2+</sup> molar ratio 50, irradiation time 30 min and pH 3.



Table 5.9 Photo-Fenton-treated and SBR effluent characteristics and combined system efficiency at different H<sub>2</sub>O<sub>2</sub>/COD molar ratio

Case	Photo-Fenton-treated effluent							SBR effluent						Combined efficiency	
	H <sub>2</sub> O <sub>2</sub> /COD (MR)	sCOD		DOC		BOD <sub>5</sub>	BOD <sub>5</sub> /COD	sCOD		DOC		MLSS	F/M	sCOD %	DOC %
		mg/L	R%	mg/L	R%	mg/L		mg/L	R%	mg/L	R%	mg/L	day <sup>-1</sup>		
PF1	3	238±2	58±1	85±2	48±1	100±2	0.42±0.1	79±4	67±2	28±2	68±2	2560	0.062	86	83
PF2	2.5	222±2	59±1	83±2	49±1	97±3	0.44±0.02	76±2	66±1	29±1	66±2	2520	0.058	86	83
PF3	2	232±5	57±1	95±2	36±1	99±1	0.43±0.01	82±1	65±1	34±1	64±2	2500	0.061	85	77
PF4	1.5	245±2	55±1	98±6	34±4	95±1	0.39±0.01	101±1	59±1	41±1	58±1	2500	0.065	81	72
PF5	1	300±2	45±12	105±1	32±3	103±1	0.34±0.01	152±1	50±1	51±3	51±3	2480	0.080	72	67

The SBR cycle period was 24 hr and it was divided into 0.25 hr filling, 22.0 hr aeration, 1.25 hr settling, 0.25 hr decanting and 0.25 hr idle period. The H<sub>2</sub>O<sub>2</sub>/COD molar ratio 3 (H<sub>2</sub>O<sub>2</sub> 1832 mg/L) was considered as the starting point. The characteristics of the photo-Fenton-treated effluent (Case PF1) were sCOD 238±2 mg/L, DOC 85±2 mg/L and BOD<sub>5</sub>/COD ratio 0.42±0.01. SBR efficiency was 67±2 and 68±2% for sCOD and DOC removal, respectively. When H<sub>2</sub>O<sub>2</sub> dose was reduced to 1527 mg/L (Case PF2), the characteristics of the photo-Fenton-treated effluent were sCOD 222±2 mg/L, DOC 83±2 mg/L and BOD<sub>5</sub>/COD ratio improved to 0.44±0.03, and SBR efficiency was 66±1 and 66±2% for sCOD and DOC removal, respectively. Comparing SBR performance of Case PF3 with that of Case PF2 and PF1, it is observed that increasing H<sub>2</sub>O<sub>2</sub>/COD molar ratio to more than 2 did not improve the SBR efficiency. This is presumably due to the fact that biodegradability (BOD<sub>5</sub>/COD ratio) of the photo-Fenton-treated effluents was more than 0.40 in all cases, which is considered biodegradable (Al-Momani *et al.*, 2002). Decreasing SBR performance with decreasing H<sub>2</sub>O<sub>2</sub>/COD molar ratios below 2 (Case PF4 and PF3) is ascribed to the decrease of biodegradability below 0.4 and that indicates inhibition of the aerobic oxidation by the antibiotic intermediates.

MLSS varied from 2560 mg/L at BOD<sub>5</sub>/COD ratio 0.42±0.01 (Case PF1) to 2480 mg/L at BOD<sub>5</sub>/COD ratio 0.34±0.01 (Case PF5). The reduction in MLSS concentration is considered small and it may be due to biomass growth on the SBR wall as well as inhibition of aerobic oxidation by antibiotic intermediates. The F/M ratio varied in the range 0.065-0.080 day<sup>-1</sup> and this is mainly due to variation in sCOD concentration of the photo-Fenton-treated effluent.

The next step was to study the effect of increasing  $\text{H}_2\text{O}_2/\text{Fe}^{2+}$  molar ratio (decrease of  $\text{Fe}^{2+}$  dose) from 10 to 20, 50, 100 and 150 on SBR performance (Case PF6-PF10, Table 5.10). The  $\text{H}_2\text{O}_2/\text{Fe}^{2+}$  molar ratio 10 ( $\text{Fe}^{2+}$  250 mg/L) was considered as the starting point. The other operating conditions of the photo-Fenton process were fixed at  $\text{H}_2\text{O}_2/\text{COD}$  molar ratio 2.5, irradiation time 30 min and pH 3. The SBR cycle period was 24 hr and it was divided into 0.25 hr filling, 22.0 hr aeration, 1.25 hr settling and 0.25 hr decanting and 0.25 hr idle period. The characteristics of the photo-Fenton-treated effluent (Case PF6) were sCOD  $183\pm 2$  mg/L, DOC  $80\pm 2$  mg/L and  $\text{BOD}_5/\text{COD}$  ratio  $0.48\pm 0.01$ . SBR efficiency was  $69\pm 1$  and  $70\pm 2\%$  for sCOD and DOC removal, respectively. When ferrous iron dose was reduced to 125 mg/L (Case PF7), the characteristics of the photo-Fenton-treated effluent were sCOD  $179\pm 2$  mg/L, DOC  $76\pm 3$  mg/L and  $\text{BOD}_5/\text{COD}$  ratio improved to  $0.50\pm 0.02$ , and SBR efficiency was  $69\pm 1$  and  $69\pm 1\%$  for sCOD and DOC removal, respectively. It is seen in Table 5.10, the photo-Fenton-treated effluent characteristics are similar in Case PF6 and PF7 and hence the SBR efficiency. Both photo-Fenton-treated effluents are considered biodegradable since the  $\text{BOD}_5/\text{COD}$  ratio threshold for a wastewater to be considered easily biodegradable is 0.4 (Al-Momani *et al.*, 2002).

The results show that ferrous iron dose ( $\text{H}_2\text{O}_2/\text{Fe}^{2+}$  molar ratio) is an important parameter of the combined photo-Fenton and SBR system. Decreasing SBR efficiency with decrease of  $\text{Fe}^{2+}$  dose (increase  $\text{H}_2\text{O}_2/\text{Fe}^{2+}$  molar ratio) is presumably due to decrease of biodegradability below 0.4 and this indicates inhibition of the aerobic oxidation by the antibiotic intermediates. It is noteworthy that SBR efficiency in terms of sCOD and DOC is very sensitive to  $\text{BOD}_5/\text{COD}$  ratio below 0.40. SBR efficiency in terms of sCOD removal decreased from  $69\pm 1\%$  at  $\text{BOD}_5/\text{COD}$  ratio  $0.48\pm 0.01$  to  $44\pm 1\%$  at  $\text{BOD}_5/\text{COD}$  ratio  $0.19\pm 0.02$ .

Table 5.10 Photo-Fenton-treated and SBR effluent characteristics and combined system efficiency at different H<sub>2</sub>O<sub>2</sub>/Fe<sup>2+</sup> molar ratios

Case	Photo-Fenton-treated effluent							SBR effluent						Combined efficiency	
	H <sub>2</sub> O <sub>2</sub> /Fe <sup>2+</sup> (MR)	sCOD		DOC		BOD <sub>5</sub>	BOD <sub>5</sub> /COD	sCOD		DOC		MLSS	F/M	sCOD	DOC
		mg/L	R%	mg/L	R%	mg/L		mg/L	R%	mg/L	R%	mg/L	day <sup>-1</sup>	%	%
PF6	10	183±2	67±1	80±2	48±2	88±2	0.48±0.01	56±1	69±1	24±1	70±2	2460	0.049	90	84
PF7	20	179±2	67±1	76±3	51±3	90±1	0.50±0.02	56±2	69±1	24±1	69±1	2400	0.049	90	85
PF8	50	225±3	59±1	84±1	45±2	101±1	0.45±0.01	83±1	63±1	30±1	65±1	2360	0.063	85	81
PF9	100	300±4	46±1	105±1	36±1	97±1	0.32±0.01	131±1	56±1	52±1	51±1	2160	0.092	77	69
PF10	150	391±2	30±1	126±3	24±2	74±8	0.19±0.02	220±4	44±1	69±1	45±1	2080	0.124	61	58

A marked decline in MLSS concentration was observed at higher influent sCOD and low BOD<sub>5</sub>/COD ratio (Case PF10). This reduction in MLSS concentration may be ascribed to wall growth (Farré *et al.*, 2007) and inhibition of aerobic oxidation by antibiotic intermediates. The F/M ratio varied in the range 0.049-0.124 day<sup>-1</sup> and this is mainly due to variation in sCOD concentration of the photo-Fenton-treated effluent as well as the change in biomass concentration.

The combined efficiency achieved by the photo-Fenton-SBR process was similar to those observed in the reported studies. Farré *et al.* (2007) reported 80% DOC removal for treatment of diuron and linuron pesticides by combined photoFenton-SBR system at H<sub>2</sub>O<sub>2</sub>/Fe<sup>2+</sup> molar ratio ~ 12.7, HRT 2 days and VSS 0.60±0.03 g /L. Garcia-Montaña *et al.* (2006a) reported 80% DOC removal for treatment of a synthetic textile effluent containing an hetero-bioreactive dye (Cibacron Red FN-R, 250 mg /L) by combined photo-Fenton-SBR system at H<sub>2</sub>O<sub>2</sub>/Fe<sup>2+</sup> molar ratio 12.5, HRT 1 day, irradiation time 90 min and VSS 0.56±0.03 g/L. Gonzalez *et al.* (2009) reported 75.7% TOC removal for treatment of a synthetic wastewater containing 200 mg/L sulfamethoxazole by photo-Fenton-sequencing batch biofilm reactor (SBBR). The treatment conditions were 300 mg/L H<sub>2</sub>O<sub>2</sub> and 10 mg/L Fe<sup>2+</sup> for photo-Fenton process and HRT 8 hr for SBBR. It is obvious from Tables 6.9 and 6.10 that discharge standard of the Malaysian Standards (B) is met by the photo-Fenton-SBR treated antibiotic wastewater (Case PF6 and PF7).

A comparison between Fenton–SBR and photo-Fenton–SBR processes is important to evaluate the beneficial effect of UV irradiation. As shown in Tables 5.2, 5.3, 5.9 and 5.10, at high chemical dosage no appreciable difference in combined efficiency between the processes were observed. However, at low chemical dosage the photo-Fenton-SBR exhibited higher efficiency compared with the Fenton–SBR process.

#### 5.2.2.2 Effect of Cycle Period on the Performance of SBR

In order to examine the effect of cycle period on SBR performance, HRT was varied in the range 12-48 hr. The SBR was operated for 203 days at HRT 48, 24 and 12 hr

and was fed by ten photo-Fenton-treated effluents (Case PF1-PF10, Table 5.8). Figures 5.15 and 5.16 show the SBR efficiency in terms of sCOD and DOC removal, respectively at HRT 48, 24 and 12 hr. No remarkable improvement in SBR efficiency in terms of sCOD and DOC removal is seen due to HRT increasing from 12 to 48 hr. This indicates that most of the substrate degradation takes place during the first 12 hr and a smaller portion is degraded in rest of the retention time. In order to confirm this, a statistical analysis (one-way ANOVA) was made on the results at a 5% level of significance. The statistical analysis results are presented in more details in Appendix (C). As shown in Table 5.11, the statistical analysis indicated that increase of HRT from 24 to 48 hr did not significantly improve sCOD removal (P-value 0.132 > 0.05) or DOC removal (P-value 0.198 > 0.05). HRT decreasing from 24 hr to 12 hr did not also significantly reduce sCOD removal (P-value 0.201 > 0.05) or DOC removal (P-value 0.096 > 0.05).

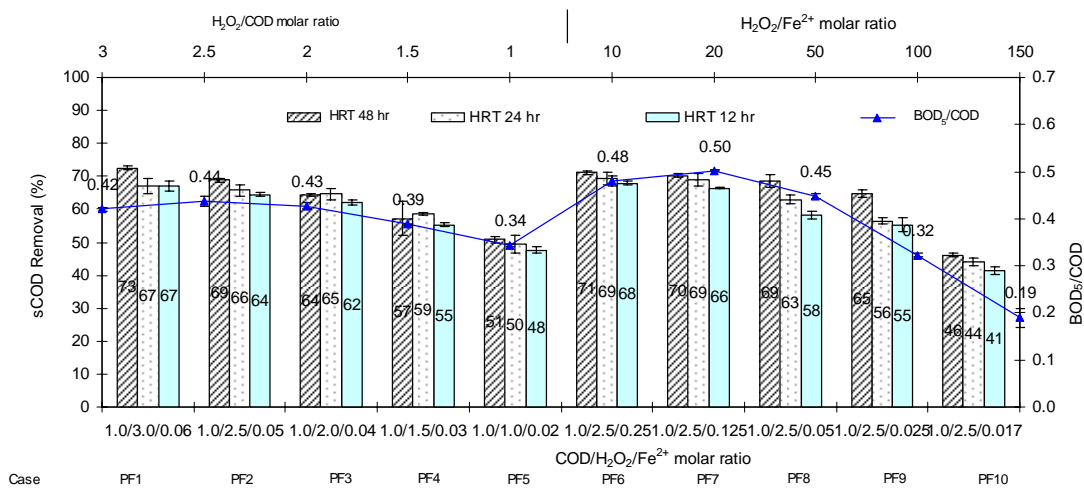


Figure 5.15 SBR efficiency of photo-Fenton-SBR in terms of sCOD removal at HRT 48, 24 and 12 hr

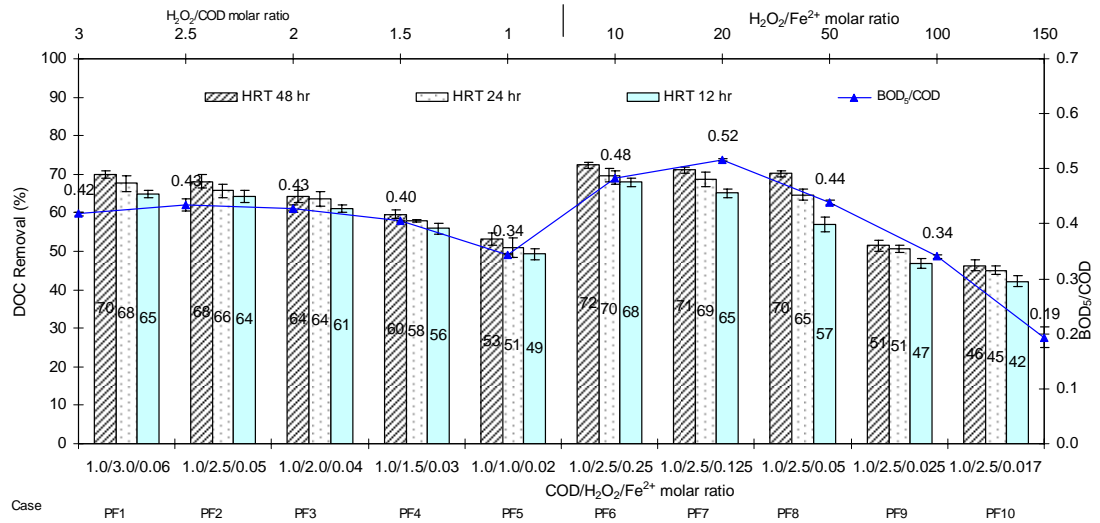


Figure 5.16 SBR efficiency of photo-Fenton-SBR in terms of DOC removal at HRT 48, 24 and 12 hr

Table 5.11 One-way ANOVA for SBR efficiency in terms of sCOD and DOC removal at different HRT (combined photo-Fenton and SBR)

One-way ANOVA	Parameter	No. of groups	F	P-value	F crit
24 hr vs. 48 hr	sCOD	2	2.3	0.132	3.9
12 hr vs. 24 hr	sCOD	2	1.7	0.201	3.9
12 hr vs. 24 hr vs. 48 hr	sCOD	3	3.9	0.023	3.1
24 hr vs. 48 hr	DOC	2	1.7	0.198	3.9
12 hr vs. 24 hr	DOC	2	2.8	0.096	3.9
12 hr vs. 24 hr vs. 48 hr	DOC	3	4.4	0.014	3.1

From the results it can be concluded that SBR efficiency mainly depends on the nature of the by-products generated in the photo-Fenton treatment and no remarkable improvement in SBR efficiency due to HRT increase. It was decided to operate the SBR at 12 hr HRT for subsequent experiments. The results agree well with the results of the combined Fenton-SBR in this work (Section 5.1.2.2). It is also agrees with the reported studies by García-Montaño *et al.* (2006a, 2006b). They reported no remarkable decrease in DOC removal due to increasing HRT from 1 to 2 and 4 days

for degradation of a commercial hetero-bioreactive dye and Procion Red H-E7B reactive dye by combined photo-Fenton-SBR system.

### 5.2.2.3 Optimization of Combined Photo-Fenton-SBR

In section 5.2.2.1 and 5.2.2.2 it was observed that  $\text{H}_2\text{O}_2/\text{COD}$  molar ratio and  $\text{H}_2\text{O}_2/\text{Fe}^{2+}$  molar ratio significantly affected the SBR performance, whereas HRT increase did not significantly improve the SBR performance. It was found that  $\text{H}_2\text{O}_2/\text{COD}$  molar ratio 2.0 and HRT 12 hr were suitable for the combined photo-Fenton-SBR process in this study. For  $\text{H}_2\text{O}_2/\text{Fe}^{2+}$  molar ratio, it was found that Case PF6 and PF7 ( $\text{H}_2\text{O}_2/\text{Fe}^{2+}$  molar ratio 10 and 20) met the discharge standard in terms of sCOD (Table 5.10). So, the next step would be to study the effect of increasing the irradiation time to more than 30 min as well as increasing  $\text{H}_2\text{O}_2/\text{Fe}^{2+}$  molar ratio (decreasing  $\text{Fe}^{2+}$  dose) on the combined system performance. The experimental design consisted of nine photo-Fenton-treated effluents (Case PF11-PF19, Table 5.12).

Table 5.12 Operating conditions for combined photo-Fenton-SBR

Case	Irradiation time (min)	$\text{H}_2\text{O}_2/\text{COD}$ (MR)	$\text{H}_2\text{O}_2/\text{Fe}^{2+}$ (MR)	$\text{COD}/\text{H}_2\text{O}_2/\text{Fe}^{2+}$ (MR)	HRT (hr)
PF11	60	2.0	50	1.0/2.0/0.04	12
PF12	90	2.0	50	1.0/2.0/0.04	12
PF13	120	2.0	50	1.0/2.0/0.04	12
PF14	60	2.0	100	1.0/2.0/0.02	12
PF15	90	2.0	100	1.0/2.0/0.02	12
PF16	120	2.0	100	1.0/2.0/0.02	12
PF17	60	2.0	150	1.0/2.0/0.013	12
PF18	90	2.0	150	1.0/2.0/0.013	12
PF19	120	2.0	150	1.0/2.0/0.013	12



The SBR was operated from day 204-239 (36 days) at HRT 12 hr and the cycle was repeated 8 times to obtain repetitive results for each feed. Figure 5.17 shows the performance of the SBR in terms of sCOD and DOC as a function of photo-Fenton operating conditions.

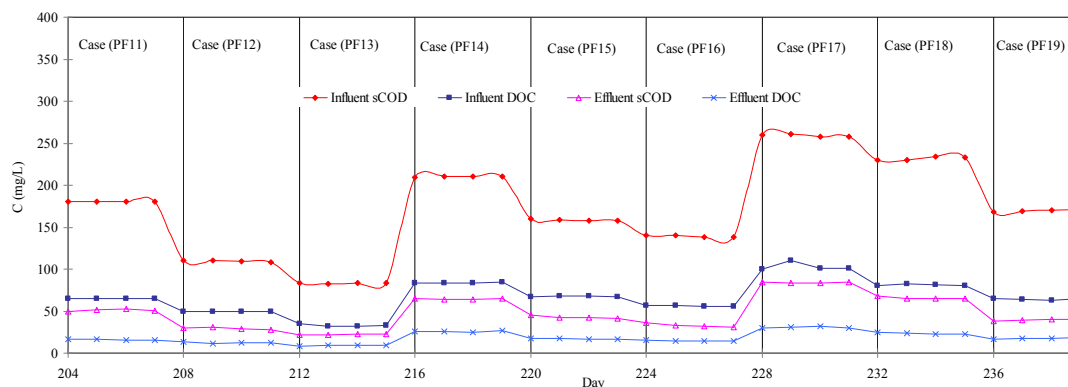


Figure 5.17 Performance of SBR in terms of sCOD and DOC as function of photo-Fenton operating condition (Case PF11-PF19)

Table 5.13 shows a summary photo-Fenton-treated and SBR effluent characteristics and combined system efficiency at different irradiation time and  $\text{H}_2\text{O}_2/\text{Fe}^{2+}$  molar ratios. The other operating conditions of the photo-Fenton process were fixed at  $\text{H}_2\text{O}_2/\text{COD}$  molar ratio 2.0 and pH 3. The SBR cycle period was 12 hr and it was divided into 0.25 hr filling, 10 hr aeration, 1.25 hr settling, 0.25 hr decanting and 0.25 hr idle period.  $\text{H}_2\text{O}_2/\text{Fe}^{2+}$  molar ratio 50 ( $\text{Fe}^{2+}$  200 mg/L) was considered as the starting point since it did not meet the discharge standard as described in Table 5.10. The irradiation time was increased from 30 to 60 min (Case PF11). The characteristics of the photo-Fenton-treated effluent (Case PF11) were sCOD  $180 \pm 1$  mg/L, DOC  $67 \pm 1$  mg/L and  $\text{BOD}_5/\text{COD}$  ratio  $0.47 \pm 0.01$ . SBR efficiency was  $71 \pm 1$  and  $76 \pm 1\%$  for sCOD and DOC removal, respectively. With regard to the final effluent, the final sCOD was  $52 \pm 1$  mg/L which met the discharge standard.

Table 5.13 Photo-Fenton-treated and SBR effluent characteristics and combined system efficiency at different irradiation time and  $\text{H}_2\text{O}_2/\text{Fe}^{2+}$  molar ratios

Case	Photo-Fenton-treated effluent								SBR effluent						Combined efficiency	
	Irradiation time	$\text{H}_2\text{O}_2/\text{Fe}^{2+}$	sCOD		DOC		BOD <sub>5</sub>	BOD <sub>5</sub> /COD	sCOD		DOC		MLSS	F/M	sCOD	DOC
	min	(MR)	mg/L	R%	mg/L	R%	mg/L		mg/L	R%	mg/L	R%	mg/L	day <sup>-1</sup>	%	%
PF11	60	50	180±1	67±1	65±1	61±1	784±1	0.47±0.01	52±1	71±1	16±1	76±1	2380	0.050	91	90
PF12	90	50	109±1	81±1	50±1	70±1	71±1	0.65±0.01	30±1	73±1	12±1	76±2	2260	0.032	95	93
PF13	120	50	83±1	86±1	33±1	80±1	57±2	0.68±0.01	23±3	73±1	9±1	73±3	2300	0.024	96	95
PF14	60	100	210±1	64±1	84±2	49±1	80±2	0.38±0.01	65±1	69±1	26±1	69±1	2260	0.061	90	88
PF15	90	100	159±1	72±1	68±1	59±1	88±1	0.55±0.01	43±2	73±1	16±1	74±1	2240	0.047	93	91
PF16	120	100	139±1	77±1	57±1	66±1	91±2	0.66±0.01	33±2	76±1	14±1	75±1	2310	0.040	95	92
PF17	60	150	259±2	56±1	103±5	39±1	94±1	0.36±0.01	84±1	68±1	31±1	70±1	2200	0.078	86	82
PF18	90	150	232±2	60±1	81±2	52±1	97±1	0.42±0.01	66±2	72±1	24±1	71±1	2160	0.071	89	86
PF19	120	150	170±1	71±1	64±1	62±1	77±2	0.45±0.01	39±1	77±1	18±1	72±1	2150	0.052	93	89

When the photo-Fenton irradiation time was increased to 90 min (Case PF12) and 120 min (Case PF13), SBR efficiency did not improve significantly. Performance of the combined photo-Fenton-SBR in Case PF11-PF13 is similar to that of the combined Fenton-SBR in Case F11-F13. This may be ascribed to the biodegradability ( $BOD_5/COD$  ratio) of the Fenton-treated and photo-Fenton-treated effluent being above 0.40.

Final SBR effluent in Case PF11, PF12 and PF13 amply meet the discharge standard of less than 100 mg/L COD and 70 mg/L sCOD and based on these results it was decided to increase the  $H_2O_2/Fe^{2+}$  molar ratio (decrease  $Fe^{2+}$ ) by 50% to 100 ( $Fe^{2+}$  100 mg/L). The irradiation time was 60 min (Case PF14), 90 min (Case PF15) and 120 min (Case PF16). The characteristics of the photo-Fenton-treated effluent (Case F14) were sCOD  $210 \pm 1$  mg/L, DOC  $84 \pm 2$  mg/L and  $BOD_5/COD$  ratio  $0.38 \pm 0.01$ . The SBR efficiency was  $69 \pm 1$  and  $69 \pm 1\%$  for sCOD and DOC removal, respectively. With regard to the final effluent, the sCOD concentration was  $65 \pm 1$  mg/L which meets the discharge standard. When irradiation time was increased further to 90 min (Case PF15) and 120 min (Case PF16), SBR efficiency improved further ( $73 \pm 1$  and  $76 \pm 1\%$ ) and the final sCOD was  $43 \pm 2$  and  $33 \pm 2$  mg/L, respectively.

From the previous results, the final SBR effluent of the combined photo-Fenton-SBR process at  $H_2O_2/Fe^{2+}$  molar ratio 100 and irradiation time 60, 90 and 120 min (Case PF14-PF16) amply met the discharge standard. In order to assess the effect of further increasing  $H_2O_2/Fe^{2+}$  molar ratio (reducing  $Fe^{2+}$  concentration) on SBR and combined system performance,  $H_2O_2/Fe^{2+}$  molar ratio 150 ( $Fe^{2+}$  66.6 mg/L) was used with irradiation time 60, 90 and 120 min (Case PF17-PF19). Characteristics of the photo-Fenton-treated effluent (Case F17) were sCOD  $259 \pm 2$  mg/L, DOC  $103 \pm 5$  mg/L and  $BOD_5/COD$  ratio  $0.36 \pm 0.01$ . The SBR efficiency was  $68 \pm 1$  and  $70 \pm 1\%$  for sCOD and DOC removal, respectively. With regard to the final effluent, the sCOD concentration was  $84 \pm 1$  mg/L which did not meet the discharge standard.

In order improve the final effluent characteristics and instead of increasing chemical dosage, irradiation time was increased from 60 min to 90 min (Case PF18)

at same  $\text{H}_2\text{O}_2/\text{Fe}^{2+}$  molar ratio 150,  $\text{H}_2\text{O}_2/\text{COD}$  2.0, pH 3 and HRT 12 hr. SBR efficiency was  $72\pm 1\%$  for sCOD and  $71\pm 1\%$  for DOC removal, and the final effluent sCOD was  $66\pm 2$  mg/L which met the discharge standard. When irradiation time was increased further to 120 min (Case F19), SBR efficiency for sCOD removal improved to  $77\pm 1\%$  and final effluent sCOD was  $39\pm 1$  mg/L.

Since the target was to minimize the use of chemicals ( $\text{Fe}^{2+}$  dose) in the treatment, it was important to know if increasing photo-Fenton irradiation time and reducing  $\text{Fe}^{2+}$  dose significantly affected the SBR performance. In order to do that, a two-way analysis of variance (ANOVA) was conducted using SPSS statistical software. Table 5.14 shows the significance of the difference between the two means for sCOD removal in SBR at  $\text{H}_2\text{O}_2/\text{Fe}^{2+}$  molar ratio 50, 100 and 150 and photo-Fenton irradiation time 60, 90 and 120 min using Tukey HSD method. The statistical analysis results are presented in more details in Appendix (D). When the value of significance is less than 0.05, it indicates that COD removal in SBR is significantly different and is not significantly different if the value of significance is more than 0.05 (the highlighted values in Table 5.14). There is no difference between the SBR efficiency at  $\text{H}_2\text{O}_2/\text{Fe}^{2+}$  molar ratio 100 and 90 min irradiation time (100 MR - 90 min), and SBR efficiency at  $\text{H}_2\text{O}_2/\text{Fe}^{2+}$  molar ratio 150 and 90 irradiation time (150 MR - 90 min). If the final SBR effluent in both cases meets the discharge standard, it may be more economic to choose  $\text{H}_2\text{O}_2/\text{Fe}^{2+}$  molar ratio 150 and 90 min photo-Fenton irradiation time as optimum condition (Case PF18, Table 5.13).

Table 5.14 Significance of the difference between two means for sCOD removal in SBR using Tukey HSD method (combined photo-Fenton-SBR)

H <sub>2</sub> O <sub>2</sub> /Fe <sup>2+</sup> (MR) and irradiation time (min)	50 MR - 60 min (PF11)	50 MR - 90 min (PF12)	50 MR - 120 min (PF13)	100 MR - 60 min (PF14)	100 MR - 90 min (PF15)	100 MR - 120 min (PF16)	150 MR - 60 min (PF17)	150 MR - 90 min (PF18)	150 MR - 120 min (PF19)
50 MR - 60 min (PF11)									
50 MR - 90 min (PF12)	0.14								
50 MR - 120 min (PF13)	0.15	1.00							
100 MR - 60 min (PF14)	0.01	0.0	0.0						
100 MR - 90 min (PF15)	0.05	1.0	1.00	0.00					
100 MR - 120 min (PF16)	0.00	0.0	0.00	0.00	0.00				
150 MR - 60 min (PF17)	0.00	0.0	0.0	0.09	0.00	0.00			
150 MR - 90 min (PF18)	0.00	0.26	0.28	0.00	0.11	0.00	0.00		
150 MR - 120 min (PF19)	1.00	0.00	0.0	0.00	0.00	0.97	0.00	0.00	

The combined system efficiency also confirmed the finding. As shown in Figure 5.18, the combined system efficiency in terms of sCOD at H<sub>2</sub>O<sub>2</sub>/Fe<sup>2+</sup> molar ratio 50, 100 and 150, and 90 min irradiation time were 95, 93 and 89%, respectively. With regards to the final effluent, the final sCOD decreased to 66±2 mg/L (Case PF18, Table 5.13) which met discharge standard of less than 100 mg/L as COD. Based on the results, we can consider the best H<sub>2</sub>O<sub>2</sub>/Fe<sup>2+</sup> molar ratio is 150 and the best irradiation time is 90 min.

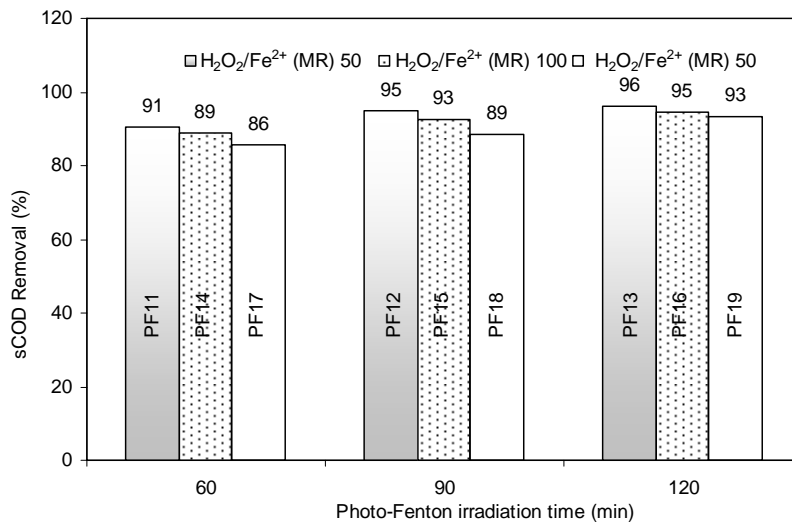


Figure 5.18 Combined photo-Fenton and SBR efficiency in terms of sCOD removal

To study biodegradation of the photo-Fenton-treated effluent and nitrification in SBR, sCOD, DOC, NH<sub>3</sub>, TKN and NO<sub>3</sub><sup>-</sup> were measured during the cycle period (12 hr) for Case PF18 and shown in Figures 5.19 and 5.20. Oxidation of NH<sub>3</sub> was complete in 6 hr, oxidation of TKN was complete in 12 hr and NO<sub>3</sub> concentration was 36 mg/L in 12 hr, indicating complete nitrification (Figure 5.20).

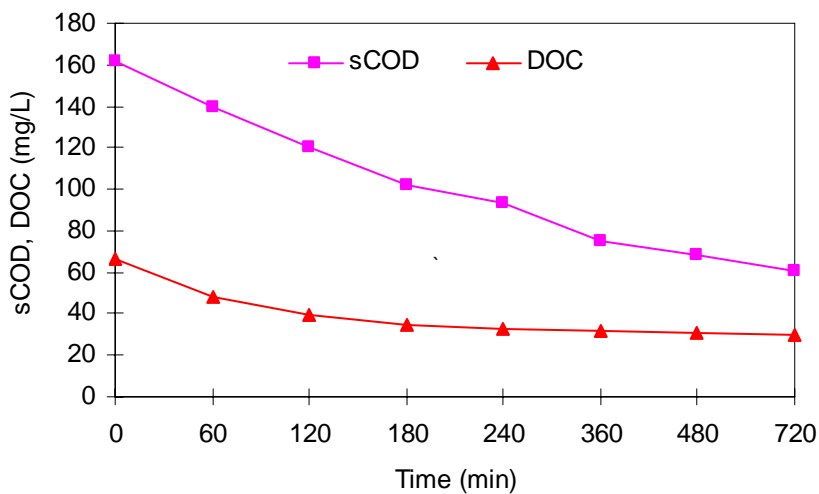


Figure 5.19 Biodegradation of the photo-Fenton-treated effluent in terms of sCOD and DOC in SBR during the cycle period (Case PF18)

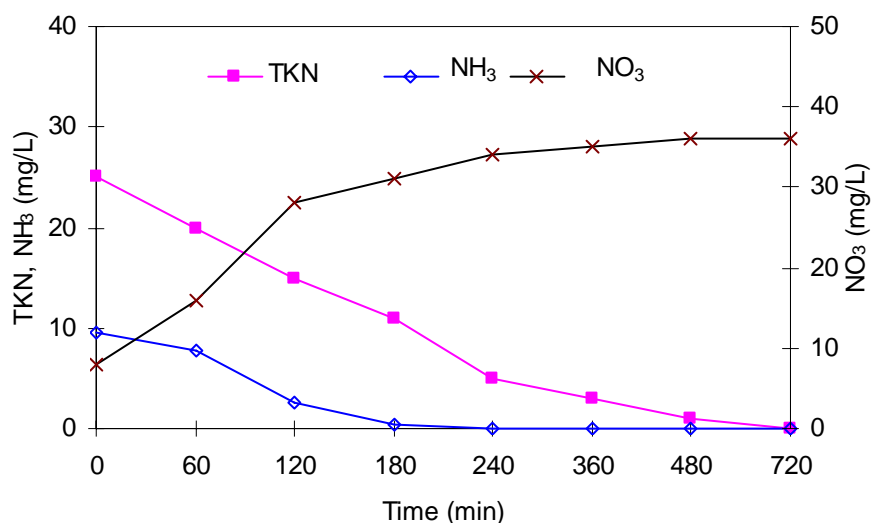


Figure 5.20 Nitrification in SBR during the cycle period (Case PF18)

In summary, the SBR was operated for 239 days and fed with photo-Fenton-treated effluent under different photo-Fenton and SBR operating conditions. The  $\text{H}_2\text{O}_2/\text{COD}$  molar ratio 2.0 was found to be the best ratio among five studied ratios (Case PF1-PF5, Table 5.9). The hydraulic retention time (HRT) of 12 hr was found suitable for the SBR and increasing HRT to 24 and 48 hr did not significantly improve the SBR efficiency in terms of sCOD and DOC removal. The  $\text{H}_2\text{O}_2/\text{Fe}^{2+}$  molar ratio and irradiation time of the photo-Fenton process were found to be the most influential parameters. Statistical analysis (two-way ANOVA) was conducted on the results to optimize the  $\text{H}_2\text{O}_2/\text{Fe}^{2+}$  molar ratio and irradiation time and it was found possible to reduce the  $\text{Fe}^{2+}$  dose and increase the photo-Fenton irradiation time. Based on the results, the best operating conditions for treatment of the antibiotics wastewater by the combined photo-Fenton-SBR were  $\text{H}_2\text{O}_2/\text{COD}$  molar ratio 2.0,  $\text{H}_2\text{O}_2/\text{Fe}^{2+}$  molar ratio 150, reaction time 90 min and HRT 12 hr. Under the best operating conditions, the photo-Fenton-SBR achieved a combined efficiency of 89% for sCOD removal. Final sCOD of the effluent was  $66\pm 2$  mg/L and complete nitrification occurred in the SBR.

### **5.3 Combined UV/H<sub>2</sub>O<sub>2</sub>/TiO<sub>2</sub> and Sequencing Batch Reactor Process (UV/H<sub>2</sub>O<sub>2</sub>/TiO<sub>2</sub>-SBR)**

The third treatment train was a combined UV/H<sub>2</sub>O<sub>2</sub>/TiO<sub>2</sub> and SBR process. The combined UV/H<sub>2</sub>O<sub>2</sub>/TiO<sub>2</sub>-SBR process may be affected by the UV/H<sub>2</sub>O<sub>2</sub>/TiO<sub>2</sub> operating conditions such as the catalyst and oxidant concentration, and UV irradiation time as well as the SBR operating conditions such as the hydraulic retention time (HRT). The key to efficient integration of the UV/H<sub>2</sub>O<sub>2</sub>/TiO<sub>2</sub> process and SBR for recalcitrant wastewater treatment is knowing the required chemical dosages and UV irradiation time for the effluent to be biodegradable, and the required hydraulic retention time of the SBR. Experiments were designed to answer these questions. In the experimental design, TiO<sub>2</sub> and H<sub>2</sub>O<sub>2</sub> concentration, and irradiation time were varied in order to study the performance of the UV/H<sub>2</sub>O<sub>2</sub>/TiO<sub>2</sub> process. The SBR was fed with the UV/H<sub>2</sub>O<sub>2</sub>/TiO<sub>2</sub>-treated effluent under different operating conditions to study the SBR and combined system performance under these conditions. In addition, the SBR cycle period was also varied.

#### **5.3.1 Pre-treatment of Antibiotic Wastewater Using UV/H<sub>2</sub>O<sub>2</sub>/TiO<sub>2</sub> process**

In this section, the effect of operating conditions (TiO<sub>2</sub> and H<sub>2</sub>O<sub>2</sub> dose) on biodegradability (BOD<sub>5</sub>/COD ratio) improvement and mineralization of the antibiotic wastewater was studied.

##### *5.3.1.1 Effect of TiO<sub>2</sub> and H<sub>2</sub>O<sub>2</sub> Dose*

Addition of other powerful oxidizing agent such as H<sub>2</sub>O<sub>2</sub> to TiO<sub>2</sub> suspension is a well-known procedure and in many cases leads to an increase in the rate of photooxidation (Malato *et al.*, 2000; Poullos *et al.*, 2003). In order to keep the efficiency of the added H<sub>2</sub>O<sub>2</sub>, it is necessary to choose the optimum dose of H<sub>2</sub>O<sub>2</sub> according to the type and concentration of the pollutants. H<sub>2</sub>O<sub>2</sub> is considered to have two functions in the photocatalytic oxidation. It accepts a photogenerated electron from the conduction band of the semiconductor according to Reaction (2.17) and



thus promotes the charge separation. In addition, it forms OH<sup>•</sup> radicals according to Reaction (4.1) (Kositzi *et al.*, 2004).

Figure 5.21 shows the effect of TiO<sub>2</sub> and H<sub>2</sub>O<sub>2</sub> dose on sCOD and DOC removal and biodegradability (BOD<sub>5</sub>/COD ratio) improvement. To study the effect of H<sub>2</sub>O<sub>2</sub> dose on UV/H<sub>2</sub>O<sub>2</sub>/TiO<sub>2</sub> process, experiments were conducted at pH 5, TiO<sub>2</sub> 1000 mg/L, irradiation time 5 hr, and H<sub>2</sub>O<sub>2</sub> dose in the range 50-350 mg/L (Case T1-T6, Figure 5.21). The COD removal was 16±1, 16±1, 20±1, 23±1, 29±1 and 25±1% at H<sub>2</sub>O<sub>2</sub> dose 50, 100, 150, 200, 250 and 350 mg/L, respectively. The biodegradability (BOD<sub>5</sub>/COD ratio) was 0.11±0.01, 0.12±0.01, 0.15±0.01, 0.19±0.01, 0.23±0.01 and 0.22±0.01 at H<sub>2</sub>O<sub>2</sub> dose 50, 100, 150, 200, 250 and 350 mg/L, respectively. The DOC removal was 10±1, 12±1, 13±2, 14±1, 16±1 and 14±1% at at H<sub>2</sub>O<sub>2</sub> dose 50, 100, 150, 200, 250 and 350 mg/L, respectively. Maximum COD and DOC removal, and biodegradability improvement were achieved at H<sub>2</sub>O<sub>2</sub> dose 250 mg/L. COD and DOC removal, and BOD<sub>5</sub>/COD ratio increased as H<sub>2</sub>O<sub>2</sub> dose increased and it reached the highest value at H<sub>2</sub>O<sub>2</sub> dose of 250 mg/L. Further increase in H<sub>2</sub>O<sub>2</sub> dose caused decrease in COD and DOC removal, and BOD<sub>5</sub>/COD ratio. This may be due to the fact that, excess H<sub>2</sub>O<sub>2</sub> reacts with OH<sup>•</sup> radicals and contributes to the OH<sup>•</sup> radicals and hole scavenging to form HO<sub>2</sub><sup>•</sup> as in Reactions 2.6 and 4.2 (Behnajady *et al.*, 2006; Zhao *et al.*, 2004). This agrees well with other reported studies such as degradation of chloramphenicol (Chatzitakis *et al.*, 2008). Based on the results, the optimum H<sub>2</sub>O<sub>2</sub> dose is 250 mg/L.

To study the effect of TiO<sub>2</sub> dose on the UV/H<sub>2</sub>O<sub>2</sub>/TiO<sub>2</sub> process, experiments were conducted by varying the TiO<sub>2</sub> dose in the range 0-1000 mg/L, pH 5, H<sub>2</sub>O<sub>2</sub> 250 mg/L, and irradiation time 5 hr. As shown in Figure 5.21 at zero TiO<sub>2</sub> dosage, sCOD and DOC removals were 14±1 and 6±1%, respectively and BOD<sub>5</sub>/COD ratio was 0.13±0.01 (Case T9). Increasing TiO<sub>2</sub> dose to 250 mg/L (Case T8) resulted in improvement of sCOD and DOC removal (18±1 and 8±2%), and BOD<sub>5</sub>/COD ratio (0.19±0.01). When TiO<sub>2</sub> dose was 500 mg/L (Case T7), sCOD and DOC removals were 21±1 and 13±1%, respectively and BOD<sub>5</sub>/COD ratio was 0.22±0.01. Further increase of TiO<sub>2</sub> dose to 1000 mg/L (Case T5) resulted in further improvement of sCOD and DOC removal (29±1 and 16±1%) and BOD<sub>5</sub>/COD ratio was 0.22±0.01. In

Phase I results, it was found that the optimum  $\text{TiO}_2$  dose for the treatment of amoxicillin, ampicillin and cloxacillin aqueous solution was 1000 mg/L.

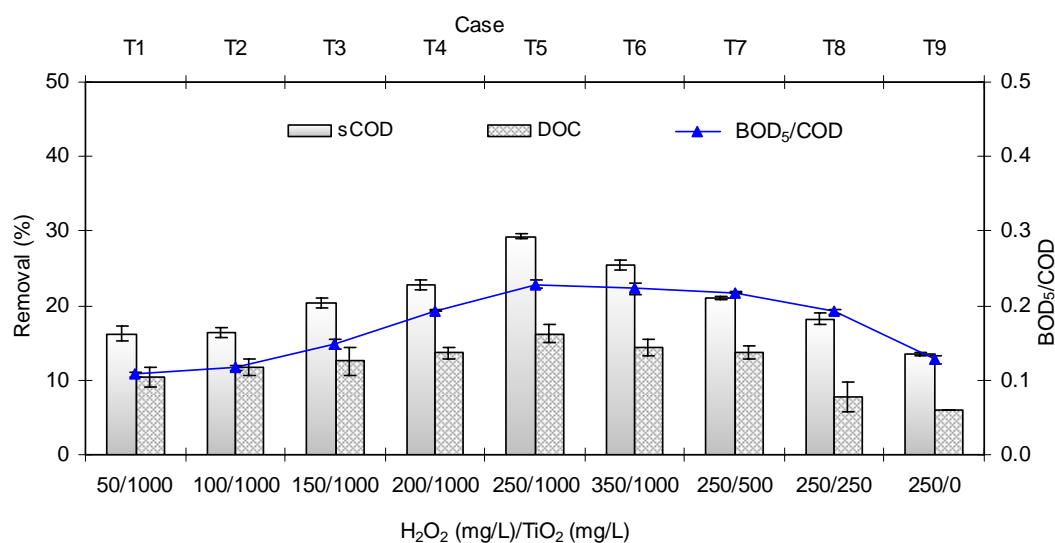


Figure 5.21 Effect of  $\text{TiO}_2$  and  $\text{H}_2\text{O}_2$  dose on the sCOD and DOC removal, and  $\text{BOD}_5/\text{COD}$  ratio

### 5.3.1.2 Degradation of Antibiotics

To confirm degradation of the antibiotics and study the matrix effect, an experiment was conducted under the following operating conditions:  $\text{TiO}_2$  dose 1000 mg/L,  $\text{H}_2\text{O}_2$  dose 250 mg/L and pH 5. HPLC analysis confirmed that complete degradation of amoxicillin and cloxacillin occurred in 30 min (Figure 5.22). Comparing with the Phase I results, the complete degradation time of the antibiotics increased from 20 min in Phase I (aqueous solution) to 30 min. This may be ascribed to the matrix effect.

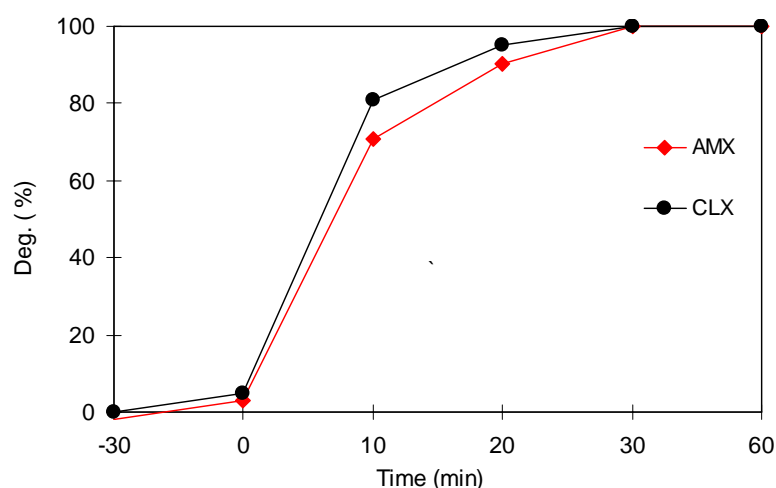


Figure 5.22 Degradation of AMX and CLX in Antibiotic Wastewater by UV/H<sub>2</sub>O<sub>2</sub>/TiO<sub>2</sub> Process

### 5.3.2 Treatment of UV/H<sub>2</sub>O<sub>2</sub>/TiO<sub>2</sub>-treated Antibiotic Wastewater by SBR

The third SBR was operated for 155 days with UV/H<sub>2</sub>O<sub>2</sub>/TiO<sub>2</sub>-treated effluent. The UV/H<sub>2</sub>O<sub>2</sub>/TiO<sub>2</sub>-treated effluent characteristics depended mainly on the UV/H<sub>2</sub>O<sub>2</sub>/TiO<sub>2</sub> operating conditions. The study covered the effect of the UV/H<sub>2</sub>O<sub>2</sub>/TiO<sub>2</sub> and SBR operating conditions on the SBR and combined system performance. These conditions are oxidant (H<sub>2</sub>O<sub>2</sub>) and catalyst (TiO<sub>2</sub>) dose, and irradiation time and SBR hydraulic retention time (HRT).

#### 5.3.2.1 Effect of UV/H<sub>2</sub>O<sub>2</sub>/TiO<sub>2</sub> Operating Conditions on SBR Performance

To study the effect of UV/H<sub>2</sub>O<sub>2</sub>/TiO<sub>2</sub> operating conditions and UV/H<sub>2</sub>O<sub>2</sub>/TiO<sub>2</sub>-treated effluent characteristics on SBR and combined system performance, nine UV/H<sub>2</sub>O<sub>2</sub>/TiO<sub>2</sub>-treated effluents (Case T1-T9, Table 5.15) at different TiO<sub>2</sub> and H<sub>2</sub>O<sub>2</sub> dosages were used to feed the SBR. The SBR was operated for 65 days at cycle period 24 hr. The cycle was repeated 6-9 times to allow cell acclimation and/or to obtain repetitive results for each feed. The performance of SBR in terms of sCOD and DOC as a function of UV/H<sub>2</sub>O<sub>2</sub>/TiO<sub>2</sub> operating conditions are shown in Figure 5.23.

Table 5.15 UV/H<sub>2</sub>O<sub>2</sub>/TiO<sub>2</sub> operating conditions for SBR

Case	TiO <sub>2</sub> (mg/L)	H <sub>2</sub> O <sub>2</sub> (mg/L)	H <sub>2</sub> O <sub>2</sub> /TiO <sub>2</sub> (mg/L)/(mg/L)
T1	1000	50	50/1000
T2	1000	100	100/1000
T3	1000	150	150/1000
T4	1000	200	200/1000
T5	1000	250	250/1000
T6	1000	350	350/1000
T7	500	250	250/500
T8	250	250	250/250
T9	0	250	250/0

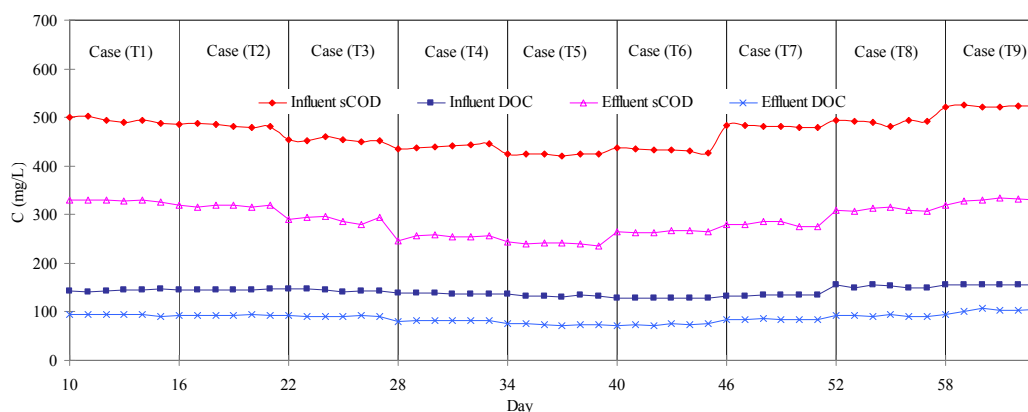


Figure 5.23 Performance of SBR in terms of sCOD and DOC as a function of UV/H<sub>2</sub>O<sub>2</sub>/TiO<sub>2</sub> operating conditions (Case T1-T9)

Table 5.16 shows the UV/H<sub>2</sub>O<sub>2</sub>/TiO<sub>2</sub> operating conditions, UV/H<sub>2</sub>O<sub>2</sub>/TiO<sub>2</sub>-treated and SBR effluent characteristics and the combined system efficiency. The effect of increasing H<sub>2</sub>O<sub>2</sub> dose from 50 to 100, 150, 200, 250 and 350 mg/L on SBR performance at TiO<sub>2</sub> dose 1000 mg/L, pH 5 and irradiation time 5 hr were examined (Case T1-T6). The results show that sCOD and DOC removal in SBR increased with increasing H<sub>2</sub>O<sub>2</sub> dose. Increasing H<sub>2</sub>O<sub>2</sub> dose from 50 to 100, 150, 200, 250 and 350 mg/L resulted in residual sCOD of 495±6, 483±3, 454±3, 440±4, 424±2 and 432±4 mg/L, respectively and residual DOC of 143±2, 145±1, 144±3, 137±1, 133±2 and

129±1 mg/L, respectively. The SBR efficiency was 33±1, 34±3, 36±1, 42±1, 43±1 and 39±1% for sCOD removal and 34±2, 36±1, 37±1, 41±1, 44±1, and 43±1% for DOC removal at H<sub>2</sub>O<sub>2</sub> dose 50, 100, 150, 200, 250 and 350 mg/L, respectively. Increasing H<sub>2</sub>O<sub>2</sub> dose beyond 250 mg/L did not improve the SBR efficiency in terms of sCOD and DOC removal and based on this it was decided to continue the next experiments using a H<sub>2</sub>O<sub>2</sub> dose of 250 mg/L. The SBR efficiency is considered low for all feeding and this is presumably due to low BOD<sub>5</sub>/COD ratio below 0.4, which is the threshold for a wastewater to be considered easily biodegradable (Al-Momani *et al.*, 2002) and indicates inhibition of aerobic oxidation by the antibiotic intermediates.

Table 5.16 UV/H<sub>2</sub>O<sub>2</sub>/TiO<sub>2</sub>-treated and SBR effluent characteristics and combined system efficiency at different H<sub>2</sub>O<sub>2</sub> and TiO<sub>2</sub> dose

Case	UV/H <sub>2</sub> O <sub>2</sub> /TiO <sub>2</sub> -treated effluent							SBR effluent					Combined efficiency		
	H <sub>2</sub> O <sub>2</sub> / TiO <sub>2</sub> (mg/L)/(mg/L)	sCOD		DOC		BOD	BOD <sub>5</sub> /COD	sCOD		DOC		MLSS	F/M	sCOD	DOC
		mg/L	R%	mg/L	R%	mg/L		mg/L	R%	mg/L	R%	mg/L	day <sup>-1</sup>	%	%
T1	50/1000	495±6	16±1	143±2	10±1	53±1	0.11±0.01	329±2	33±1	94±2	34±2	2500	0.128	41	41
T2	100/1000	483±3	16±1	145±1	12±1	56±2	0.12±0.01	318±2	34±3	93±1	36±1	2480	0.128	42	43
T3	150/1000	454±3	20±1	144±3	13±2	67±2	0.15±0.01	290±6	36±1	91±1	37±1	2450	0.122	42	45
T4	200/1000	440±4	23±1	137±1	14±1	85±1	0.19±0.01	254±5	42±1	82±1	41±1	2400	0.121	49	49
T5	250/1000	424±2	29±1	133±2	16±1	97±2	0.23±0.01	240±3	43±1	74±1	44±1	2470	0.113	57	53
T6	350/1000	432±4	25±1	129±1	14±1	96±4	0.22±0.01	265±2	39±1	74±2	43±1	2400	0.119	52	51
T7	250/500	480±2	21±1	134±12	13±1	104±1	0.22±0.01	278±5	42±1	85±1	37±1	2380	0.133	49	45
T8	250/250	491±4	18±1	152±3	8±2	94±1	0.19±0.01	310±3	37±1	92±2	39±2	2340	0.139	45	44
T9	250/0	523±1	14±1	155±1	6±1	67±3	0.13±0.01	329±5	37±1	102±4	34±3	2300	0.150	41	38

The next step was to study the effect of decreasing TiO<sub>2</sub> dose from 1000 to 500, 250 and 0 mg/L on the performance of SBR (Case T5, T7, T8 and T9, Table 5.16). The other operating conditions were fixed at H<sub>2</sub>O<sub>2</sub> dose 250 mg/L (the best dose from the pervious experiments), pH 5 and irradiation time 5 hr. The characteristics of the UV/H<sub>2</sub>O<sub>2</sub>/TiO<sub>2</sub>-treated effluent at TiO<sub>2</sub> dose 1000 mg/L (Case T5) were sCOD 424±2 mg/L, DOC 133±2 mg/L and BOD<sub>5</sub>/COD ratio 0.23±0.01 and SBR efficiency was 43±1 and 44±1% for sCOD and DOC removal, respectively. When TiO<sub>2</sub> dose was reduced to 500 mg/L (Case T7), the characteristics of the UV/H<sub>2</sub>O<sub>2</sub>/TiO<sub>2</sub>-treated effluent were sCOD 480±2 mg/L, DOC 134±12 mg/L and BOD<sub>5</sub>/COD ratio 0.22±0.01, and SBR efficiency was 42±1 and 37±1% for sCOD and DOC removal, respectively. When TiO<sub>2</sub> dose was reduced further to 250 mg/L (Case T8) and 0 mg/L (Case T9), the SBR efficiency decreased further. The results show decreasing sCOD and DOC removal in SBR with decrease of TiO<sub>2</sub> dose and this is presumably due to inhibition of aerobic oxidation by the antibiotic intermediates.

A marked decline in MLSS concentration (Table 5.16) was observed at low BOD<sub>5</sub>/COD ratio (Case T9). This reduction in MLSS concentration can be attributed to wall growth (Farré *et al.*, 2007) and inhibition of aerobic process by antibiotic intermediates. The F/M ratio varied in the range 0.113-0.150 day<sup>-1</sup> and this is mainly due to variation in sCOD concentration of the UV/H<sub>2</sub>O<sub>2</sub>/TiO<sub>2</sub>-treated effluent. With regard to the final effluent, the sCOD concentration under the best operating conditions (Case T5) was 240±3 mg/L which did not meet the discharge standard.

### 5.3.2.2 Effect of Cycle Period on the Performance of SBR

In order to improve final effluent characteristics of the UV/H<sub>2</sub>O<sub>2</sub>/TiO<sub>2</sub>-SBR and study the effect of cycle period on the SBR performance, SBR hydraulic retention time (HRT) was increased from 24 to 48 hr. The SBR was operated for 155 days at HRT 24 and 48 hr and was fed by nine UV/H<sub>2</sub>O<sub>2</sub>/TiO<sub>2</sub>-treated effluents (Case T1-T9, Table 5.15). Figures 5.24 and 5.25 show the SBR efficiencies at HRT 48 and 24 hr in terms of sCOD and DOC removal, respectively. A statistical analysis (one-way ANOVA) was performed on the results at a 5% level of significance. The statistical

analysis results are presented in more details in Appendix (E). As shown in Table 5.17, the statistical analysis indicated that increase of HRT from 24 to 48 hr significantly improved sCOD removal (P-value  $0.008 < 0.05$ ) or DOC removal (P-value  $0.005 < 0.05$ ). This disagrees with the results of the combined Fenton-SBR (Section 5.1.2.2) and combined photo-Fenton-SBR (Section 5.2.2.2) and it can be ascribed to the hardly biodegradable UV/H<sub>2</sub>O<sub>2</sub>/TiO<sub>2</sub>-treated effluent. With regard to the final effluent characteristics under the best UV/H<sub>2</sub>O<sub>2</sub>/TiO<sub>2</sub>-SBR operating conditions (H<sub>2</sub>O<sub>2</sub> dose 250 mg/L, TiO<sub>2</sub> dose 1000 mg/L pH 5, irradiation time 5 hr and HRT 48 hr), the sCOD concentration was  $236 \pm 3$  mg/L which did not meet the discharge standard.

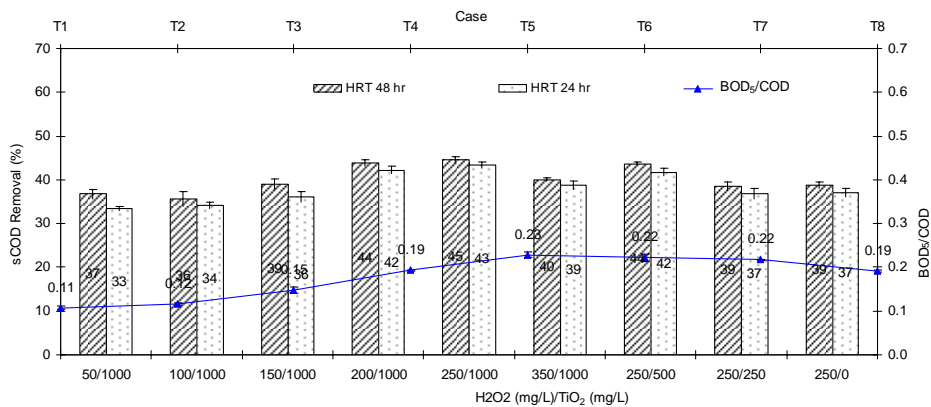


Figure 5.24 SBR efficiency of UV/H<sub>2</sub>O<sub>2</sub>/TiO<sub>2</sub>-SBR in terms of sCOD removal at HRT 48 and 24 hr

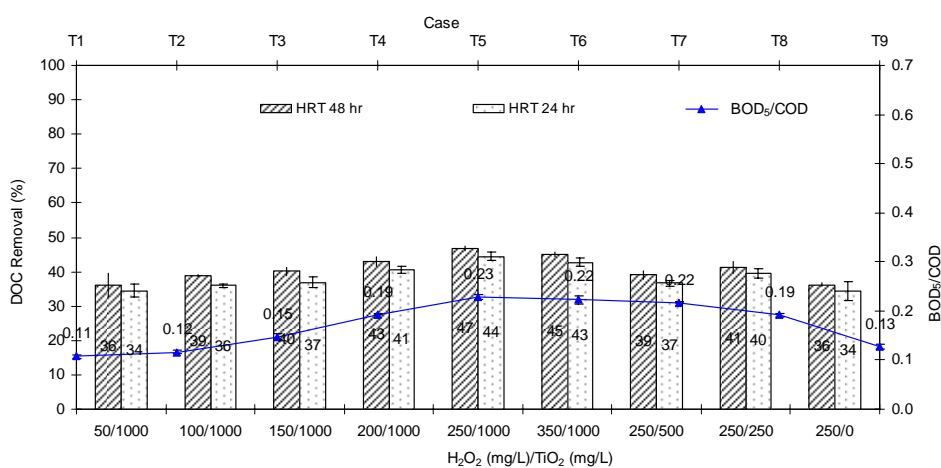


Figure 5.25 SBR efficiency of UV/H<sub>2</sub>O<sub>2</sub>/TiO<sub>2</sub>-SBR in terms of DOC removal at HRT 48 and 24 hr



Table 5.17 One-way ANOVA for SBR efficiency in terms of sCOD and DOC removal at different HRT (combined UV/H<sub>2</sub>O<sub>2</sub>/TiO<sub>2</sub>-SBR)

One-way ANOVA	Parameter	No. of groups	F	P-value	F crit
24 hr vs. 48 hr	sCOD	2	7.46	0.008	3.95
24 hr vs. 48 hr	DOC	2	8.19	0.005	3.95

In summary, the SBR was operated for 155 days and fed with UV/H<sub>2</sub>O<sub>2</sub>/TiO<sub>2</sub>-treated effluent under different UV/H<sub>2</sub>O<sub>2</sub>/TiO<sub>2</sub> and SBR operating conditions. The best TiO<sub>2</sub> and H<sub>2</sub>O<sub>2</sub> dosages were observed to be 1000 and 250 mg/L, respectively. Increasing HRT from 24 to 48 hr significantly improved the SBR efficiency in terms of sCOD and DOC removal. However, under the UV/H<sub>2</sub>O<sub>2</sub>/TiO<sub>2</sub>-SBR operating conditions H<sub>2</sub>O<sub>2</sub> dose 250 mg/L, TiO<sub>2</sub> dose 1000 mg/L, pH 5, irradiation time 5 hr and HRT 48 hr, the sCOD of the final effluent was 236±3 mg/L which did not meet the discharge standard. Based on the results, the combined UV/H<sub>2</sub>O<sub>2</sub>/TiO<sub>2</sub>-SBR is not a feasible system for treatment of antibiotic wastewater containing amoxicillin and cloxacillin, compared with the combined Fenton-SBR and combined photo-Fenton-SBR system.

#### 5.4 Kinetic Study

The kinetic study was conducted for optimum Fenton–SBR case (Case F19) and optimum photo-Fenton-SBR case (Case PF18) process. According to Equation 3.15, plot of  $\ln \frac{S}{S_0}$  versus time should give a straight line whose slope will be the biological first order kinetic constant ( $k_{ob}$ ).

Figure 5.26 shows the kinetics of SBR treatment of Fenton-treated effluent (Case F19). The Fenton operating conditions were H<sub>2</sub>O<sub>2</sub>/COD molar ratio 2.5, pH 3, H<sub>2</sub>O<sub>2</sub>/Fe<sup>2+</sup> molar ratio 150 and reaction time 120 min, and SBR operating conditions were cycle period 12 hr, MLSS 1940 mg/L and F/M 0.071 day<sup>-1</sup>. The value of the first order kinetic constant ( $k_{ob}$ ) is 0.078 hr<sup>-1</sup> (0.040 L g<sup>-1</sup> MLSS hr<sup>-1</sup>). Figure 5.27 shows the kinetics of SBR treatment of photo-Fenton-treated effluent (Case PF18).

The operating photo-Fenton conditions were  $\text{H}_2\text{O}_2/\text{COD}$  2 molar ratio, pH 3,  $\text{H}_2\text{O}_2/\text{Fe}^{2+}$  molar ratio 150 and reaction time 90 min, and SBR operating conditions were cycle period 12 hr, MLSS 2180 mg/L and F/M 0.070  $\text{day}^{-1}$ . The value of the first order kinetic constant ( $k_{ob}$ ) is 0.083  $\text{hr}^{-1}$  (0.038  $\text{L g}^{-1} \text{MLSS hr}^{-1}$ ). The value of the first order kinetic constant for both Fenton-treated effluent (Case F19) and photo-Fenton-treated effluent (Case PF18) agree well with those reported in the literature. Beltran-Heredia *et al.* (2000) studied the treatment of black olive wastewater by activated sludge process and the kinetic study was conducted assuming a first order kinetic equation. The kinetic constant was 0.037  $\text{L g MLSS}^{-1} \text{hr}^{-1}$ .

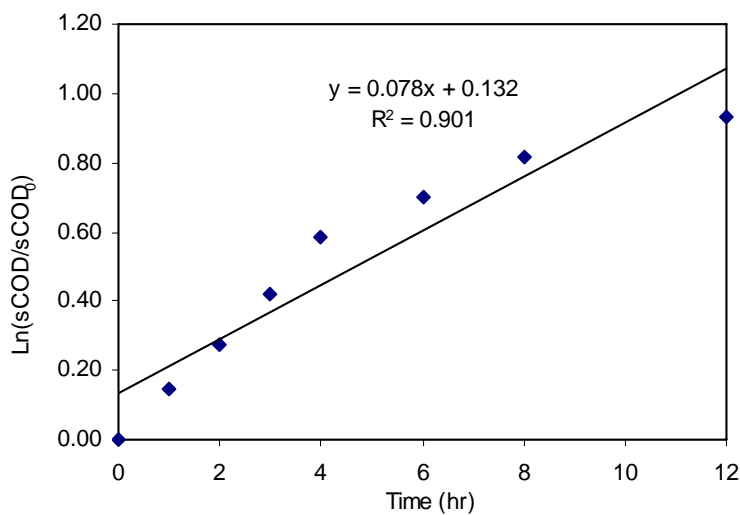


Figure 5.26 Kinetics of SBR treatment of Fenton-treated effluent (Case F19)

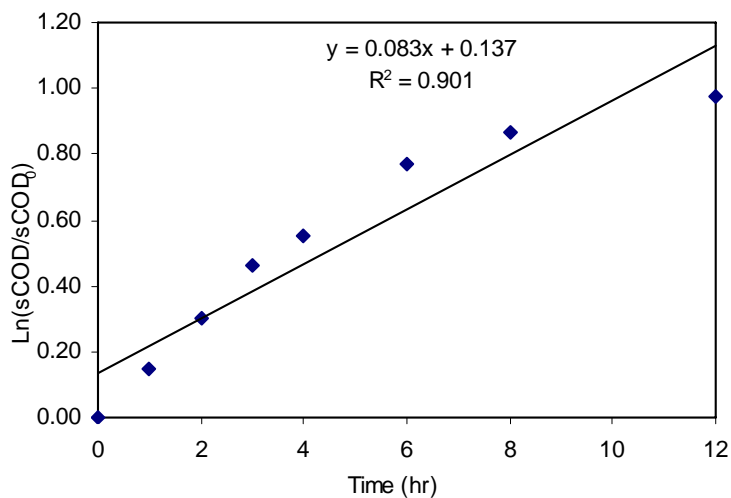


Figure 5.27 Kinetics of SBR treatment of photo-Fenton-treated effluent (Case PF18)

In biological reactor design, the parameters related to the biomass evolution over the whole cycle such as cell yield coefficient ( $Y_{X/S}$ ) and biomass decay coefficient ( $K_d$ ) are important (Ramalho, 1983; Beltran-Heredia *et al.* 2000). The first parameter represents the grams of biomass produced per gram of substrate utilized and the second parameter indicates the importance of endogenous metabolism. Taking into consideration the exponential growth and death phase, the net specific growth rate can be expressed as the following

$$\mu = Y_{X/S} q - K_d \quad \text{Equation 5.1}$$

where,  $\mu$  = specific growth rate,  $\text{hr}^{-1}$ ;  $q$  = specific substrate utilization rate;  $Y_{X/S}$  = ratio of the mass of cell formed to the mass of substrate utilized; and  $K_d$  = kinetic constant for biomass death phase,  $\text{hr}^{-1}$

A plot of  $\mu$  versus  $q$  should give a straight line whose slope and intercept will be  $Y_{X/S}$  and  $K_d$ , respectively. To perform this plot,  $\mu$  and  $q$  should be previously calculated as in the following equations:

$$\mu = \frac{1}{x} \frac{\Delta X}{\Delta t} \quad \text{Equation 5.2}$$

$$q = -\frac{1}{x} \frac{\Delta s}{\Delta t} \quad \text{Equation 5.3}$$

Figures 5.28 and 5.29 show plots of  $\mu$  versus  $q$  for Case F19 and Case PF18, respectively. The linearity of the plot indicates the validity of the proposed model for bio-oxidation. For Case F19, the values of  $Y_{X/S}$  and  $K_d$  are 0.60 (mg MLSS /mg sCOD) and  $-0.0013 \text{ hr}^{-1}$ , respectively, whereas the values of  $Y_{X/S}$  and  $K_d$  for Case PF18 are 0.64 (mg sCOD/mg MLSS) and  $-0.0014 \text{ hr}^{-1}$ , respectively. The values of  $Y_{X/S}$  and  $K_d$  for both cases (Case F19 and PF18) are similar. It is presumably due to the fact that biodegradability ( $\text{BOD}_5/\text{COD}$  ratio) for both cases are more than 0.40. The values of  $Y_{X/S}$  and  $K_d$  for both cases are in the normal range reported in the literature. Martín *et al.*, (2008) reported  $Y_{X/S}$  0.5 and  $K_d$   $0.004 \text{ hr}^{-1}$  for biodegradation of AOP-treated pesticide aqueous solution in SBR by *Pseudomonas putida* CECT 324. Beltran-Heredia *et al.* (2000) reported  $Y_{X/S}$  0.227 and  $K_d$   $0.0069 \text{ hr}^{-1}$  for biodegradation of black olive wastewater.

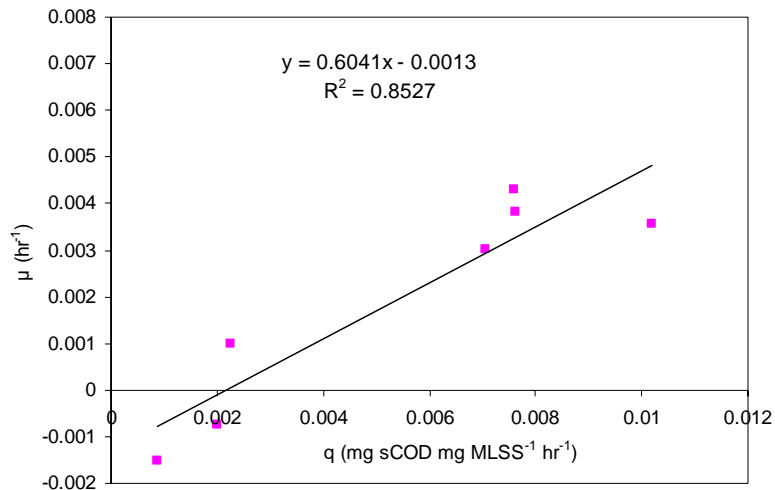


Figure 5.28 Evaluation of  $Y_{X/S}$  and  $K_d$  for SBR treatment of Fenton-treated effluent (Case F19)

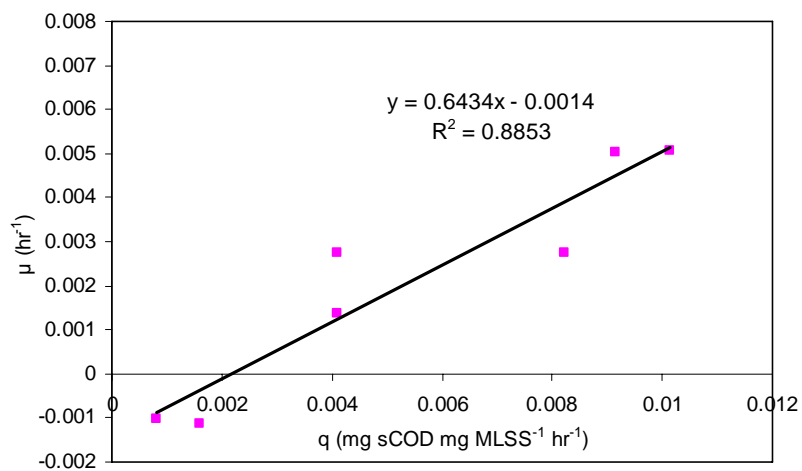


Figure 5.29 Evaluation of  $Y_{X/S}$  and  $K_d$  for SBR treatment of photo-Fenton-treated effluent (Case PF18)

## 5.5 Proposed Treatment System for Antibiotic Wastewater

The feasibility of using three combined systems (Fenton-SBR, photo-Fenton-SBR and UV/H<sub>2</sub>O<sub>2</sub>/TiO<sub>2</sub>-SBR) for treatment of antibiotic wastewater was evaluated. To propose a treatment system, it is necessary to make a technical and cost comparison among the combined systems.

The first treatment system was a combined Fenton-SBR process. The SBR was operated for 239 days and fed with Fenton-treated antibiotic wastewater under different Fenton and SBR operating conditions. The best operating conditions for treatment of the antibiotic wastewater by the combined Fenton-SBR process were found to be  $\text{H}_2\text{O}_2/\text{COD}$  molar ratio 2.5,  $\text{H}_2\text{O}_2/\text{Fe}^{2+}$  molar ratio 150, reaction time 120 min and HRT 12 hr. Under the best operating conditions, the final effluent sCOD was  $61 \pm 1$  mg/L which met the discharge standard of less than 100 mg/L COD. Combined system efficiency for sCOD was 89% and almost complete nitrification occurred in the SBR.

The second treatment system was a combined photo-Fenton-SBR process. The SBR was operated for 239 days and fed with photo-Fenton-treated antibiotic wastewater under different photo-Fenton and SBR operating conditions. The best operating conditions for treatment of the antibiotic wastewater by the combined photo-Fenton-SBR process were found to be  $\text{H}_2\text{O}_2/\text{COD}$  molar ratio 2.0,  $\text{H}_2\text{O}_2/\text{Fe}^{2+}$  molar ratio 150, irradiation time 90 min and HRT 12 hr. Under the best operating conditions, the final effluent sCOD was  $66 \pm 2$  mg/L which met the discharge standard of less than 100 mg/L COD. Combined system efficiency for sCOD was 89% and complete nitrification occurred in the SBR.

The third treatment system was a combined UV/ $\text{H}_2\text{O}_2$ / $\text{TiO}_2$ -SBR process. The SBR was operated for 155 days and fed with UV/ $\text{H}_2\text{O}_2$ / $\text{TiO}_2$ -treated antibiotic wastewater under different UV/ $\text{H}_2\text{O}_2$ / $\text{TiO}_2$  and SBR operating conditions. The best operating conditions for treatment of the antibiotic wastewater by the combined UV/ $\text{H}_2\text{O}_2$ / $\text{TiO}_2$ -SBR process were found to be  $\text{TiO}_2$  dose 1000 mg/L,  $\text{H}_2\text{O}_2$  dose 250 mg/L, pH 5, irradiation time 5 hr and HRT 48 hr. However, under the best operating conditions, the final effluent sCOD was  $236 \pm 3$  mg/L which did not meet the discharge standard of less than 100 mg/L COD.

Table 5.18 Comparison among combined Fenton-SBR, photo-Fenton-SBR and UV/H<sub>2</sub>O<sub>2</sub>/TiO<sub>2</sub>-SBR from technical point of view

	Parameter	Fenton-SBR	Photo-Fenton-SBR	UV/H <sub>2</sub> O <sub>2</sub> /TiO <sub>2</sub> -SBR
Best operating conditions	H <sub>2</sub> O <sub>2</sub> /COD (MR)	2.5	2.0	-
	H <sub>2</sub> O <sub>2</sub> /Fe <sup>2+</sup> (MR)	150	150	-
	COD/H <sub>2</sub> O <sub>2</sub> /Fe <sup>2+</sup> (MR)	1.0/2.5/0.0167	1.0/2/0.0133	-
	H <sub>2</sub> O <sub>2</sub> (mg/L)/TiO <sub>2</sub> (mg/L)	-	-	100/1000
	Reaction/irradiation time (min)	120	90	300
	pH of the AOP	3	3	5
	SBR cycle duration (hr)	12	12	48
AOP treatment	Complete antibiotics degradation	1 min	1 min	30 min
	sCOD removal (%)	64±1	60±1	29±1
	DOC removal (%)	44±1	52±1	16±1
	BOD <sub>5</sub> /COD ratio	0.42±0.01	0.42±0.01	0.23±0.01
SBR treatemnt	sCOD removal (%)	71±1	71±1	45±1
	DOC removal (%)	71±1	72±1	47±1
Final effluent characteristics	sCOD (mg/L)	61±1	66±2	236±3
	DOC (mg/L)	28±1	24±1	71±1
Combined system efficiency	COD removal (%)	89	89	57
	DOC removal (%)	84	86	55

From a technical comparison of the three combined systems shown in Table 5.18, the AOP pre-treatment is very important for biological treatment of recalcitrant wastewater (antibiotic wastewater) since it is responsible for degradation of the parent toxic compounds as well as for improving the biodegradability. Further, the combined UV/H<sub>2</sub>O<sub>2</sub>/TiO<sub>2</sub>-SBR is not a feasible treatment system for antibiotic wastewater containing amoxicillin and cloxacillin, compared with the combined Fenton-SBR and combined photo-Fenton-SBR and it will be excluded from consideration.

### 5.5.1 Cost Comparison

The estimation of the treatment cost is an important aspect. The overall cost of the treatment system is represented by the sum of the capital, operating and maintenance cost. For a full-scale system, these costs strongly depend on the nature and concentration of the pollutants, flow rate of the influent and configuration of the reactor (Andreozzi *et al.*, 1999).. A comparison between the two combined processes (Fenton-SBR and photo-Fenton-SBR) was made from economic (operation cost) point of view. The main cost items for pre-treatment processes are ferrous ion and hydrogen peroxide dosage and energy cost for UV irradiation, and the main cost item for post treatment (SBR) is the energy cost for aeration. The cost difference between the treatment systems under consideration (Fenton-SBR and photo-Fenton-SBR) is in the pre-treatment process (chemical dosages and UV irradiation time) since the aeration time is same for both combined systems.

In the literature, some efforts have been made for estimation of the electrical consumption for UV lamps (Bolton *et al.*, 1996; Andreozzi *et al.*, 1999). One of these procedures to estimate the electrical energy is based on the electrical energy (*EE*) in kilowatt hours (kWh) required to bring about the degradation of a unit mass (one kilogram, kg) of a pollutant and can be calculated using the following formula:

$$EE = \frac{P \times t \times 1000}{V \times M \times 60 \times (c_i - c_f)} \quad \text{Equation 5.4}$$

where, *EE* is the energy requirement per kilogram of organic pollutant as DOC, *P* is the lamp power (kW), *V* is the polluted wastewater volume (litres), *t* is irradiation time, *M* is the molecular weight of the pollutant (g/mol), *c<sub>i</sub>*, *c<sub>f</sub>* are the initial and final concentrations of the pollutant (mol/L) and the factor of 1000 converts g to kg.

Prices of electricity are highly dependent on the particular country and electricity price was taken \$0.10/kwh as an average value (Cañizares *et al.*, 2009). The average price of the chemical reagents are shown in Table 5.19. An estimation of the operating cost per kg of DOC was calculated (Table 5.20). The combined Fenton-SBR process appeared to be more cost-effective than combined photo-Fenton-SBR.

Figure 5.30 shows the processes diagram of the proposed combined system (Fenton-SBR) for the antibiotic wastewater treatment.

Table 5.19 Price of reagents for estimation of combined AOP-SBR cost

Reagent	Unit	Price (\$)
H <sub>2</sub> O <sub>2</sub> (35%) (Cañizares <i>et al.</i> , 2009)	kg	0.35
FeSO <sub>4</sub> ·7H <sub>2</sub> O (Cañizares <i>et al.</i> , 2009)	kg	0.5

Table 5.20 Cost estimation for combined Fenton-SBR and photo-Fenton-SBR

	Reagent	Combined Fenton-SBR	Combined Photo-Fenton -SBR
Chemical requirement (kg/kg DOC)	H <sub>2</sub> O <sub>2</sub>	19.08	15.25
	FeSO <sub>4</sub> ·7H <sub>2</sub> O	1.075	0.825
Cost estimation (\$/kg DOC)	H <sub>2</sub> O <sub>2</sub>	6.7	5.3
	FeSO <sub>4</sub> ·7H <sub>2</sub> O	0.5	0.4
	UV	-	11.3
Total cost* (\$/kg DOC)		7.2	17.0

\*Total cost is based on AOP operation cost only and one litre volume



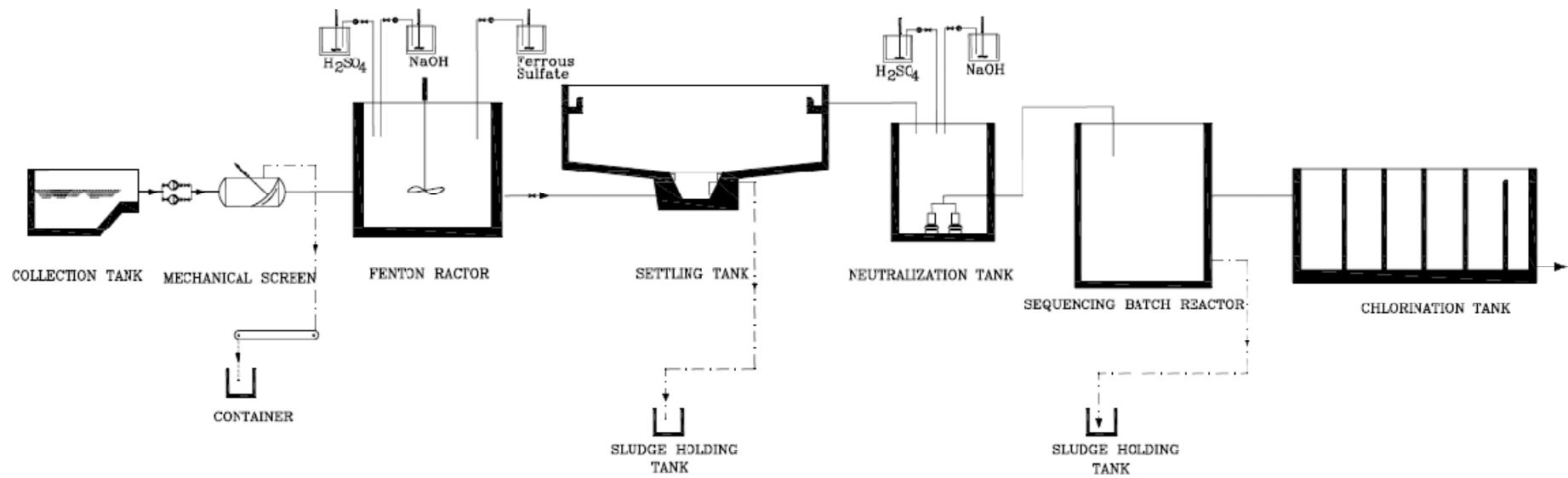


Figure 5.30 Process diagram of the proposed combined system (Fenton-SBR) for the antibiotic wastewater treatment

## 5.6 Summary

Feasibility of using three combined systems for treatment of antibiotic wastewater was evaluated. In the first combined system (Fenton-SBR), the SBR was operated for 239 days and fed with Fenton-treated antibiotic wastewater under different Fenton and SBR operating conditions. The  $\text{H}_2\text{O}_2/\text{COD}$  molar ratio 2.5 was found to be the best ratio among the five studied ratios (Case F1-F5, Table 5.2). The hydraulic retention time (HRT) of 12 hr was found suitable for the SBR and increasing HRT to 24 and 48 hr did not significantly improve the SBR efficiency in terms of sCOD and DOC removal. The  $\text{H}_2\text{O}_2/\text{Fe}^{2+}$  molar ratio and reaction time for the Fenton process were found to be the most influential parameters and they were optimized. Statistical analysis (two-way ANOVA) was made on the results to optimize the  $\text{H}_2\text{O}_2/\text{Fe}^{2+}$  molar ratio and reaction time and it was found possible to reduce the  $\text{Fe}^{2+}$  concentration and increase the Fenton reaction time. Based on the results, the best operating conditions for the treatment of antibiotic wastewater by the Fenton-SBR were  $\text{H}_2\text{O}_2/\text{COD}$  molar ratio 2.5,  $\text{H}_2\text{O}_2/\text{Fe}^{2+}$  molar ratio 150, reaction time 120 min and HRT 12 hr.

In the second combined system (photo-Fenton-SBR), the SBR was operated for 239 days and fed with photo-Fenton-treated antibiotic wastewater under different photo-Fenton and SBR operating conditions. The  $\text{H}_2\text{O}_2/\text{COD}$  molar ratio 2.0 was found to be the best ratio among the five studied ratios (Case PF1-PF5, Table 5.9). The hydraulic retention time (HRT) of 12 hr was found suitable for the SBR and increasing HRT to 24 and 48 hr did not significantly improve the SBR efficiency in terms of sCOD and DOC removal. The  $\text{H}_2\text{O}_2/\text{Fe}^{2+}$  molar ratio and irradiation time for the photo-Fenton process were found to be the most influential parameters and they were optimized. Statistical analysis (two-way ANOVA) was made on the results to optimize the  $\text{H}_2\text{O}_2/\text{Fe}^{2+}$  molar ratio and irradiation time and it was found possible to reduce the  $\text{Fe}^{2+}$  concentration and increase the photo-Fenton irradiation time. Based on the results, the best operating conditions for the treatment of antibiotic wastewater by the photo-Fenton-SBR were  $\text{H}_2\text{O}_2/\text{COD}$  molar ratio 2.0,  $\text{H}_2\text{O}_2/\text{Fe}^{2+}$  molar ratio 150, irradiation time 90 min and HRT 12 hr.

In the third combined system (combined UV/H<sub>2</sub>O<sub>2</sub>/TiO<sub>2</sub>-SBR), the SBR was operated for 155 days and fed with UV/H<sub>2</sub>O<sub>2</sub>/TiO<sub>2</sub>-treated antibiotic wastewater under different UV/H<sub>2</sub>O<sub>2</sub>/TiO<sub>2</sub> and SBR operating conditions. The best TiO<sub>2</sub> and H<sub>2</sub>O<sub>2</sub> dose were observed to be 1000 and 250 mg/L, respectively. Increasing HRT from 24 to 48 hr significantly improved the SBR efficiency in terms of sCOD and DOC removal. However, under the best operating conditions (H<sub>2</sub>O<sub>2</sub> 250 mg/L, TiO<sub>2</sub> 1000 mg/L, pH 5, irradiation time 5 hr and HRT 48 hr), the sCOD concentration in the final effluent was 236±3 mg/L, which did not meet discharge standard. The UV/H<sub>2</sub>O<sub>2</sub>/TiO<sub>2</sub>-SBR was not a feasible system for treatment of antibiotic wastewater containing amoxicillin and cloxacillin, compared with Fenton-SBR and photo-Fenton-SBR systems.

The matrix effect was not pronounced for antibiotic degradation in Fenton and photo-Fenton process; however, it increased the amoxicillin and cloxacillin degradation time from 20 to 30 min in UV/H<sub>2</sub>O<sub>2</sub>/TiO<sub>2</sub> process.

Monod kinetic model was fitted to the results of the Fenton-treated effluent biodegradation by SBR under the best combined Fenton-SBR operating conditions. The Fenton operating conditions were H<sub>2</sub>O<sub>2</sub>/COD molar ratio 2.5, pH 3, H<sub>2</sub>O<sub>2</sub>/Fe<sup>2+</sup> molar ratio 150 and reaction time 120 min, and SBR operating conditions were cycle period was 12 hr, MLSS 1940 mg/L and F/M 0.071 day<sup>-1</sup>. The value of the first order kinetic constant ( $k_{ob}$ ) was 0.078 hr<sup>-1</sup> (0.040 L g MLSS<sup>-1</sup> hr<sup>-1</sup>). The values of Y<sub>X/S</sub> and K<sub>d</sub> were 0.60 (mg MLSS /mg sCOD) and -0.0013 hr<sup>-1</sup>, respectively. The Monod kinetic model was also fitted to the results of the photo-Fenton-treated effluent biodegradation by SBR under the best combined photo-Fenton-SBR operating conditions. The photo-Fenton operating conditions were H<sub>2</sub>O<sub>2</sub>/COD molar ratio 2, pH 3, H<sub>2</sub>O<sub>2</sub>/Fe<sup>2+</sup> molar ratio 150 and irradiation time 90 min, and SBR operating conditions were cycle period 12 hr, MLSS 2180 mg/L and F/M 0.070 day<sup>-1</sup>. The value of the first order kinetic constant ( $k_{ob}$ ) was 0.083 hr<sup>-1</sup> (0.038 L g MLSS<sup>-1</sup> hr<sup>-1</sup>). The values of Y<sub>X/S</sub> and K<sub>d</sub> were 0.64 (mg sCOD/mg MLSS) and -0.0014 hr<sup>-1</sup>, respectively. The values of Y<sub>X/S</sub> and K<sub>d</sub> for both cases were similar and this is presumably due to the fact that biodegradability (BOD<sub>5</sub>/COD ratio) for both cases are more than 0.40.

From technical point of view, both combined Fenton-SBR and photo-Fenton-SBR achieved an overall efficiency of 89% and the final effluent amply met the discharge standard of less than 100 mg/L. The combined UV/H<sub>2</sub>O<sub>2</sub>/TiO<sub>2</sub>-SBR achieved an overall efficiency of 57% and a final effluent of 236 mg/L as sCOD which did not meet the discharge standard and thus was not a feasible combined system for treatment of antibiotic wastewater containing amoxicillin and cloxacillin. From economic point of view, the combined Fenton-SBR system appeared to be more cost-effective (~ 50% reduction in the operation cost) than the combined photo-Fenton-SBR system.

CHAPTER 6  
RESULTS AND DISCUSSION  
PHASE III: ARTIFICIAL NEURAL NETWORK (ANN) FOR MODELLING AND  
SIMULATION OF ADVANCED OXIDATION PROCESS

## 6.0 Chapter Overview

In Chapter 5 the combined Fenton-SBR system appeared to be more cost-effective than the combined photo-Fenton-SBR system. Fenton pre-treatment is very important for the combined Fenton-SBR system because the parent recalcitrant substances are degraded to less toxic byproducts, improving the biodegradability. Antibiotic wastewater characteristics are considered the main variable in operation of the Fenton-SBR system. Thus, application of artificial neural network for modelling, simulation and prediction of the Fenton process performance as well as studying the dynamic behaviour of the Fenton process is considered important.

This chapter introduces the implementation of artificial neural network in the area of wastewater treatment using Fenton process. The chapter is divided into five sections: selection of backpropagation training algorithm, optimization of number of neurons, test and validation of the model, sensitivity analysis and comparison between the measured and the predicted data.

## 6.1 Data Sets

Experimental data sets (120) were obtained from the results of the Fenton process in Phase I and were divided into input matrix [p] and target matrix [t] (Appendix F). The input variables were reaction time (t), H<sub>2</sub>O<sub>2</sub>/COD molar ratio, H<sub>2</sub>O<sub>2</sub>/Fe<sup>2+</sup> molar ratio, pH and COD concentration. The corresponding COD removal was used as a target. Principal component analysis (PCA) was performed on input data to filter out uncorrelated random data. The data sets were divided into training (one half),

validation (one fourth) and test (one fourth) subsets, each of which contained 60, 30 and 30 sets, respectively.

## 6.2 Selection of Backpropagation Training Algorithm

Backpropagation was used because it is the most widely used supervised learning algorithm for artificial neural networks. To determine the best backpropagation (BP) training algorithm, ten BP algorithms were studied. Tangent sigmoid transfer function (tansig) at hidden layer and a linear transfer function (purelin) at output layer were used. In addition, five neurons were used in the hidden layer as initial value for all BP algorithms. Table 6.1 shows a comparison among different backpropagation training algorithms. Levenberg–Marquardt backpropagation algorithm (LMA) showed smaller mean square error (MSE) compared to other backpropagation algorithms and hence LMA was considered the training algorithm in the present study.

Table 6.1 Backpropagation training algorithms with five neurons in the hidden layer

Backpropagation (BP) algorithms	Function	MSE	Epoch	R <sup>2</sup>	Best linear equation
Levenberg–Marquardt backpropagation	trainlm	0.0082	30	0.994	$y = 0.995X + 0.407$
Scaled conjugate gradient backpropagation	trainscg	0.0167	99	0.988	$y = 0.986X + 0.928$
BFGS quasi-Newton backpropagation	trainbfg	0.0188	55	0.987	$y = 0.989X + 0.83$
One step secant backpropagation	trainoss	0.0306	29	0.974	$y = 0.958X + 2.59$
Batch gradient descent	traingd	0.4860	100	0.703	$y = 0.387X + 33$
Vairable learning rate backpropagation	traingdx	0.4494	22	0.781	$y = 0.405X + 30$
Batch gradient descent with momentum	traingdm	0.5082	100	0.718	$y = 0.363X + 34.5$
Fletcher–Reeves conjugate gradient backpropagation	traincgf	0.0275	25	0.979	$y = 1.02X - 0.874$
Polak–Ribière conjugate gradient backpropagation	traincgp	0.0175	100	0.987	$y = 0.982X + 1.23$
Powell–Beale conjugate gradient backpropagation	traincgb	0.0203	37	0.985	$y = 0.963X + 2.09$

### 6.3 Optimization of Number of Neurons

The optimum number of neurons was determined based on the minimum value of MSE of the training and prediction set (Yetilmezsoy and Demirel, 2008). The optimization was done by using the Levenberg–Marquardt backpropagation (`trainlm`) as a training algorithm and varying the number of neurons in the range 1-20. Figure 6.1 shows the relationship between number of neurons and MSE. MSE was 0.3023 when one neuron was used and decreased to 0.0003 when 14 neurons were used. Increasing the number of neurons to more than 14 did not significantly decrease MSE. Hence, 14 neurons were selected as the best number of neurons.

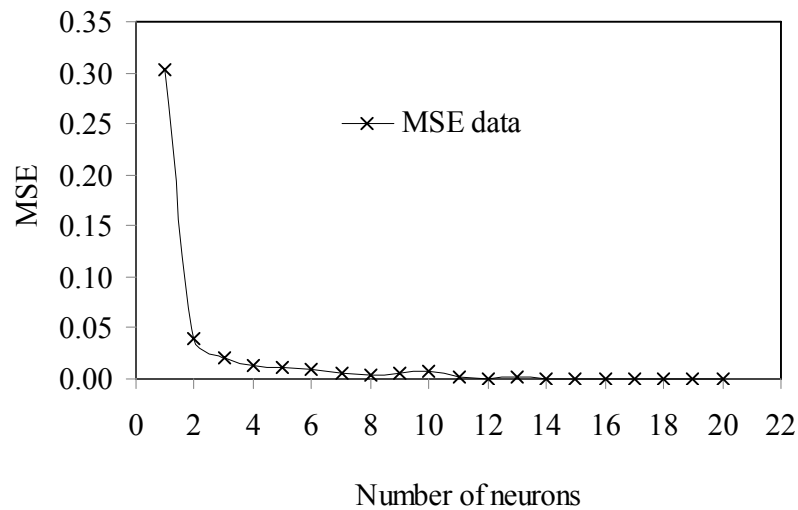


Figure 6.1 Relationship between number of neurons and MSE

Figure 6.2 shows the optimized neural network structure. It has three-layer ANN, with tangent sigmoid transfer function (*tansig*) at hidden layer with 14 neurons and linear transfer function (*purelin*) at output layer.

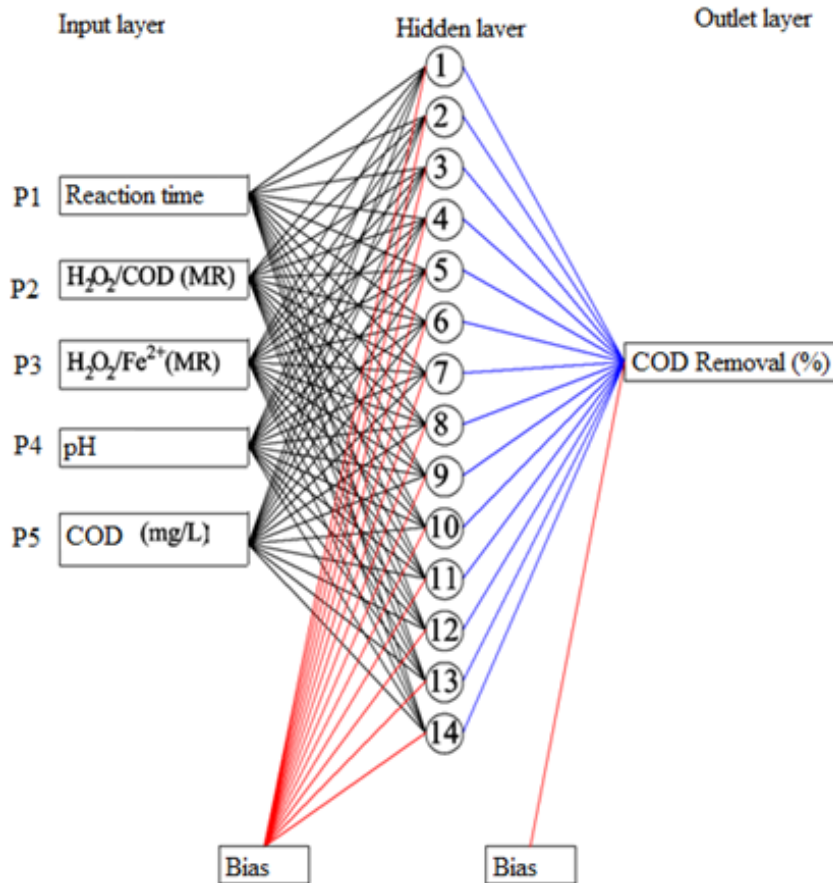


Figure 6.2 Artificial neural network optimized structure

#### 6.4 Test and Validation of the Model

As mentioned in Section 6.1, the data sets were divided into training subset (one half), validation subset (one fourth) and test subset (one fourth), each of which contained 60, 30 and 30 sets, respectively. The data sets were used to feed the optimized network in order to test and validate the model. Figure 6.3 shows a comparison between measured COD removal and the predicted COD removal using the neural network model. The figure contains two lines, one is the perfect fit  $Y = X$  (predicted value = measured value) and the other is the best fit indicated by a solid line with best liner equation  $Y = (0.999) X + 0.116$ , correlation coefficient 0.997 and MSE 0.0003. Both best liner equation and correlation coefficient show that the predicted values are in good agreement with the measured values. This agrees well



with the correlation coefficient reported in the literature – a correlation coefficient of 0.985 for prediction of nitrogen oxides removal by TiO<sub>2</sub> photocatalysis (Toma *et al.*, 2004), 0.998 for prediction of methyl tert-butyl ether (MTBE) degradation by UV/H<sub>2</sub>O<sub>2</sub> process (Salari *et al.*, 2005), 0.966 for prediction of polyvinyl alcohol degradation in aqueous solution by photo-Fenton process (Giroto *et al.*, 2006), 0.995 for removal of humic substances from the aqueous solutions by ozonation (Oguz *et al.*, 2008) and 0.98 for decolouration of Acid Orange 52 dye by UV/H<sub>2</sub>O<sub>2</sub> process (Guimarães *et al.*, 2008).

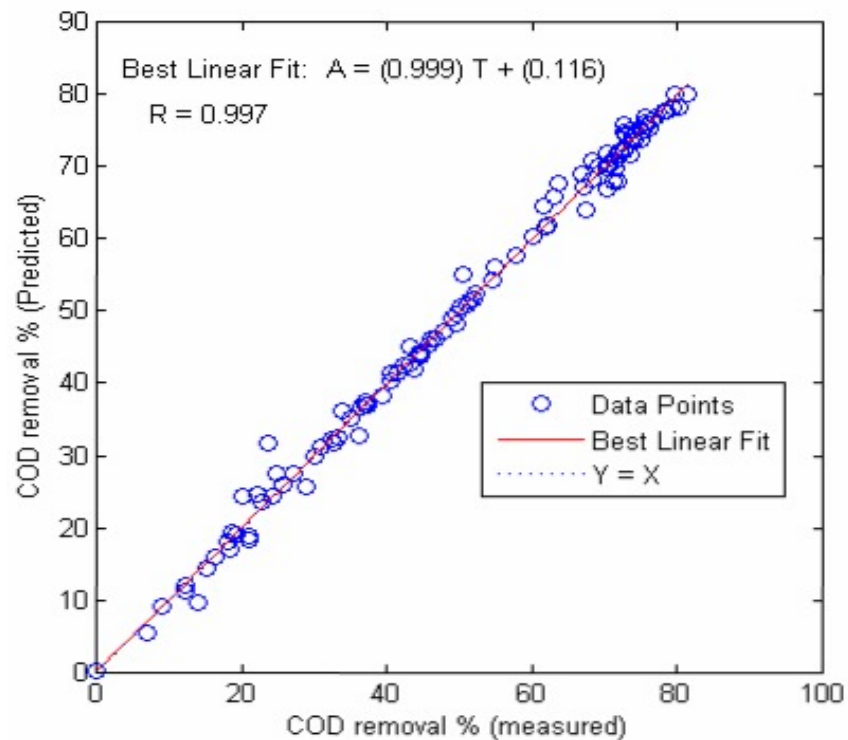


Figure 6.3 Comparison between predicted and measured values of the output

## 6.5 Sensitivity Analysis

In order to assess the relative importance of the input variables, two evaluation processes were used. The first one was based on the neural net weight matrix and Garson equation (Aleboyeh *et al.*, 2008). Garson (1991) proposed an equation based on the partitioning of connection weights:

$$I_j = \frac{\sum_{m=1}^{N_h} \left( \left( |W_{jm}^{ih}| \div \sum_{k=1}^{N_i} |W_{km}^{ih}| \right) \times |W_{mn}^{ho}| \right)}{\sum_{k=1}^{N_i} \left\{ \sum_{m=1}^{N_h} \left( |W_{km}^{ih}| \div \sum_{k=1}^{N_i} |W_{km}^{ih}| \right) \times |W_{mn}^{ho}| \right\}} \quad \text{Equation 6.1}$$

where,  $I_j$  is the relative importance of the  $j^{\text{th}}$  input variable on the output variable,  $N_i$  and  $N_h$  are the numbers of input and hidden neurons, respectively,  $W$ s are connection weights, the superscripts ‘i’, ‘h’ and ‘o’ refer to input, hidden and output layers, respectively, and subscripts ‘k’, ‘m’ and ‘n’ refer to input, hidden and output neurons, respectively.

Table 6.2 shows the weights between the artificial neurons produced by ANN model used in this work and Table 6.3 shows the relative importance of the input variables calculated by Garson equation. It is seen in Table 6.3 that all variables have strong effect on COD removal. The  $\text{H}_2\text{O}_2/\text{Fe}^{2+}$  molar ratio appears to be the most influential variable followed by pH,  $\text{H}_2\text{O}_2/\text{COD}$  molar ratio, reaction time and COD concentration. The low relative importance of COD concentration reveals that the selected  $\text{H}_2\text{O}_2/\text{COD}$  and  $\text{H}_2\text{O}_2/\text{Fe}^{2+}$  molar ratios are valid for a wide range of wastewater strength.

Table 6.2 Weight matrix, weights between input and hidden layers (W1) and weights between hidden and output layers (W2)

Neuron	W1					W2
	Input variable					Output
	Time	H <sub>2</sub> O <sub>2</sub> /COD	H <sub>2</sub> O <sub>2</sub> /Fe <sup>2+</sup>	pH	COD concentration	COD removal %
1	0.8869	0.0855	-0.7863	-0.2422	0.3197	0.7394
2	0.1251	-2.0537	-0.2143	0.8923	-2.1553	1.9441
3	0.1996	-0.0919	-0.8751	0.2114	0.0137	-1.4281
4	0.0048	0.6453	0.0236	-0.786	-0.4838	0.836
5	1.1772	0.84	0.8969	1.0508	0.045	-0.7664
6	-0.6675	-1.1887	1.4041	0.7599	0.0555	-0.5634
7	-0.8075	-1.0106	0.7954	-1.0555	0.5573	-0.9707
8	-0.6322	-0.2504	0.7846	0.4784	-0.5846	-1.0221
9	0.4747	0.2399	0.1719	0.6281	-0.2614	-1.0734
10	-0.875	0.4465	-0.0579	0.4996	0.9659	-0.1611
11	-0.9162	-0.4413	-1.73	-1.4311	0.1075	-1.4267
12	0.4797	-0.0523	-1.0736	0.2493	0.2117	-1.018
13	0.3521	0.028	0.8121	-0.5173	-0.4002	-0.3725
14	0.5326	1.355	0.4631	1.0192	1.5174	1.3226

Table 6.3 Relative importance of input variables

Input variable	Importance (%)
H <sub>2</sub> O <sub>2</sub> /Fe <sup>2+</sup>	25.8
pH	22.1
H <sub>2</sub> O <sub>2</sub> /COD	18.2
Reaction time	17.1
COD concentration	16.8
Total	100

The second evaluation process is based on the possible combination of variables (Yetilmezsoy and Demirel, 2008). Performance of the groups of one, two, three, four, and five variables were examined by the optimum ANN structure using the LMA with 14 hidden neurons. The input variables were reaction time ( $P_1$ ),  $H_2O_2/COD$  molar ratio ( $P_2$ ),  $H_2O_2/Fe^{2+}$  molar ratio ( $P_3$ ), pH ( $P_4$ ) and COD concentration ( $P_5$ ). Table 6.4 shows the results of the sensitivity analysis for different combination of input variables. The sensitivity analysis showed that  $P_3$  ( $H_2O_2/Fe^{2+}$ ) was found to be the most effective parameter among the other variable in the group of one variable. The MSE (270.141) decreased up to 0.3041, which is the minimum value of the group of two variables when  $P_4$  (pH) was used in combination with  $P_3$ . The MSE (0.3041) decreased up to 0.1172, which is the minimum value of the group of three variables when  $P_2$  ( $H_2O_2/COD$ ) was used in combination with  $P_3$  and  $P_4$ . The MSE (0.1172) decreased up to 0.0027, which is the minimum value of the group of four variables when  $P_1$  (reaction time) was used in combination with  $P_3$ ,  $P_4$  and  $P_2$ . The MSE (0.0027) decreased up to 0.0003, which is the minimum value of the group of five variables when  $P_5$  (COD concentration) was used in combination with  $P_3$ ,  $P_4$ ,  $P_2$  and  $P_1$ . The best group performances according to number of parameters are marked with asterisk in Table 6.4. MSE values decreased as the number of variables in the group increased due to the contribution of all parameters (Table 6.4). It can be concluded that  $H_2O_2/Fe^{2+}$  molar ratio is the most influential parameter. In addition, all variables have strong effect on antibiotics degradation in terms of COD removal and it agrees well with the sensitivity analysis using Garson equation.

Table 6.4 Evaluation of combination of input variables

Combination	Mean square error (MSE)	Epoch	Correlation coefficient (R <sup>2</sup> )	Best linear equation
P <sub>1</sub>	365.889	6	0.315	y = 3.71X +880
P <sub>2</sub>	276.46	8	0.599	y = 7.44X +763
P <sub>3</sub> <sup>*</sup>	270.141	10	0.616	y = 8.93X +689
P <sub>4</sub>	378.575	7	0.395	y = 3.15X +991
P <sub>5</sub>	404.727	12	0.284	y = 1,7X +953
P <sub>1</sub> +P <sub>2</sub>	0.500941	7	0.538	y = 0.409X +29.2
P <sub>1</sub> +P <sub>3</sub>	0.451707	8	0.649	y = 0.452X +25.9
P <sub>1</sub> +P <sub>4</sub>	0.65364	9	0.451	y = 0.32X +31.8
P <sub>1</sub> +P <sub>5</sub>	0.714965	6	0.391	y = 0.30X +38
P <sub>2</sub> +P <sub>3</sub>	0.415012	9	0.742	y = 0.528X +25
P <sub>2</sub> +P <sub>4</sub>	0.388861	5	0.764	y = 0.528X +24.3
P <sub>2</sub> +P <sub>5</sub>	0.552496	5	0.636	y = 0.405X +32.1
P <sub>3</sub> +P <sub>4</sub> <sup>*</sup>	0.304122	9	0.848	y = 0.701X +16.9
P <sub>3</sub> +P <sub>5</sub>	0.571864	10	0.646	y = 0.509X +23.5
P <sub>4</sub> +P <sub>5</sub>	0.755573	5	0.487	y = 0.232X +40.6
P <sub>1</sub> +P <sub>2</sub> +P <sub>3</sub>	0.313754	16	0.802	y = 0.642X +18.1
P <sub>1</sub> +P <sub>2</sub> +P <sub>4</sub>	0.2901	14	0.825	y = 0.675X +16.4
P <sub>1</sub> +P <sub>2</sub> +P <sub>5</sub>	0.453212	10	0.702	y = 0.675X +25.2
P <sub>1</sub> +P <sub>3</sub> +P <sub>4</sub>	0.141262	25	0.873	y = 0.873X +6.2
P <sub>1</sub> +P <sub>3</sub> +P <sub>5</sub>	0.43797	10	0.69	y = 0.57X +21.1
P <sub>1</sub> +P <sub>4</sub> +P <sub>5</sub>	0.583005	16	0.528	y = 0.57X +32.7
P <sub>2</sub> +P <sub>3</sub> +P <sub>4</sub> <sup>*</sup>	0.117252	12	0.936	y = 0.849X +9.37
P <sub>2</sub> +P <sub>3</sub> +P <sub>5</sub>	0.379122	47	0.77	y = 0.579X +23.1
P <sub>3</sub> +P <sub>4</sub> +P <sub>5</sub>	0.300483	25	0.85	y = 0.695X +17.1
P <sub>1</sub> +P <sub>2</sub> +P <sub>3</sub> +P <sub>4</sub> <sup>*</sup>	0.00278282	34	0.995	y = 0.997X +0.402
P <sub>1</sub> +P <sub>2</sub> +P <sub>3</sub> +P <sub>5</sub>	0.270749/0	25	0.818	y = 0.679X +15.7
P <sub>1</sub> +P <sub>2</sub> +P <sub>4</sub> +P <sub>5</sub>	0.264695	15	0.832	y = 0.682X +15.8
P <sub>1</sub> +P <sub>3</sub> +P <sub>4</sub> +P <sub>5</sub>	0.139748	15	0.912	y = 0.87X +6.27
P <sub>2</sub> +P <sub>3</sub> +P <sub>4</sub> +P <sub>5</sub>	0.113608	36	0.915	y = 0.862X +8.92
P <sub>1</sub> +P <sub>2</sub> +P <sub>3</sub> +P <sub>4</sub> +P <sub>5</sub> <sup>*</sup>	0.000376	20	0.997	y = 0.999X +0.116

\* The best group performances according to number of parameters

## **6.6 Comparison between Predicted and Experimental Results**

A comparison between predicted and experimental results under different operating conditions (reaction time,  $\text{H}_2\text{O}_2/\text{COD}$  molar ratio,  $\text{H}_2\text{O}_2/\text{Fe}^{2+}$  molar ratio and pH) was conducted and shown in the following sections.

### **6.6.1 Comparison between Measured and Predicted Results at Different $\text{H}_2\text{O}_2/\text{COD}$ Molar Ratio**

Predicted results were compared with the experimental results at  $\text{H}_2\text{O}_2/\text{COD}$  molar ratio 1, 1.5, 2, 2.5, 3 and 3.5. Initial AMX, AMP and CLX concentrations were 104, 105 and 103 mg/L, respectively. The other operating conditions were pH 3 and  $\text{H}_2\text{O}_2/\text{Fe}^{2+}$  molar ratio 50. The importance of this comparison was to study the ability of the proposed model to predict the results at different  $\text{H}_2\text{O}_2/\text{COD}$  molar ratio in order to help the operator to choose the suitable oxidant dosage. Figure 6.4 shows a comparison between the predicted results and experimental results of COD removal at  $\text{H}_2\text{O}_2/\text{COD}$  molar ratio 1.0 (Figure 6.4(A)), 1.50 (Figure 6.4(B)), 2.0 (Figure 6.4(C)), 2.50 (Figure 6.4(D)), 3.0 (Figure 6.4(E)) and 3.5 (Figure 6.4(F)), respectively. The results show that the predicted values are in good agreement with the experimental values.

### **6.6.2 Comparison between Measured and Predicted Results at Different $\text{H}_2\text{O}_2/\text{Fe}^{2+}$ Molar Ratio**

Predicted results were compared with the experimental results at  $\text{H}_2\text{O}_2/\text{Fe}^{2+}$  molar ratio 2, 5, 10, 20, 50 and 100. Initial AMX, AMP and CLX concentrations were 104, 105 and 103 mg/L, respectively. The other operating conditions were pH 3 and  $\text{H}_2\text{O}_2/\text{COD}$  molar ratio 3. The importance of this comparison was to study the ability of the proposed model to predict the results at different  $\text{H}_2\text{O}_2/\text{Fe}^{2+}$  molar ratio in order to help the operator to choose the suitable catalyst dosage. Figure 6.5 shows a comparison between the predicted results and experimental results of COD removal at  $\text{H}_2\text{O}_2/\text{Fe}^{2+}$  molar ratio 2 (Figure 6.5(A)), 5 (Figure 6.5(B)), 10 (Figure 6.5(C)), 20 (Figure 6.5(D)), 50 (Figure 6.5(E)) and 100 (Figure 6.5(F)), respectively. The results show that the predicted values are in good agreement with the experimental values.

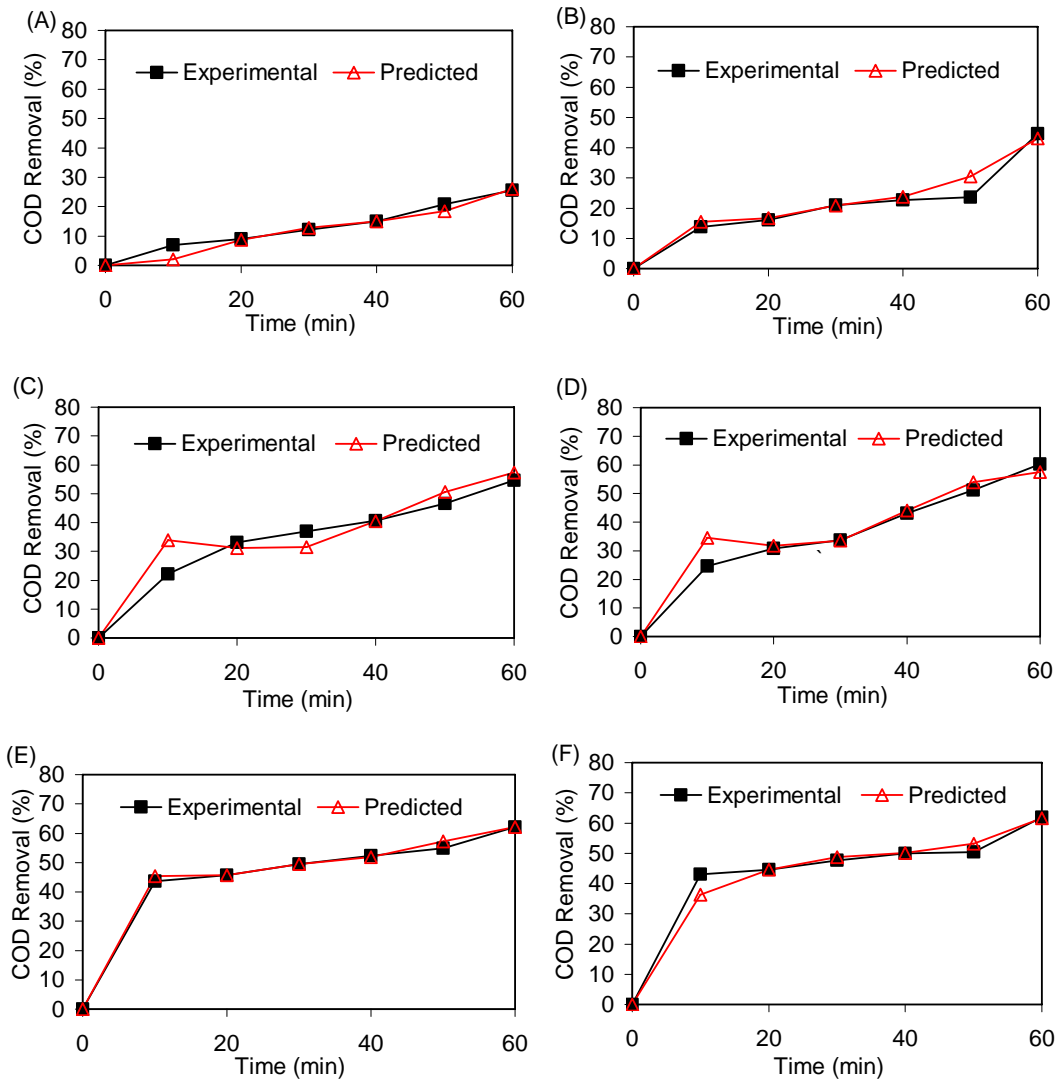


Figure 6.4 Comparison between predicted and experimental results at different H<sub>2</sub>O<sub>2</sub>/COD molar ratio: (A) 1.0, (B) 1.5, (C) 2.0, (D) 2.5, (E) 3.0 and (F) 3.5

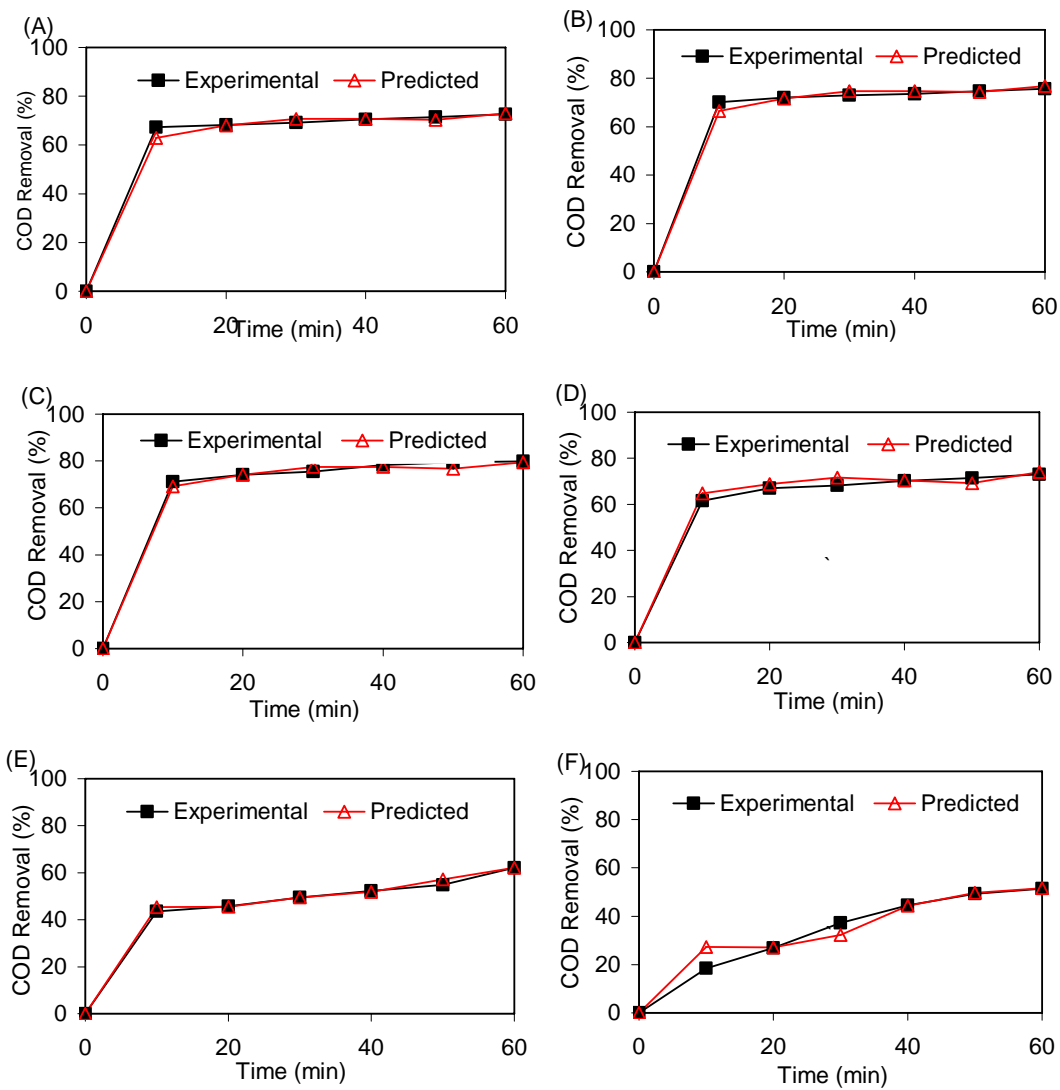


Figure 6.5 Comparison between predicted and experimental results at different  $H_2O_2/Fe^{2+}$  molar ratio: (A) 2, (B) 5, (C) 10, (D) 20, (E) 50 and (F) 100



### 6.6.3 Comparison between Measured and Predicted Results at Different pH

Predicted results were compared with the experimental results at initial pH 2, 3, 3.5 and 4. Initial AMX, AMP and CLX concentrations were 104, 105 and 103 mg/L, respectively. The other operating conditions were H<sub>2</sub>O<sub>2</sub>/COD molar ratio 3 and H<sub>2</sub>O<sub>2</sub>/Fe<sup>2+</sup> molar ratio 10. The importance of this comparison was to study the ability of the proposed model to predict the results at different initial pH since the pH of industrial wastewater fluctuates from time to time. Figure 6.6 shows a comparison between the predicted results and experimental results of COD removal at pH 2 (Figure 6.6(A)), 3 (Figure 6.6(B)), 3.5 (Figure 6.6(C)) and 4 (Figure 6.6(D)), respectively. The results show that the predicted values are in good agreement with the experimental values.

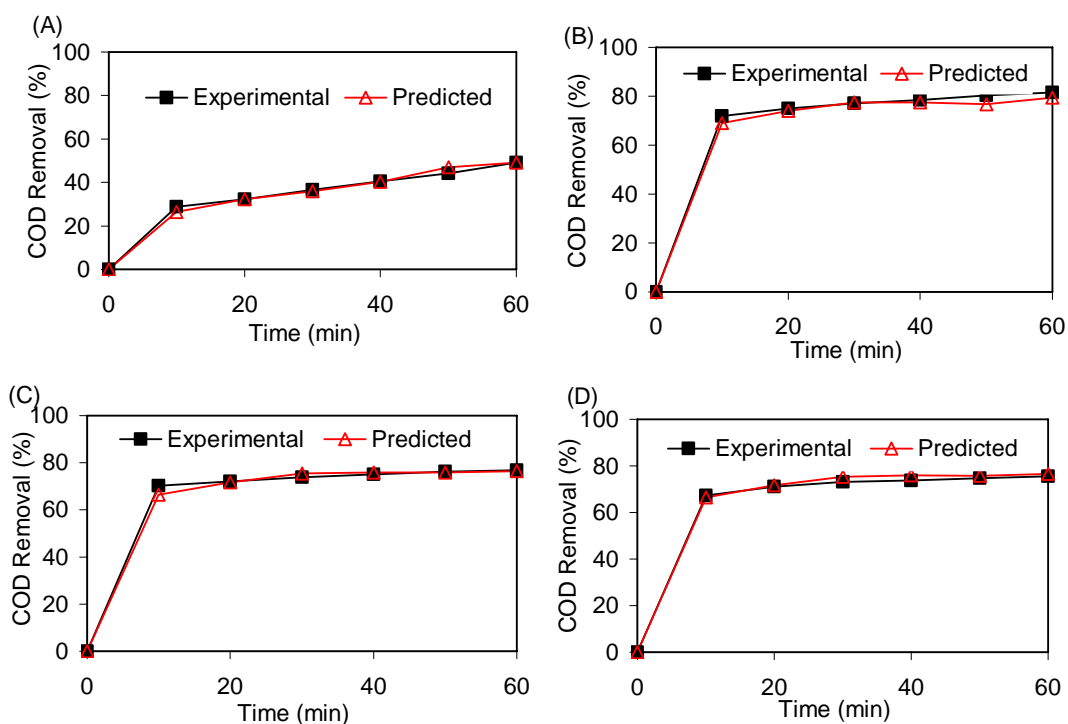


Figure 6.6 Comparison between predicted and experimental results at different pH:

(A) 2, (B) 3, (C) 3.5 and (D) 4

## 6.7 Summary

The study examined the implementation of artificial neural network (ANN) for prediction and simulation of the performance of Fenton process. The configuration of the backpropagation neural network giving the smallest mean square error (MSE) was a three-layer ANN with tangent sigmoid transfer function (tansig) at hidden layer with 14 neurons, linear transfer function (purelin) at output layer and Levenberg–Marquardt backpropagation training algorithm (LMA). ANN predicted results were very close to the experimental results with correlation coefficient ( $R^2$ ) of 0.997 and MSE of 0.000376. The sensitivity analysis showed that all studied variables (reaction time,  $H_2O_2$ /COD molar ratio,  $H_2O_2/Fe^{2+}$  molar ratio, pH and COD concentration) had a strong effect on COD removal. In addition,  $H_2O_2/Fe^{2+}$  molar ratio was the most influential parameter with relative importance of 25.8%. The results showed that neural network modeling could effectively predict and simulate the performance of the Fenton process in antibiotic wastewater treatment.

## CHAPTER 7 CONCLUSIONS AND RECOMMENDATIONS

### 7.0 Chapter Overview

This chapter presents the main conclusions and recommendations for future work. The conclusions are arranged in order to answer each objective of the study.

### 7.1 Conclusions

- 1) The first objective of the work was to study degradation of amoxicillin, ampicillin and cloxacillin antibiotics in aqueous solution by the Fenton, photo-Fenton, TiO<sub>2</sub> photocatalytic and ZnO photocatalytic process, and the effect of operating conditions of each on antibiotic mineralization and biodegradability improvement. Based on the results, the following conclusions can be drawn:
  - a. Fenton and photo-Fenton processes are effective in the treatment of an aqueous solution of amoxicillin, ampicillin and cloxacillin.
  - b. Higher hydrogen peroxide and iron dose showed negative effect on both processes. The optimum operating conditions for the processes were: Fenton process – H<sub>2</sub>O<sub>2</sub>/COD molar ratio 3, H<sub>2</sub>O<sub>2</sub>/Fe<sup>2+</sup> molar ratio 10 (COD/H<sub>2</sub>O<sub>2</sub>/Fe<sup>2+</sup> molar ratio 1:3:0.30) and pH 3; photo-Fenton process – H<sub>2</sub>O<sub>2</sub>/COD molar ratio 1.5, H<sub>2</sub>O<sub>2</sub>/Fe<sup>2+</sup> molar ratio 20 (COD/H<sub>2</sub>O<sub>2</sub>/Fe<sup>2+</sup> molar ratio 1:1.5:0.075) and pH 3.
  - c. Under the optimum Fenton operating conditions, complete degradation of the antibiotics occurred in 2 min, biodegradability improved from ~ 0 to 0.33, COD removal was 81.4% in 60 min and mineralization of

- organic carbon and nitrogen occurred (DOC removal 54.3% and  $\text{NO}_3^-$  increased from 0.3 to 10 mg/L in 60 min).
- d. Under the optimum photo-Fenton operating conditions, complete degradation of the antibiotics occurred in 2 min, biodegradability improved to  $\sim 0.4$ , COD removal was 80.8 % in 50 min and mineralization of organic carbon and nitrogen occurred (DOC removal 58% and  $\text{NO}_3^-$  increased from 0.3 to 14.2 mg/L in 50 min).
  - e. The pH had a great effect on antibiotics degradation by UV/TiO<sub>2</sub> process and the highest degradation was achieved at pH 11.
  - f. Photocatalytic degradation of the antibiotics by UV/TiO<sub>2</sub> process approximately followed a pseudo-first order kinetics and the rate constants ( $k_0$ ) were 0.007, 0.003 and 0.029 min<sup>-1</sup> for amoxicillin, ampicillin and cloxacillin, respectively.
  - g. Addition of H<sub>2</sub>O<sub>2</sub> at ambient pH  $\sim 5$  and TiO<sub>2</sub> 1.0 g/L resulted in complete degradation of amoxicillin, ampicillin and cloxacillin in 30 min.
  - h. Dissolved organic carbon (DOC) removal, and nitrate ( $\text{NO}_3^-$ ), ammonia ( $\text{NH}_3$ ) and sulphate ( $\text{SO}_4^{2-}$ ) formation during degradation indicated mineralization of organic carbon, nitrogen and sulphur.
  - i. The optimum operating conditions of the UV/ZnO process for complete degradation of the antibiotic aqueous solution containing 104, 105 and 103 mg/L amoxicillin, ampicillin, and cloxacillin, respectively were: ZnO concentration 0.5 g/L, irradiation time 180 min and pH 11.
  - j. Photocatalytic degradation of the antibiotics by the UV/ZnO process approximately followed a pseudo-first order kinetics. Cloxacillin exhibited the highest rate constant ( $k_0$ ) (0.029 min<sup>-1</sup>), followed by amoxicillin (0.018 min<sup>-1</sup>) and ampicillin (0.015 min<sup>-1</sup>).
- 2) The second objective of the work was to compare among the AOPs (Fenton, photo-Fenton, and UV/TiO<sub>2</sub> and UV/ZnO processes) in terms of technical and economic feasibility. Based on the results, the following conclusions can be drawn:

- a. All studied processes were able to degrade the antibiotics and improve biodegradability, except for UV/ZnO process which did not improve biodegradability.
  - b. The DOC removal approximately followed a pseudo-first order kinetics. Photo-Fenton process exhibited the highest rate constant ( $0.029 \text{ min}^{-1}$ ), followed by Fenton ( $0.0144 \text{ min}^{-1}$ ), UV/ZnO process ( $0.00056 \text{ min}^{-1}$ ) and UV/H<sub>2</sub>O<sub>2</sub>/TiO<sub>2</sub> process ( $0.0005 \text{ min}^{-1}$ ).
  - c. Photo-Fenton process appeared to be the most cost-effective compared to other studied processes.
- 3) The third objective of the work was to study the feasibility of using combined AOP-sequencing batch reactor (SBR) system for complete treatment of antibiotic wastewater from a local antibiotic industry producing amoxicillin, ampicillin and cloxacillin. The study was conducted using three parallel combined AOP and SBR (Fenton-SBR, photo-Fenton-SBR and UV/H<sub>2</sub>O<sub>2</sub>/TiO<sub>2</sub>-SBR) system and based on the results, the following conclusions can be drawn:
- a. Combined Fenton-SBR system
    - Hydraulic retention time (HRT) of 12 hr was found suitable for the SBR and increasing HRT to 24 and 48 hr did not significantly improve the SBR efficiency in terms of sCOD and DOC removal.
    - The best operating conditions for treatment of the antibiotic wastewater by the combined Fenton-SBR system were H<sub>2</sub>O<sub>2</sub>/COD molar ratio 2.5, H<sub>2</sub>O<sub>2</sub>/Fe<sup>2+</sup> molar ratio 150, Fenton reaction time 120 min and HRT 12 hr.
    - Under the best operating conditions, the combined Fenton-SBR system achieved an overall efficiency of 89% as sCOD removal, Final effluent sCOD was 61 mg/L, and almost complete nitrification occurred in the SBR.
  - b. Combined photo-Fenton-SBR system
    - Hydraulic retention time (HRT) of 12 hr was found suitable for the SBR and increasing HRT to 24 and 48 hr did not significantly improve the SBR efficiency in terms of sCOD and DOC removal.

- The best operating conditions for treatment of the antibiotic wastewater by the combined photo-Fenton-SBR system were  $\text{H}_2\text{O}_2/\text{COD}$  molar ratio 2.0,  $\text{H}_2\text{O}_2/\text{Fe}^{2+}$  molar ratio 150, irradiation time 90 min and HRT 12 hr.
  - Under the best operating conditions, the combined photo-Fenton-SBR system achieved an overall efficiency of 89% as sCOD removal. Final sCOD of the effluent was 66 mg/L, and complete nitrification occurred in the SBR.
- c. Combined UV/ $\text{H}_2\text{O}_2$ / $\text{TiO}_2$ -SBR system
- Increasing HRT from 24 to 48 hr significantly improved the SBR efficiency in terms of sCOD and DOC removal.
  - The best operating conditions for the treatment of antibiotic wastewater by the combined UV/ $\text{H}_2\text{O}_2$ / $\text{TiO}_2$ -SBR system were  $\text{H}_2\text{O}_2$  250 mg/L,  $\text{TiO}_2$  1000 mg/L, pH 5, irradiation time 5 hr and HRT 48 hr.
  - Under the best operating conditions, the combined UV/ $\text{H}_2\text{O}_2$ / $\text{TiO}_2$ -SBR system achieved an overall efficiency of 57% in terms of sCOD removal and final sCOD in the effluent was 236 mg/L which did not meet the discharge standard of less than 100 mg/L.
- d. SBR efficiency was found to be very sensitive to  $\text{BOD}_5/\text{COD}$  ratio below 0.40.
- e. The matrix effect was not pronounced in antibiotic degradation by Fenton and photo-Fenton processes; however, it increased the amoxicillin and cloxacillin degradation time from 20 to 30 min in UV/ $\text{H}_2\text{O}_2$ / $\text{TiO}_2$  process.
- f. The Monod kinetic model was fitted to the results of the Fenton-treated effluent biodegradation by SBR with the kinetic constants  $k_{ob}$   $0.078 \text{ hr}^{-1}$  ( $0.040 \text{ L g}^{-1} \text{ MLSS hr}^{-1}$ ),  $Y_{X/S}$  0.60) and  $K_d$   $-0.0013 \text{ hr}^{-1}$ . The values of  $k_{ob}$ ,  $Y_{X/S}$  and  $K_d$  for photo-Fenton-treated effluent were similar to those of Fenton-treated effluent.
- g. From a technical point of view, both combined Fenton-SBR system and photo-Fenton-SBR system achieved an overall efficiency of 89% as sCOD removal and the final effluent met the discharge standard.

However, the combined UV/H<sub>2</sub>O<sub>2</sub>/TiO<sub>2</sub>-SBR system is not a feasible system for treatment of antibiotic wastewater containing amoxicillin and cloxacillin.

- h. From economic point of view, combined Fenton-SBR system appeared to be more cost-effective than combined photo-Fenton-SBR system.
- 4) The fourth objective of the work was the application of artificial neural network (ANN) for modelling and simulation of advanced oxidation process in order to estimate the dynamic behaviour of the process. The ANN was applied on the Fenton process (AOP in the best combined system). Based on the results, the following conclusions can be drawn:
- a. The configuration of the backpropagation neural network giving the smallest MSE was a three-layer ANN with tangent sigmoid transfer function (tansig) at hidden layer with 14 neurons, linear transfer function (purelin) at output layer and Levenberg–Marquardt backpropagation training algorithm (LMA).
  - b. ANN predicted results are very close to the experimental results with correlation coefficient ( $R^2$ ) of 0.997 and MSE of 0.000376.
  - c. The sensitivity analysis showed that all studied variables (reaction time, H<sub>2</sub>O<sub>2</sub>/COD molar ratio, H<sub>2</sub>O<sub>2</sub>/Fe<sup>2+</sup> molar ratio, pH and COD concentration) had strong effect on COD removal. In addition, H<sub>2</sub>O<sub>2</sub>/Fe<sup>2+</sup> molar ratio was the most influential parameter with relative importance of 25.8%.
  - d. ANN results showed that neural network modelling could effectively simulate and predict the performance of the Fenton process.

## 7.2 Recommendations for Future Work

- 1) Identification of the pathway of amoxicillin, ampicillin and cloxacillin degradation by Fenton and photo-Fenton processes by analyzing the intermediates through instrumental analysis
- 2) Use of solar irradiation as a source of UV for UV based advanced oxidation processes to make the process more economical
- 3) Study the performance of other homogenous and/or heterogeneous advanced oxidation process in antibiotic degradation Such as ozonation, UV/H<sub>2</sub>O<sub>2</sub> and modified photo-Fenton (UV-Vis/H<sub>2</sub>O<sub>2</sub>/Ferrioxalate).
- 4) To study the characteristics of the iron sludge produced in Fenton and photo-Fenton processes and the potential of its recycling and reuse
- 5) Study the performance of the anaerobic SBR for treatment of AOP-treated antibiotic wastewater to make the process more economical.
- 6) Application of artificial intelligence such as Neuro-fuzzy for control of the combined AOP-SBR system.



## PUBLICATIONS AND AWARDS DERIVED FROM THIS STUDY

This study has been the basis for the following peer-reviewed journal papers, conference papers and awards.

- Peer-Reviewed Journal

1. **Emad Elmolla**, Malay Chaudhuri, Optimization of Fenton process for treatment of amoxicillin, ampicillin and cloxacillin antibiotics in aqueous solution. *Journal of Hazardous Materials*, 170 (2009), 666-672. (**Impact Factor 2.97**)
2. **Emad S. Elmolla**, Malay Chaudhuri, Degradation of the antibiotics amoxicillin, ampicillin and cloxacillin in aqueous solution by the photo-Fenton process. *Journal of Hazardous Materials* 172 (2009), 1476-1481. (**Impact Factor 2.97**)
3. **Emad Elmolla**, Malay Chaudhuri, Improvement of biodegradability of synthetic amoxicillin wastewater by photo-Fenton process. *World Applied Science Journal*, 5 (2009) 53-58.
4. **Emad S. Elmolla**, Malay Chaudhuri, Degradation of amoxicillin, ampicillin and cloxacillin antibiotics in aqueous solution by the UV/ZnO photocatalytic process. *Journal of Hazardous Materials*, 173 (2010), 445-449. (**Impact Factor 2.97**)
5. **Emad S. Elmolla**, Malay Chaudhuri, Photocatalytic degradation of amoxicillin, ampicillin and cloxacillin antibiotics in aqueous solution using using UV/TiO<sub>2</sub> and UV/H<sub>2</sub>O<sub>2</sub>/TiO<sub>2</sub> photocatalysis, *Desalination*, 252 (2010), 46-52. (**Impact Factor 1.15**)
6. **Emad S. Elmolla**, Malay Chaudhuri, Photo-Fenton treatment of antibiotic wastewater, *Nature Environment and pollution Technology*, 9 (2010) 365-370.
7. **Emad S. Elmolla**, Malay Chaudhuri, MM Eltoukhy, The use of artificial neural network (ANN) for modeling of COD removal from antibiotics aqueous solution by Fenton process. *Journal of Hazardous Materials*, 179 (2010) 127-134. (**Impact Factor 2.97**).
8. **Emad S. Elmolla**, Malay Chaudhuri, Comparison of different advanced oxidation processes for treatment of antibiotic aqueous solution. *Desalination*, 256 (2010) 43-47. (**Impact Factor 1.15**).
9. **Emad S. Elmolla**, Malay Chaudhuri, Combining Fenton process with sequencing batch reactor (SBR) for antibiotic wastewater treatment. Water research, *Communicated*
10. **Emad S. Elmolla**, Malay Chaudhuri, Combined photo-Fenton-SBR system for antibiotic wastewater treatment. *Bioresource Technology*, *Communicated*

11. **Emad S. Elmolla**, Malay Chaudhuri, Combination of TiO<sub>2</sub> photocatalysis and aerobic sequencing batch reactor for antibiotic wastewater treatment. Desalination, *Communicated*

- Conference Presentation

1. **Emad Elmolla**, Malay Chaudhuri, Antibiotics wastewater Treatment: Review. *International Seminar on Civil and Infrastructure Engineering (ISCIE08)*, 11-12 June 2008, Shah Alam, Malaysia.
2. **Emad Elmolla**, Malay Chaudhuri, Improvement of biodegradability of synthetic amoxicillin wastewater by photo-fenton process. *International Conference on Environment 2008 (ICENV 2008)*, 15-17 December, Penang, Malaysia.
3. **Emad Elmolla**, Malay Chaudhuri, Biodegradability improvement of antibiotics aqueous solution by fenton process. *National Postgraduate Conference (NPC2009)*, 25-26 March 2009, UTP, Malaysia.
4. **Emad Elmolla**, Malay Chaudhuri, Degradation of some antibiotics in aqueous solution using UV/ZnO process. *National Postgraduate Conference (NPC2009)*, 25-26 March 2009, UTP, Malaysia.
5. **Emad S. Elmolla**, Malay Chaudhuri, Photocatalytic degradation of some antibiotics in aqueous solution. *Water Malaysia Conference 2009*, 19-21 May 2009, Putra World Trade Centre, Kuala Lumpur, Malaysia.
6. **Emad S. Elmolla**, Malay Chaudhuri, Application of artificial neural network (ANN) for modelling of DOC removal from antibiotics aqueous solution by Fenton process. *Proceeding of the Fifth National Conference on Civil Engineering (AWAM'09)*, School of Civil Engineering, Universiti Sains Malaysia (2009), pp. 79-86.
7. **Emad S. Elmolla**, Malay Chaudhuri, Pretreatment of real antibiotics wastewater by Fenton process. *2<sup>nd</sup> international conference on Engineering and Technology*, 8-10 December 2009, Kuala Lumpur, Malaysia.
8. **Emad S. Elmolla**, Malay Chaudhuri, Effect of Fenton operating conditions on the performance of the combined Fenton-SBR process for antibiotic wastewater treatment. *The 1<sup>st</sup> IWA Malaysia for Young Water Professional*, 2-3 March 2010, Kuala Lumpur, Malaysia.

9. Malay Chaudhuri, **Emad S. Elmolla**, Effect of Fenton reaction time on the performance of Fenton-SBR process for antibiotic wastewater treatment. *International Conference on Sustainable Building and Infrastructure (ICSBI2010)*, 15-17 June 2010, Kuala Lumpur, Malaysia (Accepted).
10. **Emad S. Elmolla**, Malay Chaudhuri, Effect of photo-Fenton operating conditions on the performance of photo-Fenton-SBR Process for recalcitrant wastewater treatment. *International Conference on Process Engineering and Advanced Materials (ICPEAM2010)*, 15-17 June 2010, Kuala Lumpur, Malaysia (Accepted).

- Awards

1. Silver medal, Engineering Design Exhibition 22 (EDX 22) 11-12, October 2008.  
Project title: Development of a treatment method for antibiotics wastewater.
2. Silver medal, Engineering Design Exhibition 23 (EDX 23) 22-23, April 2009.  
Project title: Application of artificial neural networks (ANNs) for simulation of antibiotics degradation by Fenton process.
3. Best poster, Engineering Design Exhibition 23 (EDX 23) 22-23, April 2009.  
Project title: Application of artificial neural networks (ANNs) for simulation of antibiotics degradation by Fenton process.

## REFERENCES

- Abellán, M.N., Bayarri, B., Giménez, J., Costa, J., 2007. Photocatalytic degradation of sulfamethoxazole in aqueous suspension of TiO<sub>2</sub>. *Applied Catalysis B: Environment*, 74, 233–241.
- Aber, S., Daneshvar, N., Soroureddin, S.M., Chabok, A., Asadpour-Zeynali, K., 2007. Study of acid orange 7 removal from aqueous solutions by powdered activated carbon and modeling of experimental results by artificial neural network. *Desalination*, 211, 87–95.
- Adams, C., Wang, Y., Loftin, K., Meyer, M., 2002. Removal of antibiotics from surface and distilled water in conventional water treatment processes. *Journal of Environmental Engineering-ASCE*, 128, 253–260 .
- Addamo, M., Augugliaro, V., Paola, A.D., García-López, E., Loddo, V., Marci, G., Palmisano, L., 2005. Removal of drugs in aqueous systems by photoassisted degradation. *Journal Applied. Electrochemical*, 35, 765–774.
- Akyol, A., Yatmaz, H.C., Bayramoglu, M., 2004. Photocatalytic decolorization of remazol Red RR in aqueous ZnO suspensions. *Applied Catalyst. B: Environment*, 54, 19-24.
- Alaton, I., Dogruel, S., Baykal, E. Gerone, G., 2004. Combined chemical and biological oxidation of penicillin formulation effluent. *Journal of Environmental Management*, 73, 155–163
- Alaton, I., Gurses, F., 2004. Photo-Fenton-like and photo-Fenton-like oxidation of procaine penicillin G formulation effluent. *Journal Photochemistry and Photobiology A: Chemistry*, 165, 165–175.
- Alaton, I., Dogruel, S., 2004. Pre-treatment of penicillin formulation effluent by advanced oxidation processes. *Journal of Hazardous Materials*, 112, 105–113.
- Alaton, I., Caglayan, A.E., 2005. Ozonation of procaine penicillin G formulation effluent — Part I: process optimization and kinetics. *Chemosphere*, 59, 31–39.
- Alaton, I., Tureli, G., Olmez-Hanci, T., 2009. Treatment of azo dye production wastewaters using Photo-Fenton-like advanced oxidation processes:

- Optimization by response surface methodology. *Journal of Photochemistry and Photobiology A: Chemistry*, 202, 142-153.
- Aleboye, A., Kasiri, M.B., Olya, M.E., Aleboye, H., 2008. Prediction of azo dye decolorization by UV/H<sub>2</sub>O<sub>2</sub> using artificial neural networks. *Dyes and Pigments*, 77, 288-294.
- Al-Momani, F., Touraud, E., Degorce-Dumas, J.R., Roussy, J., Thomas, O., 2002. Biodegradability enhancement of textile dyes and textile wastewater by UV photolysis. *Journal Photochemistry and Photobiology A: Chemistry*, 153,191–197.
- Al-Momani, F., 2006. Impact of photo-oxidation technology on the aqueous solutions of nitrobenzene: Degradation efficiency and biodegradability enhancement. *Journal of Photochemistry and Photobiology A: Chemistry*, 179, 184-192.
- Anderson, P.D., D'Aco, V.J., Shanahan, P., Chapra, S.C., Buzby, M.E., Cunningham, V.L., Duplessie, B.M., Hayes, E.P., Mastrocco, F.J., Parke, N.J., Rader, J.C., Samuelian, J.H., Schwab, B.W., 2004. Screening analysis of human pharmaceutical compounds in US surface waters. *Environmental Science and Technology*, 38, 839–849.
- Andreozzi, R., Caprio, V., Insola, A., Marotta, R., 1999. Advanced oxidation processes (AOP) for water purification and recovery. *Catalyst Today*, 53, 51-59.
- Andreozzi, R., Canterino, M., Marotta, R., Paxeus, N., 2005. Antibiotic removal from wastewaters: The ozonation of amoxicillin. *Journal of Hazardous Materials*, 122, 243-250.
- APHA, 1992. Standard Methods for the Examination of Water and Wastewater, 18th ed., American Public Health Association, American Water Works Association, Water Pollution Control Federation, Washington, DC, USA.
- Artificial neural network tutorial, 2008, <http://www.learnartificialneuralnetworks.com/> access September 2009
- Ash, R.J., Mauck, B., Morgan, M., 2002. Antibiotic resistance of gram-negative bacteria in rivers, United States. *Emerging Infectious Disease*, 8, 713-716.

- Arasasinghan, R.D., Cornman, C.R., Balch, A.L., 1989. Detection of alkylperoxo and ferryl,  $(\text{FeIV}=\text{O})^{2+}$ , intermediates during the reaction of tert-butyl Hydroperoxide with iron porphyrins in toluene solution. *Journal of the American Chemical Society*, 111, 7800-7805.
- Aubrun, C., Theilliol, D., Harmand, J., Steyer, J.P., 2001. Software sensor design for COD estimation in an anaerobic fluidized bed reactor. *Water Science & Technology*, 43, 115-120.
- Bailey, J.E., Ollis, D.F., 1986, Fundamentals of Bio-chemical Engineering. McGraw-Hill, New York.
- Balcioglu, I.A., Ötöker, M., 2003. Treatment of pharmaceutical wastewater containing antibiotics by  $\text{O}_3$  and  $\text{O}_3/\text{H}_2\text{O}_2$  processes. *Chemosphere*, 50, 85–95.
- Ballesteros, M.M.M., Pérez, J.A.S., López, J.L.C., Oller, I., Rodríguez, S.M., 2009. Degradation of a four-pesticide mixture by combined photo-Fenton and biological oxidation. *Water Research*, 43, 653- 660.
- Baruch, I.S., Georgieva, P., Barrera-Cortes, J., Feyo de Azevedo, S., 2005. Adaptive recurrent neural network control of biological wastewater treatment. *International Journal of Intelligent Systems*, 20, 173-193.
- Bauer, R., Fallman, H., 1997. The photo-Fenton oxidation—a cheap and efficient wastewater treatment method. *Research on Chemical Intermediate*, 23, 341-354.
- Bautitz, I. R., Nogueira, R.F.P., 2007. Degradation of tetracycline by photo-Fenton process—Solar irradiation and matrix effects. *Journal of Photochemistry and Photobiology A: Chemistry*, 187, 33–39.
- Behnajady, M.A., Modirshahla, N., Hamzavi, R., 2006. Kinetic study on photocatalytic degradation of c.i. Acid yellow 23 by ZnO photocatalyst. *Journal of Hazardous Materials*, B133, 226–232.
- Beltran-Heredia, J., Torregrosa, j., Dominguez, R. j., Garcia, j., Treatment of black-olive wastewaters by ozonation and aerobic biologicaldegradation. *Water Research*, 34, 3515-3522.

- Benkelberg, H.J., Warneck, P., 1995. Photodecomposition of Fe(III) hydroxo- and sulfato-complexes in aqueous solution: Wavelength dependence of OH and  $\text{SO}_4^-$  quantum yields. *Journal of Physical Chemistry A*, 99, 5214-5221.
- Bertelli, M., Selli, E., 2004. Kinetic analysis on the combined use of photocatalysis,  $\text{H}_2\text{O}_2$  photolysis, and sonolysis in the degradation of methyl *tert*-butyl ether. *Applied Catalysis B: Environmental*, 52, 205-212.
- Bhatkhande, D.S., Pangarkar, V.G., Beenackers, A.A.C.M., 2002. Photocatalytic degradation for environmental applications-a review. *Journal of Chemical Technology & Biotechnology*, 77, 102-116.
- Bolton, J.R., Bircher, K.G., Tumas, W., Tolman, C.A., 1996. Figures-of-merit for the technical development and application of advanced oxidation processes. *Journal Advanced Oxidation Technology*, 1, 13-23.
- Bossmann, S.H., Oliveros, E., Göb, S., Siegwart, S., Dahlen, E.P., Payawan, L., Straub, M., Wörner, M., Braun, A.M., 1998. New evidence against hydroxyl radicals as reactive intermediates in the thermal and photochemically enhanced Fenton reactions. *The Journal of Physical Chemistry A*, 102, 5542-5550.
- Bowers, A.R., Gaddipati, P., Eckenfelder, W.W., Monsen, R.M., 1989. Treatment of toxic or refractory wastewaters with hydrogen peroxide. *Water Science and Technology*, 21, 477-486.
- Calza, P., Medana, C., Pazzi, M., Baiocchi, C., Pelizzetti, E., 2004. Photocatalytic Transformations of Sulphonamides on Titanium Dioxide. *Applied Catalysis B: Environmental*, 53, 63-69.
- Calza, P., Pelizzetti, E., Minero, C., 2005. The fate of organic nitrogen in photocatalysis: an overview, *Journal of Applied Electrochemistry*, 35, 665-673.
- Calza, P., Sakkas, V.A., Villioti, A., Massolino, C., Boti, V., Pelizzetti, E., Albanis T., 2008. Multivariate experimental design for the photocatalytic degradation of imipramine: Determination of the reaction pathway and identification of intermediate products, *Applied Catalysis B: Environmental*, 84, 379-388.

- Cañizares, P., Paz, R., Sáez, C., Rodrigo M.A., 2009. Costs of the electrochemical oxidation of wastewaters: A comparison with ozonation and Fenton oxidation processes, *Journal of Environmental Management*, 90, 410-420.
- Carballa, M., Omil, F., Lema, J.M., Liompart, M., Garcia-Jares, C., Rodriguez, I., Gomez, M., Ternes, T., 2004. Behavior of pharmaceuticals, cosmetics and hormones in a sewage treatment plant. *Water Research*, 38, 2918-2926.
- Cardona, S.P.P., 2001. Coupling of photocatalytic and biological processes as a contribution to the detoxification of water: catalytic and technological aspects. PhD thesis, Thesis No. 2470, *Institute of Environmental Engineering, Department of Rural Engineering*, EPFL, Lausanne, Switzerland.
- Casero, I., Sicilia, D., Rubio, S., Perez-Bendito, D., 1997. Chemical degradation of aromatic amines by Fenton's reagent. *Water Research*, 31, 1985-1995.
- Chacon, J. M., Leal, M.T., Sanchez, M., Bandala, E.R., 2006. Solar photocatalytic degradation of azo-dyes by photo-Fenton process. *Dyes and Pigments*, 69, 144-150.
- Chatzitakis, A., Berberidou, C., Paspalsis, I., Kyriakou, G., Sklaviadis, T., Poullos, I., 2008. Photocatalytic degradation and drug activity reduction of chloramphenicol. *Water Research*, 42, 386-394.
- Chemie, V.F., 2005. New methods for determination of  $\beta$ -lactam antibiotics by means of diffuse reflectance spectroscopy using polyurethane foam as sorbent. PhD thesis, Duisburg University, Germany.
- Chen, R., Pignatello, J., 1997. Role of quinone intermediates as electron shuttles in Fenton and photoassisted Fenton oxidations of aromatic compounds. *Environmental Science & Technology*, 31, 2399-2406.
- Chen, Z., McHale, J.M., 2009. Antimicrobial glaze and porcelain enamel via double layer glaze with high zinc content, *US Patent*, US 2009/0117173A1.
- Chiron, S., Fernández-Alba, A., Rodríguez, A., García-Calvo, E., 2000. Pesticide chemical oxidation: State of the art. *Water Research*, 34, 366-377.



- Chu, W., Choy, W.K., So, T.Y., 2007. The effect of solution pH and peroxide in the TiO<sub>2</sub>-induced photocatalysis of chlorinated aniline. *Journal of Hazardous Materials*, 141, 86-91.
- Cokgor, E.U., Alaton, I.A., Karahan, O., Dogruel, S., Orhon, D., 2004. Biological treatability of raw and ozonated penicillin formulation effluent. *Journal of Hazardous Materials*, 116, 159–166.
- Cote, M., Grandjean, B.P.A., Lessard, P., Thibault, J., 1995. Dynamic modeling of activated sludge process: improving prediction using neural networks. *Water Research*, 29, 995-1004.
- Curcó, D., Malato, S., Blanco, J., Giménez, J., Marco, P., 1996. Photocatalytic degradation of phenol: comparison between pilot-plant scale and laboratory results. *Solar Energy*, 56, 387–400.
- Curcó, D., Giménez, J., Addardak, A., Cervera-March, S., Esplugas, S., 2002. Effects of radiation absorption and catalyst concentration on the photocatalytic degradation of pollutants. *Catalysis Today*, 76, 177-188.
- Daneshvar, N., Salari, D., Khataee, A. R., 2004. Photocatalytic degradation of azo dye Acid Red 14 in water on ZnO as an alternative catalyst TiO<sub>2</sub>. *Journal of Photochemistry and Photobiology A: Chemistry*, 162, 317–322.
- Daneshvar, N., Khataee, A.R., Djafarzadeh, N., 2006. The use of artificial neural networks (ANN) for modeling of decolorization of textile dye solution containing C.I. Basic Yellow 28 by electrocoagulation process. *Journal of Hazardous Materials*, B137, 1788-1795.
- Danion, A., Disdier, J., Guillard, C., Païssé, O., Jaffrezic-Renault, N., 2006. Photocatalytic degradation of imidazolinone fungicide in TiO<sub>2</sub>-coated optical fiber reactor. *Applied Catalysis B: Environmental*, 62, 274-281.
- Daosud, W., Thitiyasook, P., Arpornwichanop, A., Kittisupakorn, P., Hussain, M., 2005. Neural network inverse model-based controller for the control of a steel pickling process. *Computers and Chemical Engineering*, 29, 2110–2119.
- Deshpande, A. D., Baheti, K. G., Chatterjee, C. N. R., 2004. Degradation of  $\beta$ -lactam antibiotics. *Current Science*, 87, 1684-1695.

- Dillert, R., Bahnemann, D., Hidaka, H., 2007. Light-induced degradation of perfluorocarboxylic acids in the presence of titanium dioxide. *Chemosphere*, 67, 785-792.
- Dinga, H, Suna, H., Shan, Y., 2005. Preparation and characterization of mesoporous SBA-15 supported dye-sensitized TiO<sub>2</sub> photocatalyst. *Journal of Photochemistry and Photobiology A: Chemistry*, 169, 101-107.
- Durán, A., Monteagudo, J.M., Mohedano, M., 2006. Neural networks simulation of photo-Fenton degradation of Reactive Blue 4. *Applied Catalysis B: Environmental*, 65,127–134.
- Edgerton, B.D., McNevin, D., Wong, C.H., Menoud, P., Barford, J.P., Mitchell, C.A., 2000. Strategies for dealing with piggery effluent in Australia: the sequencing batch reactor as a solution. *Water Science and Technology*, 41, 123–126.
- Essam, T., Amin, M.A., El Tayeb, O., Mattiasson, B., Guieysse, B., 2007. Sequential photochemical–biological degradation of chlorophenols. *Chemosphere*, 66, 2201-2209.
- Estrada, L.A.P., Maldonado, M.I., Gernjak, W., Aguera, A., Fernandez-Alba, A.R., Ballesteros, M.M., Malato, S., 2005. Decomposition of diclofenac by solar driven photocatalysis at pilot scale. *Catalysis Today*, 101. 219-226.
- Evgenidou, E., Fytianos, K., Poullos, I., 2005. Semiconductor-sensitized photodegradation of dichlorvos in water using TiO<sub>2</sub> and ZnO as catalysts. *Applied Catalysis B: Environmental*, 59, 81.
- Faisal, M., Abu Tariq, M., Muneer, M., 2007. Photocatalysed degradation of two selected dyes in UV-irradiated aqueous suspensions of Titania. *Dyes Pigments*, 72, 233-239.
- Farré, M.J., Doménech, X., Peral, J., 2007. Combined photo-Fenton and biological treatment for Diuron and Linuron removal from water containing humic acid. *Journal of Hazardous Materials*, 147, 167–174.

- Feitz, A.J., Waite, T.D., Jones G.J., Boyden, B.H., Orr, P.T., 1999. Photocatalytic degradation of the blue green algal toxin microcystin-LR in a natural organic-aqueous matrix. *Environmental Science & Technology*, 33, 243–249.
- Fenton, H.J.H., 1894. Oxidation of tartaric acid in the presence of iron. *Journal of the Chemical Society*, 65, 899-910.
- Fu, X., Clark, L.A., Zeltner, W.A., Anderson, M.A., 1996. Effects of reaction temperature and water vapor content on the heterogeneous photocatalytic oxidation of ethylene. *Journal of Photochemistry and Photobiology A: Chemistry*, 97, 181-186.
- Galindo, C., Jacques, P., Kalt, A., 2000. Photodegradation of the aminoazobenzene acid orange 52 by three advanced oxidation process: UV/H<sub>2</sub>O<sub>2</sub>, UV/TiO<sub>2</sub> and VIS/TiO<sub>2</sub>, comparative mechanistic and kinetics investigations. *Journal of Photochemistry and Photobiology A: Chemistry*, 130, 35-47.
- Gallert, C., Fund, K., Winter, J., 2005. Antibiotic resistance of bacteria in raw and biologically treated sewage and in groundwater below leaking sewers. *Applied Microbiology and Biotechnology*, 69, 106-112.
- Gao, Y., Liu, H., 2005. Preparation and catalytic property study of a novel kind of suspended photocatalyst of TiO<sub>2</sub>-activated carbon immobilized on silicone rubber film. *Materials Chemistry and Physics*, 92, 604-608.
- García-Montaño, J., Pèrez-Estrada, L., Oller, I., Maldonado, M. I., Torrades, F., Peral, J., 2008. Pilot plant scale reactive dyes degradation by solar photo-Fenton and biological processes. *Journal of Photochemistry and Photobiology A: Chemistry*, 195, 205–214
- García-Montaño, J., Torrades, F., García-Hortal, J.A., Doménech, X., Peral, J., 2006a. Combining photo-Fenton process with aerobic sequencing batch reactor for commercial hetero-bireactive dye removal. *Applied Catalysis B: Environmental*, 67, 86–92.
- García-Montaño, J., Torrades, F., García-Hortal, J.A., Doménech, X., Peral, J., 2006b. Degradation of Procion Red H-E7B reactive dye by coupling a photo-

- Fenton system with a sequencing batch reactor. *Journal of Hazardous Materials*, 134, 120–129.
- Garson, GD, 1991. Interpreting neural-network connection weights. *AI Expert*, 6, 47-51.
- Giménez, J., Curcó, D., Marco, P., 1997. Reactor modelling in the photocatalytic oxidation of wastewater. *Water Science and Technology*, 35, 207–213.
- Giménez, J., Curcó, D., Queral, MA., 1999. Photocatalytic treatment of phenol and 2,4-dichlorophenol in a solar plant in the way to scaling-up. *Catalysis Today*, 54, 229-43.
- Giroto, J.A., Guardani, R., Teixeira, A.C.S.C., Nascimento, C.A.O., 2006. Study on the photo-Fenton degradation of polyvinyl alcohol in aqueous solution. *Chemical Engineering and Processing*, 45, 523–532.
- Glaze, W.H., Kang, J.W., Chapin, D.H., 1987. The chemistry of water treatment processes involving ozone, hydrogen peroxide and ultraviolet radiation. *Ozone: Science & Engineering*, 9, 335-352.
- Gontarski, C.A., Rodrigues, P.R., Mori, M., Prenem, L.F., 2000. Simulation of an industrial wastewater treatment plant using artificial neural networks. *Computers and Chemical Engineering*, 24, 1719-1723.
- González, O., Esplugas, M., Sans, C., Esplugas, S., 2007. Sulfamethoxazole abatement by photo-Fenton Toxicity, inhibition and biodegradability assessment of intermediates. *Journal of Hazardous Materials*, 146, 459–464.
- González, O., Esplugas, M., Sans, C., Torres, A., Esplugas, S., 2009. Performance of a sequencing batch biofilm reactor for the treatment of pre-oxidation sulfamethoxazole solutions. *Water Research*, 43, 2149-2158.
- Guillard, C., Disdier, J., Herrmann, J.M., Lehaut, C., Chopin, T., Malato, S., Blanco, J., 1999. Comparison of various titania samples of industrial origin in the solar photocatalytic detoxification of water containing 4-chlorophenol. *Catalysis Today*, 54, 217-228.

- Guimarães, O.L.C., Chagas, M.H.D.R., Filho, D.N.V., Siqueira, A.F., Filho, H.J. I., Aquino, H.O.Q.D., Silva, M.B., 2008a. Discoloration process modeling by neural network. *Chemical Engineering Journal*, 140, 71–76.
- Guimarães, O.L.C., Filho, M.H.d.R., Siqueira, A.F., Filho, H.J. I., Silva, M. B., 2008b. Optimization of the AZO dyes decoloration process through neural networks: Determination of the H<sub>2</sub>O<sub>2</sub> addition critical point. *Chemical Engineering Journal*, 141, 35–41
- Haber, F., Weiss, J., 1934. The catalytic decomposition of hydrogen peroxide by iron salts. *Proceedings of the Royal Society of London. Series A, Mathematical and Physical Sciences*, 147, 332-351.
- Hach, 2002. Water analysis handbook. 4th ed. *Hach Company*, Loveland Colorado.
- Hack, M., Kohne, M., 1996. Estimation of wastewater process parameters using neural networks. *Water Science & Technology*, 33, 101-115.
- Halling-Sørensen, B., Nielsen, S.N., Lanzky, P.F., Ingerslev, F., Lützhøft, H.C.H., Jørgensen, S.E., 1998. Occurrence, fate and effects of pharmaceutical substances in the environment—A review. *Chemosphere*, 36, 357–394.
- Haque, M.M., Muneer, M., 2003. Heterogeneous photocatalysed degradation of a herbicide derivative, isoproturon in aqueous suspension of titanium dioxide. *Journal of Environmental Management*, 69, 169-176.
- Heberer, T., 2002. Occurrence, fate, and removal of pharmaceutical residues in the aquatic environment: A Review of Recent Research Data. *Toxicology Letters*, 131, 5-17.
- Herrmann, J.M., Guillard, C., Pichat, P., 1993. Heterogeneous photocatalysis: an emerging technology for water treatment. *Catalysis Today*, 17, 7-20.
- Hideyuki, K., Satoshi, K., Tohru, S., Kiyohisa, O. and Yoshihiro, Y., 2005. Photo-Fenton degradation of alachlor in the presence of citrate solution. *Journal of Photochemistry and Photobiology A: Chemistry*, 180, 38–45.
- Hirsch, R., Ternes, T., Haberer, K., Kratz, K.L., 1999. Occurrence of antibiotics in the aquatic environment. *The Science of the Total Environment*, 225, 109-118.

- Hoffmann, M.R., Martin, S.T., Choi, W.Y., Bahnemann, D.W., 1995. Environmental applications of semiconductor photocatalysis. *Chemical Reviews*, 95, 69–96.
- Hong, S.H., Lee, M.W., Lee, D.S., Park, J.M., 2007. Monitoring of sequencing batch reactor for nitrogen and phosphorus removal using neural networks. *Biochemical Engineering Journal*, 35, 365-370.
- Holubar, P., Zani, L., Hager, M., Froschl, W., Radak, Z., Braun, R., 2002. Advanced controlling of anaerobic digestion by means of hierarchical neural networks. *Water Resaerch*, 36, 2582-2588.
- Hou, J.P., Poole, J.W., 1971. Beta-lactam antibiotics, their physicochemical properties and biological activity in relation to structure. *Journal of Pharmaceutical Sciences*, 60, 503-509.
- <http://www.eguide.com.my/MY/SEARCH/Pharmaceutical+Companies/3?>
- Huber, W.G., 1971. Antibacterial drugs as environmental contaminants. *Advances in Environmental Science and Technology*, 2, 289-320.
- Huston, P.L., Pignatello, J., 1999. Degradation of selected pesticide active ingredients and commercial formulations in water by the photo-assisted Fenton reaction. *Water Research*, 33, 1238-1246.
- Ikehata, K., Naghashkar, N.J., El-Din M. G., 2006. Degradation of Aqueous Pharmaceuticals by Ozonation and Advanced Oxidation Processes: A Review. *Ozone: Science & Engineering*, 28, 353- 414.
- Jones, O.A.H., Voulvoulis, N., Lester, J.N., 2005. Human Pharmaceuticals in Wastewater Treatment Processes. *Critical Reviews in Environmental Science and Technology*, 35, 401–427.
- Jones D.E., 2006. Pharmaceutical Waste Analysis, *Quality Environmental Solutions, Inc.* February, 1-4
- Joseph, J.M., Destailats, H., Hung, H.M., Hoffmann, M.R., 2000. The sonochemical degradation of azobenzene and related azo dyes: rate enhancements via Fenton's reactions. *Journal of Physical Chemistry A*, 104, 301–307.

- Kabra, K., Chaudhary, R., Sawhney, R.L., 2004. Treatment of hazardous organic and inorganic compounds through aqueous- phase photocatalysis: a review. *Industrial & Engineering Chemistry Research*, 43, 7683–7696.
- Kanay, H., 1983. Drug-resistance and distribution of conjugative R-plasmids in *E. coli* strains isolated from healthy adult animals and humans. *Japanese Journal of Veterinary Science*, 45, 171-178.
- Kaneco, S., Rahman, M.A., Suzuki, T., Katsumata, H., Ohta, K., 2004. Optimization of solar photocatalytic degradation conditions of bisphenol A in water using titanium dioxide. *Journal of Photochemistry and Photobiology A: Chemistry*, 163, 419-424.
- Kansal, S.K., Singh, M., Sud, D., 2007. Studies on photodegradation of two commercial dyes in aqueous phase using different photocatalysts. *Journal of Hazardous Materials*, 141, 581-590.
- Kansal, S. K., Singh, M., Sud, D., 2008. Studies on TiO<sub>2</sub>/ZnO photocatalysed degradation of lignin. *Journal of Hazardous Materials*, 153, 412-417.
- Katzung, B.G., 2004. Basic and clinical pharmacology, Lange Medical Books, *McGraw-Hill*, 9th edition, New York.
- Kavitha, V., Palanivelu, K., 2005a. Destruction of cresols by Fenton oxidation process. *Water Research*, 39, 3062–3072.
- Kavitha, V., Palanivelu, K., 2005b. Degradation of nitrophenols by Fenton and photo-Fenton processes. *Journal of Photochemistry and Photobiology A: Chemistry*, 170, 83-95.
- Kiwi, J., Pulgarin, C., Peringer, P., 1994. Effect on Fenton and photo-Fenton reactions on the degradation and biodegradability of 2 and 4-nitrophenols in water treatment. *Applied Catalysis B: Environmental*, 3, 335-350.
- Kolpin, D.W., Furlong, E.T., Meyer, M.T., Thurman, E.M., Zaugg, S.D., Barber, L.B., Buxton, H.T., 2002. Pharmaceuticals, hormones, and other organic wastewater contaminants in US streams, 1999–2000: a national reconnaissance. *Environmental Science and Technology*. 36, 1202–1211.

- Konstantinou, I.K., Albanis, T.A., 2004. TiO<sub>2</sub>-assisted photocatalytic degradation of azo dyes in aqueous solution: kinetic and mechanistic investigations: a review. *Applied Catalysis B: Environmental*, 49, 1–14.
- Kositzki, M., Antoniadis, A., Poullos, I., Kiridis, I., Malato, S., 2004. Solar photocatalytic treatment of simulated dyestuff effluents. *Solar Energy*, 77, 591-600.
- Krutzler, T., Fallmann, H., Bauer, R., Malato, S., Blanco, J., 1999. Applicability of the photo-Fenton method for treating water containing pesticides. *Catalysis Today*, 54. 309-319.
- Kwon, B.G., Lee, D.S., Kang, N., Yoon, J., 1999. Characteristics of p-chlorophenol oxidation by Fenton's reagent. *Water Research*, 33, 2110–2118.
- Lapertot, M., Ebrahimi, S., Dazio, S., Rubinelli, A., Pulgarin, C., 2007. Photo-Fenton and biological integrated process for degradation of a mixture of pesticides. *Journal of Photochemistry and Photobiology A: Chemistry*, 186, 34–40.
- Larsen, T.A., Lienert, J., Joss, A., Siegrist, H., 2004. How to avoid pharmaceuticals in the aquatic environment. *Journal of Biotechnology*, 113, 295–304.
- Larsson, D.G. J., Fick J., 2009. Transparency throughout the production chain—a way to reduce pollution from the manufacturing of pharmaceuticals. *Regulatory Toxicology and Pharmacology* 53, 161–163.
- Larsson, D.G.J., De Pedro, C., Paxéus, N., 2007. Effluent from drug manufactures contains extremely high levels of pharmaceuticals. *Journal of Hazardous Materials*. 148, 751–755.
- Lewis, R. 1995. The Rise of Antibiotic-Resistant Infections. *FDA Consumer Magazine*, 29 September.
- Lin, S.H., Jiang, C.D., 2003. Fenton oxidation and sequencing batch reactor (SBR) treatments of high strength semiconductor wastewater. *Desalination*, 154, 107–116.
- Liou, M.J., Lu, M.C., Chen, J.N., 2003. Oxidation of explosives by Fenton and photo-Fenton processes. *Water Research*, 37, 3172-3179.



- Low, G.K.C., McEvoy, S.R., Matthews, R.W., 1991. Formation of nitrate and ammonium ions in titanium dioxide mediated photocatalytic degradation of organic compounds containing nitrogen atoms. *Environmental Science Technology*, 25, 460-467.
- Luccarini, L., Porr, E., Spagni, A., Ratini, P., Grilli, S., Longhi, S., Bortone, G. 2002. Soft sensors for control of nitrogen and phosphorus removal from wastewaters by neural networks. *Water Science & Technology*, 45, 101-107.
- Machón, I., López, H., Rodríguez-Iglesias, J., Marañón, E., Vázquez I., 2007. Simulation of a coke wastewater nitrification process using a feed-forward neuronal net. *Environmental Modelling and Software*, 22, 1382-1387.
- Maier, H.R., Dandy, G.C., 1998. Understanding the behavior and optimizing the performance of back-propagation neural networks: an empirical study. *Environmental Modelling and Software*, 13, 179-191.
- Maira, A.J., Yeung, K.L., Soria, J., Coronado, Belver, J.M.C., Lee, C.Y., Augugliaro, V., 2001. Gas-phase photo-oxidation of toluene using nanometer-size TiO<sub>2</sub> catalysts. *Applied Catalysis B: Environmental*, 29, 327.
- Malato, S., Blanco, J., Maldonado, M., Fernandez-Ibanez, P., Campos, A., 2000. Optimising solar photocatalytic mineralisation of pesticides to the recycling of pesticide containers. *Applied Catalysis B: Environmental*, 28, 163-174.
- Malato, S., Blanco, J., Vidal, A., Alarcón, D., Maldonado, M.I., Cáceres, J., Gernjak, W., 2003. Applied studies in solar photocatalytic detoxification: an overview. *Solar Energy*, 75, 329-336.
- Malaysian Environmental Quality (Sewage and Industrial Effluents) Regulations, 1979.
- Marco, A., Esplugas, S., Saum, G., 1997. How and why to combine chemical and biological processes for wastewater treatment. *Water Science & Technology*, 35, 321-327.
- Mariana, N., Yedilera, A., Siminiceanub I., Kettrupa, A., 2003. Oxidation of commercial reactive azo dye aqueous solutions by the photo-Fenton and

- Fenton-like processes. *Journal of Photochemistry and Photobiology A: Chemistry*, 161, 87-83.
- Martín, M.M.B., Pèrez, J.A. S., Fernández, F.G. A., Sánchez, J.L.G., López, J.L.C., Rodríguez, S.M., A., 2008. Kinetics study on the biodegradation of synthetic wastewater simulating effluent from an advanced oxidation process using *Pseudomonas putida* CECT 324. *Journal of Hazardous Materials*, 151, 780–788.
- Martín, M.M.B., Pèrez, J.A.S., López, J.L.C., Oller, I., Rodríguez, S.M., 2009. Degradation of a four-pesticide mixture by combined photo-Fenton and biological oxidation. *Water Research*, 43, 653- 660.
- Martinez, N.S.S., Fernández, J.F., Segura, X.F., Ferrer, A.S., 2003. Pre-oxidation of an extremely polluted industrial wastewater by the Fenton's reagent. *Journal of Hazardous Materials*, B101, 315–322.
- Metcalf & Eddy, Inc., 2003. Wastewater engineering: treatment and reuse, Fourth Edition, McGraw-Hill, Inc., New York, NY.
- Miao, X.S., Koenig, B.G., Metcalfe, C.D., 2002. Analysis of acidic drugs in the effluents of sewage treatment plants using liquid chromatography-electrospray ionization tandem mass spectrometry. *Journal of Chromatography A*, 952, 139–147.
- Mills, A., Le Hunte, S., 1997. An overview of semiconductor photocatalysis. *Journal of Photochemistry and Photobiology A: Chemistry*, 108, 1–35.
- Monod, J., 1949. The growth of bacterial cultures. *Annual Review of Microbiology*, 3, 371-376.
- Moral, H., Aksoy, A., Gokcay, C.F., 2008. Modeling of the activated sludge process by using artificial neural networks with automated architecture screening. *Computers and Chemical Engineering*, 32, 2471-2478.
- Morese, A.N., 2003. Fate and effect of amoxicillin in space and terrestrial water reclamation systems. Ph D thesis, Texas Tech University.

- Mrowetz, M., Pirola, C., Selli E., 2003. Degradation of organic water pollutants through sonophotocatalysis in the presence of TiO<sub>2</sub>. *Ultrasonics Sonochemistry*, 10, 247-254.
- Muradov, N.Z., T-Raissi, a., Muzzey, D., Painter, C.R., Kemme, M.R., 1996. Selective photocatalytic destruction of airborne VOCs. *Solar Energy*, 56, 445-453
- Nesheiwat, F.K., Swanson, A.G., 2000. Clean contaminated sites using Fenton's reagent. *Chemical Engineering Progress*, 96, 61-66.
- Nikolaou, A., Meric, S., Fatta, D., 2007. Occurrence patterns of pharmaceuticals in water and wastewater environments. *Analytical and Bioanalytical Chemistry*, 387,1225–1234.
- Nogueira, R.F.P., Trovo, A.G., Mode, P.F., 2002. Solar photodegradation of dichloromethic acid and 2,4-dichlorophenol using an enhanced photo-Fenton process. *Chemosphere*. 48, 385-391.
- Nogueira, R.F.P., Silva, M.R.A., Trovó, A.G., 2005. Influence of the iron source on the solar photo-Fenton degradation of different classes of organic compounds. *Solar Energy*, 79, 384-392
- Oguz, E., Tortum, A., Keskinler, B., 2008. Determination of the apparent rate constants of the degradation of humic substances by ozonation and modeling of the removal of humic substances from the aqueous solutions with neural network. *Journal of Hazardous Materials*, 157, 455–463.
- Oliveros, E., Legrini, O., Hohl, M., Mueller, T., Braun, A.M., 1997. Large scale development of a light-enhanced Fenton reaction by optimal experimental design. *Water Science and Technology*, 35, 223-230.
- Oller, I., Malato, S., Sánchez-Pérez, J.A., Maldonado, M.I., Gassó, R. 2007. Detoxification of wastewater containing five common pesticides by solar AOPs–biological coupled system. *Catalysis Today*, 129, 69–78.
- Orhon, D., Cimsit, Y., Tunay, O., 1986. Substrate removal mechanisms for sequencing batch reactors. *Water Science and Technology*, 18, 21-33.

- Pai, T.Y., Tsai, Y.P., Lo, H.M., Tsai, C.H., Lin, C.Y., 2007. Grey and neural network prediction of suspended solids and chemical oxygen demand in hospital wastewater treatment plant effluent. *Computers & Chemical Engineering*, 31, 1272-1281.
- Paola, A.D., Addamo, M., Augugliaro, V., Garcia-López, E., Loddo, V., Marci, G., Palmisano, L., 2004. Photolytic and TiO<sub>2</sub>-assisted photodegradation of aqueous solutions of tetracycline. *Fresenius Environmental Bulletin*, 13, 1275–1280.
- Paola, A.D., Addamo M., Augugliaro V., Garcia-López E., Loddo V., Marci G., Palmisano, L., 2006. Photodegradation of lincomycin in aqueous solution. *International Journal of Photoenergy*, Article ID 47418, 1–6.
- Pareek, V.K., Brungs, M.P., Adesina, A.A., Sharma, R., 2002. Artificial neural network modeling of a multiphase photodegradation system. *Journal of Photochemistry and Photobiology A: Chemistry*, 149, 139-146.
- Pelizzetti, E., Minero, C., 1993. Mechanism of the photooxidative degradation of organic pollutants over TiO<sub>2</sub> particles. *Electrochimica Acta*, 38, 47-54.
- Pelizzetti, E., 1995. Concluding remarks on heterogeneous solar photocatalysis. *Solar energy materials and solar cells*, 38, 453-457.
- Pera-Titus, M., Garcia-Molina, V., Banos, M.A., Giménez, J., Esplugas, S., 2004. Degradation of Chlorophenols by means of advanced oxidation processes: a general review. *Applied Catalysis B: Environmental*, 47, 219–256.
- Pignatello, J., 1992. Dark and photoassisted Fe<sup>3+</sup>-catalyzed degradation of chlorophenoxy herbicides by hydrogen peroxide. *Environmental Science and Technology*, 26, 944-951.
- Pignatello, J., Oliveros, E., MacKay, A., 2006. Advanced oxidation processes for organic contaminant destruction based on the Fenton reaction and related chemistry, *Critical Reviews in Environmental Science and Technology*, 36, 1-84.

- Pillai, S.D., Widmer, K.W., Maciorowski, K.G., Ricke, S.C., 1997. Antibiotic resistance profiles of *Escherichia coli* isolated from rural and urban environment. *Journal of Environmental Science and Health*, 32, 1665-1675.
- Poulios, I., Micropoulou, E., Panou, R., Kostopoulou, E., 2003. Photooxidation of eosin Y in the presence of semiconducting oxides. *Applied Catalysis B: Environmental*, 41, 345-355.
- Prakash, S.N., Manikandan, A., Govindarajan, L., Vijayagopal, V., 2008. Prediction of biosorption efficiency for the removal of copper (II) using artificial neural networks. *Journal of Hazardous Materials*, 152, 1268–1275.
- Pulgarin, C., Invernizzi, M., Parra, S., Sarria, V., Polania, R., Peringer, P., 1999. Strategy for the coupling of photochemical and biological flow reactors useful in mineralization of biorecalcitrant industrial pollutants. *Catalysis Today*, 54, 341-352.
- Qamar, M., Saquib, M., Muneer, M., 2004. Semiconductor-mediated photocatalytic degradation of anazo dye, chrysoidine Y in aqueous suspensions. *Desalination*, 171, 185-193.
- Qamar, M., Muneer, M., Bahnemann, D., 2006. Heterogeneous photocatalysed degradation of two selected pesticide derivatives, triclopyr and daminozid in aqueous suspensions of titanium dioxide. *Journal of Environmental Management*, 80, 99-106.
- Rabiet, M., Togola, A., Brissaud, F., Seidel, J.L., Budzinski, H., Elbaz-Poulichet, F., 2006. Consequences of treated water recycling as regards pharmaceuticals and drugs in surface and ground waters of a medium-sized Mediterranean catchment. *Environmental Science and Technology*, 40, 5282–5288.
- Raj, D.S.S., Anjaneyulu, Y., 2005. Evaluation of biokinetic parameters for pharmaceutical wastewaters using aerobic oxidation integrated with chemical treatment. *Process Biochemistry*, 40, 165–175.
- Ramalho, R.S., 1983. Introduction to Wastewater Treatment Processes. Academic Press, London.

- Ranalli, G., Belli, C., Lustrato, G., Pizzella, L., Liberatore, L., Bressan, M., 2008. Effects of combined chemical and biological treatments on the degradability of vulcanization accelerators. *Water, Air, and Soil Pollution*, 192, 199–209.
- Rao, A.N., Sivasankar, B., Sadasivam, V., 2009. Kinetic study on the photocatalytic degradation of salicylic acid using ZnO catalyst. *Journal of Hazardous Materials*, 166, 1357-1361.
- Ren, N., Chen, Z., Wang, X., Hu, D., Wang, A., 2005. Optimized operational parameters of a pilot scale membrane bioreactor for high-strength organic wastewater treatment. *International Biodeterioration & Biodegradation*, 56, 216-223.
- Rodríguez, M., Tmokhin, V., Michl, F., Contretas, S., Gimenez, J., Esplugas, S., 2002. The influence of different irradiation sources on the treatment of nitrobenzene. *Catalysis Today*, 76, 291-300.
- Rodríguez, M., Malatod, S., Pulgarinc, C., Contrerasb, S., Curcób, D., Giménezb J., Esplugas, S., 2005. Optimizing the solar photo-Fenton process in the treatment of contaminated water. Determination of intrinsic kinetic constants for scale-up. *Solar Energy*, 79, 360-368
- Sadik, W.A., Nashed, A.W., El-Demerdash, A.M., 2007. Photodecolourization of ponceau 4R by heterogeneous photocatalysis. *Journal of Photochemistry and Photobiology A: Chemistry*, 189, 135–140.
- Safarzadeh-Amiri, A., Bolton, J.R., Cater, S.R., 1996. The use of iron in advanced oxidation processes. *Journal of Advanced Oxidation Technologies*, 1, 18-26.
- Salari, D., Daneshvar, N., Aghazadeh, F., Khataee, A.R., 2005. Application of artificial neural networks for modeling of the treatment of wastewater contaminated with methyl tert-butyl ether (MTBE) by UV/H<sub>2</sub>O<sub>2</sub> process. *Journal of Hazardous Materials*, B125, 205–210.
- San, N., Kilic, M., Tuiebakhova, Z., Cinar, Z., 2007. Enhancement and modeling of the photocatalytic degradation of benzoic acid. *Journal of Advanced Oxidation Technologies*, 10, 43–50.

- Sakthivel, S., Neppolian, B., Shankar, M.V., Arabindoo, B., Palanichamy, M., Murugesan, V., 2003. Solar photocatalytic degradation of azo dye: comparison of photocatalytic efficiency of ZnO and TiO<sub>2</sub>. *Solar energy materials and solar cells*, 77, 65–82.
- Sarria, V., Parra, S., Adler, N., Péringier, P., Benítez, N., Pulgarín, C., 2002. Recent developments in the coupling of photoassisted and aerobic biological processes for the treatment of biorecalcitrant compounds. *Catalysis Today*, 76, 301-315.
- Sarria, V., Kenfack, S., Guillod, O., Pulgarin, C., 2003. An innovative coupled solar-biological system at field pilot scale for the treatment of biorecalcitrant pollutants. *Journal of Photochemistry and Photobiology A: Chemistry*, 159, 89–99.
- Scott, J.P., Oills, O.F., 1995. Integration of chemical and biological oxidation processes for water treatment: review and recommendations. *Environmental Progress*, 14, 88-103.
- Selvam, K., Muruganandham, M., Swaminathan, M., 2005. Enhanced heterogeneous ferrioxalate photo-fenton degradation of reactive orange 4 by solar light. *Solar Energy Materials and Solar Cells*, 89, 61-74.
- Shuler, M.L, Kargi, F., 2002. Bioprocess Engineering: Basic concept. *Prentice Hall*
- Sinha, S., Bose, P., Jawed, M., John, S., Tare, V., 2002. Application of neural network for simulation of upflow anaerobic sludge blanket (UASB) reactor performance. *Biotechnology and bioengineering*, 77, 806-814.
- Sioi, M., Bolosis, A., Kostopoulou, E., Poullos, I., 2006. Photocatalytic treatment of colored wastewater from medical laboratories: photocatalytic oxidation of hematoxylin. *Journal of Photochemistry and Photobiology A: Chemistry*, 184, 18–25.
- Sirtori, C., Zapata, A., Oller, I., Gernjak, W., Agüera, A., Malato, S., 2009. Decontamination industrial pharmaceutical wastewater by combining solar photo-Fenton and biological treatment. *Water Research*, 43, 661-668.

- Slokar, Y.M., Zupan, J., Marechal, A.M.L., 1999. The use of artificial neural network (ANN) for modeling of the H<sub>2</sub>O<sub>2</sub>/UV decoloration process: part I. *Dyes and Pigments*, 42, 123-135
- So, C.M., Cheng, M.Y., Yu, J.C., Wong, P.K., 2002. Degradation of azo dye Procion Red MX-5B by photocatalytic oxidation. *Chemosphere*, 46, 905–912.
- Solozhenko, E.G., Soboleva, N.M., Goncharuk, V.V., 1995. Decolourization of Azo dye solutions by Fenton's oxidation. *Water Research*, 29, 2206-2210.
- Soulet, B., Tauxe, A., Tarradellas, J., 2002. Analysis of acidic drugs in swiss wastewaters. *International Journal of Environmental Analytical Chemistry*, 82, 659–667.
- Stackelberg, P.E., Furlong, E.T., Meyer, M.T., Zaugg, S.D., Henderson, A.K., Reissman, D.B., 2004. Persistence of pharmaceutical compounds and other organic wastewater contaminants in a conventional drinking-water treatment plant. *Science of the Total Environment*, 329, 99–113.
- Stephenson, R.L., Blackburn, J.B., 1998. Biological treatment processes. In: Stephenson R.L. and Blackburn J.B. (Eds). *The industrial wastewater systems. Handbook*. (Ed) Lewis Publishers. New York, USA.
- Strik, D.P.B.T.B., Domnanovich, A.M, Zani, L., Braun, R., Holubar, P., 2005, Prediction of trace compounds in biogas from anaerobic digestion using the MATLAB neural network toolbox. *Environmental Modelling & Software*, 20, 803-810.
- Sun, J., Sun, S., Fan, M., Guo, H., Lee, Y., Sun, R., 2008. Oxidative decomposition of p-nitroaniline in water by solar photo-Fenton advanced oxidation process. *Journal of Hazardous Materials*, 153 187–193.
- Sychev, A.Y., Isaak, V.G., 1995. Iron compounds and the mechanisms of the homogeneous catalysis of the activation of O<sub>2</sub> and H<sub>2</sub>O<sub>2</sub> and of the oxidation of organic substrates. *Russian Chemical Reviews Articles*, 64, 1105-1129.
- Talinli, I., Anderson, G.K., 1992. Interference of hydrogen peroxide on the standard COD test. *Water Research*, 26, 107–110.



- Tamimi, M., Qourzal, S., Barka, N., Assabbane, A., Ait-Ichou, Y., 2008. Methomyl degradation in aqueous solutions by Fenton's reagent and the photo-Fenton system. *Separation and Purification Technology*, 61, 103–108.
- Tang, W.Z., Tassos, S., 1997. Oxidation kinetics and mechanisms of trihalomethanes by Fenton's reagent. *Water Research*, 31, 1117–1125.
- Tang, W.Z., Huang, C.P., 1997. Stoichiometry of Fenton's reagent in the oxidation of chlorinated aliphatic organic pollutants. *Environmental Technology*, 18, 13-23.
- Tantak, N.P., Chaudhari, S., 2006. Degradation of azo dyes by sequential Fenton's oxidation and aerobic biological treatment. *Journal of Hazardous Materials*, B136, 698–705.
- Tekin, H., Bilkay, O., Ataberk, S.S., Balta, T.H., Ceribasi, I.H., Sanin, F.D., Dilek, F.B., Yetis, U., 2006. Use of Fenton oxidation to improve the biodegradability of a pharmaceutical wastewater. *Journal of Hazardous Materials*, 136, 258-265.
- Toma, F.L., Guessasma, S., Klein, D., Montavon, G., Bertrand, G., Coddet C., 2004. Neural computation to predict TiO<sub>2</sub> photocatalytic efficiency for nitrogen oxides removal. *Journal of Photochemistry and Photobiology A: Chemistry*, 165, 91–96.
- Torrades, F., Garcia-Montano, J., Garcia-Hortal, J.A., Domenech, X., Peral, J., 2004. Decolorization and Mineralization of commercial reactive dyes under solar light assisted photo-Fenton conditions. *Journal of Solar Energy Engineering*, 77, 573-581.
- Trovó, A.G., Melo, S.A.S., Nogueira, R.F.P., 2008. Photodegradation of the pharmaceuticals amoxicillin, bezafibrate and paracetamol by the photo-Fenton process: Application to sewage treatment plant effluent. *Journal of Photochemistry and Photobiology A: Chemistry*, 198, 215–220.
- Tu, J.V., 1996. Advantages and disadvantages of using artificial neural networks versus logistic regression for predicting medical outcomes. *Journal of Clinical Epidemiology*, 49, 1225-1231.

- Tunesi, S., Anderson, M.A., 1987. Photocatalysis of 3, 4-DCB in TiO<sub>2</sub> aqueous suspensions; effects of temperature and light intensity; CIR-FTIR interfacial analysis. *Chemosphere*, 16, 1447-1456.
- US EPA, 2006. Permit Guidance Document: Pharmaceutical Manufacturing Point Source Category (40 CFR Part 439) in: U. EPA (Ed.) EPA 821-F-05-006, Washington, DC.
- Vandevivere, P.C., Bianchi, R., Verstraete, W., 1998. Treatment and reuse of wastewater from the textile wet-processing industry: review of emerging technologies. *Journal of Chemical Technology & Biotechnology*, 72, 289-302.
- Vorontsov, A.V., Savinov, E.N., Smirniotis, P.G., 2000. Vibrofluidized- and fixed-bed photocatalytic reactors: case of gaseous acetone photooxidation. *Chemical Engineering Science*, 55, 5089-5098.
- Walter, M.V., Vennes, J.W., 1985. Occurrence of multiple-antibiotic resistant enteric bacteria in domestic sewage and oxidative lagoons. *Applied and Environmental Microbiology*, 50, 930-933.
- Wang, K.H., Hsieh, Y.H., Wu, C.H., Chang, C.Y., 2000. The pH and anion effects on the heterogeneous photocatalytic degradation of o-methylbenzoic acid in TiO<sub>2</sub> aqueous suspension. *Chemosphere*, 40, 389-394.
- Yang, L., Yu, L.E., Ray, M.B., 2008. Degradation of paracetamol in aqueous solutions by TiO<sub>2</sub> photocatalysis. *Water Research*, 42, 3480-3488.
- Yaziz, M.1., 1981. The occurrence of antibiotic resistant salmonellas in sewage and the effect of primary sedimentation on their numbers. *Pertanika* 4, 39-42.
- Yetilmezsoy, K., Demirel, S., 2008. Artificial neural network (ANN) approach for modeling of Pb(II) adsorption from aqueous solution by Antep pistachio (*Pistacia Vera L.*) shells. *Journal of Hazardous Materials*, 153, 1288–1300.
- Yim, G., 2007. Attack of the superbugs: Antibiotic resistance, the Science Creative Quarterly,(2),URL:<http://www.scq.ubc.ca/attack-of-the-superbugs-antibioticresistance>.
- Yu, Y., Hu, S., 1994. Preoxidation of chlorophenolic wastewaters for their subsequent biological treatment. *Water Science and Technology*, 29, 313-320.

- Yu, R-F., Chen, H-W., Cheng, W-P., Hsieh, P-H., 2009. Dosage control of the fenton process for color removal of textile wastewater applying orp monitoring and artificial neural networks. *Journal of Environmental Engineering*, 135, 325-332.
- Zainal, Z., Hui, L.K., Hussein, M.Z., Taufiq-Yap, Y.H., Abdullah, A.H., Ramli, I., 2005. Removal of dyes using immobilized titanium dioxide illuminated by fluorescent lamps. *Journal of Hazardous Materials*, B 125, 113-120.
- Zeng, G.M., Qin, X.S., He, L., Huang, G.H., Liu, H.L., Lin, Y.P., 2003. A neural network predictive control system for paper mill wastewater treatment. *Engineering Application of Artificial Intelligence*, 410, 121-129.
- Zitomer, D.H., Speece, R.E., 1993. Sequential environments for enhanced biotransformation of aqueous contaminants. *Environmental Science & Technology*, 27, 227-244
- Zhang, H., Choi, H.J. , Huang, C., 2005. Optimization of Fenton process for the treatment of landfill leachate. *Journal of Hazardous Materials*, B125, 166–174.
- Zhang, G., Ji, S., Xi, B., 2006. Feasibility study of treatment of amoxillin wastewater with a combination of extraction, Fenton oxidation and reverse osmosis. *Desalination*, 196, 32–42.
- Zheng, S.R., Huang, Q.G., Zhou, J., Wang, B.K., 1997. A study on dye photoremoval on TiO<sub>2</sub> suspension solution. *Journal of Photochemistry and Photobiology A: Chemistry*, 108, 235-238.
- Zhao, X., Yang, G., Wang, Y., Gao, X., 2004. Photochemical degradation of dimethyl phthalate by Fenton reagent. *Journal of Photochemistry and Photobiology A: Chemistry*, 161, 215–220.
- Zhao, H., Xu, S., Zhong, J., Bao, X., 2004. Kinetic study of photo-catalytic degradation of pyridine in TiO<sub>2</sub> suspension. *Catalysis Today*, 93-95, 857-861.
- Zhua, J., Zurcher, J., Raoc, M., Menga, M.Q.H., 1998. An on-line wastewater quality predication system based on a time-delay neural network. *Engineering Application of Artificial Intelligence*, 11, 747-758.

APPENDIX (A) One-way ANOVA for sCOD and DOC removal at different HRT  
 using Fenton-SBR process  
 One-way ANOVA for sCOD removal

Anova: Single Factor 48 hr vs. 24 hr

SUMMARY

<i>Groups</i>	<i>Count</i>	<i>Sum</i>	<i>Average</i>	<i>Variance</i>
Column 1	50	2795.95	55.919	101.5292
Column 2	50	2674.419	53.48838	98.13053

ANOVA

<i>Source of Variation</i>	<i>SS</i>	<i>df</i>	<i>MS</i>	<i>F</i>	<i>P-value</i>	<i>F crit</i>
Between Groups	147.697	1	147.697	1.479488	0.226776	3.938111
Within Groups	9783.325	98	99.82985			
Total	9931.022	99				

Anova: Single Factor 12 hr vs. 24 h

SUMMARY

<i>Groups</i>	<i>Count</i>	<i>Sum</i>	<i>Average</i>	<i>Variance</i>
Column 1	50	2674.419	53.48838	98.13053
Column 2	50	2491.48	49.8296	80.30883

ANOVA

<i>Source of Variation</i>	<i>SS</i>	<i>df</i>	<i>MS</i>	<i>F</i>	<i>P-value</i>	<i>F crit</i>
Between Groups	334.6668	1	334.6668	3.751042	0.055655	3.938111
Within Groups	8743.529	98	89.21968			
Total	9078.195	99				

Anova: Single Factor 12 hr vs.24 hr vs. 12 hr

SUMMARY

<i>Groups</i>	<i>Count</i>	<i>Sum</i>	<i>Average</i>	<i>Variance</i>
Column 1	50	2795.95	55.919	101.5292
Column 2	50	2674.419	53.48838	98.13053
Column 3	50	2476.632	49.53265	90.39442

ANOVA

<i>Source of Variation</i>	<i>SS</i>	<i>df</i>	<i>MS</i>	<i>F</i>	<i>P-value</i>	<i>F crit</i>
Between Groups	1039.02	2	519.51	5.373239	0.005595	3.057621
Within Groups	14212.65	147	96.6847			
Total	15251.67	149				

## One-way ANOVA for DOC removal

Anova: Single Factor 48 hr vs. 24 hr

<i>Groups</i>	<i>Count</i>	<i>Sum</i>	<i>Average</i>	<i>Variance</i>
Column 1	50	2912.427	58.24853	44.41436
Column 2	50	2807.253	56.14507	52.86647

ANOVA

<i>Source of Variã</i>	<i>SS</i>	<i>df</i>	<i>MS</i>	<i>F</i>	<i>P-value</i>	<i>F crit</i>
Between G	110.614	1	110.614	2.274117	0.134767	3.938111
Within Gro	4766.761	98	48.64042			
Total	4877.375	99				

Anova: Single Factor

SUMMARY

<i>Groups</i>	<i>Count</i>	<i>Sum</i>	<i>Average</i>	<i>Variance</i>
Column 1	50	2807.253	56.14507	52.86647
Column 2	50	2689.638	53.79276	51.20559

ANOVA

<i>Source of Variã</i>	<i>SS</i>	<i>df</i>	<i>MS</i>	<i>F</i>	<i>P-value</i>	<i>F crit</i>
Between G	138.3335	1	138.3335	2.658418	0.106213	3.938111
Within Gro	5099.531	98	52.03603			
Total	5237.865	99				

Anova: Single Factor 12 hr vs. 24 h

SUMMARY

<i>Groups</i>	<i>Count</i>	<i>Sum</i>	<i>Average</i>	<i>Variance</i>
Column 1	50	2912.427	58.24853	44.41436
Column 2	50	2807.253	56.14507	52.86647
Column 3	50	2689.638	53.79276	51.20559

Anova: Single Factor 12 hr vs.24 hr vs. 12 hr

<i>Source of Variã</i>	<i>SS</i>	<i>df</i>	<i>MS</i>	<i>F</i>	<i>P-value</i>	<i>F crit</i>
Between G	496.863	2	248.4315	5.019277	0.007787	3.057621
Within Gro	7275.835	147	49.49548			
Total	7772.698	149				

APPENDIX (B) Two-way ANOVA for sCOD removal at different H<sub>2</sub>O<sub>2</sub>/COD molar ratio and Fenton reaction time using Fenton-SBR process

Multiple Comparisons, Dependent Variable: Percent removal, Tukey HSD

(I) H <sub>2</sub> O <sub>2</sub> /Fe <sup>2+</sup> - Reaction Time	(J) H <sub>2</sub> O <sub>2</sub> / Fe <sup>2+</sup> - Reaction Time	Mean Dif.*(I- J)	Std. Error	Sig.	95% Confidence Interval	
					Lower Bound	Upper Bound
H <sub>2</sub> O <sub>2</sub> /Fe <sup>2+</sup> (MR) 50 -T30 (min)	H <sub>2</sub> O <sub>2</sub> /Fe <sup>2+</sup> (MR)50 -T60 (min)	-16.0	0.9	0.0	-19.1	-12.9
	H <sub>2</sub> O <sub>2</sub> /Fe <sup>2+</sup> (MR)50 -T90 (min)	-17.0	0.9	0.0	-20.0	-13.9
	H <sub>2</sub> O <sub>2</sub> /Fe <sup>2+</sup> (MR)) 50 - T120(min)	-21.1	0.9	0.0	-24.2	-18.0
	H <sub>2</sub> O <sub>2</sub> /Fe <sup>2+</sup> (MR) 100 -T30 (min)	15.6	0.8	0.0	12.9	18.4
	H <sub>2</sub> O <sub>2</sub> /Fe <sup>2+</sup> (MR)100 -T60 (min)	-12.9	0.9	0.0	-16.0	-9.8
	H <sub>2</sub> O <sub>2</sub> /Fe <sup>2+</sup> (MR)100 -T90 (min)	-16.2	0.9	0.0	-19.3	-13.1
	H <sub>2</sub> O <sub>2</sub> /Fe <sup>2+</sup> (MR)100 -T120 (min)	-20.4	0.9	0.0	-23.5	-17.3
	H <sub>2</sub> O <sub>2</sub> /Fe <sup>2+</sup> (MR)150 -T30 (min)	22.0	0.8	0.0	19.3	24.8
	H <sub>2</sub> O <sub>2</sub> /Fe <sup>2+</sup> (MR)150 -T60 (min)	0.7	0.9	1.0	-2.4	3.8
	H <sub>2</sub> O <sub>2</sub> /Fe <sup>2+</sup> (MR)150 -T90 (min)	-11.6	0.9	0.0	-14.7	-8.5
	H <sub>2</sub> O <sub>2</sub> /Fe <sup>2+</sup> (MR)150 -T120 (min)	-14.1	0.9	0.0	-17.2	-11.0
	H <sub>2</sub> O <sub>2</sub> /Fe <sup>2+</sup> (MR)50 -T30 (min)	16.0	0.9	0.0	12.9	19.1
	H <sub>2</sub> O <sub>2</sub> /Fe <sup>2+</sup> (MR)50 -T90 (min)	-1.0	1.0	1.0	-4.4	2.4
	H <sub>2</sub> O <sub>2</sub> /Fe <sup>2+</sup> (MR)50 -T120 (min)	-5.1	1.0	0.0	-8.5	-1.7
H <sub>2</sub> O <sub>2</sub> / Fe <sup>2+</sup> (MR) 50 -T60 (min)	H <sub>2</sub> O <sub>2</sub> /Fe <sup>2+</sup> (MR)100 -T30 (min)	31.6	0.9	0.0	28.5	34.7
	H <sub>2</sub> O <sub>2</sub> /Fe <sup>2+</sup> (MR)100 -T60 (min)	3.1	1.0	0.1	-0.3	6.5
	H <sub>2</sub> O <sub>2</sub> /Fe <sup>2+</sup> (MR)100 -T90 (min)	-0.2	1.0	1.0	-3.6	3.2
	H <sub>2</sub> O <sub>2</sub> /Fe <sup>2+</sup> (MR)100 -T120 (min)	-4.5	1.0	0.0	-7.8	-1.1
	H <sub>2</sub> O <sub>2</sub> /Fe <sup>2+</sup> (MR)150 -T30 (min)	38.0	0.9	0.0	34.9	41.1
	H <sub>2</sub> O <sub>2</sub> /Fe <sup>2+</sup> (MR)150 -T60 (min)	16.7	1.0	0.0	13.3	20.1
	H <sub>2</sub> O <sub>2</sub> /Fe <sup>2+</sup> (MR)150 -T90 (min)	4.4	1.0	0.0	1.0	7.8
	H <sub>2</sub> O <sub>2</sub> /Fe <sup>2+</sup> (MR)150 -T120	1.8	1.0	0.8	-1.5	5.2

	(min)					
	H <sub>2</sub> O <sub>2</sub> /Fe <sup>2+</sup> (MR) 50 -T30	17.0	0.9	0.0	13.9	20.0
	(min)					
	H <sub>2</sub> O <sub>2</sub> /Fe <sup>2+</sup> (MR)50 -T60	1.0	1.0	1.0	-2.4	4.4
	(min)					
	H <sub>2</sub> O <sub>2</sub> /Fe <sup>2+</sup> (MR) 50 -T120	-4.2	1.0	0.0	-7.5	-0.8
	(min)					
	H <sub>2</sub> O <sub>2</sub> /Fe <sup>2+</sup> (MR)100 -T30	32.6	0.9	0.0	29.5	35.7
	(min)					
	H <sub>2</sub> O <sub>2</sub> /Fe <sup>2+</sup> (MR)100 -T60	4.1	1.0	0.0	0.7	7.5
	(min)					
H <sub>2</sub> O <sub>2</sub> /Fe <sup>2+</sup> (MR)	H <sub>2</sub> O <sub>2</sub> /Fe <sup>2+</sup> (MR)100 -T90	0.8	1.0	1.0	-2.6	4.1
50 -T90 (min)	(min)					
	H <sub>2</sub> O <sub>2</sub> /Fe <sup>2+</sup> (MR)100 -T120	-3.5	1.0	0.0	-6.9	-0.1
	(min)					
	H <sub>2</sub> O <sub>2</sub> /Fe <sup>2+</sup> (MR)150 -T30	39.0	0.9	0.0	35.9	42.1
	(min)					
	H <sub>2</sub> O <sub>2</sub> /Fe <sup>2+</sup> (MR)150 -T60	17.7	1.0	0.0	14.3	21.0
	(min)					
	H <sub>2</sub> O <sub>2</sub> /Fe <sup>2+</sup> (MR)150 -T90	5.3	1.0	0.0	2.0	8.7
	(min)					
	H <sub>2</sub> O <sub>2</sub> /Fe <sup>2+</sup> (MR)150 -T120	2.8	1.0	0.2	-0.6	6.2
	(min)					
	H <sub>2</sub> O <sub>2</sub> /Fe <sup>2+</sup> (MR)50 -T30	21.1	0.9	0.0	18.0	24.2
	(min)					
	H <sub>2</sub> O <sub>2</sub> /Fe <sup>2+</sup> (MR) 50 -T60	5.1	1.0	0.0	1.7	8.5
	(min)					
	H <sub>2</sub> O <sub>2</sub> /Fe <sup>2+</sup> (MR) 50 -T90	4.2	1.0	0.0	0.8	7.5
	(min)					
	H <sub>2</sub> O <sub>2</sub> /Fe <sup>2+</sup> (MR) 100 -T30	36.7	0.9	0.0	33.7	39.8
	(min)					
	H <sub>2</sub> O <sub>2</sub> /Fe <sup>2+</sup> (MR) 100 -T60	8.2	1.0	0.0	4.8	11.6
	(min)					
H <sub>2</sub> O <sub>2</sub> /Fe <sup>2+</sup> (MR)	H <sub>2</sub> O <sub>2</sub> /Fe <sup>2+</sup> (MR) 100 -T90	4.9	1.0	0.0	1.5	8.3
50 -T120 (min)	(min)					
	H <sub>2</sub> O <sub>2</sub> /Fe <sup>2+</sup> (MR) 100 -T120	0.7	1.0	1.0	-2.7	4.1
	(min)					
	H <sub>2</sub> O <sub>2</sub> /Fe <sup>2+</sup> (MR) 150 -T30	43.1	0.9	0.0	40.1	46.2
	(min)					
	H <sub>2</sub> O <sub>2</sub> /Fe <sup>2+</sup> (MR) 150 -T60	21.8	1.0	0.0	18.4	25.2
	(min)					
	H <sub>2</sub> O <sub>2</sub> /Fe <sup>2+</sup> (MR) 150 -T90	9.5	1.0	0.0	6.1	12.9
	(min)					
	H <sub>2</sub> O <sub>2</sub> /Fe <sup>2+</sup> (MR) 150 -T120	7.0	1.0	0.0	3.6	10.4
	(min)					
	H <sub>2</sub> O <sub>2</sub> /Fe <sup>2+</sup> (MR) 50 -T30	-15.6	0.8	0.0	-18.4	-12.9
	(min)					
	H <sub>2</sub> O <sub>2</sub> /Fe <sup>2+</sup> (MR) 50 -T60	-31.6	0.9	0.0	-34.7	-28.5
	(min)					
H <sub>2</sub> O <sub>2</sub> /Fe <sup>2+</sup> (MR)	H <sub>2</sub> O <sub>2</sub> /Fe <sup>2+</sup> (MR) 50 -T90	-32.6	0.9	0.0	-35.7	-29.5
100 -T30 (min)	(min)					
	H <sub>2</sub> O <sub>2</sub> /Fe <sup>2+</sup> (MR) 50 -T120	-36.7	0.9	0.0	-39.8	-33.7
	(min)					

	H <sub>2</sub> O <sub>2</sub> /Fe <sup>2+</sup> (MR) 100 -T60 (min)	-28.5	0.9	0.0	-31.6	-25.4
	H <sub>2</sub> O <sub>2</sub> /Fe <sup>2+</sup> (MR) 100 -T90 (min)	-31.8	0.9	0.0	-34.9	-28.8
	H <sub>2</sub> O <sub>2</sub> /Fe <sup>2+</sup> (MR) 100 -T120 (min)	-36.1	0.9	0.0	-39.2	-33.0
	H <sub>2</sub> O <sub>2</sub> /Fe <sup>2+</sup> (MR) 150 -T30 (min)	6.4	0.8	0.0	3.6	9.2
	H <sub>2</sub> O <sub>2</sub> /Fe <sup>2+</sup> (MR) 150 -T60 (min)	-14.9	0.9	0.0	-18.0	-11.9
	H <sub>2</sub> O <sub>2</sub> /Fe <sup>2+</sup> (MR) 150 -T90 (min)	-27.2	0.9	0.0	-30.3	-24.2
	H <sub>2</sub> O <sub>2</sub> /Fe <sup>2+</sup> (MR) 150 -T120 (min)	-29.8	0.9	0.0	-32.9	-26.7
	H <sub>2</sub> O <sub>2</sub> /Fe <sup>2+</sup> (MR) 50 -T30 (min)	12.9	0.9	0.0	9.8	16.0
	H <sub>2</sub> O <sub>2</sub> /Fe <sup>2+</sup> (MR) 50 -T60 (min)	-3.1	1.0	0.1	-6.5	0.3
	H <sub>2</sub> O <sub>2</sub> /Fe <sup>2+</sup> (MR) 50 -T90 (min)	-4.1	1.0	0.0	-7.5	-0.7
	H <sub>2</sub> O <sub>2</sub> /Fe <sup>2+</sup> (MR) 50 -T120 (min)	-8.2	1.0	0.0	-11.6	-4.8
	H <sub>2</sub> O <sub>2</sub> /Fe <sup>2+</sup> (MR) 100 -T30 (min)	28.5	0.9	0.0	25.4	31.6
H <sub>2</sub> O <sub>2</sub> /Fe <sup>2+</sup> (MR) 100 -T60 (min)	H <sub>2</sub> O <sub>2</sub> /Fe <sup>2+</sup> (MR) 100 -T90 (min)	-3.3	1.0	0.1	-6.7	0.1
	H <sub>2</sub> O <sub>2</sub> / Fe <sup>2+</sup> (MR) 100 -T120 (min)	-7.6	1.0	0.0	-10.9	-4.2
	H <sub>2</sub> O <sub>2</sub> /Fe <sup>2+</sup> (MR) 150 -T30 (min)	34.9	0.9	0.0	31.8	38.0
	H <sub>2</sub> O <sub>2</sub> /Fe <sup>2+</sup> (MR) 150 -T60 (min)	13.6	1.0	0.0	10.2	17.0
	H <sub>2</sub> O <sub>2</sub> /Fe <sup>2+</sup> (MR) 150 -T90 (min)	1.3	1.0	1.0	-2.1	4.7
	H <sub>2</sub> O <sub>2</sub> /Fe <sup>2+</sup> (MR) 150 -T120 (min)	-1.3	1.0	1.0	-4.6	2.1
	H <sub>2</sub> O <sub>2</sub> /Fe <sup>2+</sup> (MR) 50 -T30 (min)	16.2	0.9	0.0	13.1	19.3
	H <sub>2</sub> O <sub>2</sub> /Fe <sup>2+</sup> (MR) 50 -T60 (min)	0.2	1.0	1.0	-3.2	3.6
	H <sub>2</sub> O <sub>2</sub> /Fe <sup>2+</sup> (MR) 50 -T90 (min)	-0.8	1.0	1.0	-4.1	2.6
	H <sub>2</sub> O <sub>2</sub> /Fe <sup>2+</sup> (MR) 50 -T120 (min)	-4.9	1.0	0.0	-8.3	-1.5
H <sub>2</sub> O <sub>2</sub> /Fe <sup>2+</sup> (MR) 100 -T90 (min)	H <sub>2</sub> O <sub>2</sub> /Fe <sup>2+</sup> (MR) 100 -T30 (min)	31.8	0.9	0.0	28.8	34.9
	H <sub>2</sub> O <sub>2</sub> /Fe <sup>2+</sup> (MR) 100 -T60 (min)	3.3	1.0	0.1	-0.1	6.7
	H <sub>2</sub> O <sub>2</sub> /Fe <sup>2+</sup> (MR) 100 -T120 (min)	-4.2	1.0	0.0	-7.6	-0.8
	H <sub>2</sub> O <sub>2</sub> /Fe <sup>2+</sup> (MR) 150 -T30 (min)	38.2	0.9	0.0	35.2	41.3
	H <sub>2</sub> O <sub>2</sub> /Fe <sup>2+</sup> (MR) 150 -T60 (min)	16.9	1.0	0.0	13.5	20.3



	(min)	H <sub>2</sub> O <sub>2</sub> /Fe <sup>2+</sup> (MR) 150 -T90	4.6	1.0	0.0	1.2	8.0
	(min)	H <sub>2</sub> O <sub>2</sub> /Fe <sup>2+</sup> (MR) 150 -T120	2.1	1.0	0.6	-1.3	5.5
	(min)	H <sub>2</sub> O <sub>2</sub> /Fe <sup>2+</sup> (MR) 50 -T30	20.4	0.9	0.0	17.3	23.5
	(min)	H <sub>2</sub> O <sub>2</sub> /Fe <sup>2+</sup> (MR) 50 -T60	4.5	1.0	0.0	1.1	7.8
	(min)	H <sub>2</sub> O <sub>2</sub> /Fe <sup>2+</sup> (MR) 50 -T90	3.5	1.0	0.0	0.1	6.9
	(min)	H <sub>2</sub> O <sub>2</sub> /Fe <sup>2+</sup> (MR) 50 -T120	-0.7	1.0	1.0	-4.1	2.7
	(min)	H <sub>2</sub> O <sub>2</sub> /Fe <sup>2+</sup> (MR) 100 -T30	36.1	0.9	0.0	33.0	39.2
H <sub>2</sub> O <sub>2</sub> /COD(MR)	(min)	H <sub>2</sub> O <sub>2</sub> /Fe <sup>2+</sup> (MR) 100 -T60	7.6	1.0	0.0	4.2	10.9
100 -T120 (min)	(min)	H <sub>2</sub> O <sub>2</sub> /Fe <sup>2+</sup> (MR) 100 -T90	4.2	1.0	0.0	0.8	7.6
	(min)	H <sub>2</sub> O <sub>2</sub> /Fe <sup>2+</sup> (MR) 150 -T30	42.5	0.9	0.0	39.4	45.6
	(min)	H <sub>2</sub> O <sub>2</sub> /Fe <sup>2+</sup> (MR) 150 -T60	21.1	1.0	0.0	17.7	24.5
	(min)	H <sub>2</sub> O <sub>2</sub> /Fe <sup>2+</sup> (MR) 150 -T90	8.8	1.0	0.0	5.4	12.2
	(min)	H <sub>2</sub> O <sub>2</sub> /Fe <sup>2+</sup> (MR) 150 -T120	6.3	1.0	0.0	2.9	9.7
	(min)	H <sub>2</sub> O <sub>2</sub> /Fe <sup>2+</sup> (MR) 50 -T30	-22.0	0.8	0.0	-24.8	-19.3
	(min)	H <sub>2</sub> O <sub>2</sub> /Fe <sup>2+</sup> (MR) 50 -T60	-38.0	0.9	0.0	-41.1	-34.9
	(min)	H <sub>2</sub> O <sub>2</sub> /Fe <sup>2+</sup> (MR) 50 -T90	-39.0	0.9	0.0	-42.1	-35.9
	(min)	H <sub>2</sub> O <sub>2</sub> /Fe <sup>2+</sup> (MR) 50 -T120	-43.1	0.9	0.0	-46.2	-40.1
	(min)	H <sub>2</sub> O <sub>2</sub> /Fe <sup>2+</sup> (MR) 100 -T30	-6.4	0.8	0.0	-9.2	-3.6
H <sub>2</sub> O <sub>2</sub> /Fe <sup>2+</sup> (MR)	(min)	H <sub>2</sub> O <sub>2</sub> /Fe <sup>2+</sup> (MR) 100 -T60	-34.9	0.9	0.0	-38.0	-31.8
150 -T30 (min)	(min)	H <sub>2</sub> O <sub>2</sub> /Fe <sup>2+</sup> (MR) 100 -T90	-38.2	0.9	0.0	-41.3	-35.2
	(min)	H <sub>2</sub> O <sub>2</sub> /Fe <sup>2+</sup> (MR) 100 -T120	-42.5	0.9	0.0	-45.6	-39.4
	(min)	H <sub>2</sub> O <sub>2</sub> /Fe <sup>2+</sup> (MR) 150 -T60	-21.3	0.9	0.0	-24.4	-18.3
	(min)	H <sub>2</sub> O <sub>2</sub> /Fe <sup>2+</sup> (MR) 150 -T90	-33.6	0.9	0.0	-36.7	-30.6
	(min)	H <sub>2</sub> O <sub>2</sub> /Fe <sup>2+</sup> (MR) 150 -T120	-36.2	0.9	0.0	-39.3	-33.1
H <sub>2</sub> O <sub>2</sub> /Fe <sup>2+</sup> (MR)	(min)	H <sub>2</sub> O <sub>2</sub> /Fe <sup>2+</sup> (MR) 50 -T30	-0.7	0.9	1.0	-3.8	2.4
150 -T60 (min)	(min)	H <sub>2</sub> O <sub>2</sub> /Fe <sup>2+</sup> (MR) 50 -T60	-16.7	1.0	0.0	-20.1	-13.3

	H <sub>2</sub> O <sub>2</sub> /Fe <sup>2+</sup> (MR) 50 -T90 (min)	-17.7	1.0	0.0	-21.0	-14.3
	H <sub>2</sub> O <sub>2</sub> /Fe <sup>2+</sup> (MR) 50 -T120 (min)	-21.8	1.0	0.0	-25.2	-18.4
	H <sub>2</sub> O <sub>2</sub> /Fe <sup>2+</sup> (MR) 100 -T30 (min)	14.9	0.9	0.0	11.9	18.0
	H <sub>2</sub> O <sub>2</sub> /Fe <sup>2+</sup> (MR) 100 -T60 (min)	-13.6	1.0	0.0	-17.0	-10.2
	H <sub>2</sub> O <sub>2</sub> /Fe <sup>2+</sup> (MR) 100 -T90 (min)	-16.9	1.0	0.0	-20.3	-13.5
	H <sub>2</sub> O <sub>2</sub> /Fe <sup>2+</sup> (MR) 100 -T120 (min)	-21.1	1.0	0.0	-24.5	-17.7
	H <sub>2</sub> O <sub>2</sub> /Fe <sup>2+</sup> (MR) 150 -T30 (min)	21.3	0.9	0.0	18.3	24.4
	H <sub>2</sub> O <sub>2</sub> /Fe <sup>2+</sup> (MR) 150 -T90 (min)	-12.3	1.0	0.0	-15.7	-8.9
	H <sub>2</sub> O <sub>2</sub> /Fe <sup>2+</sup> (MR) 150 -T120 (min)	-14.8	1.0	0.0	-18.2	-11.4
	H <sub>2</sub> O <sub>2</sub> /Fe <sup>2+</sup> (MR) 50 -T30 (min)	11.6	0.9	0.0	8.5	14.7
	H <sub>2</sub> O <sub>2</sub> /Fe <sup>2+</sup> (MR) 50 -T60 (min)	-4.4	1.0	0.0	-7.8	-1.0
	H <sub>2</sub> O <sub>2</sub> /Fe <sup>2+</sup> (MR) 50 -T90 (min)	-5.3	1.0	0.0	-8.7	-2.0
	H <sub>2</sub> O <sub>2</sub> /Fe <sup>2+</sup> (MR) 50 -T120 (min)	-9.5	1.0	0.0	-12.9	-6.1
	H <sub>2</sub> O <sub>2</sub> /Fe <sup>2+</sup> (MR) 100 -T30 (min)	27.2	0.9	0.0	24.2	30.3
H <sub>2</sub> O <sub>2</sub> /Fe <sup>2+</sup> (MR) 150 -T90 (min)	H <sub>2</sub> O <sub>2</sub> /Fe <sup>2+</sup> (MR) 100 -T60 (min)	-1.3	1.0	1.0	-4.7	2.1
	H <sub>2</sub> O <sub>2</sub> /Fe <sup>2+</sup> (MR) 100 -T90 (min)	-4.6	1.0	0.0	-8.0	-1.2
	H <sub>2</sub> O <sub>2</sub> /Fe <sup>2+</sup> (MR) 100 -T120 (min)	-8.8	1.0	0.0	-12.2	-5.4
	H <sub>2</sub> O <sub>2</sub> /Fe <sup>2+</sup> (MR) 150 -T30 (min)	33.6	0.9	0.0	30.6	36.7
	H <sub>2</sub> O <sub>2</sub> /Fe <sup>2+</sup> (MR) 150 -T60 (min)	12.3	1.0	0.0	8.9	15.7
	H <sub>2</sub> O <sub>2</sub> /Fe <sup>2+</sup> (MR) 150 -T120 (min)	-2.5	1.0	0.3	-5.9	0.9
	H <sub>2</sub> O <sub>2</sub> / Fe <sup>2+</sup> (MR) 50 -T30 (min)	14.1	0.9	0.0	11.0	17.2
	H <sub>2</sub> O <sub>2</sub> /Fe <sup>2+</sup> (MR) 50 -T60 (min)	-1.8	1.0	0.8	-5.2	1.5
	H <sub>2</sub> O <sub>2</sub> /Fe <sup>2+</sup> (MR) 50 -T90 (min)	-2.8	1.0	0.2	-6.2	0.6
H <sub>2</sub> O <sub>2</sub> /Fe <sup>2+</sup> (MR) 150 -T120 (min)	H <sub>2</sub> O <sub>2</sub> /Fe <sup>2+</sup> (MR) 50 -T120 (min)	-7.0	1.0	0.0	-10.4	-3.6
	H <sub>2</sub> O <sub>2</sub> /Fe <sup>2+</sup> (MR) 100 -T30 (min)	29.8	0.9	0.0	26.7	32.9
	H <sub>2</sub> O <sub>2</sub> /Fe <sup>2+</sup> (MR) 100 -T60 (min)	1.3	1.0	1.0	-2.1	4.6
	H <sub>2</sub> O <sub>2</sub> /Fe <sup>2+</sup> (MR) 100 -T90	-2.1	1.0	0.6	-5.5	1.3

(min)					
H <sub>2</sub> O <sub>2</sub> /Fe <sup>2+</sup> (MR) 100 -T120	-6.3	1.0	0.0	-9.7	-2.9
(min)					
H <sub>2</sub> O <sub>2</sub> /Fe <sup>2+</sup> (MR) 150 -T30	36.2	0.9	0.0	33.1	39.3
(min)					
H <sub>2</sub> O <sub>2</sub> /Fe <sup>2+</sup> (MR) 150 -T60	14.8	1.0	0.0	11.4	18.2
(min)					
H <sub>2</sub> O <sub>2</sub> /Fe <sup>2+</sup> (MR) 150 -T90	2.5	1.0	0.3	-0.9	5.9
(min)					

Based on observed means.

\* The mean difference is significant at the .05 level.

APPENDIX (C) One-way ANOVA for sCOD and DOC removal at different HRT  
 using photo-Fenton-SBR process  
 One-way ANOVA for sCOD removal

Anova: Single Factor 48 hr vs. 24 h

SUMMARY

Groups	Count	Sum	Average	Variance
Column 1	50	3171.178	63.42356	78.34026
Column 2	50	3041.004	60.82008	68.55222

ANOVA

Source of Variation	SS	df	MS	F	P-value	F crit
Between Groups	169.4524	1	169.4524	2.307162	0.131999	3.938111
Within Groups	7197.732	98	73.44624			
Total	7367.184	99				

Anova: Single Factor 12 hr vs. 24 h

SUMMARY

Groups	Count	Sum	Average	Variance
Column 1	50	3041.004	60.82008	68.55222
Column 2	50	2932.947	58.65894	72.63489

ANOVA

Source of Variation	SS	df	MS	F	P-value	F crit
Between Groups	116.7628	1	116.7628	1.654014	0.201444	3.938111
Within Groups	6918.169	98	70.59356			
Total	7034.931	99				

Anova: Single Factor 12 hr vs. 24 h vs. 48 hr

SUMMARY

Groups	Count	Sum	Average	Variance
Column 1	50	3171.178	63.42356	78.34026
Column 2	50	3041.004	60.82008	68.55222
Column 3	50	2932.947	58.65894	72.63489

ANOVA

Source of Variation	SS	df	MS	F	P-value	F crit
Between Groups	569.1692	2	284.5846	3.889054	0.022603	3.057621
Within Groups	10756.84	147	73.17579			
Total	11326.01	149				

## One-way ANOVA for DOC removal

Anova: Single Factor 48 hr vs. 24 h

### SUMMARY

<i>Groups</i>	<i>Count</i>	<i>Sum</i>	<i>Average</i>	<i>Variance</i>
Column 1	50	3131.53	62.63061	82.41131
Column 2	50	3015.996	60.31991	76.68358

### ANOVA

<i>Source of Variance</i>	<i>SS</i>	<i>df</i>	<i>MS</i>	<i>F</i>	<i>P-value</i>	<i>F crit</i>
Between Groups	133.4827	1	133.4827	1.678026	0.19823	3.938111
Within Groups	7795.65	98	79.54745			
Total	7929.132	99				

Anova: Single Factor 12 hr vs. 24 h

### SUMMARY

<i>Groups</i>	<i>Count</i>	<i>Sum</i>	<i>Average</i>	<i>Variance</i>
Column 1	50	3015.996	60.31991	76.68358
Column 2	50	2869.873	57.39746	74.7705

### ANOVA

<i>Source of Variance</i>	<i>SS</i>	<i>df</i>	<i>MS</i>	<i>F</i>	<i>P-value</i>	<i>F crit</i>
Between Groups	213.5179	1	213.5179	2.819573	0.096307	3.938111
Within Groups	7421.25	98	75.72704			
Total	7634.768	99				

Anova: Single Factor 12 hr vs. 24 h vs. 48 hr

### SUMMARY

<i>Groups</i>	<i>Count</i>	<i>Sum</i>	<i>Average</i>	<i>Variance</i>
Column 1	50	3131.53	62.63061	82.41131
Column 2	50	3015.996	60.31991	76.68358
Column 3	50	2869.873	57.39746	74.7705

### ANOVA

<i>Source of Variance</i>	<i>SS</i>	<i>df</i>	<i>MS</i>	<i>F</i>	<i>P-value</i>	<i>F crit</i>
Between Groups	687.7638	2	343.8819	4.41128	0.013788	3.057621
Within Groups	11459.4	147	77.95513			
Total	12147.17	149				

APPENDIX (D) Two-way ANOVA for sCOD removal at different H<sub>2</sub>O<sub>2</sub>/COD molar ratio and photo-Fenton irradiation time using photo-Fenton-SBR process

Multiple Comparisons

Dependent Variable: Percent removal

Tukey HSD

(I) H <sub>2</sub> O <sub>2</sub> /Fe <sub>2</sub> +&R eaction Time	(J) H <sub>2</sub> O <sub>2</sub> /Fe <sub>2</sub> +&Reaction Time	Mean Differe nce (I-J)	Std. Error	Sig.	95% Confidence Interval	
					Lower Boun d	Upp er Boun d
H <sub>2</sub> O <sub>2</sub> /Fe <sub>2</sub> +(M R) 50 -T60 (min)	H <sub>2</sub> O <sub>2</sub> /Fe <sub>2</sub> +(MR) 50 -T90 (min)	-1.600	.55419	.137	-3.465	.2647
	H <sub>2</sub> O <sub>2</sub> /Fe <sub>2</sub> +(MR) 50 -T120 (min)	-1.575	.55419	.149	-3.440	.2897
	H <sub>2</sub> O <sub>2</sub> /Fe <sub>2</sub> +(MR) 100 -T60 (min)	2.1750*	.55419	.013	.3103	4.040
	H <sub>2</sub> O <sub>2</sub> /Fe <sub>2</sub> +(MR) 100 -T90 (min)	-1.850	.55419	.053	-3.715	.0147
	H <sub>2</sub> O <sub>2</sub> /Fe <sub>2</sub> +(MR) 100 -T120 (min)	-4.850*	.55419	.000	-6.715	-2.99
	H <sub>2</sub> O <sub>2</sub> /Fe <sub>2</sub> +(MR) 150 -T60 (min)	3.9000*	.55419	.000	2.0353	5.765
	H <sub>2</sub> O <sub>2</sub> /Fe <sub>2</sub> +(MR) 150 -T90 (min)	-2.000	.55419	1.000	-2.065	1.665
	H <sub>2</sub> O <sub>2</sub> /Fe <sub>2</sub> +(MR) 150 -T120 (min)	-5.450*	.55419	.000	-7.315	-3.59
H <sub>2</sub> O <sub>2</sub> /Fe <sub>2</sub> +(M R) 50 -T90 (min)	H <sub>2</sub> O <sub>2</sub> /Fe <sub>2</sub> +(MR) 50 -T60 (min)	1.6000	.55419	.137	-.2647	3.465
	H <sub>2</sub> O <sub>2</sub> /Fe <sub>2</sub> +(MR) 50 -T120 (min)	.0250	.55419	1.000	-1.840	1.890
	H <sub>2</sub> O <sub>2</sub> /Fe <sub>2</sub> +(MR) 100 -T60 (min)	3.7750*	.55419	.000	1.9103	5.640
	H <sub>2</sub> O <sub>2</sub> /Fe <sub>2</sub> +(MR) 100 -T90 (min)	-2.500	.55419	1.000	-2.115	1.615
	H <sub>2</sub> O <sub>2</sub> /Fe <sub>2</sub> +(MR) 100 -T120 (min)	-3.250*	.55419	.000	-5.115	-1.39
	H <sub>2</sub> O <sub>2</sub> /Fe <sub>2</sub> +(MR) 150 -T60 (min)	5.5000*	.55419	.000	3.6353	7.365
	H <sub>2</sub> O <sub>2</sub> /Fe <sub>2</sub> +(MR) 150 -T90 (min)	1.4000	.55419	.264	-.4647	3.265
	H <sub>2</sub> O <sub>2</sub> /Fe <sub>2</sub> +(MR) 150 -T120 (min)	-3.850*	.55419	.000	-5.715	-1.99

Based on observed means.

**Multiple Comparisons**

Dependent Variable: Percent removal  
Tukey HSD

(I) H2O2/Fe2+&R eaction Time	(J) H2O2/Fe2+&Reaction Time	Mean Differe nce (I-J)	Std. Error	Sig.	95% Confidence Interval	
					Lower Boun d	Upp er Boun d
H2O2/Fe2+(M R) 50 -T120 (min)	H2O2/Fe2+(MR) 50 -T60 (min)	1.5750	.55419	.149	-2.897	3.440
	H2O2/Fe2+(MR) 50 -T90 (min)	-.0250	.55419	1.000	-1.890	1.840
	H2O2/Fe2+(MR) 100 -T60 (min)	3.7500*	.55419	.000	1.8853	5.615
	H2O2/Fe2+(MR) 100 -T90 (min)	-.2750	.55419	1.000	-2.140	1.590
	H2O2/Fe2+(MR) 100 -T120 (min)	-3.275*	.55419	.000	-5.140	-1.41
	H2O2/Fe2+(MR) 150 -T60 (min)	5.4750*	.55419	.000	3.6103	7.340
	H2O2/Fe2+(MR) 150 -T90 (min)	1.3750	.55419	.284	-.4897	3.240
	H2O2/Fe2+(MR) 150 -T120 (min)	-3.875*	.55419	.000	-5.740	-2.01
H2O2/Fe2+(M R) 100 -T60 (min)	H2O2/Fe2+(MR) 50 -T60 (min)	-2.175*	.55419	.013	-4.040	-.3103
	H2O2/Fe2+(MR) 50 -T90 (min)	-3.775*	.55419	.000	-5.640	-1.91
	H2O2/Fe2+(MR) 50 -T120 (min)	-3.750*	.55419	.000	-5.615	-1.89
	H2O2/Fe2+(MR) 100 -T90 (min)	-4.025*	.55419	.000	-5.890	-2.16
	H2O2/Fe2+(MR) 100 -T120 (min)	-7.025*	.55419	.000	-8.890	-5.16
	H2O2/Fe2+(MR) 150 -T60 (min)	1.7250	.55419	.086	-.1397	3.590
	H2O2/Fe2+(MR) 150 -T90 (min)	-2.375*	.55419	.006	-4.240	-.5103
	H2O2/Fe2+(MR) 150 -T120 (min)	-7.625*	.55419	.000	-9.490	-5.76

Based on observed means.

**Multiple Comparisons**

Dependent Variable: Percent removal

Tukey HSD

(I) H2O2/Fe2+&R eaction Time	(J) H2O2/Fe2+&Reaction Time	Mean Differe nce (I-J)	Std. Error	Sig.	95% Confidence Interval	
					Lower Boun d	Upp er Boun d
H2O2/Fe2+(M R) 100 -T90 (min)	H2O2/Fe2+(MR) 50 -T60 (min)	1.8500	.55419	.053	-.0147	3.715
	H2O2/Fe2+(MR) 50 -T90 (min)	.2500	.55419	1.000	-1.615	2.115
	H2O2/Fe2+(MR) 50 -T120 (min)	.2750	.55419	1.000	-1.590	2.140
	H2O2/Fe2+(MR) 100 -T60 (min)	4.0250*	.55419	.000	2.1603	5.890
	H2O2/Fe2+(MR) 100 -T120 (min)	-3.000*	.55419	.000	-4.865	-1.14
	H2O2/Fe2+(MR) 150 -T60 (min)	5.7500*	.55419	.000	3.8853	7.615
	H2O2/Fe2+(MR) 150 -T90 (min)	1.6500	.55419	.114	-.2147	3.515
	H2O2/Fe2+(MR) 150 -T120 (min)	-3.600*	.55419	.000	-5.465	-1.74
H2O2/Fe2+(M R) 100 -T120 (min)	H2O2/Fe2+(MR) 50 -T60 (min)	4.8500*	.55419	.000	2.9853	6.715
	H2O2/Fe2+(MR) 50 -T90 (min)	3.2500*	.55419	.000	1.3853	5.115
	H2O2/Fe2+(MR) 50 -T120 (min)	3.2750*	.55419	.000	1.4103	5.140
	H2O2/Fe2+(MR) 100 -T60 (min)	7.0250*	.55419	.000	5.1603	8.890
	H2O2/Fe2+(MR) 100 -T90 (min)	3.0000*	.55419	.000	1.1353	4.865
	H2O2/Fe2+(MR) 150 -T60 (min)	8.7500*	.55419	.000	6.8853	10.61
	H2O2/Fe2+(MR) 150 -T90 (min)	4.6500*	.55419	.000	2.7853	6.515
	H2O2/Fe2+(MR) 150 -T120 (min)	-.6000	.55419	.972	-2.465	1.265

Based on observed means.



**Multiple Comparisons**

Dependent Variable: Percent removal

Tukey HSD

(I) H2O2/Fe2+&R eaction Time	(J) H2O2/Fe2+&Reaction Time	Mean Differe nce (I-J)	Std. Error	Sig.	95% Confidence Interval	
					Lower Boun d	Upp er Boun d
H2O2/Fe2+(M R) 150 -T60 (min)	H2O2/Fe2+(MR) 50 -T60 (min)	-3.900*	.55419	.000	-5.765	-2.04
	H2O2/Fe2+(MR) 50 -T90 (min)	-5.500*	.55419	.000	-7.365	-3.64
	H2O2/Fe2+(MR) 50 -T120 (min)	-5.475*	.55419	.000	-7.340	-3.61
	H2O2/Fe2+(MR) 100 -T60 (min)	-1.725	.55419	.086	-3.590	.1397
	H2O2/Fe2+(MR) 100 -T90 (min)	-5.750*	.55419	.000	-7.615	-3.89
	H2O2/Fe2+(MR) 100 -T120 (min)	-8.750*	.55419	.000	-10.61	-6.89
	H2O2/Fe2+(MR) 150 -T90 (min)	-4.100*	.55419	.000	-5.965	-2.24
	H2O2/Fe2+(MR) 150 -T120 (min)	-9.350*	.55419	.000	-11.21	-7.49
H2O2/Fe2+(M R) 150 -T90 (min)	H2O2/Fe2+(MR) 50 -T60 (min)	.2000	.55419	1.000	-1.665	2.065
	H2O2/Fe2+(MR) 50 -T90 (min)	-1.400	.55419	.264	-3.265	.4647
	H2O2/Fe2+(MR) 50 -T120 (min)	-1.375	.55419	.284	-3.240	.4897
	H2O2/Fe2+(MR) 100 -T60 (min)	2.3750*	.55419	.006	.5103	4.240
	H2O2/Fe2+(MR) 100 -T90 (min)	-1.650	.55419	.114	-3.515	.2147
	H2O2/Fe2+(MR) 100 -T120 (min)	-4.650*	.55419	.000	-6.515	-2.79
	H2O2/Fe2+(MR) 150 -T60 (min)	4.1000*	.55419	.000	2.2353	5.965
	H2O2/Fe2+(MR) 150 -T120 (min)	-5.250*	.55419	.000	-7.115	-3.39
H2O2/Fe2+(M R) 150 -T120 (min)	H2O2/Fe2+(MR) 50 -T60 (min)	5.4500*	.55419	.000	3.5853	7.315
	H2O2/Fe2+(MR) 50 -T90 (min)	3.8500*	.55419	.000	1.9853	5.715
	H2O2/Fe2+(MR) 50 -T120 (min)	3.8750*	.55419	.000	2.0103	5.740
	H2O2/Fe2+(MR) 100 -T60 (min)	7.6250*	.55419	.000	5.7603	9.490
	H2O2/Fe2+(MR) 100 -T90 (min)	3.6000*	.55419	.000	1.7353	5.465
	H2O2/Fe2+(MR) 100 -T120 (min)	.6000	.55419	.972	-1.265	2.465
	H2O2/Fe2+(MR) 150 -T60 (min)	9.3500*	.55419	.000	7.4853	11.21
	H2O2/Fe2+(MR) 150 -T90 (min)	5.2500*	.55419	.000	3.3853	7.115

Based on observed means.

APPENDIX (E) One-way ANOVA for sCOD and DOC removal at different HRT  
using TiO<sub>2</sub> photocataysis-SBR process

Anova: Single Factor 48 hr vs. 24 h

SUMMARY

<i>Groups</i>	<i>Count</i>	<i>Sum</i>	<i>Average</i>	<i>Variance</i>
Column 1	45	1804.651	40.10336	10.32046
Column 2	45	1718.657	38.19237	11.69746

ANOVA

<i>Source of Variation</i>	<i>SS</i>	<i>df</i>	<i>MS</i>	<i>F</i>	<i>P-value</i>	<i>F crit</i>
Between Groups	82.16688	1	82.16688	7.463636	0.007607	3.949321
Within Groups	968.7886	88	11.00896			
Total	1050.955	89				

APPENDIX (F) Input data for ANN

Table F.1 Input data for artificial neural network

Experiment No.	Input					Output COD Removal (%)
	Time (min)	H <sub>2</sub> O <sub>2</sub> /COD (MR)	H <sub>2</sub> O <sub>2</sub> /Fe <sup>2+</sup> (MR)	pH	Antibiotics (mg/L)	
1	0	1	50	3	300	0
2	10	1	50	3	300	7
3	20	1	50	3	300	9
4	30	1	50	3	300	12
5	40	1	50	3	300	15
6	50	1	50	3	300	21
7	60	1	50	3	300	26
8	10	1.5	50	3	300	14
9	20	1.5	50	3	300	16
10	30	1.5	50	3	300	21
11	40	1.5	50	3	300	23
12	50	1.5	50	3	300	24
13	60	1.5	50	3	300	45
14	10	2	50	3	300	22
15	20	2	50	3	300	33
16	30	2	50	3	300	37
17	40	2	50	3	300	41
18	50	2	50	3	300	47
19	60	2	50	3	300	55
20	10	2.5	50	3	300	25
21	20	2.5	50	3	300	31
22	30	2.5	50	3	300	34
23	40	2.5	50	3	300	43
24	50	2.5	50	3	300	51
25	60	2.5	50	3	300	60
26	10	3	50	3	300	44
27	20	3	50	3	300	46
28	30	3	50	3	300	49
29	40	3	50	3	300	52
30	50	3	50	3	300	55
31	60	3	50	3	300	62
32	10	3.5	50	3	300	43
33	20	3.5	50	3	300	45
34	30	3.5	50	3	300	48
35	40	3.5	50	3	300	50
36	50	3.5	50	3	300	50
37	60	3.5	50	3	300	62

Table F.1 (continued)

Experiment No.	Input	Output				
	Time (min)	H <sub>2</sub> O <sub>2</sub> /COD (MR)	H <sub>2</sub> O <sub>2</sub> /Fe <sup>2+</sup> (MR)	pH	Antibiotics (mg/L)	COD Removal (%)
38	10	3	2	3	300	67
39	20	3	2	3	300	68
40	30	3	2	3	300	69
41	40	3	2	3	300	71
42	50	3	2	3	300	72
43	60	3	2	3	300	73
44	10	3	5	3	300	70
45	20	3	5	3	300	72
46	30	3	5	3	300	73
47	40	3	5	3	300	74
48	50	3	5	3	300	75
49	60	3	5	3	300	76
50	10	3	10	3	300	71
51	20	3	10	3	300	74
52	30	3	10	3	300	76
53	40	3	10	3	300	78
54	50	3	10	3	300	79
55	60	3	10	3	300	80
56	10	3	20	3	300	62
57	20	3	20	3	300	67
58	30	3	20	3	300	68
59	40	3	20	3	300	70
60	50	3	20	3	300	71
61	60	3	20	3	300	73
62	10	3	50	3	300	44
63	20	3	50	3	300	46
64	30	3	50	3	300	49
65	40	3	50	3	300	52
66	50	3	50	3	300	55
67	60	3	50	3	300	62
68	10	3	100	3	300	18
69	20	3	100	3	300	27
70	30	3	100	3	300	37
71	40	3	100	3	300	45
72	50	3	100	3	300	49
73	60	3	100	3	300	51
74	10	3	150	3	300	18
75	20	3	150	3	300	19
76	30	3	150	3	300	24

Table F.1 (continued)

Experiment No.	Input	Output			Antibiotics (mg/L)	COD Removal (%)
	Time (min)	H <sub>2</sub> O <sub>2</sub> /COD (MR)	H <sub>2</sub> O <sub>2</sub> /Fe <sup>2+</sup> (MR)	pH		
77	40	3	150	3	300	32
78	50	3	150	3	300	39
79	60	3	150	3	300	42
80	10	3	10	2	300	29
81	20	3	10	2	300	32
82	30	3	10	2	300	37
83	40	3	10	2	300	40
84	50	3	10	2	300	44
85	60	3	10	2	300	49
86	10	3	10	2.5	300	33
87	20	3	10	2.5	300	37
88	30	3	10	2.5	300	41
89	40	3	10	2.5	300	46
90	50	3	10	2.5	300	52
91	60	3	10	2.5	300	58
92	10	3	10	3	300	72
93	20	3	10	3	300	75
94	30	3	10	3	300	77
95	40	3	10	3	300	78
96	50	3	10	3	300	80
97	60	3	10	3	300	82
98	10	3	10	3.5	300	70
99	20	3	10	3.5	300	72
100	30	3	10	3.5	300	74
101	40	3	10	3.5	300	75
102	50	3	10	3.5	300	76
103	60	3	10	3.5	300	77
104	10	3	10	4	300	12
105	20	3	10	4	300	18
106	30	3	10	4	300	20
107	40	3	10	4	300	30
108	50	3	10	4	300	36
109	60	3	10	4	300	35
110	10	3	10	3	750	64
111	20	3	10	3	750	72
112	30	3	10	3	750	73
113	40	3	10	3	750	76
114	50	3	10	3	750	73
115	60	3	10	3	750	76
116	10	3	10	3	1500	63

Table F.1 (continued)

Experiment No.	Input	Output			Antibiotics (mg/L)	COD Removal (%)
	Time (min)	H <sub>2</sub> O <sub>2</sub> /COD (MR)	H <sub>2</sub> O <sub>2</sub> /Fe <sup>2+</sup> (MR)	pH		
17	20	3	10	3	1500	67
118	30	3	10	3	1500	70
119	40	3	10	3	1500	73
120	50	3	10	3	1500	74

## APPENDIX (G) Raw results

Effect of H<sub>2</sub>O<sub>2</sub>/COD molar ratio of Fenton process

time min	COD						COD R %					
	H2O2/COD						H2O2/COD					
	F1	F2	F3	F4	F5	F6	F1	F2	F3	F4	F5	F6
	1	1.5	2	2.5	3	3.5	1	1.5	2	2.5	3	3.5
0	520	520	520	520	520	520	0.0	0.0	0.0	0.0	0.0	0.0
10	484	448	405	392	293	296	6.9	13.8	22.1	24.6	43.7	43.1
20	473	436	348	360	282	288	9.0	16.2	33.1	30.8	45.8	44.6
30	457	411	328	345	263	272	12.1	21.0	36.9	33.7	49.4	47.7
40	442	402	309	296	248	260	15.0	22.7	40.6	43.1	52.3	50.0
50	412	397	278	254	235	258	20.8	23.7	46.5	51.2	54.8	50.4
60	387	288	236	207	197	198	25.6	44.6	54.6	60.2	62.1	61.9

time min	BOD5						BOD5/COD					
	H2O2/COD						H2O2/COD					
	F1	F2	F3	F4	F5	F6	F1	F2	F3	F4	F5	F6
	1	1.5	2	2.5	3	3.5	1	1.5	2	2.5	3	3.5
0	0	0	0	0	0	0	0.00	0.00	0.00	0.00	0.00	0.00
10	5	25	24	32	30	39	0.01	0.06	0.06	0.08	0.10	0.13
20	7	30	22	37	35	35	0.01	0.07	0.06	0.10	0.12	0.12
30	10	34	37	45	42	47	0.02	0.08	0.11	0.13	0.16	0.17
40	12	25	42	55	56	51	0.03	0.06	0.14	0.19	0.23	0.20
50	17	22	55	65	70	55	0.04	0.06	0.20	0.26	0.30	0.21
60	20	20	50	58	62	57	0.05	0.07	0.21	0.28	0.31	0.29

time min	DOC						DOC R %					
	H2O2/COD						H2O2/COD					
	F1	F2	F3	F4	F5	F6	F1	F2	F3	F4	F5	F6
	1	1.5	2	2.5	3	3.5	1	1.5	2	2.5	3	3.5
0	149	149	149	149	149	149	0.0	0.0	0.0	0.0	0.0	0.0
10	143	139	139	132	131	119	3.8	6.5	6.7	11.1	12.0	20.0
20	141	140	126	122	118	111	5.3	6.2	15.2	18.4	20.9	25.2
30	139	135	117	116	117	106	6.5	9.1	21.3	22.4	21.6	29.1
40	136	129	119	112	117	103	8.6	13.4	20.3	25.2	21.2	31.2
50	132	124	112	109	102	101	11.3	16.7	24.7	26.7	31.8	32.3
60	129	120	104	103	98	96	13.3	19.8	30.1	31.0	34.4	35.6

Effect of  $H_2O_2/Fe^{2+}$  molar ratio of Fenton process

Time mi	COD							COD R %						
	$H_2O_2/Fe^{2+}$							$H_2O_2/Fe^{2+}$						
	F12	F13	F7	F8	F9	F10	F11	F12	F13	F7	F8	F9	F10	F11
	2	5	10	20	50	100	150	2	5	10	20	50	100	150
0	520	520	520	520	520	520	520	0.0	0.0	0.0	0.0	0.0	0.0	0.0
10	170	155	150	200	293	424	425	67.3	70.2	71.2	61.5	43.7	18.5	18.3
20	165	145	135	172	282	380	420	68.3	72.1	74.0	66.9	45.8	26.9	19.2
30	160	140	127	165	263	326	394	69.2	73.1	75.6	68.3	49.4	37.3	24.2
40	153	137	113	155	248	288	352	70.6	73.7	78.3	70.2	52.3	44.6	32.3
50	148	131	107	149	235	263	316	71.5	74.8	79.4	71.3	54.8	49.4	39.2
60	142	127	105	140	197	253	300	72.7	75.6	79.8	73.1	62.1	51.3	42.3

Time mi	BOD <sub>5</sub>							BOD <sub>5</sub> /COD						
	$H_2O_2/Fe^{2+}$							$H_2O_2/Fe^{2+}$						
	F12	F13	F7	F8	F9	F10	F11	F12	F13	F7	F8	F9	F10	F11
	2	5	10	20	50	100	150	2	5	10	20	50	100	150
0	0	0	0	0	0	0	0	0.00	0.00	0.00	0.00	0.00	0.00	0.00
10	36	36	27	50.7	30	28	14	0.21	0.23	0.18	0.25	0.10	0.07	0.03
20	38	25	30	40	35	30	22	0.23	0.17	0.22	0.23	0.12	0.08	0.05
30	38	27	29	45	42	33	33	0.24	0.19	0.23	0.27	0.16	0.10	0.08
40	32	29	39	50	56	40	31	0.21	0.21	0.35	0.32	0.23	0.14	0.09
50	29	31	42	53	70	48	36	0.20	0.24	0.39	0.36	0.30	0.18	0.11
60	28	30	48	52	62	38	23	0.20	0.24	0.46	0.37	0.31	0.15	0.08

Time mi	DOC							DOC R %						
	$H_2O_2/Fe^{2+}$							$H_2O_2/Fe^{2+}$						
	F12	F13	F7	F8	F9	F10	F11							
	2	5	10	20	50	100	150	2	5	10	20	50	100	150
0	149	149	149	149	149	149	149	0.0	0.0	0.0	0.0	0.0	0.0	0.0
10	100	98	103	125	131	144	147	32.8	34.4	30.6	15.8	12.0	3.2	1.1
20	96	96	100	120	118	139	146	35.5	35.5	32.8	19.4	20.9	7.0	2.2
30	94	95	94	113	117	135	143	37.1	36.6	37.2	24.4	21.6	9.1	3.8
40	92	80	78	104	117	131	139	38.2	46.2	47.4	30.1	21.2	12.0	7.0
50	91	78	77	97	102	129	128	39.2	47.8	48.4	34.9	31.8	13.5	14.1
60	88	74	75	92	98	121	127	41.0	50.5	50.0	38.2	34.4	18.5	14.9



## Effect of pH of Fenton process

Time mi	COD					COD R%				
	pH					pH				
	F14	F15	F7	F16	F17	F14	F15	F7	F16	F17
	2	2.5	3	3.5	4	2	2.5	3	3.5	4
0	520	520	520	520	520	0.0	0.0	0.0	0.0	0.0
10	370	350	146	155	170	28.8	32.7	71.9	70.2	67.3
20	352	327	130	145	150	32.3	37.1	75.0	72.1	71.2
30	330	305	119	136	140	36.5	41.3	77.1	73.8	73.1
40	310	280	112	130	137	40.4	46.2	78.5	75.0	73.7
50	290	250	102	124	131	44.2	51.9	80.4	76.2	74.8
60	265	220	96	120	127	49.0	57.7	81.5	76.9	75.6

Time mi	BOD <sub>5</sub>					BOD <sub>5</sub> /COD				
	pH					pH				
	F14	F15	F7	F16	F17	F14	F15	F7	F16	F17
	2	2.5	3	3.5	4	2	2.5	3	3.5	4
0	0	0	0	0	0	0.00	0.00	0.00	0.00	0.00
10	12	20	54	44	33	0.03	0.06	0.37	0.28	0.19
20	18	25	47	45	39	0.05	0.08	0.36	0.31	0.26
30	20	30	37	35	35	0.06	0.10	0.31	0.26	0.25
40	30	36	35	34	26	0.10	0.13	0.31	0.26	0.19
50	36	45	33	31	25	0.12	0.18	0.32	0.25	0.19
60	35	42	32	30	25	0.13	0.19	0.33	0.25	0.20

Time mi	DOC					DOC R%				
	pH					pH				
	F14	F15	F7	F16	F17	F14	F15	F7	F16	F17
	2	2.5	3	3.5	4					
0	149	149	149	149	149	0.0	0.0	0.0	0.0	0.0
10	127	108	103	103	116	15	27.4	31.2	30.6	22.0
20	120	104	89	100	109	19	30.1	40.3	32.8	26.9
30	116	99	82	94	97	22	33.9	45.2	37.2	34.9
40	110	92	75	78	91	26	38.2	50.0	47.4	39.2
50	103	87	71	77	82	31	41.9	52.2	48.4	45.2
60	99	84	68	75	77	34	43.5	54.3	50.0	48.4

Effect of antibiotic concentration of Fenton process

Time min.	COD			COD R%		
	antibiotic conc.			antibiotic conc.		
	F7	F18	F19	F16	F18	F19
	100	250	500	100	250	500
0	520	1229	2440	0.0	0.0	0.0
10	146	447	900	71.9	63.6	63.1
20	130	350	800	75.0	71.5	67.2
30	119	335	724	77.1	72.7	70.3
40	112	300	670	78.5	75.6	72.5
50	102	335	645	80.4	72.7	73.6
60	96	290	595	81.5	76.4	75.6

Time min.	BOD <sub>5</sub>			BOD <sub>5</sub> /COD		
	antibiotic conc.			antibiotic conc.		
	F7	F18	F19	F16	F18	F19
	100	250	500	100	250	500
0	0	0	0	0.00	0.00	0.00
10	54	60	169	0.37	0.13	0.19
20	47	126	186	0.36	0.36	0.23
30	37	90	200	0.31	0.27	0.28
40	35	85	241	0.31	0.28	0.36
50	33	83	232	0.32	0.25	0.36
60	32	80	170	0.33	0.28	0.29

Time min.	DOC			DOC R%		
	antibiotic conc.			antibiotic conc.		
	F7	F18	F19	F16	F18	F19
	100	250	500	100	250	500
0	149	439	884	0	0.0	0.0
10	103	316	625	128	28.1	29.3
20	89	299	544	111	32.0	38.5
30	82	287	533	102	34.6	39.7
40	75	270	518	93	38.5	41.4
50	71	265	493	89	39.6	44.3
60	68	250	467	85	43.1	47.1

Effect of H<sub>2</sub>O<sub>2</sub>/COD molar ratio of photo-Fenton process

Tme min.	COD				COD R %			
	H <sub>2</sub> O <sub>2</sub> /COD				H <sub>2</sub> O <sub>2</sub> /COD			
	F1	F2	F3	F4	F1	F2	F3	F4
	1	1.5	2	2.5	1	1.5	2	2.5
0	520	520	520	520	0.0	0.0	0.0	0.0
10	350	300	365	365	32.7	42.3	29.8	29.8
20	275	250	315	340	47.1	51.9	39.4	34.6
30	270	225	270	315	48.1	56.7	48.1	39.4
40	240	185	240	305	53.8	64.4	53.8	41.3
50	175	145	205	280	66.3	72.1	60.6	46.2

Tme min.	BOD <sub>5</sub>				BOD <sub>5</sub> /COD			
	H <sub>2</sub> O <sub>2</sub> /COD				H <sub>2</sub> O <sub>2</sub> /COD			
	F1	F2	F3	F4	F1	F2	F3	F4
	1	1.5	2	2.5	1	1.5	2	2.5
0	0	0	0	0	0.00	0.00	0.00	0.00
10	38	40	39	35	0.11	0.13	0.11	0.10
20	39	43	43	41	0.14	0.17	0.14	0.12
30	37	40	41	38	0.14	0.18	0.15	0.12
40	35	36	35	34	0.15	0.19	0.15	0.11
50	32	34	33	31	0.18	0.23	0.16	0.11

Tme min.	DOC				DOC R %			
	H <sub>2</sub> O <sub>2</sub> /COD				H <sub>2</sub> O <sub>2</sub> /COD			
	F1	F2	F3	F4	F1	F2	F3	F4
	1	1.5	2	2.5	1	1.5	2	2.5
0	149	149	149	149	0.0	0.0	0.0	0.0
10	99	96	97.5	97.5	33.6	35.6	34.6	34.6
20	95	92	96	96	36.2	38.3	35.6	35.6
30	92	90	94	94	38.3	39.6	36.9	36.9
40	90	87	92	91	39.6	41.6	38.3	38.9
50	88	81	89	88	40.9	45.6	40.3	40.9

Effect of  $H_2O_2/Fe^{2+}$  molar ratio of photo-Fenton process

Time min.	COD					COD R %				
	$H_2O_2/Fe^{2+}$					$H_2O_2/Fe^{2+}$				
	F5	F6	F7	F8	F9	F5	F6	F7	F8	F9
	10	20	50	100	150	10	20	50	100	150
0	520	520	520	520	520	0.0	0.0	0.0	0.0	0.0
10	205	225	300	300	340	60.6	56.7	42.3	42.3	34.6
20	175	195	250	290	310	66.3	62.5	51.9	44.2	40.4
30	150	180	225	285	295	71.2	65.4	56.7	45.2	43.3
40	140	145	185	250	285	73.1	72.1	64.4	51.9	45.2
50	125	130	145	240	270	76.0	75.0	72.1	53.8	48.1

Time min.	BOD <sub>5</sub>					BOD <sub>5</sub> /COD				
	$H_2O_2/Fe^{2+}$					$H_2O_2/Fe^{2+}$				
	F5	F6	F7	F8	F9	F5	F6	F7	F8	F9
	10	20	50	100	150	10	20	50	100	150
0	0	0	0	0	0	0.00	0.00	0.00	0.00	0.00
10	39	47	40	38	30	0.19	0.21	0.13	0.13	0.09
20	45	46	43	42	31	0.26	0.24	0.17	0.14	0.10
30	41	46	40	38	33	0.27	0.26	0.18	0.13	0.11
40	39	45	36	35	36	0.28	0.31	0.19	0.14	0.13
50	43	44	34	33	33	0.34	0.34	0.23	0.14	0.12

Time min.	DOC					DOC R %				
	$H_2O_2/Fe^{2+}$					$H_2O_2/Fe^{2+}$				
	F5	F6	F7	F8	F9	F5	F6	F7	F8	F9
	10	20	50	100	150	10	20	50	100	150
0	149	149	149	149	149	0.0	0.0	0.0	0.0	0.0
10	99	100	96	100	102	33.6	32.9	35.6	32.9	31.5
20	95	97.5	92	99	101	36.2	34.6	38.3	33.6	32.2
30	90	94.5	90	98	100	39.6	36.6	39.6	34.2	32.9
40	85	87.5	87	97	99.5	43.0	41.3	41.6	34.9	33.2
50	79.5	80	81	96	99	46.6	46.3	45.6	35.6	33.6

## Effect of pH of photo-Fenton process

Time min.	COD					COD R %				
	pH					pH				
	F14	F15	F7	F16	F17	F14	F15	F7	F16	F17
	2	2.5	3	3.5	4	2	2.5	3	3.5	4
0	520	520	520	520	520	0.0	0.0	0.0	0.0	0.0
10	390	265	210	225	285	25.0	49.0	59.6	56.7	45.2
20	375	237	177	195	230	27.9	54.4	66.0	62.5	55.8
30	350	180	145	180	220	32.7	65.4	72.1	65.4	57.7
40	320	160	125	145	175	38.5	69.2	76.0	72.1	66.3
50	300	150	100	130	140	42.3	71.2	80.8	75.0	73.1

Time min.	BOD <sub>5</sub>					BOD <sub>5</sub> /COD				
	pH					pH				
	F14	F15	F7	F16	F17	F14	F15	F7	F16	F17
	2	2.5	3	3.5	4	2	2.5	3	3.5	4
0	0	0	0	0	0	0.00	0.00	0.00	0.00	0.00
10	20	28	44	47	23	0.05	0.11	0.21	0.21	0.08
20	25	28	48	46	32	0.07	0.12	0.27	0.24	0.14
30	29	32	52	46	33	0.08	0.18	0.36	0.26	0.15
40	34	43	48	45	34	0.11	0.27	0.38	0.31	0.19
50	40	42	39	44	38	0.13	0.28	0.39	0.34	0.27

Time min.	DOC					DOC R %				
	pH					pH				
	F14	F15	F7	F16	F17	F14	F15	F7	F16	F17
	2	2.5	3	3.5	4	2	2.5	3	3.5	4
0	149	149	149	149	149	0.0	0.0	0.0	0.0	0.0
10	110	100	97	100	97	26.2	32.9	34.9	32.9	34.9
20	107	98	91	97.5	93	28.2	34.2	38.9	34.6	37.6
30	105	92.5	81	94.5	90.5	29.5	37.9	45.6	36.6	39.3
40	103	91	73	87.5	85	30.9	38.9	51.0	41.3	43.0
50	100	89	62	80	81	32.9	40.3	58.4	46.3	45.6

Effect of antibiotic concentration of photo-Fenton process

Time min.	COD			COD R %		
	Antibiotic conc.			Antibiotic conc.		
	F16	F18	F19	F16	F18	F19
	100	250	500	100	250	500
0	520	1203	2455	0.0	0.0	0.0
10	210	475	940	59.6	60.5	61.7
20	177	383	790	66.0	68.2	67.8
30	145	332	725	72.1	72.4	70.5
40	125	317	699	76.0	73.6	71.5
50	100	302	680	80.8	74.9	72.3

Time min.	BOD <sub>5</sub>			BOD <sub>5</sub> /COD		
	Antibiotic conc.			Antibiotic conc.		
	F16	F18	F19	F16	F18	F19
	100	250	500	100	250	500
0	0	0	0	0.00	0.00	0.00
10	44	110	242	0.21	0.23	0.26
20	48	118	239	0.27	0.31	0.30
30	52	120	237	0.36	0.36	0.33
40	48	117	239	0.38	0.37	0.34
50	39	109	236	0.39	0.36	0.35

Time min.	DOC			DOC R %		
	Antibiotic conc.			Antibiotic conc.		
	F16	F18	F19	F16	F18	F19
	100	250	500	100	250	500
0	149	321	650	0.0	0.0	0.0
10	97	281	535	34.9	12.5	17.7
20	91	250	505	38.9	22.1	22.3
30	81	224	485	45.6	30.2	25.4
40	73	190	460	51.0	40.8	29.2
50	62	169	434	58.4	47.4	33.2

Effect of TiO<sub>2</sub> concentration on antibiotic degradation by TiO<sub>2</sub> photocatalysis

**AMX**

Time min.			1		1.5		2	
		%	mg/l	%	mg/l	%	mg/l	%
-30	104	0.0	104	0.0	104.0	0.0	105	0.0
0	100	3.8	100	3.8	99.0	4.8	98	6.7
60	97	6.7	88	15.4	88.0	15.4	81	22.9
120	87	16.3	77	26.0	77.0	26.0	75	28.6
180	69	33.7	65	37.5	63.0	39.4	62	41.0
240	65	37.5	50	51.9	51.0	51.0	55	47.6
300	60	42.3	47	54.8	46.0	55.8	47	55.2

**AMP**

Time m	0.5		1		1.5		2	
	mg/l	%	mg/l	%	mg/l	%	mg/l	%
-30	105	0.0	105	0.0	105.0	0.0	105	0.0
0	100	4.8	100	4.8	99.0	5.7	100	4.8
60	93	11.4	87	17.1	83.0	21.0	91	13.3
120	89	15.2	78	25.7	76.0	27.6	89	15.2
180	81	22.9	65	38.1	65.0	38.1	78	25.7
240	77	26.7	60	42.9	57.0	45.7	63	40.0
300	70	33.3	50	52.4	48.0	54.3	50	52.4

**CLX**

Time m	0.5		1		1.5		2	
	mg/l	%	mg/l	%	mg/l	%	mg/l	%
-30	103	0.0	103	0.0	103.0	0.0	103	0.0
0	100	2.9	100	2.9	101.0	1.9	98	4.9
60	90	12.6	92	10.7	96.0	6.8	96	6.8
120	82	20.4	79	23.3	82.0	20.4	81	21.4
180	77	25.2	68	34.0	70.0	32.0	69	33.0
240	72	30.1	50	51.5	52.0	49.5	59	42.7
300	55	46.6	43	58.3	42.0	59.2	41	60.2

Effect of pH on antibiotic degradation by TiO<sub>2</sub> photocatalysis

Time m	AMX							
	3		5		8		11	
	mg/l	%	mg/l	%	mg/l	%	mg/l	%
-30	103	0.0	104	0.0	103.0	0.0	103	0.0
0	95	7.8	100	3.8	86.0	16.5	90	12.6
60	84	18.4	88	15.4	74.0	28.2	76	26.2
120	74	28.2	77	26.0	67.0	35.0	65	36.9
180	67	35.0	65	37.5	58.0	43.7	55	46.6
240	49	52.4	50	51.9	49.0	52.4	40	61.2
300	40	61.2	47	54.8	42.0	59.2	30	70.9

Time m	AMP							
	3		5		8		11	
	mg/l	%	mg/l	%	mg/l	%	mg/l	%
-30	105	0.0	105	0.0	105.0	0.0	105	0.0
0	78	25.7	100	4.8	84.0	20.0	80	23.8
60	55	47.6	87	17.1	79.0	24.8	33	68.6
120	42	60.0	78	25.7	71.0	32.4	20	81.0
180	37	64.8	65	38.1	61.0	41.9	13	87.6
240	31	70.5	60	42.9	42.0	60.0	12	88.6
300	23	78.1	50	52.4	27.0	74.3	9	91.4

Time m	CLX							
	3		5		8		11	
	mg/l	%	mg/l	%	mg/l	%	mg/l	%
-30	104	0.0	103	0.0	104.0	0.0	103	0.0
0	71	31.7	100	2.9	94.0	9.6	70	32.0
60	41	60.6	92	10.7	86.0	17.3	12	88.3
120	31	70.2	79	23.3	77.0	26.0	2	98.1
180	18	82.7	68	34.0	59.0	43.3	1	100.0
240	10	90.4	50	51.5	32.0	69.2	0	100.0
300	5	95.2	43	58.3	19.0	81.7	0	100.0



Effect of ZnO concentration on antibiotic degradation by ZnO photocatalysis

Time min.	AMX											
	0.2		0.35		0.5		1		1.5		2	
	mg/l	%	mg/l	%	mg/l	%	mg/l	%	mg/l	%	mg/l	%
-30	104	0.0	104	0.0	105	0.0	104	0.0	104.0	0.0	105	0.0
0	100	3.8	98	5.8	93	10.6	84	19.2	96.0	7.7	91	13.3
60	96	7.7	85	18.3	84	19.2	77	26.0	86.0	17.3	86	18.1
120	89	14.4	78	25.0	65	37.5	60	42.3	76.0	26.9	75	28.6
180	78	25.0	71	31.7	43	58.7	41	60.6	50.0	51.9	45	57.1
240	66	36.5	62	40.4	38	63.5	37	64.4	42.0	59.6	37	64.8
300	58	44.2	50	51.9	29	72.1	30	71.2	31.0	70.2	33	68.6

Time min.	AMP											
	0.2		0.35		0.5		1		1.5		2	
	mg/l	%	mg/l	%	mg/l	%	mg/l	%	mg/l	%	mg/l	%
-30	105	0.0	105	0.0	105	0.0	105	0.0	105.0	0.0	105	0.0
0	98	6.7	93	11.4	92	12.4	88	16.2	85.0	19.0	82	21.9
60	84	20.0	83	21.0	71	32.4	73	30.5	78.0	25.7	77	26.7
120	70	33.3	64	39.0	59	43.8	65	38.1	65.0	38.1	65	38.1
180	60	42.9	55	47.6	48	54.3	56	46.7	58.0	44.8	60	42.9
240	48	54.3	43	59.0	37	64.8	42	60.0	45.0	57.1	41	61.0
300	42	60.0	33	68.6	28	73.3	31	70.5	33.0	68.6	34	67.6

Time min.	CLX											
	0.2		0.35		0.5		1		1.5		2	
	mg/l	%	mg/l	%	mg/l	%	mg/l	%	mg/l	%	mg/l	%
-30	103	0.0	103	0.0	103	0.0	103	0.0	103.0	0.0	103	0.0
0	74	28.2	60	41.7	60	41.7	45	56.3	40.0	61.2	40	61.2
60	50	51.5	40	61.2	30	70.9	30	70.9	19.0	81.6	17	83.5
120	27	73.8	31	69.9	5	95.1	15	85.4	2.0	98.1	2	98.1
180	16	84.5	16	84.5	0	100.0	10	90.3	0.0	100.0	0	100.0
240	7	93.2	2	98.1	0	100.0	0	100.0	0.0	100.0	0	100.0
300	4	96.1	0	100.0	0	100.0	0	100.0	0.0	100.0	0	100.0

Effect of pH on antibiotic degradation by ZnO photocatalysis

Time min.	<b>AMX</b>					
	5		8		11	
	mg/l	%			mg/l	%
-30	103	0.0	104	0.0	103	0.0
0	95	7.8	93	10.6	94	8.7
60	85	17.5	84	19.2	35	66.0
120	79	23.3	65	37.5	10	90.3
180	63	38.8	43	58.7	0	100.0
240	49	52.4	38	63.5	0	100.0
300	42	59.2	29	72.1	0	100.0

Time min.	<b>AMP</b>					
	5		8		11	
	mg/l	%	mg/l	%	mg/l	%
-30	105	0.0	105.0	0.0	105	0.0
0	96	8.6	92.0	12.4	95	9.5
60	84	20.0	71.0	32.4	31	70.5
120	78	25.7	59.0	43.8	15	85.7
180	72	31.4	48.0	54.3	0	100.0
240	65	38.1	37.0	64.8	0	100.0
300	60	42.9	30.0	71.4	0	100.0

Time min.	<b>CLX</b>					
	5		8		11	
	mg/l	%	mg/l	%	mg/l	%
-30	104	0.0	103.0	0.0	103	0.0
0	75	27.9	60.0	41.7	65	36.9
60	48	53.8	30.0	70.9	23	77.7
120	5	95.2	5.0	95.1	2	98.1
180	2	98.1	0.0	100.0	0	100.0
240	3	97.1	0.0	100.0	0	100.0
300	0	100.0	0.0	100.0	0	100.0